RESEARCH ARTICLE

Taxonomic study of *Baeosega* and its allies, with description of a new species of *Nipponosega* (Hymenoptera, Chrysididae, Amiseginae)

Toshiharu Mita[1]

1 *Entomological Laboratory, Faculty of Agriculture, Kyushu University, Motooka 744, Nishi-ku, Fukuoka 819-0395, Japan*

Corresponding author: Toshiharu Mita (t3mita@agr.kyushu-u.ac.jp)

Citation: Mita T (2021) Taxonomic study of *Baeosega* and its allies, with description of a new species of *Nipponosega* (Hymenoptera, Chrysididae, Amiseginae). ZooKeys 1041: 1–25. https://doi.org/10.3897/zookeys.1041.66267

Abstract

Three related genera of Asian Amiseginae, *Baeosega* Krombein, *Nipponosega* Kurzenko & Lelej, and *Okinawasega* Terayama are revised. The male of *N. yamanei* Kurzenko & Lelej and the female of *O. eguchii* Terayama are newly described. The following new synonymies are proposed: *Baeosega humida* Krombein, 1984 = *B. laticeps* Krombein, 1984, **syn. nov.**; *Nipponosega yamanei* Kurzenko & Lelej, 1994 = *N. kantoensis* Nagase, 1995, **syn. nov.** A new species of *Nipponosega*, *N. lineata* **sp. nov.** is described based on a female from Thailand. A key to genera and species of *Baeosega*, *Nipponosega* and *Okinawasega* is given.

Keywords

Asia, egg parasitoid, stick insects, synonymy

Introduction

Amiseginae (Hymenoptera: Chrysididae) are egg parasitoids of stick insects (Phasmatodea) (Krombein 1983; Kimsey et al. 2013). They often show distinct sexual dimorphism: females are brachypterous; their wings are reduced to small pads reaching at most the anterior margin of the propodeum, whereas the males are macropterous.

Because brachypterous females are seldom collected in the field and their morphological characters are greatly different from males, it is difficult to make correct sex association and thus many species have been known by only one sex (Kimsey and Bohart 1991; Kimsey et al. 2016).

Egg parasitoid wasps of stick insects are abundant in tropical and subtropical forests (Krombein 1983; Kimsey and Bohart 1991). However, some species occur in temperate regions. For example, Japan is known as the eastern and northern borders of their distribution in Asia and four genera have been recorded: *Nipponosega* Kurzenko & Lelej, 1994 (*N. yamanei* Kurzenko & Lelej, 1994 and *N. kantoensis* Nagase, 1995), *Cladobethylus* Kieffer, 1922 (*C. japonicus* Kimsey, 1986), *Calosega* Terayama, 1999 (*C. kamiteta* Terayama, 1999), and *Okinawasega* Terayama, 1999 (*O. eguchii* Terayama, 1999) (Kimsey 1986; Kurzenko and Lelej 1994; Nagase 1995; Terayama 1999). Except for *Calosega*, only the female or male of the species has been recognized. Although their life history is almost unknown, *N. yamanei* is considered to attack the eggs of *Micadina phluctainoides* (Rehn, 1904) (Diapheromeridae) (Mita 2014).

In the genus *Nipponosega*, three species are known from mainland China to Japan (Kurzenko and Lelej 1994; Nagase 1995; Xu et al. 2003). Although their males are unknown, the morphology of the female is closely related to *Baeosega* Krombein, 1983 and *Serendibula* Krombein, 1980. However, the female of *Serendibula* is clearly separated from *Baeosega* and *Nipponosega* by having a costate second metasomal tergite (Krombein 1983) and developed inner tooth of its claw. The monotypic genus *Okinawasega* was established on the basis of the male (Terayama 1999). The only known species, *O. eguchii* Terayama, endemic to southern Ryukyus, Japan, is apparently similar to the male of *Baeosega*. The genus has been insufficiently defined and thus it is difficult to distinguish it from *Baeosega* by the known diagnostic characters. Therefore, a comparative study of *Baeosega* and its allies is needed. *Baeosega* is known from three species from Sri Lanka (Krombein 1983) and Krombein (1983) mentioned the presence of a female of an undescribed species from Madras, southern India. In addition, Kimsey (1995) included southern Japan in its distribution, although species information was not provided. As for other related genera, the male of *Baeosega* is separated from *Serendibula*, the most similar taxon in Asia, by having longer setae on antennal flagellomeres, shorter metanotum (almost half as long as mesoscutum), and the absence of a developed inner tooth on the claw. For both genera, R1 on forewing is not indicated; however, unlike *Baeosega*, the distal apex of the pterostigma forms a sharp streak in *Serendibula*.

Although *Baeosega* is currently unknown outside of South Asia, the presence of *Nipponosega* and *Okinawasega* in East Asia suggests that other related taxa should be widely distributed. During the investigation of the Amiseginae fauna in Asia, several unknown females and males similar to *Baeosega* were found in Japan and Thailand. They provide helpful insights to understand taxonomic placement of the genera and species.

Materials and methods

Examined materials are deposited in the collections of the following institutes:

ELKU   Entomological Laboratory, Faculty of Agriculture, Kyushu University, Fukuoka, Japan;

ELMU   Entomological Laboratory, Faculty of Agriculture, Meijo University, Nagoya, Japan (K. Yamagishi);

MNHAH Museum of Nature and Human Activities, Hyogo, Sanda, Japan (Y. Hashimoto);

FFPRI Forestry and Forest Products Research Institute, Tsukuba, Japan (S. Makino);

NSMT   National Museum of Nature and Science, Tsukuba, Japan (T. Ide);

THNHM Natural History Museum of the National Science Museum, Thailand (W. Jaitrong);

USNM   U.S. National Museum of Natural History, Smithsonian Institution, Washington D.C., U.S.A. (S. Brady).

Specimens were collected using flight interception traps (FIT), Malaise traps (MsT), yellow pan traps (YPT), emergence traps using leaf litter (EmT), leaf litter sifting, or net sweeping. Photos were obtained using an Olympus SZX10 stereomicroscope with an Olympus E-5 digital camera, or a Leica S8APO stereomicroscope with a Canon EOS Kiss X-5 digital camera. Images were combined using Zerene stacker ver. 1.04 (Zerene Systems, LLC, Richland, USA).

Morphological terminology follows that used by Krombein (1983) and Kimsey and Bohart (1991). The following abbreviations are used in the description:

F1–F11 flagellomere numbers;

MOD   anterior ocellus diameter;

MS   maximum length of malar space;

OL   distance between median ocellus and lateral ocellus;

OOL   distance between lateral ocellus and compound eye;

OPL   distance between lateral ocellus to posterior margin of vertex or occipital carina;

POL   distance between lateral ocelli;

T1–T3 metasomal tergite numbers.

Antennal articles were measured at the point of greatest breadth and compared with the total length of the article. The length of the pronotum was measured on the midline.

Taxonomic account

Family Chrysididae Latreille, 1802
Subfamily Amiseginae Mocsáry, 1889

Key to the genera and species of *Baeosega* and its allies

Based on the key to genera of Amiseginae provided by Kimsey and Bohart (1991). Males of *Nipponosega kurzenkoi* and *N. lineata* sp. nov. are unknown.

1	Micropterous (female) **2**	
–	Macropterous (male)..**7**	
2	Deep malar sulcus present (Fig. 10D); mesosoma black (*Okinawasega*)...*O. eguchii* Terayama (Japan)	
–	Malar sulcus absent or only faintly indicated (Fig. 7C); mesosoma partly reddish or brownish **3**	
3	Occipital carina distinct from posterior margin of head to gena (Fig. 8C), rarely indistinct; head punctate with interspaces smooth (*Nipponosega*).......**4**	
–	Occipital carina absent, at most posterior margin of vertex forming corner (Fig. 3C, D); head punctate with interspaces finely granulate (*Baeosega*) **6**	
4	Pronotum longitudinally costate (Fig. 7D)....*N. lineata* sp. nov. (Thailand)	
–	Pronotum sparsely punctate with smooth interspaces (Fig. 8E)...................**5**	
5	Mesopleuron fully testaceous; maximum interocular distance 1.2 × longer than width of frons ....*N. kurzenkoi* Xu, He & Terayama (China)	
–	Mesopleuron at least partly blackish; maximum interocular distance 1.5–2.0 × longer than width of frons ....*N. yamanei* Kurzenko & Lelej (Japan)	
6	Metasoma shagreened and dull (Fig. 5D); declivous anterior surface of T1 with weak longitudinal rugulae: silvery subdecumbent setae stout, conspicuous... *B. torrida* Krombein (Sri Lanka)	
–	Metasoma smooth, at most with faint granules; declivous anterior surface of T1 smooth; setae thinner, not conspicuous..*B. humida* Krombein, 1983 (Sri Lanka)	
7	F3 2.3 × as long as wide; and pronotum 0.7–0.9 × as long as mesoscutum (*Nipponosega*) ....*N. yamanei* Kurzenko & Lelej	
–	F3 usually more than 3.5 ×, at least 2.7 × (*Baeosega humida*) as long as wide; and pronotum 1.0–1.1 × as long as mesoscutum **8**	
8	Forewing with R1 clearly indicated, linear (Fig. 11D); F3 3.8–4.3 × as long as wide; setae on flagellum 0.7 × as long as diameter of flagellomere (*Okinawasega*)..*O. eguchii* Terayama (Japan)	
–	Forewing with R1 not indicated (Fig. 4B); F3 2.7–3.5 × as long as wide; setae on flagellum 0.5 × as long as diameter of flagellomere (*Baeosega*) **9**	
9	Head and pronotum testaceous (Fig. 6); F3 3.5 × as long as wide .... *B. torrida* Krombein (Sri Lanka)	
–	Dorsum of head blackish, pronotal disk reddish dark brown (Fig. 4); F3 2.7 × as long as wide .... *B. humida* Krombein (Sri Lanka)	

Genus *Baeosega* Krombein

Baeosega Krombein, 1983. Type species: *Baeosega torrida* Krombein, 1983, original designation.

Diagnosis. The female of *Baeosega* is superficially similar to *Nipponosega* and *Okinawasega*. However, the occipital carina is developed and reaching lower gena in *Nipponosega* (absent in *Baeosega*) and the deep malar sulcus is present in *Okinawasega* (only faintly indicated in *Baeosega*). The male is very similar to *Okinawasega*. The longer setae on flagellum and remarkably long R1 of the forewing are useful characters distinguishing *Okinawasega* from *Baeosega*. Compared to the above two genera, the male of *Nipponosega* has the pronotum short. The pronotum of *Baeosega* and *Okinawasega* is as long as or longer than mesoscutum but it is shorter in *Nipponosega*. Compared to genera found in South Asia, *Baeosega* is most similar to *Serendibula*. In the female of *Baeosega*, the metasomal T2 is lacking fine longitudinal carinae whereas T2 of *Serendibula* is covered with fine carinae. The male of *Baeosega* can be distinguished from *Serendibula* by having longer setae on antennal flagellomeres, the shorter metanotum, almost half as long as mesoscutellum (metanotum is longer, almost as long as mesoscutellum in *Serendibula*) and the tubular distal apex of pterostigma (very sharp in *Serendibula*). The inner tooth of tarsal claw is minute and indistinct in both female and male of *Baeosega*, whereas the inner tooth is distinctively large in *Serendibula*.

Description. Female. Clypeal apex not thickened; malar sulcus absent or indicated as faint track; scapal basin shallow, cross-ridged, median longitudinal carina absent; occipital carina absent, at most posterior margin of vertex forming corner behind ocellar triangle; eye setose; flagellum fusiform, intermediate segments broader than long, and with ventral surface flattened. Mesosoma slender, dorsum more or less punctate; pronotum with median groove and shallow pit before lateral lobe, 1.0–1.4 × as long as combined length of mesoscutum, mesoscutellum and metanotum; mesoscutum with notauli; parapsides lacking; posterolateral corner of mesoscutum not lobate; micropterous (Fig. 1A, B), forewing pads extending to posterior margin of mesoscutellum; mesopleuron with omaulus, without scrobal sulcus; metanotum triangular and small, ca. 2/3 as long as mesoscutellum; propodeum with long dorsal surface and a pair of recumbent teeth present, meeting or almost meeting together, dorsal posterolateral angles bluntly angulate, lateral and posterior surfaces abruptly declivous. Hind coxa with dorsobasal carina; tarsal claws with a minute inner tooth. Metasoma smooth, shagreened or weakly granulated, without longitudinally striate area.

Male. Clypeal apex not thickened; scapal basin flat or weakly excavated, cross-ridged; malar sulcus present; occipital carina absent; eye setose; antenna elongate, F3 2.7–3.5 × longer than wide. Mesosoma slender, dorsum densely punctate; pronotum with median groove and shallow pit before lateral lobe, slightly longer than mesoscutum, 0.5–0.6 × as long as combined length of mesoscutum, mesoscutellum and metanotum; mesoscutum with notauli; parapsidal line faintly indicated; mesopleuron without omaulus and scrobal sulcus; metanotum approximately half mesoscutellum; a pair of recumbent teeth present, meeting or almost meeting together; propodeum with dorsal posterolateral angles bluntly angulate, posterior surface abruptly declivous; fully winged (Fig. 1C),
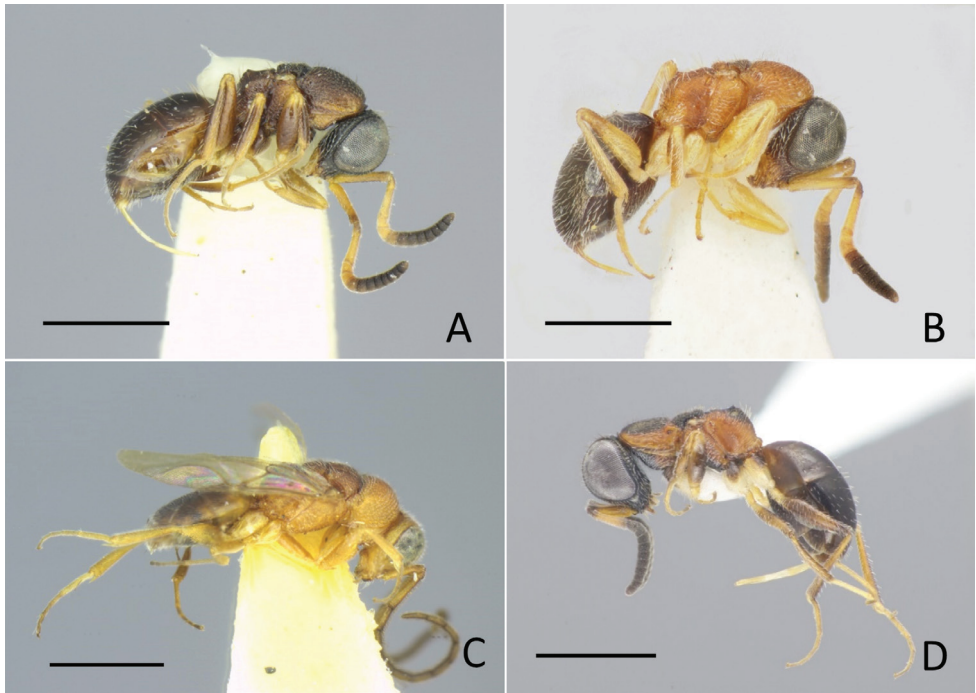
Figure 1. General habitus of Amiseginae **A** *Baeosega humida* Krombein, holotype ♀ **B** *B. torrida* Krombein, holotype ♀ **C** ditto, allotype ♂ **D** *Nipponosega lineata* sp. nov., holotype ♀. Scale bars: 1.0 mm.

pterostigma thin; R1 not indicated, distal apex tubular; Rs extended by weakly curved dark streak; medial vein arising before cu-a. Hind coxa with dorsobasal carina; tarsal claws with a minute inner tooth. Metasoma sparsely punctate with smooth interspaces.

Distribution. Oriental region: Sri Lanka.

Hosts. Unknown.

Remarks. According to Krombein (1983), the female of *Baeosega* has no malar groove. However, a trace of a groove is present from the lower margin of the eye to the mandibular base. A minute inner tooth is also present in the claws of both female and male, but the size of tooth is remarkably small compared to *Serendibula*.

Baeosega humida Krombein, 1983
Figures 1A, 3, 4

Baeosega humida Krombein, 1983: 46, holotype ♀ by original designation. Type local-
　ity: Central Province, Kandy District, Kandy, Udawattakele Sanctuary (Sri Lanka).
Baeosega laticeps Krombein, 1983: 48, holotype ♀ by original designation, new syn-
　onymy. Type locality: Central Province, Kandy District, Kandy, Udawattakele
　Sanctuary (Sri Lanka).

Specimens examined. *Holotypes. Baeosega humida*: Sri Lanka ♀, "SRI LANKA: Kan. Dist./ Udawattakele Sanct./ Elevation 1800 ft./ 23–25-IX-1980", "Collected/ on or in/ leaf litter", "K.V. Krombein/ P.B. Karunaratne/ L. Jayawickrema/ V. Gunawardane/ P. Liyanage" "HOLOTYPE/ BAEOSEGA/ HUMIDA/ Karl V. Krombein", "Type No./ 100454/ U.S.N.M." (USNM); ***Baeosega laticeps*:** Sri Lanka ♀, "SRI LANKA: Kan. Dist./ Udawattakele Sanct./ 25–27-IV-1981", "collected on or/ in leaf litter", "K.V. Krombein/ T. Wijesinhe/ L. Jayawickrema", "HOLOTYPE/ BAEOSEGA/ LATICEPS/ Karl V. Krombein", "Type No./ 100455/ U.S.N.M." (USNM). ***Paratypes. B. humida*:** Sri Lanka 1♂ (allotype), same locality as holotype, but collected at 21–22.IX.1980 (USNM); 4♀, same as above but K.V. Krombein, L. Jayawickrema, V. Gunawardane, T. Wijesinhe leg. (USNM); 4♀1♂, same locality as above, but collected at 23–25.IX.1980, K.V. Krombein, P.B. Karunaratne, L. Jayawickrema, V. Gunawardane, P. Liyanage leg. (USNM); 1♀, same locality as above, but 12–14.X.1980, K.V. Krombein, P.B. Karunaratne, L. Jayawickrema, V. Gunawardane, T. Wijesinhe leg. (USNM); 8♀, same locality as above, but 25–27.IV.1981, K.V. Krombein, T. Wijesinhe, L. Weeratunge leg. (USNM); 1♂, same locality and collectors as above, but 22.V.1981 (USNM); ***B. laticeps*:** Sri Lanka 2♀, same as locality as holotype of *B. laticeps*, but 12–14.X.1980, K.V. Krombein, P.B. Karunaratne, L. Jayawickrema, V. Gunawardane leg. (USNM).

Diagnosis. The female of *Baeosega humida* Krombein can be distinguished from *B. torrida* Krombein, the other known species of *Baeosega*, by having the smooth metasoma. The male is similar to *B. torrida*, however, *B. humida* can be distinguished from *B. torrida* by the short F3 (2.7 × as long as wide). Punctures on mesepisternum are often separated with each other, but sometimes contiguous as in *B. torrida*. The body color of both female and male is brownish unlike *B. torrida*. Other diagnostic characters are as follows: (female) body length 2.3–2.7 mm; head (Figs 1A, 3A, B) black, bearing faint bronzy tint, punctate with interspaces granulated, except the costate scapal basin; malar sulcus indicated by a faint groove; occipital carina absent, only posterior margin of vertex forming corner behind ocellar triangle; mesosoma (Fig. 3C, D) dark brown to brown, part of pronotum, mesoscutum and metanotum darkened; surface punctate with interspaces granulated; (male) body length 2.3–2.7 mm; head (Fig. 4A) dorsally dark brown with face testaceous, punctate by densely located punctures; occipital carina absent; mesosoma (Fig. 4C) dark brown with mesoscutum blackish, punctate as head; postero-lateral corner of propodeum with distinctly producing angle.

Distribution. Sri Lanka (Central Province, Kandy District).

Remarks. According to Krombein (1983), the slender proportion of the head and mesosoma of *Baeosega laticeps* Krombein is the important diagnostic character separating it from *B. humida* Krombein. However, the body proportion can be variable to some extent. This variation is probably caused by the different shape of the host egg. Because there is no significant difference except for the proportion (slightly compressed laterally or not), *B. laticeps* is considered to be a junior subjective synonym of *B. humida*.

Baeosega torrida Krombein, 1983
Figures 1B, C, 5, 6

Baeosega torrida Krombein, 1983: 44, holotype ♀ by original designation. Type local-
ity: Angunakolapelessa, Uva District, Southern Province, Sri Lanka.

Specimens examined. *Holotype.* Sri Lanka ♀, "SRI LANKA: Mon. Dist./ Angu-
nakolapelessa/ 22-28-III-1981", "collected on or/ in leaf litter", "K. V. Krombein/
T. Wijesinhe/ L. Weeratunge", "HOLOTYPE/ BAEOSEGA/ TORRIDA/ Karl V.
Krombein", "Type No./ 100453/ U.S.N.M." (hand-written) "2083468". *Paratypes.*
Sri Lanka 1♂ (allotype), same as holotype, but 100 m alt., 23.I.1979, MsT (USNM);
1♂, same as above (USNM).

Diagnosis. The female of *Baeosega torrida* Krombein can be distinguished from
B. humida Krombein by having the rugulose anterior declivity of T1 (Fig. 5C) and the
strongly granulated dorsum of metasoma (Fig. 5D). Superficially, the reddish mesosoma
is similar to *Nipponosega* females and *Serendibula deraniyagalai* Krombein. The male of
B. torrida is similar to *B. humida*, however, the F3 is longer (3.5 × as long as wide) unlike
B. humda. Other diagnostic characters are as follows: (female) body length 1.8–2.7 mm;
head (Figs 1B, 5A, B) black, bearing faint bronzy tint, punctate with interspaces granu-
lated; malar sulcus indicated by a faint groove; occipital carina absent; mesosoma (Figs
1B, 5C) punctate with interspaces strongly granulated; metasoma (Fig. 5D) blackish;
stout silvery subdecumbent setae on mesosoma and metasoma; (male) body length 2.3–
2.5 mm; head (Figs 1C, 6A, B) testaceous with dark flagellum, rarely around ocellar
region brown, punctate by densely located punctures; occipital carina absent; mesosoma
(Figs 1C, 6C) testaceous with mesoscutum, mesoscutellum, metanotum and dorsum
of propodeum brown or rarely reddish, punctate as head; punctures on mesepisternum
largely contiguous; postero-lateral corner of propodeum with weakly producing angle.

Distribution. Sri Lanka (Uva Province: Monaragala District; Southern Province:
Hambantota District; Central Province: Kandy District, Matale District)

Genus *Nipponosega* Kurzenko & Lelej

Nipponosega Kurzenko & Lelej, 1994: 83. Type species: *Nipponosega yamanei* Kurzen-
ko & Lelej, 1994, original designation.

Diagnosis. General characters of *Nipponosega* are similar to those of *Baeosega* and
Okinawasega. The distinctive characters of *Nipponosega* are in the developed occipital
carina in the female, the short setae on flagellum and the short pronotum in the male.
More details, see the diagnosis of *Baeosega*.

Description. Female. Clypeal apex not thickened; malar sulcus absent or indicated
as faint track; scapal basin shallow, cross-ridged, median longitudinal smooth strip pre-
sent; occipital carina present, reaching gena (Fig. 8C); eye setose; flagellum fusiform,

intermediate segments broader than long, and with ventral surface flattened. Mesosoma slender, punctate or longitudinally striate; pronotum with median groove and shallow pit before lateral lobe, as long as combined length of mesoscutum, mesoscutellum and metanotum; mesoscutum with notauli and without parapsides; posterolateral corner of mesoscutum not lobate; micropterous (Figs 1D, 2A), forewing pads extending to posterior margin of mesoscutellum; mesopleuron with omaulus; scrobal sulcus lacking; metanotum triangular, longer than mesoscutellum; propodeum with long dorsal surface and a pair of recumbent teeth present, almost meeting together, dorsal posterolateral angles bluntly angulate, lateral surfaces abruptly declivous and posterior surface rounded. Hind coxa with dorsobasal carina; tarsal claws without inner tooth. Metasoma smooth.

Male. Clypeal apex not thickened; scapal basin flat, cross-ridged, median longitudinal smooth strip present; malar sulcus present; occipital carina absent (Fig. 9C); eye setose; antenna elongate, F3 2.3 × longer than wide. Mesosoma stout, dorsum punctate; pronotum with median groove and shallow pit before lateral lobe, 0.7–0.9 × as long as mesoscutum (Fig. 9E); median length of pronotum 0.4–0.5 × as long as combined length of mesoscutum, mesoscutellum and metanotum; mesoscutum with notauli; parapsidal line faintly indicated; mesopleuron without omaulus
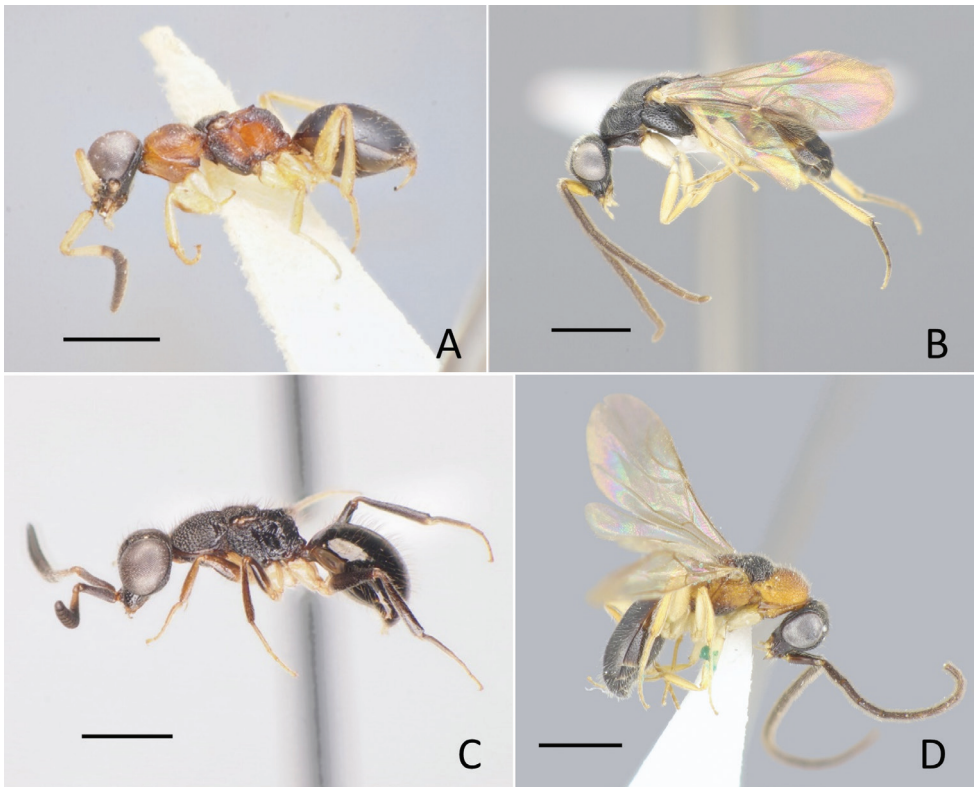
Figure 2. General habitus of Amiseginae **A** *Nipponosega yamanei* Kurzenko & Lelej, holotype ♀ **B** ditto, ♂ **C** *Okinawasega eguchii* Terayama ♀ **D** ditto, holotype ♂. Scale bars: 1.0 mm.
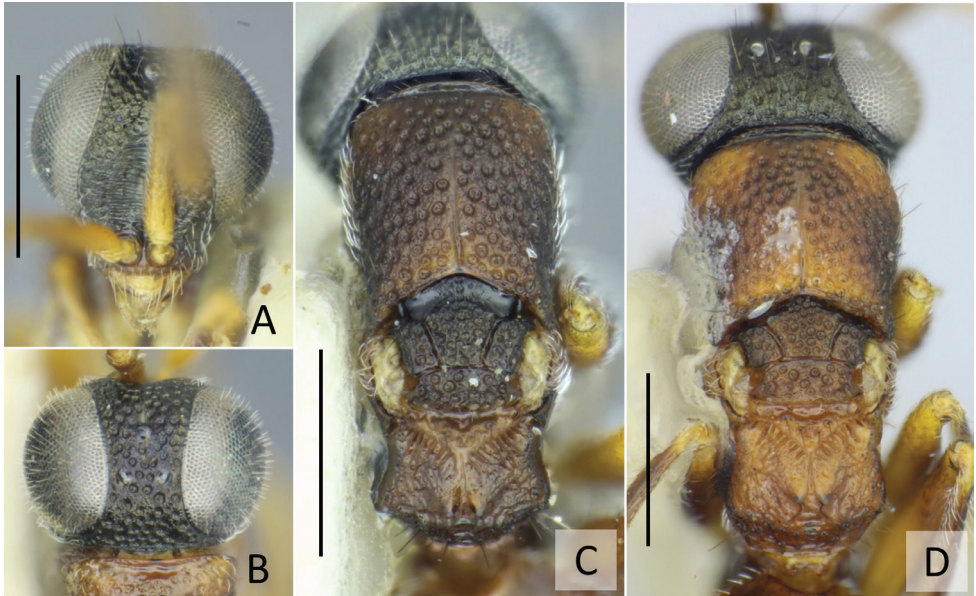
Figure 3. *Baeosega humida* Krombein ♀ **A** holotype of *B. humida*, head in frontal view **B** ditto, dorsal view **C** ditto, mesosoma **D** holotype of *B. laticeps*, mesosoma. Scale bars: 0.5 mm.
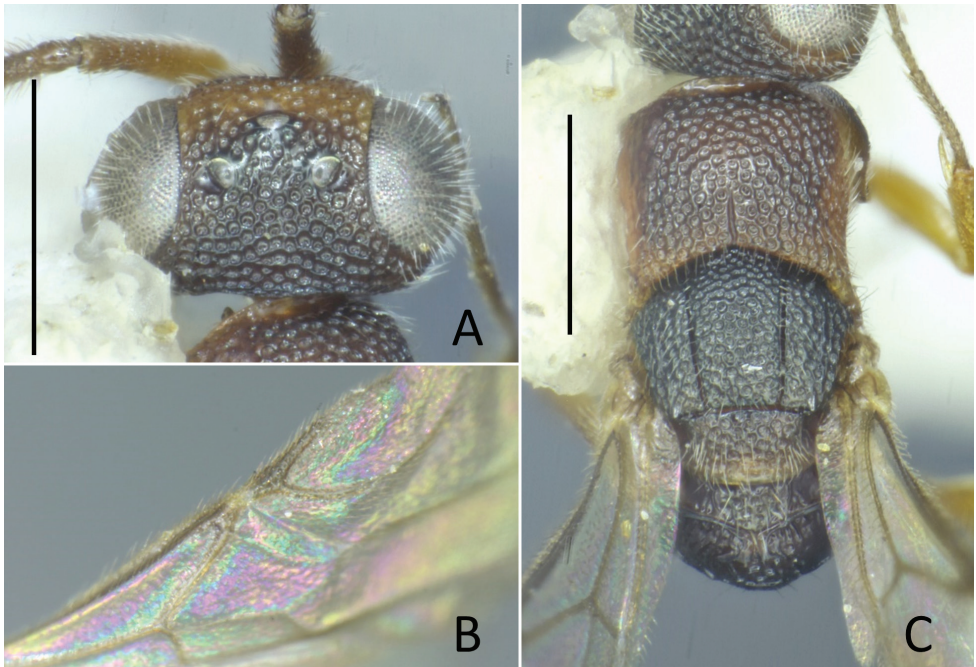
Figure 4. *Baeosega humida* Krombein, allotype ♂ **A** head in dorsal view **B** forewing **C** mesosoma. Scale bars: 0.5 mm.
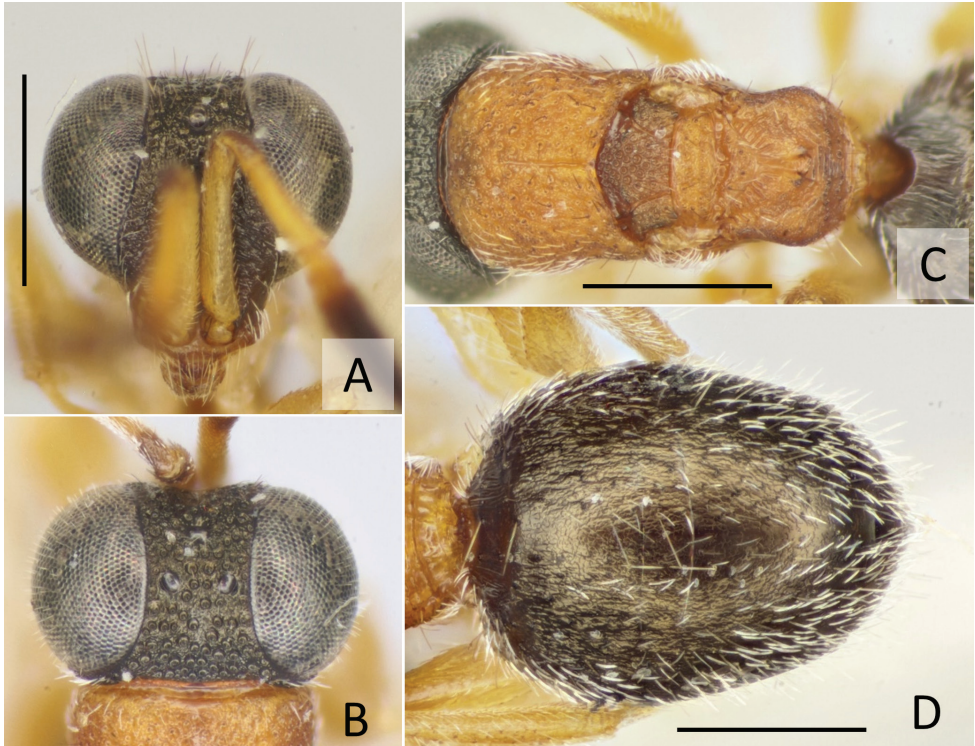
Figure 5. *Baeosega torrida* Krombein, holotype ♀ **A** head in frontal view **B** ditto, dorsal view **C** mesosoma **D** metasoma. Scale bars: 0.5 mm.

and scrobal sulcus; metanotum ca. 0.6 × as long as mesoscutellum; a pair of recumbent teeth present, slightly separated each other; propodeum with dorsal posterolateral angles rounded, posterior surface abruptly declivous; fully winged (Fig. 2B), R1 tubular, thick (Fig. 9D), not clearly differentiated from pterostigma; Rs extended by weakly curved dark streak; medial vein arising at or before cu-a. Hind coxa with dorsobasal carina; tarsal claws with one small inner tooth. Metasoma punctate with smooth interspaces.

Distribution. Palaearctic region: Japan (Honshu, Shikoku, Kyushu, northern Ryukyus); Oriental region: China (Zhejiang); Thailand.

Hosts. *Micadina phluctainoides* (Rehn, 1904) (Diapheromeridae) is considered to be the host of *Nipponosega yamanei* in Japan (Mita 2014).

Nipponosega kurzenkoi Xu, He & Terayama, 2003

Nipponosega kurzenkoi Xu, He & Terayama, 2003: 195, holotype ♀ by original designation. Type locality: Mt. Jiulong, Suichang, Zhejiang Province, China (Type no.
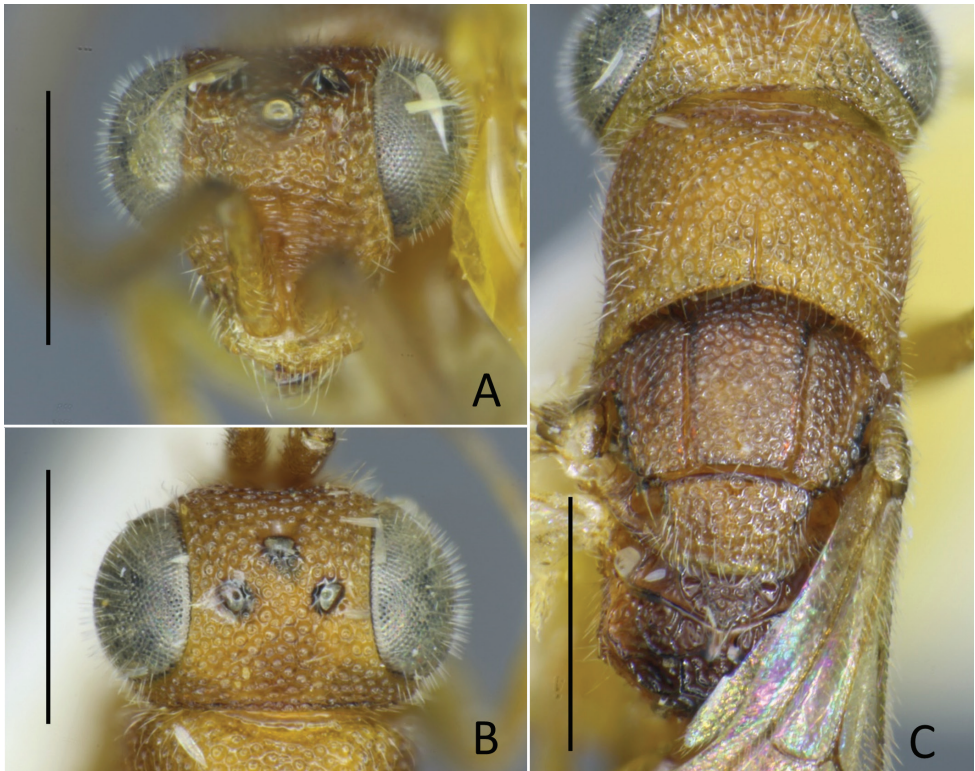
Figure 6. *Baeosega torrida* Krombein ♂ **A** head in frontal view, paratype **B** ditto, dorsal view, allotype **C** ditto, mesosoma. Scale bars: 0.5 mm.

944347, no type depository information, but likely Zhejiang University, Hangzhou). Not examined.

Diagnosis. *Nipponosega kurzenkoi* is closely related to *N. yamanei* from Japan. It can be distinguished from *N. yamanei* by the fully testaceous mesopleuron, whereas it is blackish in *N. yamanei* (Fig. 2A). Also, the frons is wider than in *N. yamanei*. The maximum interocular distance (measured at the lower end of the face) is 1.2 × longer than the width of frons (1.5–2.0 in *N. yamanei*). Other diagnostic characters are as follows: body length 3.0 mm; head black, smooth with scattered punctures; lateral ocelli well separated from the inner margin of eye; mesosoma largely testaceous with mesoscutum and mesoscutellum black; pronotum smooth with scattered punctures; legs yellow; metasoma dark brown. Male is unknown.

Distribution. China (Zhejiang).

Remarks. Although the body color could be variable to some extent, no specimen of *N. yamanei* with completely testaceous mesopleuron has been found; a closely related species showing different distribution. The morphology of *N. kurzenkoi* should be evaluated

in more detail to discuss their identification. However, diagnostic characters shown above do not overlap with those of *N. yamanei*. In the original description of *N. kurzenkoi* Xu et al., 2003, the evaluation of POD is different from the POD (= POL herein) used in Nagase (1995). The POD *sensu* Xu et al. (2003) is correspond to OOL herein.

Nipponosega lineata, sp. nov.

http://zoobank.org/F30DAD50-8FC6-4A01-A304-8240DD8EC4F5

Figures 1D, 7

Specimen examined. *Holotype*. THAILAND ♀ (THNHM-I-23985), "[NW Thailand] / Tak prov., / Umphang WS, / nr Pha Lueat stn.", "28. i 2015 / Sk. Yamane leg. / 390 m alt.; leaf /& surface soil", "Sk Yamane Collection" (THNHM).

Diagnosis. *Nipponosega lineata* sp. nov. is readily distinguished from other *Nipponosega* species by the longitudinally costate pronotum (Fig. 7D). Other characters useful to distinguish from other species are as follows: body length 2.8 mm; head black, punctate with interspaces smooth, posterior margin of vertex longitudinally costate (Fig. 7D); maximum interocular distance 2.9 × longer than width of frons; lateral ocelli almost touching the inner margin of eye; malar sulcus indicated as a faint track (Fig. 7C); outer orbit of eye with a row of punctures; occipital carina present (Fig. 7B, D), reaching lower gena; antenna blackish with scape and F1 testaceous; mesosoma reddish but dorsum largely black; mesoscutum and mesoscutellum punctate; legs brownish; metasoma dark brown, smooth. Male is unknown.

Description. *Holotype* female. Body length 2.81 mm. Head (Fig. 7A–C) punctate except scapal basin and posterior margin of vertex, as long as wide in dorsal view, 0.82 × as wide as deep in frontal view; punctures 0.5–1.0 × MOD, 0.5–2.0, 2.0–3.0, and, 0.5–1.0 punctures diameter apart on frons, ocellar region and vertex, respectively; interspaces among punctures smooth; scapal basin moderately excavated, transversely costate by fine grooves, upper part with short median unsculptured line; malar sulcus indicated as faint track; frons narrow, shortest distance between eyes 0.23 × head width; maximum interocular distance 2.9 × as long as narrowest width of frons; MS 0.23 × as long as eye height; outer orbit of eye with a row of deep punctures; ocellar triangle acute, lateral ocelli almost touching inner margin of eye; OL 1.3, OPL 2.2, POL 1.0, OOL 0.2, MOD 0.3; posterior margin of vertex longitudinally costate; occipital carina present, reaching gena. Clypeus thickened. Mandible without inner tooth, cylindrical. Antenna stout, F4–F9 wider than long; length (width) of F1 to F4 following ratio: 5.8 (1.5): 1.8 (1.7): 1.8 (1.8): 1.5 (2.0).

Pronotum (Fig. 7D) longitudinally costate by fine grooves except anterior narrow region smooth with several punctures; medial longitudinal line reaching 3/4 of pronotum; length of pronotum measured mesad 0.89 × as long as wide, 1.6 × mesoscutum plus mesoscutellum. Mesoscutum roughly punctate-reticulate: punctures as long as or slightly smaller than MOD; notauli complete, diverging anteriorly.
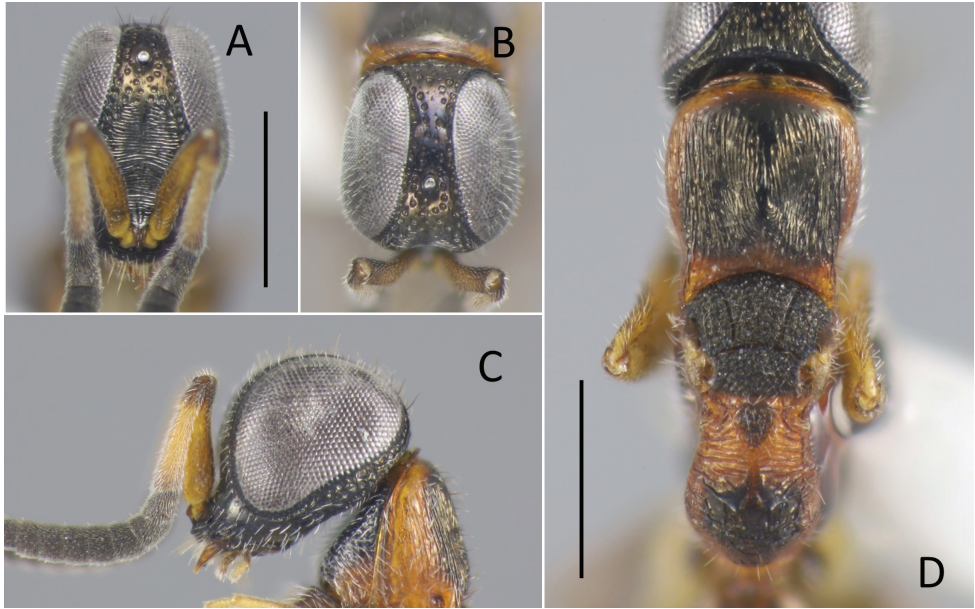
Figure 7. *Nipponosega lineata* sp. nov., holotype ♀ **A** head in frontal view **B** ditto, dorsal view **C** ditto, lateral view **D** vertex and mesosoma. Scale bars: 0.5 mm.

Mesoscutellum punctate as mesoscutum, 0.59 × longer than mesoscutum. Mesopleuron punctate with smooth interspaces: punctures as long as MOD. Metanotum triangular, as long as mesoscutellum mesad, punctate. Propodeum (Fig. 7D) with postero-lateral corner rounded; dorsal surface long, smooth, transversely rugose; posterior surface transversely rugose; lateral surface obliquely rugose; metapleural region smooth but behind meso-metapleural suture costate. Middle and hind coxae transversely costate.

Metasoma smooth, covered with sparse setae; setae 2.5 × MOD.

Color. Head black. Antenna basally testaceous with distal apex of scape and pedicel dark brown, F2–F10 black. Mandible brown. Mesosoma reddish but following parts blackish: dorsal surface of pronotum, anterior 2/3 of propleuron, mesoscutum, mesoscutellum, ventral surface of mesepisternum, median enclosure of metanotum, postero-dorsal surface of propodeum. Tegula and wings brown. Coxae whitish with postero-dorsal dark spot; trochanters testaceous; fore femur brown with basal and distal parts testaceous; middle and hind femora brown with basal parts testaceous; tibiae brown with basal parts of fore and hind tibiae testaceous; tarsi testaceous with fore and hind tarsi basally brownish. Metasoma dark brown with anterior surface of T1 and S1 paler.

Distribution. Thailand (Tak Province).

Etymology. The specific name derives from the Latin word *lineata*, referring to the presence of striae on the pronotum.

Remarks. The holotype was collected from the leaf litter.

Nipponosega yamanei Kurzenko & Lelej, 1994
Figures 2A, B, 8, 9

Nipponosega yamanei Kurzenko & Lelej, 1994: 83, holotype ♀ by original designation.
Type locality: Shishitsuka Ohike, Tsuchiura City, Ibaraki Pref., Honshu (Japan).
Nipponosega kantoensis Nagase, 1995: 104, holotype ♀ by original designation, new synonymy. Type locality: Tonbo-Park, Sueno, Yoriimachi, Saitama Pref., Honshu (Japan).

Specimens examined. *Holotypes. Nipponosega yamanei*: JAPAN – **Honshu** ♀, "JAPAN Ibaraki-ken / Shishitsuka Ohike / Tsuchiura City / Lelej 17 viii 1993", "NSMT-HYM / 62329", "Holotypus ♀ / *Nipponosega* / *yamanei* / Kurzenko et Lelej"(NSMT); ***Nipponosega kantoensis***: JAPAN ♀, "Tonbo-Park / Sueno, Yorii / Saitama / 11. VIII. 1991 / T. Nambu leg", "NSMT-HYM / 62328", "HOLOTYPE / *Nipponosega* / *kantoensis* / H. Nagase 1995"(NSMT).

Other materials. JAPAN – **Honshu** 1♀2♂, Ogawa (600–800 m alt.), Kitaibaraki, Ibaraki Pref., 14–28.VIII.2002, MsT, H. Goto et al. leg. (ELKU); 1♂, same data, but (FFPRI); 3♀, Okami, Satomi-mura, Ibaraki Pref., 9–24.IX.2003, MsT, S. Makino et al. leg. (FFPRI); 1♀, Fujisawa-shi, Kanagawa Pref., 24–25.IX.2009, pit fall trap, T. Shimada leg. (ELKU); 1♂, Yawata (650 m alt.), Asahi, Aichi Pref., 29.VII–11.VIII.1998, MsT, A. Hanai, K. Yamagishi leg. (ELMU); 1♀, Yawata Shrine (400 m alt.), Asahi, Aichi Pref., 12–21.VIII.1998, MsT, M. Ozawa leg. (ELMU); 1♀, Kurisu, Inuyama, Aichi Pref., 19–25.VII.1996, EmT, T. Mabuchi leg.; 1♀, Mt. Sanage, Aichi Pref., 7–13. VIII.1992, EmT, K. Shima leg. (ELMU); 2♂, Takiwaki, Toyota, Aichi Pref., 8–14.
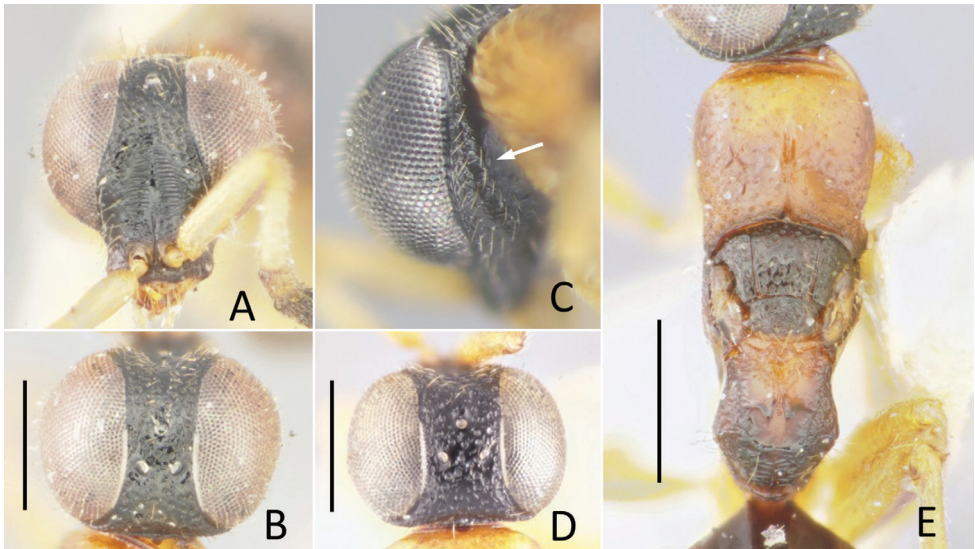
Figure 8. *Nipponosega yamanei* Kurzenko & Lelej ♀ **A** holotype of *N. yamanei*, head in frontal view **B** ditto, dorsal view **C** female from Aichi, gena (arrow indicates occipital carina) **D** holotype of *N. kantoensis* Nagase, head in dorsal view **E** holotype of *N. yamanei*, mesosoma. Scale bars: 0.5 mm.

VII.2002, MsT, Y. Kurahashi Leg. (ELMU); 1♀, same data, but 19–25.VIII.2002; 1♀, Tougoku, Seto, Aichi Pref., 10–16.VIII.1997, MsT, M. Kenmotsu leg. (ELMU); 1♀, Kurotani, Y., Hiroshima Pref., 7–13.VIII.1995, YPT, A. Morimoto leg. (ELMU); – **Shikoku** 1♀, Mt. Takanawa, Matsuyama, Ehime Pref., 26.VII.2017, K. Kuroda leg. (ELKU); 1♀, Jikiba-machi, Matsuyama-shi, Ehime Pref., 25.VII.2017, shifting, Y. Hisasue leg. (ELKU); – **Kyushu** 1♀, Mt. Kaya, Itoshima-shi, Fukuoka Pref., 2.X.2018, shifting, S. Inoue leg. (ELKU); 1♀, same locality as above, but Mt. Iwara, 8.IX.2019, K. Nishiya leg. (ELKU); 1♀, Hikosan Biological Laboratory, Kyushu University, Mt. Hiko (670 m alt.), Fukuoka Pref., 2.X.1968, MsT, K. Takeno leg.; 1♀, same data but 28–29.IX.1968; 1♀, same data but 15.X.1968; 1♂, same data but 4.IX.1970; 1♀, Mt. Hiko (700 m alt.), Fukuoka Pref., 20–28.VIII.2008, MsT, T. Mita, S. Sato leg. (ELKU); 1♀, Gokasho Plateau (860 m alt.), Takachiho-cho, Miyazaki Pref., 22.VIII.2015, Sk. Yamane leg. (ELKU); 2♀, same data but 23.VIII.2015; 1♀, Mt. Tatera, Tsushima Isl., Nagasaki Pref., 25–26. IX. 2015, YPT, Y. Hisasue leg. (ELKU); 1♀, same as above, but Mt. Shimizu, Izuhara-machi, 19.X.2019, T. Hashizume leg. (ELKU); – **Ryukyus** 2♀, Kurio, Yakushima Isl., 13.VII.1970, K. Yamagishi leg. (ELMU); 1♂, same island, but Miyanoura, 21.VI–11.VII.1999, MsT, T. Murota (A. Hanai) leg. (ELMU).

Diagnosis. In the genus *Nipponosega*, *N. yamanei* Kurzenko & Lelej is the only species known by both female and male. The female is similar to *N. kurzenkoi* in China. They can be distinguished by the body coloration and the width of frons. The mesopleuron is blackish in *N. yamanei* (Fig. 2A), whereas it is fully testaceous in *N. kurzenkoi*. The frons is narrower, the maximum interocular distance is 1.5–2.0 × longer than the width of frons in full face view (1.2 in *N. kurzenkoi*). Other diagnostic characters of the female are as follows: body length 2.5–3.9 mm; head black, smooth with scattered punctures; posterior ocelli well separated from the inner margin of eye; pronotum reddish, smooth with scattered punctures; mesoscutum, mesoscutellum, anterior part of mesepisternum and often propodeum black; legs yellow; metasoma dark brown. The body length of the male is 3.2–3.8 mm. The male of other species of *Nipponosega* is unknown. Compared to other genera found in Japan, the male of *N. yamanei* can be distinguished by the head without occipital carina and impunctate welt; the body black, without metallic reflection; and the forewing with R1 thick, not clearly separated from pterostigma.

Description. Female. Body length 2.5–3.9 mm. Head (Fig. 8A–D) punctate except scapal basin, 0.65–0.81 × as long as wide in dorsal view, 0.89–1.18 × as wide as deep in frontal view; punctures 0.3–0.5 × diameter of median ocellus, 0.3–1.0 punctures diameter apart on frons, 1.0–3.0 punctures diameter apart on ocellar region and vertex; interspaces among punctures smooth; scapal basin moderately excavated to almost flat, transversely costate by fine grooves, with median unsculptured line; malar sulcus absent; narrowest width of frons 0.24–0.33 × head width; maximum interocular distance 1.5–2.0 × as long as narrowest width of frons; MS 0.24–0.34 × as long as eye height; ocellar triangle variable, OL 0.7–1.6 × as long as POL, OL 0.8–1.2, OPL 2.0–2.5, POL 0.5–1.0, OOL 0.3–0.6, MOD 0.4–0.5; occipital carina present, reaching lower gena (Fig. 8C), occasionally present only behind ocellar triangle, only upper gena, or rarely

almost invisible. Clypeus not thickened, with thin square transparent lobe. Mandible without inner tooth. Antenna stout, F2–F7 wider than long; length (width) of F1–F4 following ratio: 2.7–3.2 (1.0–1.2): 0.7–1.0 (1.0–1.3): 0.9–1.0 (1.1–1.3): 1.0 (1.1–1.4).

Pronotum (Fig. 8E) punctate with faintly coriaceous interspace; punctures slightly smaller than those on frons, 0.3–0.4 MOD, 3–5 PD apart; medial longitudinal line reaching 2/3 of pronotum, rarely groove fully developed; median length of pronotum 0.72–0.86 × as long as wide, 1.2–1.6 × mesoscutum plus mesoscutellum. Mesoscutum 0.43–0.50 × longer than pronotum, sculptured as vertex; notauli complete, diverging anteriorly. Mesoscutellum 0.5–0.75 × longer than mesoscutum, punctate as mesoscutum with interspaces faintly transversely rugulose. Mesopleuron sculptured as pronotum. Metanotum triangular, median length 0.67–0.87 × mesoscutellum, with shallow punctures. Propodeum with postero-lateral corner forming blunt angle (Fig. 8E), angle sometimes weak; dorsal surface of propodeum short, medially smooth, laterally rugose, sometimes irregularly reticulate; transverse or arched carina present behind; sometimes lateral carina present; posterior surface transversely costate with median longitudinal carina, sometimes laterally reticulate; lateral surface faintly costate with carinae anterodorsally effaced; metapleural region polished or faintly transversely rugose. Middle and hind coxae transversely costate.

Metasoma faintly coriaceous, sparsely covered with setae; length of setae 2 MOD.

Color. Head black. Antenna basally testaceous, F2–F10 dark brown, sometimes dorsal half of F2 testaceous. Mandible testaceous with reddish teeth. Mesosoma with prothorax, posterior half of mesopleuron and lateral surface of propodeum reddish to light brownish, remainder of mesothorax, metanotum and dorsal to posterior surface of propodeum brownish to blackish; dorsum of pronotum blackish in the female from Mt. Takanawa (Ehime Pref.); metanotum and propodeum sometimes paler especially in smaller specimens. Tegulae and wings testaceous to brown. Legs testaceous, sometimes femora and tibiae brownish. Metasoma brown to dark brown, rarely blackish, usually anterior surface of T1 and sterna paler.

Male. Body length 3.2–3.8 mm. Head (Fig. 9A–C) densely punctate except scapal basin, 0.5–0.57 × as long as wide in dorsal view, 1.16–1.46 × as wide as deep in frontal view; punctures 0.2–0.3 MOD, almost contiguous to 0.3 puncture diameter apart each; scapal basin excavated, transversely rugose with median unsculptured line; MS 0.3–0.4 × as long as eye height; narrowest width of frons 0.6–0.7 × head width; ocellar triangle obtuse, OL 0.5–0.6 × as long as POL, OL 0.8, OPL 2.0–2.8, POL 1.5, OOL 0.5–0.6, MOD 0.8–1.0. Clypeus not thickened, with thin transparent lamella. Mandible distally truncate. Antenna cylindrical, flagellum densely covered with setae; length of setae ca. 0.6 × flagellomere diameter; length (width) of F1 to F4 following ratio: 3.3–4.0 (0.8–1.0): 1.8–2.5 (0.8–1.1): 1.8–2.3 (0.8–1.0): 1.8–2.0 (0.8–1.0).

Pronotum (Fig. 9E) densely punctate as vertex; medial longitudinal groove present on posterior 3/5; median length of pronotum 0.46–0.58 × as long as wide, 0.7–0.9 × mesoscutum. Mesoscutum densely punctate as vertex; on posterior half interspaces faintly granulate; notauli complete, diverging anteriorly. Mesoscutellum punctate as mesoscutum, 0.45–0.63 × longer than mesoscutum. Mesopleuron punctate with
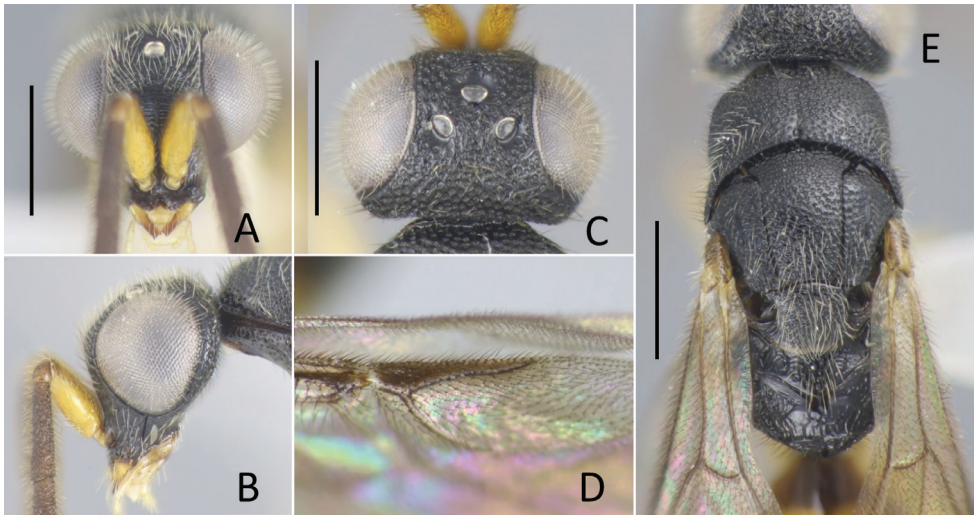
Figure 9. *Nipponosega yamanei* Kurzenko & Lelej ♂ **A** Head in frontal view **B** ditto, lateral view **C** ditto, dorsal view **D** forewing, pterostigma and R1 **E** mesosoma. Scale bars: 0.5 mm.

polished interspaces; punctures slightly larger than those on pronotum, 0.3–1.5 puncture diameter apart; surface near pleural suture polished, without puncture. Metanotum with sparse punctures, median length 0.52–0.68 × mesoscutellum; punctures 1–3 puncture diameter apart. Propodeum postero-laterally forming dully corner, without teeth or distinct angle; dorsal surface more or less rugose, sometimes only median longitudinal carina present; transverse carina present between dorsal and posterior surface; posterior surface finely reticulate rugose with median longitudinal carina; lateral surface with ventral 2/3 finely reticulate, dorsal 1/3 smooth; metapleural region polished, more or less rugose and longitudinally excavated behind pleural suture. R1 tubular, thick, not clearly distinguished from pterostigma (Fig. 9D); Rs extended by weakly curved dark streak; medial vein arising at or before cu-a. Legs with surface of coxae smooth; hind coxa with dorsobasal carina; tarsal claws with one small inner tooth.

Dorsal surface of terga and sterna with fine punctures; punctures on T1 and T2 1–2 puncture diameters apart, with interspaces polished.

Color. Head, mesosoma and metasoma black but anterior polished surface of T1 brownish, lateral surface of T1, T2 brown. Antenna with scape testaceous, flagellomere dark brown to brown, distally slightly paler. Mandible testaceous with apex reddish. Maxillary and labial palpus testaceous. Tegula brown. Wings faintly tinged with brown; veins brown. Legs testaceous with hind tibia dark brown.

Distribution. Japan (Honshu; Shikoku; Kyushu; Tsushima Isl.; Yakushima Isl.).

Hosts. Diapheromeridae: *Micadina phluctainoides* (Rehn, 1904).

Remarks. Although ocelli and head proportions of the female have been considered useful for species classification (Nagase 1995), they actually show great variation. The holotypes of *N. yamanei* (Fig. 8B) and *N. kantoensis* (Fig. 8D) are examples of the two extremes and intermediate females are more frequently found. This makes it difficult to distinguish between the two types.

Males of *N. yamanei* were only obtained by Malaise traps and occasionally they were collected together with *Cladobethylus japonicus* Kimsey, 1997. The males of both species have been unknown; however, the morphological characters of the trapped males were close to those of *Baeosega*. As *Cladobethylus* is a genus showing little sexual dimorphism (Kimsey 2019), they are considered as *Nipponosega*. Compared to the abundance of the female, the male of *N. yamanei* is rarely collected. Some females were found above the ground surface (1 m or more) (Nagase 1995; Tomura 2020), but in fact they are more likely on the ground floor or in the leaf litter. Multiple females were obtained in Malaise traps, suggesting that females actively walk around the forest floor and climb understory vegetation. Females were observed to carry the host eggs for oviposition (Y. Hisaue, personal communication).

Genus *Okinawasega* Terayama

Okinawasega Terayama, 1999: 99. Type species: *Okinawasega eguchii* Terayama, 1999, original designation.

Diagnosis. General characters of *Okinawasega* are similar to those of *Baeosega* and *Nipponosega*; however, there are some distinctive differences, e.g., the deep malar sulcus in the female, the elongated linear R1 in the male. For more details, see the diagnosis of *Baeosega*.

Description. Female. Clypeal apex not thickened; malar sulcus present (Fig. 10D); scapal basin shallow, cross-ridged, median longitudinal carina present; occipital carina absent but posterior margin of vertex forming distinct corner behind ocellar triangle; eye setose; flagellum fusiform, intermediate segments broader than long, and with ventral surface flattened. Mesosoma slender, punctate by dense punctures; pronotum with median groove and shallow pit before lateral lobe, as long as combined length of mesoscutum, mesoscutellum and metanotum; mesoscutum with notauli and without parapsides; posterolateral corner of mesoscutum not lobate; micropterous (Fig. 2C), forewing pads extending to posterior margin of mesoscutellum; mesopleuron with omaulus, without scrobal sulcus; metanotum triangular and small, slightly shorter than mesoscutellum; propodeum with long dorsal surface and a pair of recumbent teeth present, almost meeting together, dorsal posterolateral angles bluntly angulate, lateral and posterior surfaces abruptly declivous. Hind coxa with dorsobasal carina; tarsal claws without inner tooth. Metasoma smooth.

Male. Clypeal apex not thickened; scapal basin flat or weakly excavated, cross-ridged; malar sulcus present; occipital carina absent but posterior corner of vertex forming distinct corner behind ocellar triangle, occasionally trace of occipital carina present on upper gena; eye setose; antenna elongate, F3 3.5–4.3 × longer than wide. Mesosoma slender, dorsum punctate by dense punctures; pronotum with median groove and shallow pit before lateral lobe; pronotum as long as mesoscutum, 2/3 of combined length of mesoscutum, mesoscutellum; mesoscutum with notauli; parapsidal line faintly indicated; mesopleuron without omaulus and scrobal sulcus; metanotum approximately
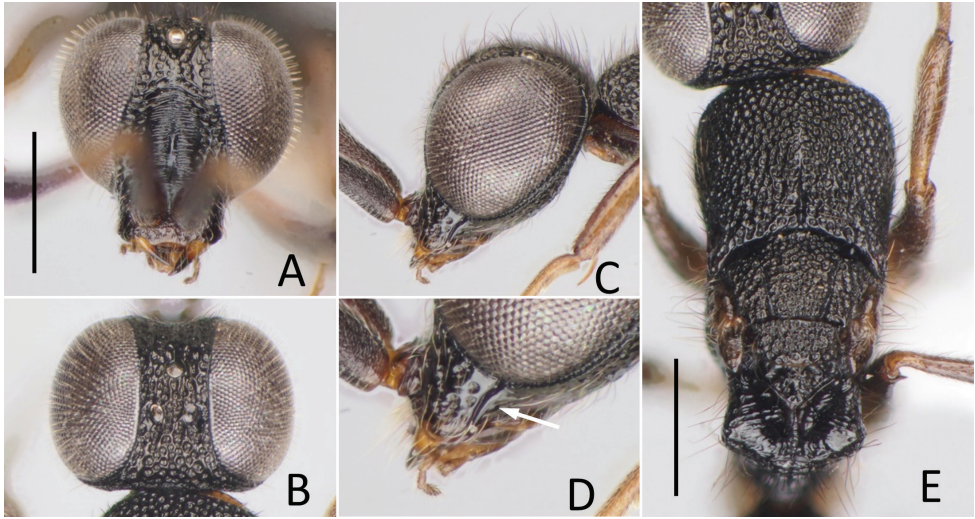
Figure 10. *Okinawasega eguchii* Terayama ♀ **A** head in frontal view **B** ditto, dorsal view **C** ditto, lateral view **D** ditto, malar space (arrow indicates malar sulcus) **E** mesosoma. Scale bars: 0.5 mm.

half mesoscutellum (Fig. 11E); a pair of recumbent teeth present, meeting or almost meeting together; propodeum with dorsal posterolateral angles bluntly angulate, posterior surface abruptly declivous; fully winged (Fig. 2D), pterostigma normal, with linear extension of R1 indicated, long (Fig. 11D, arrow); Rs extended by weakly curved dark streak; medial vein arising before cu-a. Hind coxa with dorsobasal carina; tarsal claws without inner tooth. Metasoma sparsely punctate with smooth interspaces.

Distribution. Oriental region: Japan (Yaeyama Islands, southern Ryukyus).

Hosts. Unknown.

Remarks. The previous record of *Baeosega* in southern Ryukyus (Kimsey 1995) should probably be attributed to *Okinawasega*.

Okinawasega eguchii Terayama, 1999
Figures 2C, D, 10, 11

Okinawasega eguchii Terayama, 1999: 100, holotype ♂, original designation. Type locality: Iriomote Island, Ryukyus, Japan.

Specimens examined. *Holotype.* Japan – **Ryukyus** ♂, "Holotype", "*Okinawasega eguchii* Terayama, 1999", "Genotype *Okinawasega* Terayama, 1999", "Iriomote-jima, Yaeyama Is., Okinawa Pref.", "Japan", "1. XI. 1995, K. Eguchi leg.", "951101, Iriomote Is., Q1" (NMHAH).

Other materials. Japan – **Ryukyus** 1♂, Shiramizu, Ishigaki Isl., 9.V.2004, T. Mita leg. (ELKU); 7♂, same data, but 10.V.2004 (ELKU); 4♂, same as above,
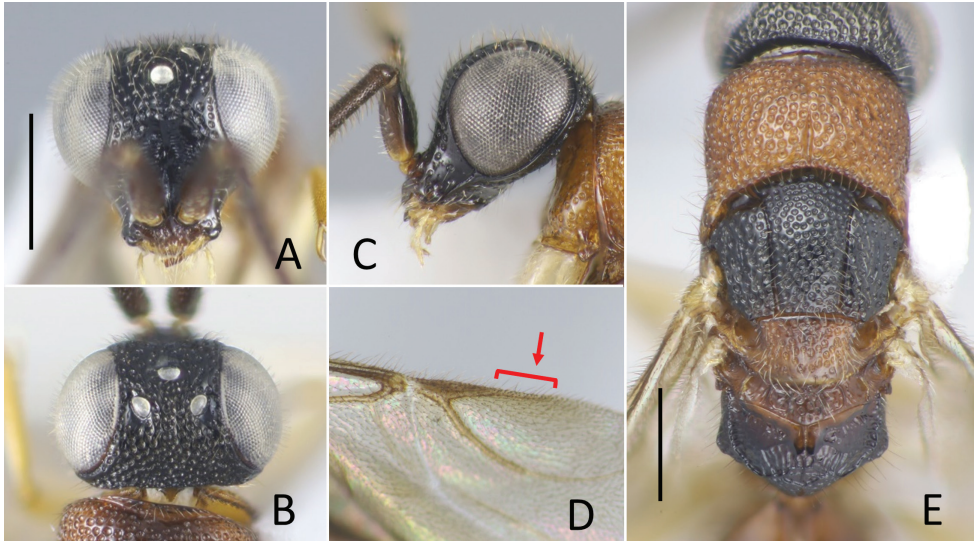
Figure 11. *Okinawasega eguchii* Terayama ♂ **A** head in frontal view **B** ditto, dorsal view **C** ditto, lateral view **D** forewing **E** mesosoma. Scale bars: 0.5 mm.

but Mt. Omoto-dake, 15.V.2004, T. Tsuru leg. (ELKU); 3♂, Aira-gawa, Iriomote Isl., 8–12.X.2004, FIT, T. Ishikawa leg. (ELKU); 1♂, same data, but 14.V.2014, T. Mita leg. (ELKU); 17♂, same data, but 24–26.VI.2016, YPT, K. Komeda leg. (ELKU); 1♀24♂, same data, but 22–25.VI.2016 (ELKU); 1♀, same data, but 4.VII.2017, T. Kawano leg. (ELKU); 1♀, same island, but Mt. Tedou, 3.X.2017, K. Narita leg. (ELKU).

Diagnosis. Conspicuous species in the southern Ryukyus (Japan). The female is blackish and covered with long setae, the body length is 3.5–3.6 mm. The male has long antennae and reddish body, the body length is 3.2–3.8 mm.

Description. Female. Body length 3.5–3.6 mm. Head (Fig. 10A–D) densely punctate except scapal basin, 0.65–0.70 × as long as wide in dorsal view, 0.95–1.00 × as wide as deep in frontal view; punctures 0.3 MOD, almost contiguous but part of frons 1.0 puncture diameter apart each; scapal basin weakly excavated, transversely costate by fine grooves, with median unsculptured line; interspaces among punctures smooth; malar sulcus present (Fig. 10D); narrowest width of frons 0.3 × head width; MS 0.3 × as long as eye height; ocellar triangle acute, OL 1.0–1.2, OPL 2.3, POL 0.8–0.9, OOL 0.4–0.5, MOD 0.5–0.7; occipital carina absent but posterior margin of vertex forming distinct corner behind ocellar triangle. Clypeus not distinctly thickened, with thin square transparent lobe. Mandible without inner tooth. Antenna stout, F2–F9 wider than long; length (width) of F1 to F4 following ratio: 2.6–2.7 (1.1–1.2): 1.0 (1.3–1.4): 1.0 (1.4–1.5): 1.0 (1.5–1.7).

Pronotum (Fig. 10E) covered with densely located punctures, punctures same with those on head in size but deeper, slightly smaller mesad, somewhat longitudinally contiguous; medial longitudinal groove present on posterior 1/3 but polished strip

leaching ca. 2/3; length of pronotum mesad 0.7–0.8 × as long as wide, 1.1–1.3 × mesoscutum plus mesoscutellum. Mesoscutum roughly puncto-reticulate, punctures 0.7 × larger than those on pronotum; notauli complete, diverging anteriorly. Mesoscutellum punctate as mesoscutum, 0.5–0.6 × longer than mesoscutum. Mesopleuron densely punctate; punctures larger, 0.7 MOD. Metanotum triangular, 0.7–0.9 × mesoscutellum mesad, punctate by shallow punctures. Propodeum with dorsal, posterior and lateral surface transversely rugose by obscure striae; median longitudinal carina present; metapleural region polished, finely rugose behind meso-metapleural suture, carinated above metacoxa; postero-lateral corner forming dully angle.

Metasoma smooth, sparsely covered with long setae; setae 3 × longer than MOD.

Color. Head, mesosoma and metasoma black but lateral surface of T1 brown, S1 dark brown. Antenna black but scape dark brown, pedicel and F1 brown. Mandible pale brown with apex black. Maxillary and labial palpi brown. Tegula and wings dark brown. Coxae and trochanters testaceous; remainder of fore and middle legs brown; remainder of hind leg dark brown.

Male. Body length 3.6–3.7 mm. Head (Fig. 11A–C) densely punctate except scapal basin, 0.59–0.66 × as long as wide in dorsal view, 1.14–1.21 × as wide as deep in frontal view; punctures 0.2–0.3 MOD, interspaces ca. 0.3–1.0 puncture diameter; scapal basin faintly excavated, transversely rugose with median unsculptured line; MS 0.4–0.5 × as long as eye height; narrowest width of frons 0.63–0.76 × head width; ocellar triangle obtuse, OL 0.8–1.0, OPL 2.3–3.0, POL 1.3–1.5, OOL 0.05, MOD 0.8; occipital carina absent but posterior corner of vertex forming distinct corner behind ocellar triangle, occasionally trace of occipital carina present on upper gena. Clypeus thin. Mandible distally truncate. Antenna cylindrical, flagellum densely covered with long setae; length of setae ca. 0.8 × flagellomere diameter; length (width) of F1 to F4 following ratio: 4.3–4.7 (0.7–1.0): 3.0 (0.7–1.0): 3.0 (0.7–0.8): 2.8–3.0 (0.7–0.8).

Pronotum (Fig. 11E) punctate as vertex; medial longitudinal groove variable, present posterior 1/3 to reaching anterior margin of disc; length of pronotum mesad 0.7–0.8 × as long as wide, 0.9–1.1 × mesoscutum. Mesoscutum punctate as head, but punctures slightly smaller than those on vertex, 0.2–0.5 puncture diameter apart; notauli complete, diverging anteriorly. Mesoscutellum scattered with shallow punctures with polished interspace, 0.50–0.58 × longer than mesoscutum. Mesopleuron punctate with polished interspace; punctures slightly larger than those on pronotum, 0.3–1.0 puncture diameter apart; subalar fossa indicated by continuous row of punctures or groove, rarely absent; usually surface near pleural suture polished, without punctures. Metanotum 0.48–0.60 × mesoscutellum, punctate as mesoscutellum. Propodeum (Fig. 11E) postero-laterally forming dull corner; dorsal surface reticulate-rugose with median and usually two pairs of longitudinal carinae present; transverse carina present between dorsal and posterior surface; posterior and lateral surface reticulate-rugose; median longitudinal carina present on posterior surface; metapleural region polished, more or less rugose and longitudinally excavated behind meso-metapleural suture, carinated above hind coxa. Pterostigma narrow, with linear

extension of R1 indicated, long (Fig. 11D, arrow); Rs extended by weakly curved dark streak; medial vein arising before cu-a. Hind coxa with dorsobasal carina; tarsal claws without inner tooth.

Color. Head black. Antenna dark brown, rarely blackish. Mandible testaceous with apex dark brown. Maxillary and labial palpus testaceous. Mesosoma mostly reddish to dark reddish except mesoscutum black, tegula brown, propodeum with posterior surface darker, rarely entirely blackish; rarely dorsum of mesosoma blackish. Wings faintly tinged with brown; veins brown, rarely dark brown. Legs testaceous. Metasoma blackish except anterior polished surface of T1 brownish.

Distribution. Japan: Yaeyama Islands, Southern Ryukyus (Ishigaki Isl., Iriomote Isl.)

Remarks. No species in *Baeosega*-related genera are known from Ishigaki-jima and Iriomote-jima except for the male of *Okinawasega eguchii* Terayama. The newly found female was clearly related to *Baeosega*, and was therefore assigned to *Okinawasega*. Compared to males, females are seldom collected. The females actively walk on the ground surface and sometimes leap a small distance.

Discussion

The discovery of previously unknown sexes of *Nipponosega* and *Okinawasega* revealed that the male morphology of the two genera and *Baeosega* is rather conservative, even though females show clear differences. Males share following features: the absence of the occipital carina; mesopleuron without omaulus and scrobal sulcus; the relatively shorter metanotum, which is 0.5–0.7 × as long as mesoscutellum; the tarsal claw without large inner tooth, at most one small tooth. As for the posterior margin of the head in females, an indistinct occipital carina is sometimes present behind the ocellar triangle in *Baeosega* and *Okinawasega*. However, the structure is not clearly cariniform. It is observed only as faintly suppressed posterior margin (Fig. 3C). The distinct occipital carina is present only in the female of *Nipponosega* (Figs 7D, 8C). In males, some genera have the forewing with R1 distinguishable from the distal part of pterostigma (e.g., *Imasega* Krombein and *Mahinda* Krombein). This linear extension of R1 is not indicated in *Baeosega* (Fig. 4B) and *Nipponosega* (Fig. 9D) but a long linear R1 is clearly indicated in *Okinawasega* (Fig. 11D). While further research is required, the R1 condition can be a diagnostic character of amisegine genera (Krombein 1983; Kimsey and Bohart 1991).

In *B. humida* and *N. yamanei*, the body proportions of females can vary within a species. Although only a few records on the host of Amiseginae are available, the adult body size of egg parasitoids is usually affected by the host, for example, the size and age of the host egg (Da Rocha et al. 2007). Additionally, discontinuous differences can be observed in egg parasitoids if they attack different host eggs, as is known in Scelionidae (Arakawa et al. 2004; Abram et al. 2016; Botch and Delfosse 2018). Further studies on their host and their life history will provide a clearer picture of the background of the host-dependent variation.

Acknowledgements

References

Abram PK, Parent J-P, Brodeur J, Boivin G (2016) Size-induced phenotypic reaction norms in a parasitoid wasp: an examination of life-history and behavioural traits. Biological Journal of the Linnean Society 117: 620–632. https://doi.org/10.1111/bij.12658

Arakawa R, Miura M, Fujita M (2004) Effects of host species on the body size, fecundity, and longevity of *Trissolcus mitsukurii* (Hymenoptera: Scelionidae), a solitary egg parasitoid of stink bugs. Applied Entomology and Zoology 39: 177–181. https://doi.org/10.1303/aez.2004.177

Botch PS, Delfosse ES (2018) Host-acceptance behavior of *Trissolcus japonicus* (Hymenoptera: Scelionidae) reared on the invasive *Halyomorpha halys* (Heteroptera: Pentatomidae) and non-target species. Environmental Entomology 47: 403–411. https://doi.org/10.1093/ee/nvy014

Da Rocha L, Kolberg R, de Mendonça MS, Redaelli LR (2007) Body size variation in *Gryon gallardoi* related to age and size of the host. BioControl 52: 161–173. https://doi.org/10.1007/s10526-006-9024-6

Kimsey LS (1986) New species and genera of Amiseginae from Asia (Chrysididae, Hymenoptera). Psyche 93: 153–165. https://doi.org/10.1155/1986/31631

Kimsey LS (1995) New amisegine wasps from Southeast Asia (Hymenoptera: Chrysididae). Entomological Society of Washington 97: 590–595.

Kimsey LS (2019) Revision of the south Asian amisegine genus *Cladobethylus* Kieffer, 1922 (Hymenoptera, Chrysididae, Amiseginae). Journal of Hymenoptera Research 70: 41–64. https://doi.org/10.3897/jhr.70.34206

Kimsey LS, Bohart RM (1991 [1990]) The chrysidid wasps of the world. Oxford Science Publications, New York, 652 pp.

Kimsey LS, Dewhurst CF, Nyaure S (2013) New species of egg parasites from the Oil Palm Stick Insect (*Eurycantha insularis*) in Papua New Guinea (Hymenoptera, Chrysididae,

Phasmatodea, Phasmatidae). Journal of Hymenoptera Research 30: 19–28. https://doi.org/10.3897/jhr.30.4010

Kimsey LS, Mita T, Pham HT (2016) New species of the genus *Mahinda* Krombein, 1983 (Hymenoptera, Chrysididae, Amiseginae). ZooKeys 551: 145–154. https://doi.org/10.3897/zookeys.551.6168

Krombein KV (1983) Biosystematic studies of Ceylonese wasps, XI: a monograph of the Amiseginae and Loboscelidiinae (Hymenoptera: Chrysididae). Journal of the Kansas Entomological Society (376): 1–79. https://doi.org/10.5479/si.00810282.376

Kurzenko NV, Lelej AS (1994) *Nipponosega yamanei* gen. et sp. nov., a new remarkable Cuckoo Wasp (Hymenoptera, Chrysididae, Amiseginae) from Japan. Bulletin of the National Science Museum. Series A, Zoology 20: 83–86.

Mita T (2014) Bees and wasps. In: Okajima S (Ed.) Pictorial book of Gakken, Live, Insects. Gakken Plus, Tokyo, 134–146. [in Japanese]

Nagase H (1995) A new species of *Nipponosega* (Hymenoptera, Chrysididae, Amiseginae) from central Japan. Bulletin of the National Science Museum. Series A, Zoology 21: 103–107.

Terayama M (1999) Descriptions of new species and genera of the Chrysidoidea (Insecta: Hymenoptera) from the Ryukyus, Japan. Biogeography 1: 99–106.

Tomura S (2020) Two species of Chrysidoidea collected by light trap at Takanosu-yama, Fukuoka, Japan. Pulex (99): 824–825. [in Japanese]

Xu Z-F, He J-H, Terayama M (2003) The genus *Nipponosega* Kurzenko et Lelej, 1994 firstly recorded from China, with a new species description (Hymenoptera, Chrysididae, Amiseginae) Bulletin de L'Institut Royal des Sciences Naturelles de Belgique, Entomologie 73: 195–196.

RESEARCH ARTICLE

Integrative taxonomy of Nearctic and Palaearctic Aleocharinae: new species, synonymies, and records (Coleoptera, Staphylinidae)

Adam J. Brunke[1], Mikko Pentinsaari[2], Jan Klimaszewski[3]

1 *Agriculture and Agri-Food Canada, Canadian National Collection of Insects, Arachnids and Nematodes, 960 Carling Avenue, Ottawa, Ontario, K1A 0C6, Canada* **2** *Centre for Biodiversity Genomics, 50 Stone Road East, University of Guelph, Guelph, Ontario, N1G 2W1, Canada* **3** *Natural Resources Canada, Canadian Forest Service, Laurentian Forestry Centre, 1055 du PEPS, PO Box 10380, Stn. Sainte-Foy, Québec, QC, G1V 4C7, Canada*

Corresponding author: Adam J. Brunke (adam.brunke@canada.ca)

Abstract

A long tradition of separate Nearctic and Palaearctic taxonomic studies of the diverse aleocharine rove beetles (Coleoptera: Staphylinidae) has obscured the recognition of Holarctic species and detection of adventive species in both regions. Recently, integrated study of the two regions through detailed morphological comparisons and development of an authoritatively identified DNA barcode reference library has revealed the degree to which these two aleocharine faunas are interconnected, both naturally and through human activity. Here this approach is adopted to recognize new species, reveal Holarctic species, and recognize adventive species in both North America and Europe. The following new species are described: *Isoglossa triangularis* Klimaszewski, Brunke & Pentinsaari, **sp. nov.** from British Columbia; *Gnypeta impressicollis* Klimaszewski, Brunke & Pentinsaari, **sp. nov.**, from Ontario, Maryland and North Carolina; *Aloconota pseudogregaria* Klimaszewski, Brunke & Pentinsaari, **sp. nov.**, from Ontario and Virginia; and *Philhygra pseudolaevicollis* Klimaszewski, Brunke & Pentinsaari, **sp. nov.** from eastern Canada. *Dasygnypeta velata* and *Philhygra angusticauda* are revealed to be Holarctic species, resulting in the following synonymies: *Dasygnypeta velata* (Erichson, 1839) = *Gnypeta minuta* Klimaszewski & Webster, 2008, **syn. nov.** and *Philhygra angusticauda* (Bernhauer, 1909) = *Atheta* (*Philhygra*) *pinegensis* Muona, 1983, **syn. nov.** The Nearctic species *Hylota ochracea* (and genus *Hylota*), *Thecturota tenuissima*, and *Trichiusa robustula* are newly reported from the Palaearctic region as adventive, resulting in the following synonymies: *Hylota ochracea*

Casey, 1906 = *Stichoglossa* (*Dexiogyia*) *forticornis* Strand, 1939, **syn. nov.**; *Thecturota tenuissima* Casey, 1893 = *Atheta marchii* Dodero, 1922, **syn. nov.**; and *Trichiusa robustula* Casey, 1893 = *T. immigrata* Lohse, 1984, **syn. nov.** The Palaearctic species *Amarochara forticornis*, *Anomognathus cuspidatus*, *Oligota pumilio*, and *Parocyusa rubicunda* are newly confirmed from the Nearctic region as adventive, resulting in the following synonymies: *Parocyusa rubicunda* (Erichson, 1837) = *Chilopora americana* Casey, 1906, **syn. nov.** and *Anomognathus cuspidatus* (Erichson, 1839) = *Thectura americana* Casey, 1893, **syn. nov.** The genus *Dasygnypeta*, **sensu nov.** is newly reported from North America, *Paradilacra* is newly reported from eastern North America, and *Haploglossa* is newly reported from Canada, resulting in the following synonymy: *Paradilacra densissima* (Bernhauer, 1909) = *Gnypeta saccharina* Klimaszewski & Webster, 2008, **syn. nov.** Native *Cyphea wallisi* is newly reported from across Canada and *C. curtula* is removed from the Nearctic fauna. The status of both *Gyrophaena affinis* and *Homalota plana* is uncertain but these species are no longer considered to be adventive in North America. Three new combinations are proposed: *Dasygnypeta baranowskii* (Klimaszewski, 2020) and *D. nigrella* (LeConte, 1863) (both from *Gnypeta*) and *Mocyta scopula* (Casey, 1893) (from *Acrotona*). *Dolosota* Casey, 1910, **syn. nov.** (type species *Eurypronota scopula* Casey), currently a subgenus of *Acrotona*, is therefore synonymized with *Mocyta* Mulsant & Rey, 1874. Additionally, four new Canadian records and 18 new provincial and state records are reported.

Keywords

Canada, DNA barcodes, faunistics, morphology, North America, rove beetles, United States

Introduction

Historically, taxonomic research on the hyperdiverse aleocharine rove beetle (Coleoptera: Staphylinidae) faunas of North America and better-known Europe has been conducted separately, with a few exceptions (e.g., Klimaszewski et al. 1979). More recently, a closer examination of Aleocharinae in these two regions has demonstrated that a number of species are shared between the Nearctic and Palaearctic, either naturally (Holarctic) or through human activity (adventive) (e.g., Muona 1984; Klimaszewski et al. 2007; Klimaszewski et al. in press). The interconnectedness of these assemblages, combined with the sheer diversity of the subfamily, have made it difficult to avoid describing synonyms of taxa from other regions, especially when those taxa have been described in entirely different genera (e.g., Gusarov 2003a). One strategy to broadly address this challenge is the publication of detailed illustrations of habitus and genitalia in comprehensive faunal treatments such as the recently available 'Aleocharinae of Eastern Canada' (Klimaszewski et al. 2018) and 'the Danish Beetle Bank' website (Hansen et al. 2017), the latter an online resource for the Danish beetle fauna. In the past few years, resources such as these have made it possible to efficiently cross-check Nearctic and Palaearctic aleocharines without consulting a comprehensive reference collection for each region.

In combination with careful morphological study, large-scale DNA barcoding (e.g., deWaard et al. 2019) has accelerated the discovery of Holarctic species, and the detection of new adventive species and potential synonyms in the Canadian beetle fauna (e.g., Pentinsaari et al. 2019) by algorithmically flagging potential taxonomic issues

and novelties, and connecting authoritatively identified specimens to unidentifiable females, damaged specimens, or other life stages. This integrated taxonomic approach, as applied to Aleocharinae, has already resulted in the detection of adventive species of genera *Amischa*, *Atheta*, and *Myllaena* in North America (Pentinsaari et al. 2019), and has refined the classification of Holarctic species in *Atheta* (Klimaszewski et al. in press), *Boreophilia* (Klimaszewski et al. 2019), and *Gnathusa* (Klimaszewski et al. in press).

Here we broadly compare morphological and molecular data across the Nearctic and West Palaearctic Aleocharinae in order to better integrate the taxonomic knowledge of these two regions. We describe four new Nearctic species, propose revised generic concepts, report new distributional records, and propose a number of new synonyms that impact our understanding of Holarctic and adventive species.

Materials and methods

Almost all specimens used in this study were dissected and their genitalia were subsequently examined on microslides. The genital structures were dehydrated in absolute ethanol, mounted in Canada balsam on celluloid microslides, and pinned with the specimens from which they originated. The photographs of the entire body and the genital structures were taken using an image processing system (Nikon SMZ 1500 stereoscopic microscope; Nikon Digital Camera DXM 1200F) and processed in Adobe Photoshop. Terminology mainly follows that used by Lohse et al. (1990) and Klimaszewski et al. (2018). The ventral part of the median lobe of the aedeagus is considered to be the part of the bulbus containing the foramen mediale, the entrance of the ductus ejaculatorius, and the adjacent venter (ventral part of the tubus of the median lobe) of the tubus; the opposite side is referred to as the dorsal part.

Depository abbreviations:

CBG   Centre for Biodiversity Genomics, University of Guelph, Guelph, Ontario, Canada;

CNC   Canadian National Collection of Insects, Arachnids and Nematodes, Ottawa, Ontario, Canada;

cRW   Personal collection of Reginald P. Webster, Charters Settlement, New Brunswick, Canada (also known as RWC);

LFC   Laurentian Forestry Centre, Québec, Quebec, Canada;

MCZ   Museum of Comparative Zoology, Harvard University, Cambridge, Massachusetts, United States (C. Maier);

NHMD Natural History Museum of Denmark, Copenhagen University, Copenhagen, Denmark (A. Solodovnikov);

NMNH National Museum of Natural History, Washington D.C., United States (F. Shockley);

UAM   University of Alaska Museum Insect Collection, Fairbanks, Alaska, United States (D. Sikes);

ZFMK   Zoologisches Forschungsmuseum Alexander Koenig, Bonn, Germany;
ZMHB   Museum für Naturkunde, Berlin, Germany (B. Jaeger);
ZMUO   Zoology Museum, University of Oulu, Oulu, Finland (M. Mutanen);
ZSM   Zoologische Staatssammlung, Munich, Germany (F. Koehler).

We have examined all DNA barcode data for Aleocharinae previously generated by a variety of projects in both Europe and North America (e.g., Rulik et al. 2017; Sikes et al. 2017; McClenaghan et al. 2019; and other studies summarized by Pentinsaari et al. 2019). Fifty-three barcode sequences, the majority of which are Canadian sequence records originating from various projects coordinated by CBG, are published here for the first time. All sequences were analyzed using the workbench tools of the BOLD platform (http://www.boldsystems.org) after applying filters to exclude those flagged as misidentifications, those with sequence lengths under 100 bp, those with stop codons, and those flagged as contaminated. Sequences were generally visualized as clusters in neighbour-joining trees (using the Taxon ID Tree tool). In addition, BIN Discordance Reports, which compare the taxonomy of the specimen records to their BIN assignments, were used to detect potential misidentifications and synonyms.

All COI barcode sequences in BOLD that fulfill quality criteria (minimum length 500 bp, less than 1% ambiguous bases) are automatically assigned into BIN clusters (Barcode Index Numbers; Ratnasingham and Hebert 2013). In addition, sequences between 300–500 bp can be assigned as members of an existing BIN, but they will not be accepted as founding members of a new BIN. BINs correspond to species at a high accuracy in northern and central European beetles (Hendrich et al. 2015; Pentinsaari et al. 2017), and we treat BINs here as provisional hypothetical species.

The DNA barcode sequences studied here, including both previously unpublished data and the sequences published in earlier studies, have been compiled into a publicly available dataset on BOLD (DS-ALEO2020, https://doi.org/10.5883/DS-ALEO2020) along with collecting data, images of the specimens (if available), and other metadata related to the specimens and sequences. The sequences are also available through GenBank (accessions provided in Suppl. material 1: Table S1).

Taxonomic accounts

Tribe Aleocharini Fleming, 1821

***Amarochara forticornis* (Lacordaire, 1835)**
BOLD:ACF6186
Fig. 1A–H

Material (DNA barcoded specimens). Canada: Ontario: Fergus, Centre Wellington District High School, 43.704, -80.358, Malaise trap, 3.V.2013, M. Cottrill (1, CBG); Guelph, Biodiversity Institute of Ontario, 43.528, -80.229, Malaise trap, 25.VII.2013, BIO Collections Staff (1, CBG); Rouge National Urban Park, west of
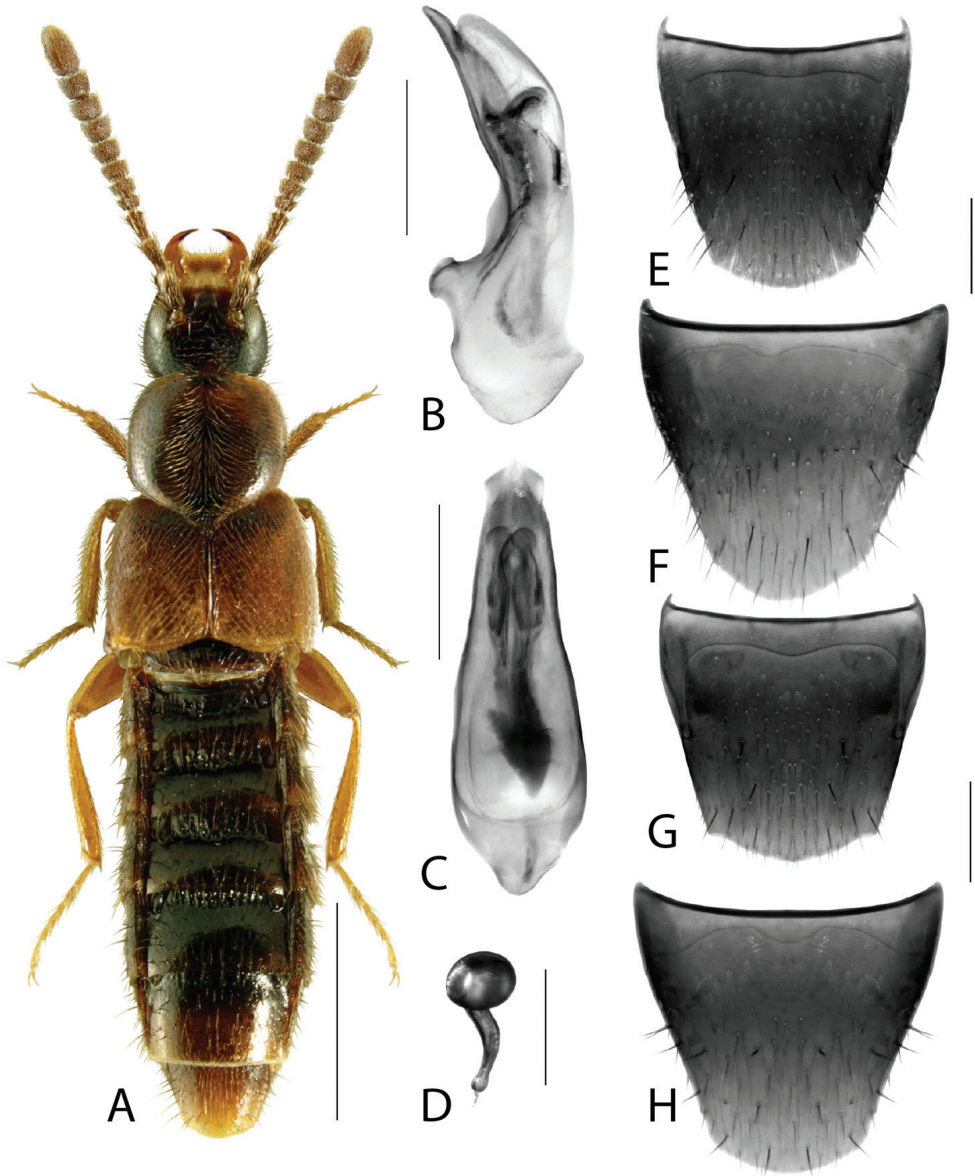
Figure 1. *Amarochara forticornis* (Lacordaire) **A** habitus **B** median lobe of aedeagus in lateral view **C** median lobe of aedeagus in dorsal view **D** spermatheca **E** male tergite VIII **F** male sternite VIII **G** female tergite VIII **H** female sternite VIII. Scale bars: 1 mm (**A**); 0.2 mm (**B–H**).

Glen Rouge campground, 43.804, -79.146, marsh scrub along riverside, pitfall trap, 9.VI.2013, BIObus 2013 (1, CBG); Cambridge, rare Charitable Research Reserve, Preston Flats, 43.3908, -80.3747, grassy wetland, pitfall trap, 31.V.2015, BIO Collections staff (2, CBG); Peterborough, 44.318, -78.372, farm, malaise trap, B. McClenaghan (1, CBG).

Distribution. Origin: Palaearctic (adventive in Nearctic). **Canada**: ON [new record].

Diagnosis. *Amarochara forticornis* may be easily recognized among the other Canadian species of the genus by the distal antennomeres, which are less than twice as wide as long. The species is also unique within the genus by having a distinct basal impression on abdominal tergite VI.

Bionomics. In its native range, *A. forticornis* occurs in a variety of open and forested habitats, including forests, edges of waterways, grasslands, agricultural fields, and gardens (Assing 2002). It has been mostly collected by pitfall traps in the spring and summer, and then from flood debris in the cooler months of the year (Assing 2002). Assing (2002) suggested that beetles in flood debris were washed from some cryptic, subterranean microhabitat. Canadian specimens were collected in similar ways as in Europe.

Comments. Newly reported as adventive in North America, from several localities in southern and eastern Ontario. It is native to the West Palaearctic and is known from most of Central Europe, Russian Central Territory, Armenia, and Georgia (Newton 2019).

The key to Eastern Canadian *Amarochara* in Klimaszewski et al. (2018) should be modified as follows

1A	Antennomere 10 only weakly transverse (Fig. 1A); abdominal tergite VI with distinct basal impression in addition to coarse punctures ....*Amarochara forticornis* **(Lacordaire)**
–	Antennomere 10 strongly transverse, at least twice as wide as long (native species); abdominal tergite VI with, at most, coarse punctures at base........... **1B**
1B	Pronotum with strong microsculpture and coarse, dense punctation, surface almost matte..*A. duryi* **(Casey)**
–	Pronotum without microsculpture or with fine microsculpture, and with fine sparse to moderately dense punctation, surface moderately to highly glossy....**2**

Tribe Oxypodini C.G. Thomson, 1859
Subtribe Microglottina Fenyes, 1918

Haploglossa nebulosa (Casey, 1906)
BOLD:ACK6454
Fig. 2A–H

Material (DNA barcoded specimens). Canada: Ontario: Rouge National Urban Park, Toronto Zoo, 43.8223, -79.1897, forest, malaise trap, 21.V.2013, L. Attard and K. Greenham (1, CBG).

Distribution. Origin: Nearctic. **Canada**: ON [new record]. **United States**: OK, PA.

Diagnosis. *Haploglossa nebulosa* may be easily distinguished from the other Nearctic species of the genus, *H. barberi* (Fenyes), by the bicolored elytra and fusiform body (Klimaszewski and Ashe 1991). Based on the shape of the spermatheca with its narrow capsule and broadly rounded apex, *H. nebulosa* may be most closely related to Palaearctic *H. marginalis* (Gravenhorst) as is suggested by barcode clustering. However,
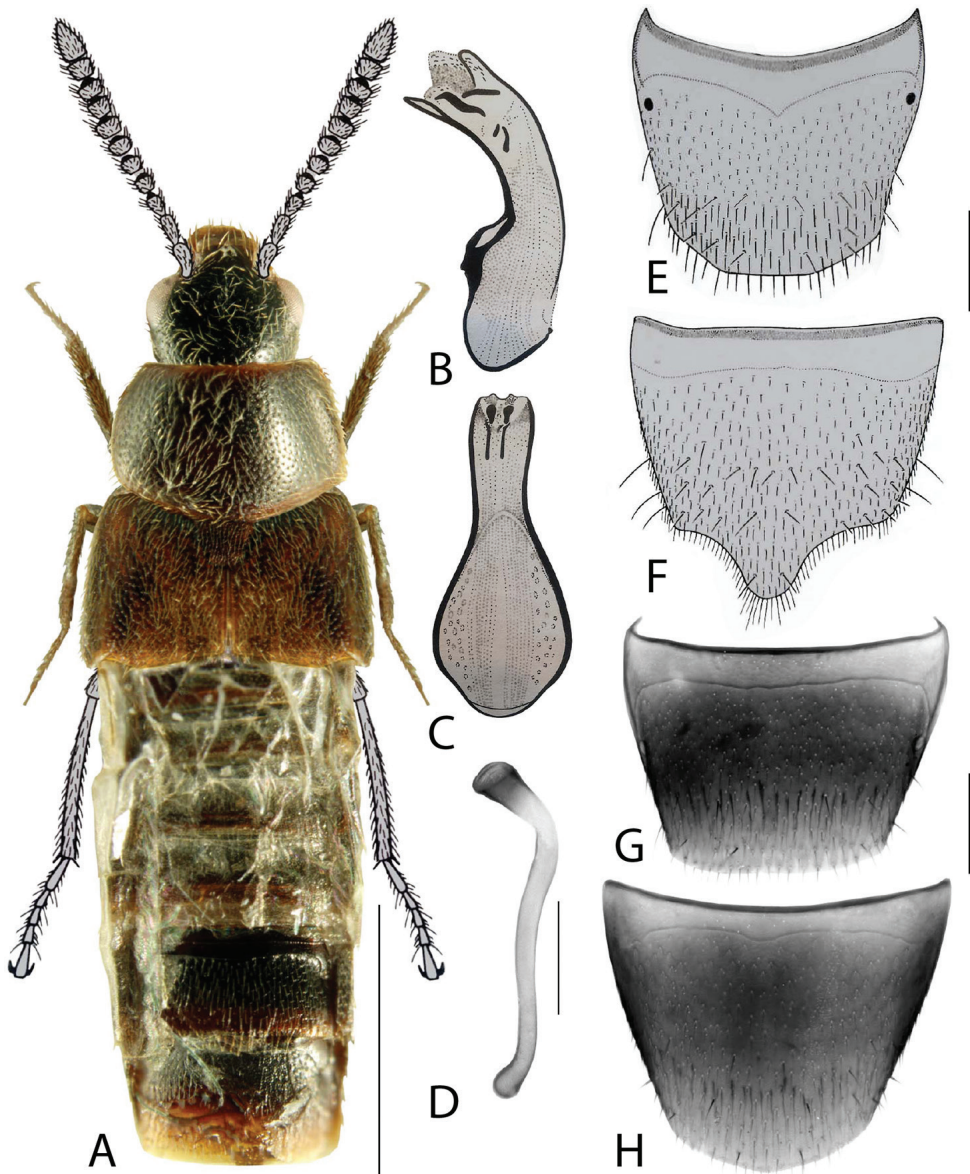
Figure 2. *Haploglossa nebulosa* (Casey) **A** habitus **B** median lobe of aedeagus in lateral view (adapted from Klimaszewski and Ashe (1991)) **C** median lobe of aedeagus in dorsal view (adapted from Klimaszewski and Ashe (1991)) **D** spermatheca **E** male tergite VIII **F** male sternite VIII **G** female tergite VIII **H** female sternite VIII. Scale bars: 1 mm (**A**); 0.2 mm (**B–H**).

H. nebulosa can be readily distinguished by the pronotum, which is dark and paler only along the margins, while *H. marginalis* has broad pale areas laterally. *Haploglossa nebulosa* was compared to Palaearctic *H. villosula* (Stephens) by Klimaszewski and Ashe (1991; as *H. pulla* (Gyllenhal)), but the species is quite different externally (much

darker, finer pronotal punctation) and the spermatheca of the latter species is of the type with a large, rounded capsule.

Bionomics. All members of *Haploglossa* are nidicolous, mostly in bird nests but also in mammal and ant nests (summarized by Staniec et al. 2010). Some species with well-known life histories appear to specialize on particular types of host nests, such as birds of prey (*H. picipennis* (Gyllenhal)) or bank swallows (*H. nidicola* (Fairmaire)) (Staniec et al. 2010). The genus is very rarely collected in North America. The Nearctic species *H. barberi* (Fenyes) was collected in long series from bank swallow nests (Klimaszewski and Ashe 1991). One specimen of *H. nebulosa* has been found in a rodent nest within a hollow tree (Klimaszewski and Ashe 1991) but bird and mammal nests have been poorly sampled in the Nearctic and more collecting is needed to determine the biology of the Nearctic *Haploglossa* (Brunke and Buffam 2018).

Comments. The genus *Haploglossa* and *H. nebulosa* are newly reported from Canada, from a single locality in southern Ontario. The species is also known from Oklahoma and Pennsylvania, United States (Klimaszewski and Ashe 1991).

The key to genera of Oxypodini in Eastern Canada in Klimaszewski et al. (2018) should be modified as follows

8A	Pronotum strongly converging anteriad; posterolateral margin of elytra with strong sinuate emargination **8B**
–	Pronotum not or, at most, weakly converging anteriad **9**
8B	Pronotum with fine punctures, not clearly visible at moderate magnification, shape strongly transverse, ~ 1.5 × wider than long ....***Crataraea* Thomson**
–	Pronotum with coarse punctures, clearly visible with low magnification, shape weakly transverse, no more than 1.4 × wider than long ....***Haploglossa* Kraatz**

Subtribe Oxypodina C.G. Thomson, 1859

Hylota cryptica Klimaszewski & Webster, 2016
BOLD:ACN2725
Fig. 3A–G

Material (DNA barcoded specimens). Canada: Ontario: Guelph, Hanlon Preservation Park, 43.506, -80.213, mixed forest, dead wood and beating, 11.VI.2017, M. Pentinsaari (1, CBG); Hartington, Eel Lake Cottage, 44.5628, -76.553, Lindgren funnel, 12.VII.2017, G. Blagoev (1, CBG); Kawartha Lakes, 44.28, -78.529, farm, malaise trap, 5.V.2016, B. McClenaghan (1, CBG); Murphy's Point Provincial Park, 44.7812, -76.2336, forest, malaise trap, 19.VI.2014, CBG Collections staff (1, CBG); **Newfoundland:** Terra Nova National Park, Blue Hill Road, 48.598, -53.9702, malaise trap, old balsam fir forest, 2.VII.2013, E. Perry (1, CBG).

Distribution. Origin: Nearctic. **Canada:** AB, NB, NF [new record], ON [new record].
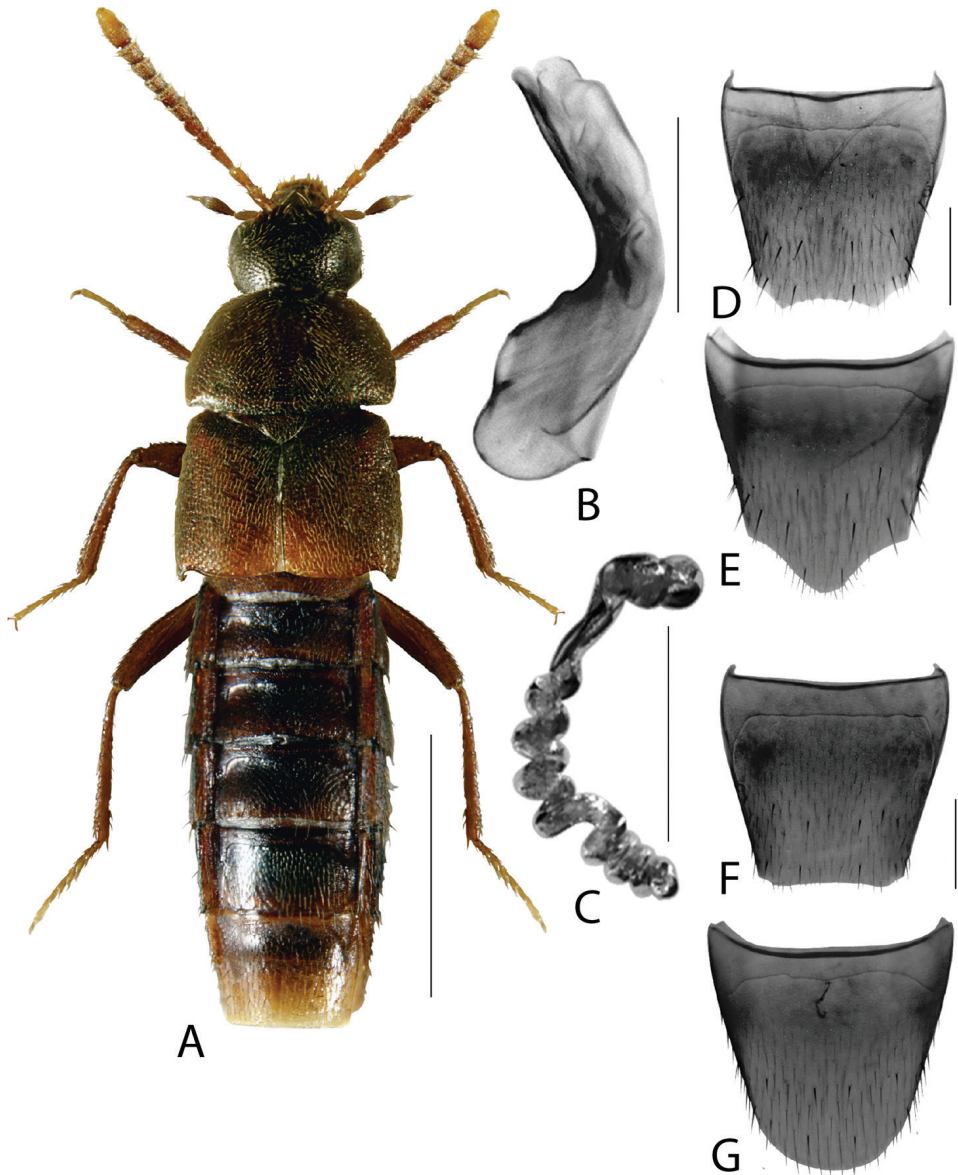
Figure 3. *Hylota cryptica* Klimaszewski & Webster **A** habitus **B** median lobe of aedeagus in lateral view **C** spermatheca **D** male tergite VIII **E** male sternite VIII **F** female tergite VIII **G** female sternite VIII. Scale bars: 1 mm (**A**); 0.2 mm (**B–G**). Illustrations after Webster et al. (2016).

Bionomics. Little is known about the microhabitat preferences of this species, but it likely occurs in in nests or cavities within trees as does *H. ochracea* (Klimaszewski et al. 2018).

Comments. This recently described species, previously known from New Brunswick and Alberta (Klimaszewski et al. 2018) is newly recorded from Ontario and Newfoundland. It is likely to be widely distributed in North America east of the Rocky Mountains.

Hylota ochracea Casey, 1906
BOLD:ABW9176
Fig. 4A–H

Stichoglossa (*Dexiogyia*) *forticornis* Strand, 1939, syn. nov.

Material (DNA barcoded specimens). Canada: Ontario: Guelph, Dovercliffe Road, 43.51, -80.254, backyard, compost and mouldy hay piles, 6.VI.2018, M. Pentinsaari (3, CBG); Guelph, Hanlon Preservation Park, 43.51, -80.221, mixed forest, at UV light, 30.VI.2018, M. Pentinsaari (1, CBG); Whitby, Julie Payette Public School, Malaise trap, 43.886, -78.934, 22.IV.-03.V.2013, Z. Turner (1, CBG). **Quebec:** Montreal, Montreal Botanical Garden, 45.559, -73.566, Malaise trap, 24.VII-02.VIII.2014, M. Larrivee (1, CBG). **Finland:** Al: Lemland, Äspholm, 60.0675, 19.9583, 9.X.2011, M. Pentinsaari (1, ZMUO); Al: Lemland, Nåtö, 60.046, 19.981, 26.VI.2014, M. Pentinsaari (2, ZMUO); N: Sipoo, Sipoonkorpi, 60.304, 25.202, window trap, 2.VIII.2013, S. Karjalainen and P. Martikainen (1, ZMUO).

Distribution. Origin: Nearctic (adventive in Europe). **Canada**: NB, NS, NT, ON, QC, SK. **United States**: NY, VT.

Bionomics. *Hylota ochracea* is strongly associated with bird nests in forested habitats. It has also been collected from artificial analogs such as a pigeon coup, manmade nest boxes, and a plastic composter bin containing carrion and decaying vegetables (Klimaszewski et al. 2018). The specimens recently collected in Ontario, Canada were found in compost and at UV light.

Comments. *Hylota ochracea*, a widespread Nearctic species (Klimaszewski et al. 2018), is newly reported from the Palaearctic region and had been previously known from Finland, Denmark, Germany, Norway, Sweden, and Switzerland (Lundberg 2006; Schülke and Smetana 2015; Newton 2019) under the synonym *Dexiogyia forticornis*. *Hylota* is also a new genus record for the Palaearctic region. Nearctic *Hylota ochracea* and Palaearctic *D. forticornis* share a BIN and do not form separate clusters. One of the DNA barcode haplotypes is shared between Finnish and Canadian specimens. Nearctic and Palaearctic populations also have identical male and female genitalia. Based on its specialization on microhabitats in forests, we do not consider *H. ochracea* to be a naturally occurring Holarctic species. Holarctic beetles are generally those that occur north of the treeline and have crossed treeless Beringia in the last 2.8 Mya (reviewed in Brunke et al. 2020). *Hylota ochracea* may have been introduced to the Palaearctic region with the nest material of poultry or domestic pigeons, or with another form of decaying plant matter. A similar situation has occurred with the bird nest-associated staphylinid *Bisnius palmi* (Smetana), which was originally described from Italy but later found to be a native Nearctic species (Smetana 1995).

With the above synonymy, the genus *Dexiogyia* is now known only from externally similar sister species *D. angustiventris* (Casey) (Nearctic) and *D. corticina* (Erichson) (West Palaearctic), plus Afrotropical *D. congoensis* (Scheerpeltz). As in the former *D. forticornis*, *D. congoensis* is probably misplaced due to superficial similarity. *Hylota*
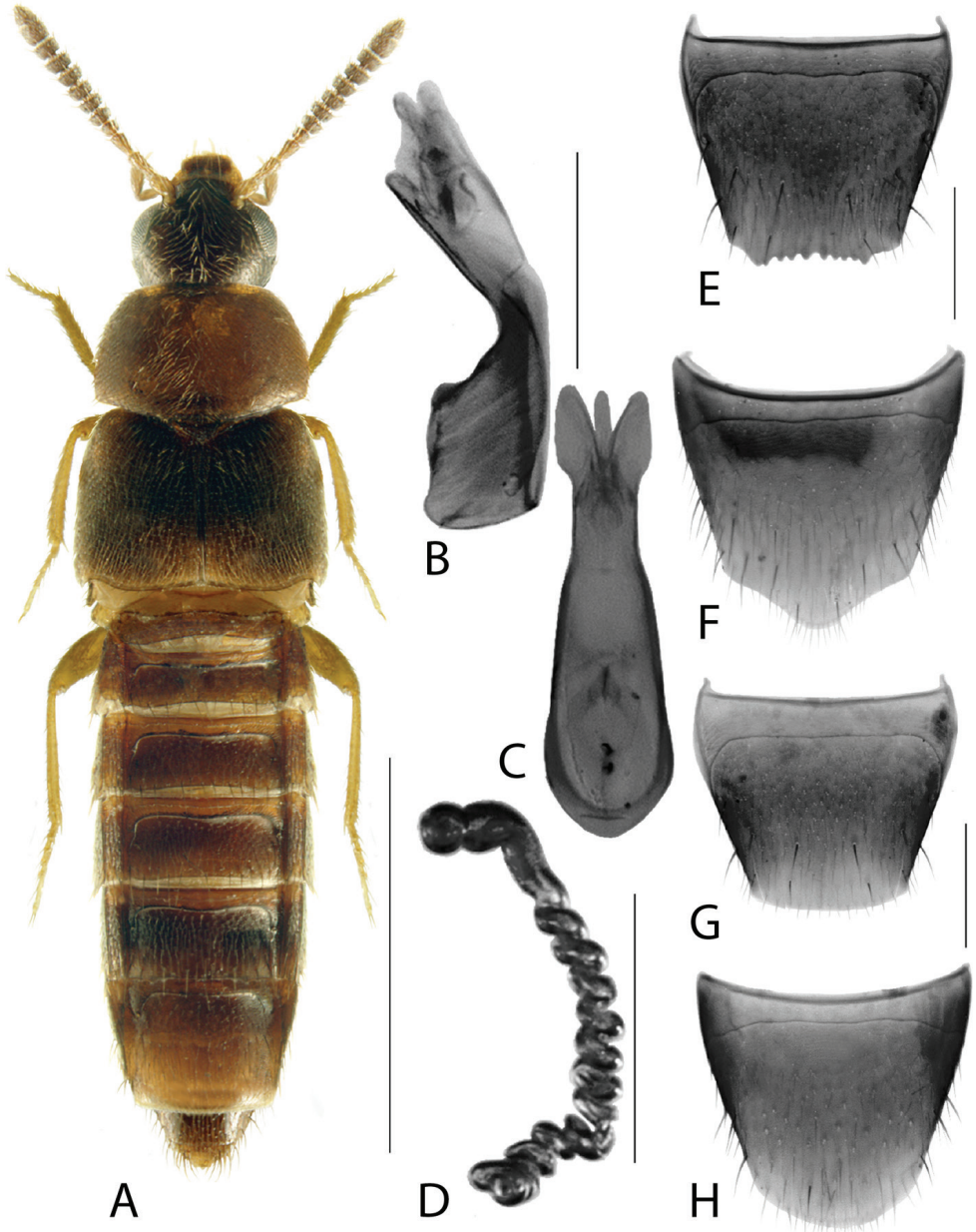
Figure 4. *Hylota ochracea* Casey **A** habitus **B** median lobe of aedeagus in lateral view **C** median lobe of aedeagus in dorsal view **D** spermatheca **E** male tergite VIII **F** male sternite VIII **G** female tergite VIII **H** female sternite VIII. Scale bars: 1 mm (**A**); 0.2 mm (**B–H**). Illustrations after Klimaszewski et al. (2018), reproduced with permission.

is readily separated from *Dexiogyia* by the shape of the pronotum, which is strongly convergent anteriad, such that its apical width is subequal to the width of the head. In *Dexiogyia*, the head is distinctly narrower than the pronotum.

Isoglossa **Casey, 1893**

Rheobioma Casey, 1906; Klimaszewski and Pelletier (2004), syn. of *Neoisoglossa*
Athetalia Casey, 1910 (in part); Klimaszewski and Pelletier (2004) syn. of *Neoisoglossa*
Neoisoglossa Klimaszewski & Pelletier, 2004; Gouix and Klimaszewski (2007), syn. of
    Isoglossa, unnecessary replacement name; Klimaszewski et al. (2020) as valid genus,
    incorrectly attributed to Casey (1893).

Comments. In Klimaszewski et al. (2020), *Neoisoglossa* was incorrectly attributed to
Casey but was actually proposed by Klimaszewski and Pelletier (2004), apparently as
an unnecessary replacement name for *Isoglossa* Casey 1893. The previous treatment of
these generic names and two other synonyms in the catalog of Gouix and Klimasze-
wski (2007) is correct and followed here. Blackwelder (1952) was wrong and there is
no *Isoglossa* Newman that preoccupied Casey's name, so *Isoglossa* Casey stands as valid
with *Neoisoglossa* as a synonym.

Isoglossa triangularis **Klimaszewski, Brunke & Pentinsaari, sp. nov.**
http://zoobank.org/A8A0402E-2950-4394-B9CF-25E3DD629804
BOLD:ACU5806
Fig. 5A–H

Type material. *Holotype.* (male): Canada, British Columbia, Prince George, Nukko
Lake Elementary EQP-CLL-574, 54.0831°N, 122.988°W, 764 m asl, Holly Sapun
04/20/2015 to 05/08/2015, Barcode of life, DNA voucher specimen, Sample ID:
BIOUG22036-B02, Process ID: SMTPM2682-15 (CNC). *Paratypes* (3, CBG):
Canada, British Columbia, Prince George, Nukko Lake Elementary EQP-CLL-574,
54.0831°N, 122.988°W, 764 m asl, Holly Sapun 04/20/2015 to 05/08/2015, Barcode
of life, DNA voucher specimen, Sample ID: BIOUG22036-B07, Process ID: SMT-
PM2682-15 (1 male, CBG); same label data except: Sample ID: BIOUG22035-H08,
Process ID: SMTPM2665-15 (1 female, CBG); Sample ID: BIOUG22036-A04, Pro-
cess ID: SMTPM2672-15 (1 female, CBG).
    Etymology. The species epithet refers to the remarkably separated triangular apex
of the median lobe of the aedeagus, distinguishing it from all other members of the
Ocalea group.
    Distribution. Origin: Nearctic. **Canada**: BC.
    Diagnosis. *Isoglossa triangularis* can be easily distinguished from all Nearctic spe-
cies of the *Ocalea* group of genera by a combination of the strongly transverse and
sparsely punctate pronotum, transverse antennomere 4, distinct triangular apex of the
median lobe in lateral view (Fig. 5B), and distinct and simple 'walking cane' shape of
the spermatheca (Fig. 5D).
    Description. Body length 3.0–3.3 mm, dark brown with elytra, antennomeres
1–2 or 1–3, legs and apical part of abdomen yellow-brown, forebody moderately
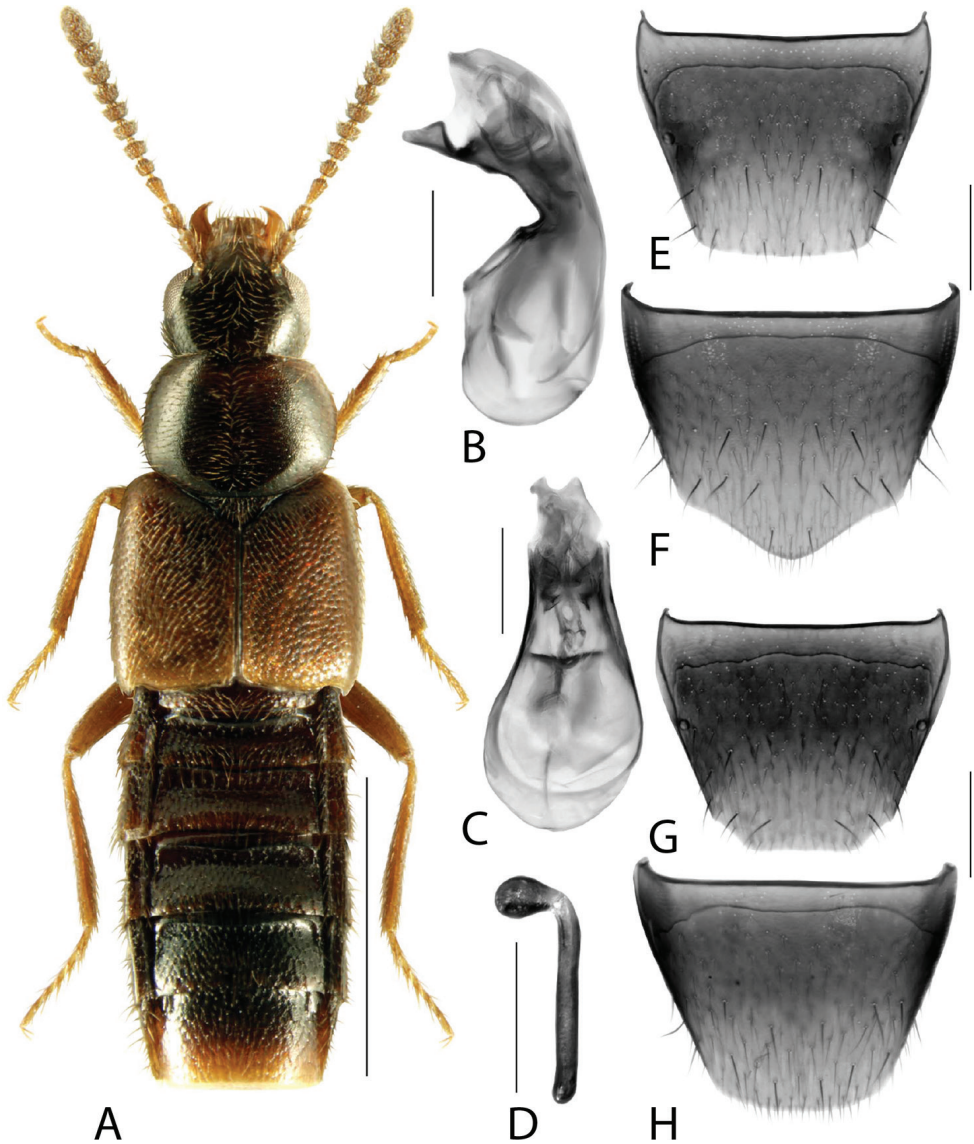
Figure 5. *Isoglossa triangularis* Klimaszewski, Brunke & Pentinsaari, sp. nov. **A** habitus **B** median lobe of aedeagus in lateral view **C** median lobe of aedeagus in dorsal view **D** spermatheca **E** male tergite VIII **F** male sternite VIII **G** female tergite VIII **H** female sternite VIII. Scale bars: 1 mm (**A**); 0.2 mm (**B–H**).

glossy and abdomen strongly so (Fig. 5A); antenna moderately stout, antennomere 4 slightly transverse, antennomeres 5–10 strongly transverse, terminal antennomere ca. as long as two preceding ones combined; pronotum transverse (width/length ratio = 1.6), impressed medially at base, lateral edges evenly arcuate, length ratio of base to apex 1.2 ×, punctures fine and sparse, distance between punctures ~ 3 × diameter of a puncture, space between punctures with faint isodiametric microsculpture, pubescence

directed laterad from midline of disc forming arcuate lines on both sides; elytra transverse (width/length ratio = 1.3), 1.5 × as long as pronotum; abdomen arcuate laterally and gradually narrowing toward apex. MALE. Tergite VIII broadly arcuate apically (Fig. 5E); sternite VIII with apical part broadly triangularly produced (Fig. 5F); median lobe of aedeagus in lateral view with narrowly elongate crista apicalis at base of bulbus, tubus moderately long, strongly produced ventrally, apex narrowly triangular constricted baso-dorsally in lateral view (Fig. 5B), internal sac structures not pronounced (Fig. 5B, C). FEMALE. Tergite VIII truncate apico-medially (Fig. 5G); sternite VIII arcuate apically (Fig. 5H); spermatheca with capsule approximately spherical with short neck, stem narrow, long and straight (Fig. 5D).

Bionomics. The specimens were collected in a Malaise trap on an open field surrounded by mixed forest.

Comments. Based on a combination of small size (< 4.5 mm), superficial, meshed microsculpture, sparse pronotal punctation, with punctures separated by more than two puncture diameters, pronotum transverse, shorter and narrower than elytra, and the transverse antennomeres 5–10, *I. triangularis* keys to genus *Isoglossa* Casey in Klimaszewski and Pelletier (2004). However, barcode sequences of this species do not cluster with *Isoglossa agnita* but rather form a cluster with *Gennadota canadensis* and the species of *Neothetalia* which bear a spermatheca with broad, circular loops, similar to those of *Gennadota*. *Isoglossa triangularis* has a simple spermatheca with a long straight stem and is not externally similar to these taxa (see above), and the barcode divergence between these species and *I. triangularis* is 11–12%. It is likely that *I. triangularis* belongs in a separate genus, but this is outside of the scope of this study. We here place *I. triangularis* tentatively in *Isoglossa* as not to disturb the existing morphological diagnoses of the genera and identification keys (e.g., Klimaszewski and Pelletier 2004; Klimaszewski et al. 2020), pending generic revision of the *Ocalea* group.

Parocyusa rubicunda (Erichson, 1837)
Fig. 6A–D

Tachyusa rubicunda Erichson, 1837
Chilopora americana Casey, 1906, syn. nov.
Tetralaucopora americana: Klimaszewski et al. 2018 (as valid species)
Parocyusa americana: Assing 2021 (possible synonym of *P. rubicunda*)

Material (DNA barcoded specimens). Austria: Innervillgraten, Arntal, 46.8362, 12.3348, 1580 m, 22.VIII.2010, F. Koehler and J. Koehler (2, ZSM). **Canada: Ontario:** Northumberland County, Peter's Woods Protected Natural Area, 44.124, -78.039, under rock in streambed,12.IX.2011, A. Brunke and S. Paiero (1, DEBU); Crieff Bog, 3 km W Puslinch, sedge meadow, 26.VI.1987, D. Blades (1, DEBU). **United States: Connecticut:** East Hartford, Two Rivers Magnet Middle School, 41.757, -72.655, 4.VI.2005, J. DeWaard (1, CBG).
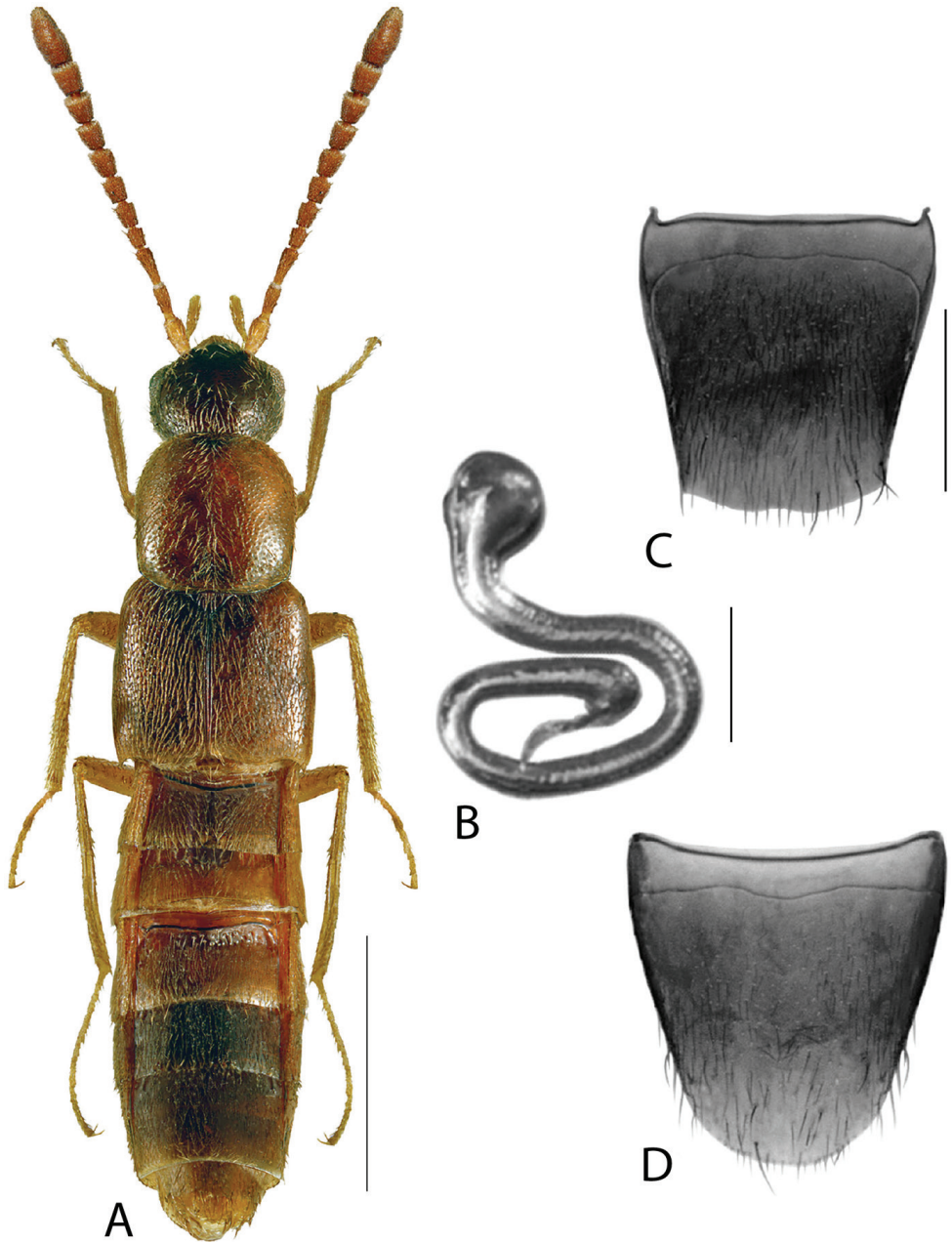
Figure 6. *Parocyusa rubicunda* (Erichson) **A** habitus **B** spermatheca **C** female tergite VIII **D** female sternite VIII. Scale bars: 1 mm (**A**); 0.2 mm (**B–D**). Illustrations after Klimaszewski et al. (2016c).

Additional non-barcoded material. Canada: Ontario: Ancaster, 21.X.1967 (1, CNC); Rondeau Prov. Pk., Tulip Tree Trail, *Carex* and moss on logs in pond, 5.VI.1985, A. Davies and J.M. Campbell (1, CNC); **Quebec:** Montreal, 20.IX.1969, E.J. Kiteley, 1 (CNC); Mt. Orford Park, 20.IX.-11.X.1972, Dondale and Redner, 1 (CNC).

Distribution. Origin: West Palaearctic (adventive in North America). **Canada**: BC, ON, QC, NB, NF. **United States**: CT, NY, PA.

Bionomics. In North America, most specimens of this species have been collected from near water, including a sandy creek bank, in a dried streambed and in moss near the splash zone of a waterfall (Klimaszewski et al. 2018). Nearctic populations of this species are only known from female specimens and the species may be parthenogenetic in North America. In its native distribution, the northern and northwestern populations are also parthenogenetic (Assing 2021) and most likely represent the source population for the Nearctic introduction.

Comments. *Parocyusa rubicunda* is a widespread West Palaearctic species (Europe, European Russia, Turkey, Georgia, Iran, Kazakhstan, Kyrgyzstan, Tajikistan, Uzbekistan) (Assing 2021). It is confirmed as established in the Nearctic region and had been previously known from North America under the synonym *Tetralaucopora americana* (Casey) (Klimaszewski et al. 2018). Assing (2021) recently reported this species from BC and treated *T. americana* as a tentative synonym based on the results presented in this paper.

Although all available sequences of this species are partial (382–407 bp) and a BIN has not been established as that would require at least one founding member with a minimum sequence length of 500 bp, Nearctic and Palaearctic sequences form a distinct cluster with only a single variable nucleotide site. External morphology and that of the spermatheca are identical. As spermathecae are of generally poor diagnostic value (especially the distal part) in *Parocyusa* (Assing 2021), the barcode evidence was quite critical for the resolution of this issue. Based on this evidence and a distribution centered around populated areas in northeastern and western North America, we here consider this species to be adventive in the Nearctic region. At the moment, it is not yet possible to determine whether the population in BC is a separate introduction from the northeastern population.

Recently, Assing (2021) revalidated *Parocyusa* as a genus separate from *Tectusa* after the discovery that *Tectusa* was not a monophyletic group. The type species of *Parocyusa* was found to be congeneric with that of *Tetralaucopora*, and the latter became a junior synonym of the former.

Tribe Tachyusini C.G. Thomson
Revised key to the Canadian genera of Tachyusini

Adapted from Klimaszewski et al. 2018.

1 Elytra at humerus only slightly broader than pronotum at base (Figs 7, 8); impressions of abdominal tergites shallow, with punctation similar to that of disc (Figs 7, 8) **2**
– Elytra at humerus distinctly broader than pronotum at base (Figs 9–13); impressions of abdominal tergites with at least a few coarse punctures and glossy areas, punctation distinctly different from that of disc (Figs 9–13)..............**3**

2   Pronotum with pubescence directed straight posteriad; hind tarsus subequal in length to hind tibia or longer (Fig. 8) .... ***Brachyusa* Mulsant & Rey**

–   Pronotum with pubescence directly posteriolaterad from midline; hind tarsus shorter, slightly longer than half the length of hind tibia or shorter (Fig. 7) .. ..***Paradilacra* Bernhauer**

3   Abdomen clavate, at base distinctly narrower than head (Fig. 9); tergite III ca. as long as wide or longer; tergal impressions with median carina (Fig. 9) ....***Tachyusa* Erichson**

–   Abdomen at most slightly constricted at base, subequal to or wider than head (Figs 10–13); tergite III ca. twice as wide as long or wider; tergal impressions never with median carina (Figs 10–13) **4**

4   Abdomen at base elongate and moderately constricted, ca. as wide as head (Figs 10–12); tergite III, at most, twice as wide as long; tergal impressions deep and sharply delineated from strongly convex disc (Figs 10–12)............. ....***Dasygnypeta* Lohse, sensu nov.**

–   Abdomen at base at most slightly constricted, wider than head (Fig. 13); tergite III strongly transverse, ~ 2.5 × wider than long or wider; tergal impressions shallower, gradually sloping to disc at base (Fig. 13) ....***Gnypeta* Thomson**

Paradilacra densissima (Bernhauer, 1909)
BOLD:ACF7668
Fig. 7A–H

Atheta (*Paradilacra*) *densissima* Bernhauer, 1909
Gnypeta saccharina Klimaszewski & Webster, 2008, syn. nov.

Material (DNA barcoded specimens). Canada: Alberta: Waterton Lakes National Park, Highway 6 pulloff, 49.065, -113.779, 1569 m, intercept trap, montane forest, 27.VI.2012, BIOBus 2012 (1, CBG); **British Columbia:** 10 km W Kamloops, New Afton Mine, Wetland Protected Area, 50.662, -120.504, 702 m, malaise trap, 22.VIII.2013, C. Simon (1, CBG); **New Brunswick:** York Co., Fredericton at Saint John River, 45.959, -66.625, margin of river in flood debris, 7.VII.2005, R.P. Webster [note: paratype of *G. saccharina*] (1, LFC); **Ontario:** Guelph, University of Guelph Arboretum, 43.53, -80.21, 12.VI.2019, M. Pentinsaari (1, CBG).

  Distribution. Origin: Nearctic. **Canada**: AB, BC, NB, ON [new record], SK [new record]. **United States**: CA, MT, NV, ND, OR, UT.

  Bionomics. This species has been collected from various wetland microhabitats including the edges of lakes, rivers, and a beaver pond (Gusarov 2003a).

  Comments. *Paradilacra densissima* and the genus *Paradilacra*, widespread in western and central North America (Gusarov 2003a), are newly reported from SK (records in Klimaszewski et al. 2016a, as *G. saccharina*) and eastern North America based on
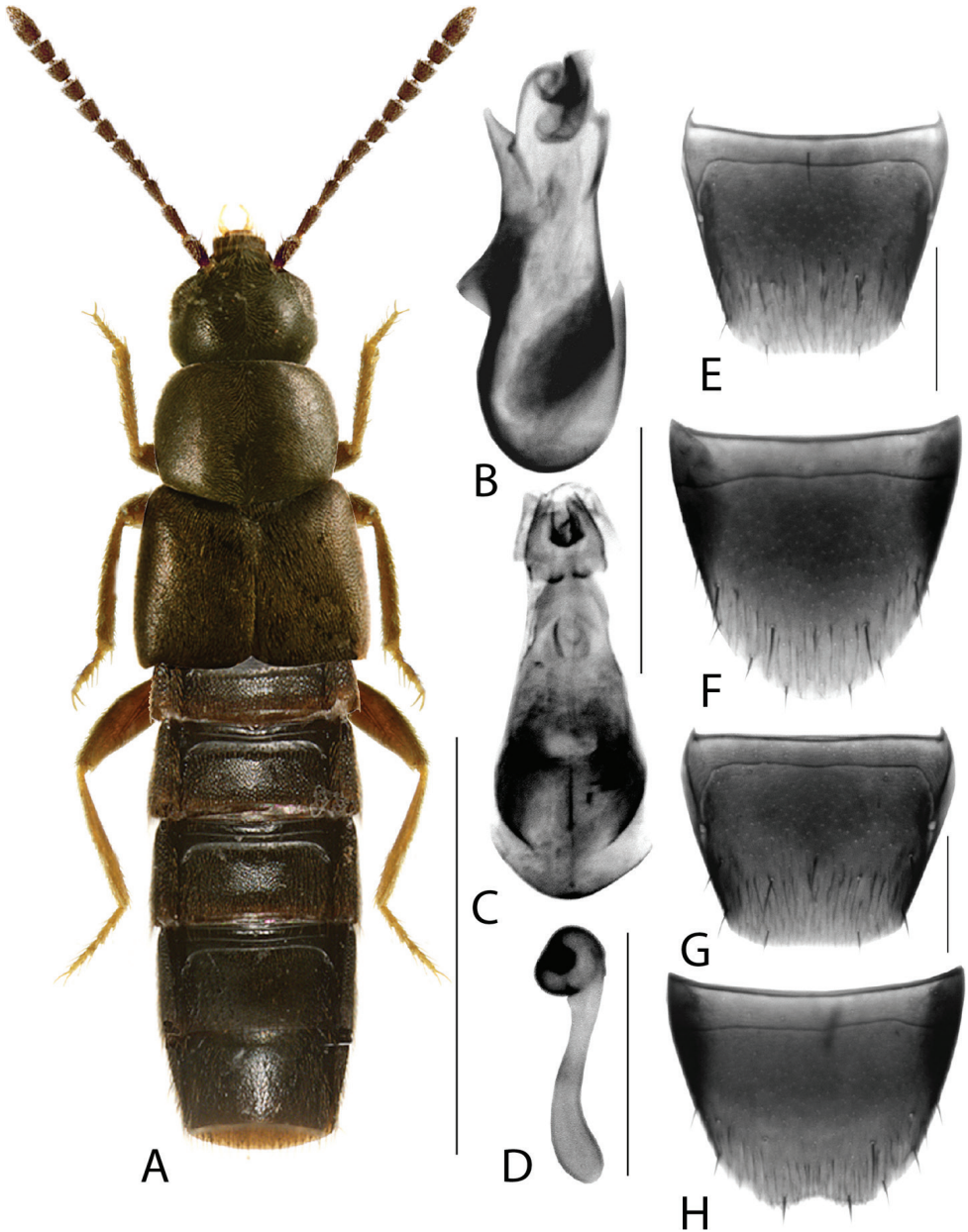
Figure 7. *Paradilacra densissima* (Bernhauer) **A** habitus **B** median lobe of aedeagus in lateral view **C** median lobe of aedeagus in dorsal view **D** spermatheca **E** male tergite VIII **F** male sternite VIII **G** female tergite VIII **H** female sternite VIII. Scale bars: 1 mm (**A**); 0.2 mm (**B–H**). Illustrations after Klimaszewski et al. (2018), used with permission.

records from NB (Klimaszewski et al. 2008) and ON (this study), including one sequenced paratype of synonym *Gnypeta saccharina*. Under the present concept, only one widespread species of this genus is known.
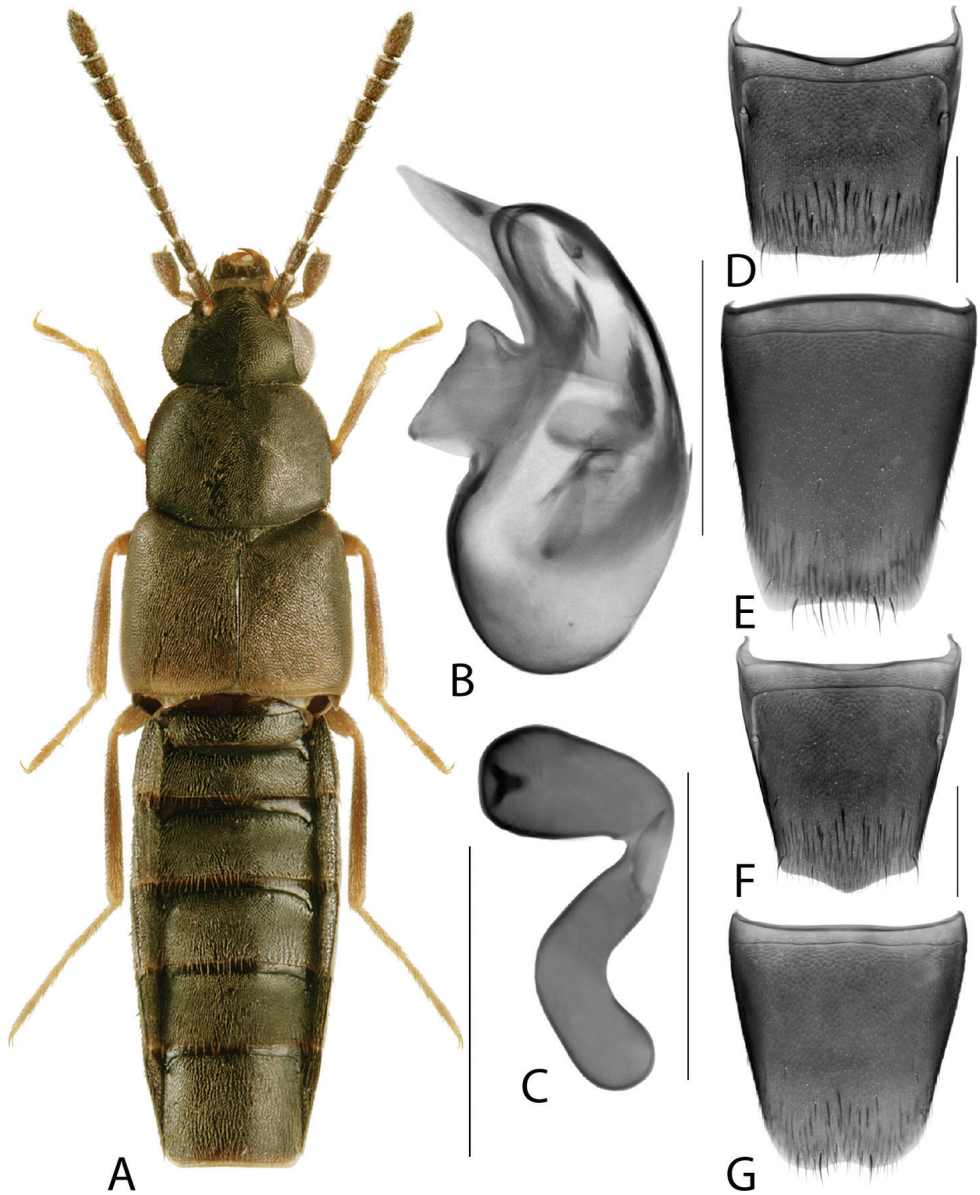
Figure 8. *Brachyusa helenae* (Casey) **A** habitus **B** median lobe of aedeagus in lateral view **C** spermatheca **D** male tergite VIII **E** male sternite VIII **F** female tergite VIII **G** female sternite VIII. Scale bars: 1 mm (**A**); 0.2 mm (**B–G**). Illustrations after Klimaszewski et al. (2016a).

Dasygnypeta Lohse, 1974, sensu nov.

In his key to the genera of Tachyusini, Paśnik (2010) distinguished *Dasygnypeta*, with its single Palaearctic species *Dasygnypeta velata* (Erichson), from the Nearctic genera by the following features: the narrow and slender abdomen with base approximately as wide as head, the 'very deep' tergal impressions, abdominal pubes-
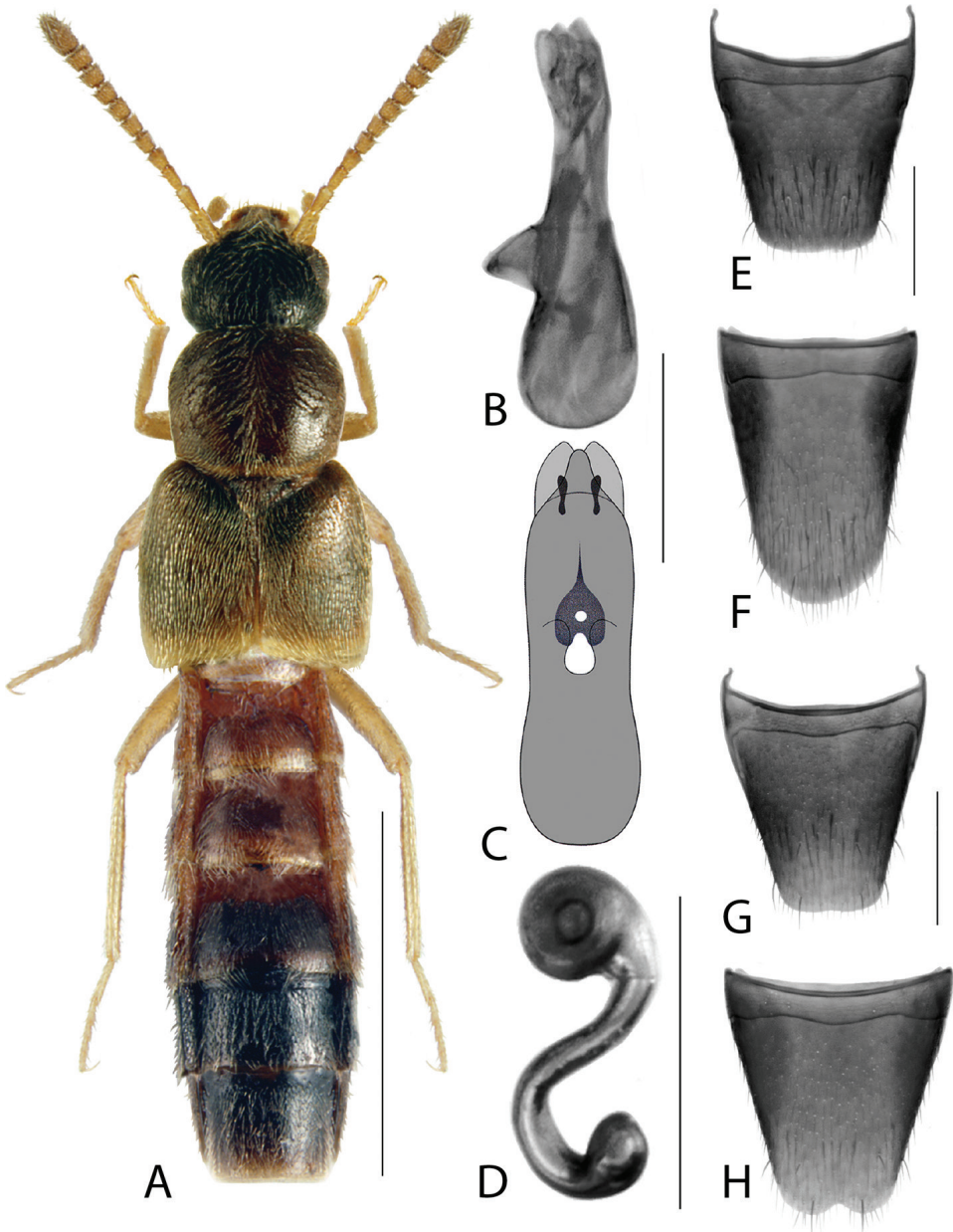
Figure 9. *Tachyusa obsoleta* Casey **A** habitus **B** median lobe of aedeagus in lateral view **C** median lobe of aedeagus in dorsal view (adapted from Paśnik 2006) **D** spermatheca **E** male tergite VIII **F** male sternite VIII **G** female tergite VIII **H** female sternite VIII. Scale bars: 1 mm (**A**); 0.2 mm (**B–H**). Illustrations after Klimaszewski et al. (2018), used with permission.

cence of tergites III–V directed posteriad, basal segment of metatarsus shorter than following two segments. Through an analysis of barcode data, we have discovered that the recently described *Gnypeta minuta* Klimaszewski & Webster is a synonym

of *D. velata* (see below). A re-examination of other Nearctic *Gnypeta* species re-vealed two others that are closely related to *D. velata*: *G. baranowskii* Klimaszewski, and *G. nigrella* (LeConte). Their morphological divergence from other *Gnypeta* was represented by an earlier placement in the 'Nigrella species group' of *Gnypeta* by Kli-maszewski et al. (2008), together with *G. saccharina* (now a synonym of *Paradilacra densissima*). In corroboration with morphology, DNA barcodes of *D. velata* and *G. nigrella* form sister clusters (sequences of *G. baranowskii* not available). Transfer of these two *Gnypeta* species to *Dasygnypeta* required a new concept for this genus as most of the distinguishing features were apomorphies of *D. velata* or found not to be of diagnostic value due to variability or overlap with other genera. Here we distinguish members of *Dasygnypeta* by their characteristic abdomen (Figs 10–12): base of abdomen ca. as wide as head; basal half of abdomen elongate, tergite III (first visible) only moderately transverse, ~ 2 × as wide as long (at least 2.5 × in *Gnypeta*); tergites III–V with very deep basal impressions, each creating strongly convex areas on the disc. Members of *Dasygnypeta* could be confused with *Tachyusa*, which also bears an elongate basal abdomen, but in the latter genus tergites III–V are far more elongate and the abdominal base is narrower than the head (Fig. 9). *Dasygnypeta nigrella* was even originally described by LeConte (1863) in *Tachyusa*, likely based on this similarity.

Dasygnypeta baranowskii (Klimaszewski, 2020), comb. nov.
Fig. 10A–H

Gnypeta baranowskii Klimaszewski, 2020

Distribution. Origin: Nearctic. **Canada**: BC.

Bionomics. The type series was collected by sifting litter (Klimaszewski et al. 2020).

Comments. We here transfer this species to *Dasygnypeta* sensu nov. based on morphology illustrated by Klimaszewski et al. (2020). This recently described western species is most similar to eastern *D. nigrella* based on the moderately elongate anten-nae, more robust body and the distinctive deep emargination of female sternite VIII. However, it is easily distinguished by the coarser pronotal punctation, and male and female genitalia (Fig. 10). The aedeagus of *D. baranowskii* is superficially similar to *P. densissima* but these taxa are externally quite different.

Dasygnypeta nigrella (LeConte, 1863), comb. nov.
BOLD:ACS6831
Fig. 11A–H

Tachyusa nigrella LeConte, 1863
Gnypeta nigrella: Klimaszewski et al. 2008
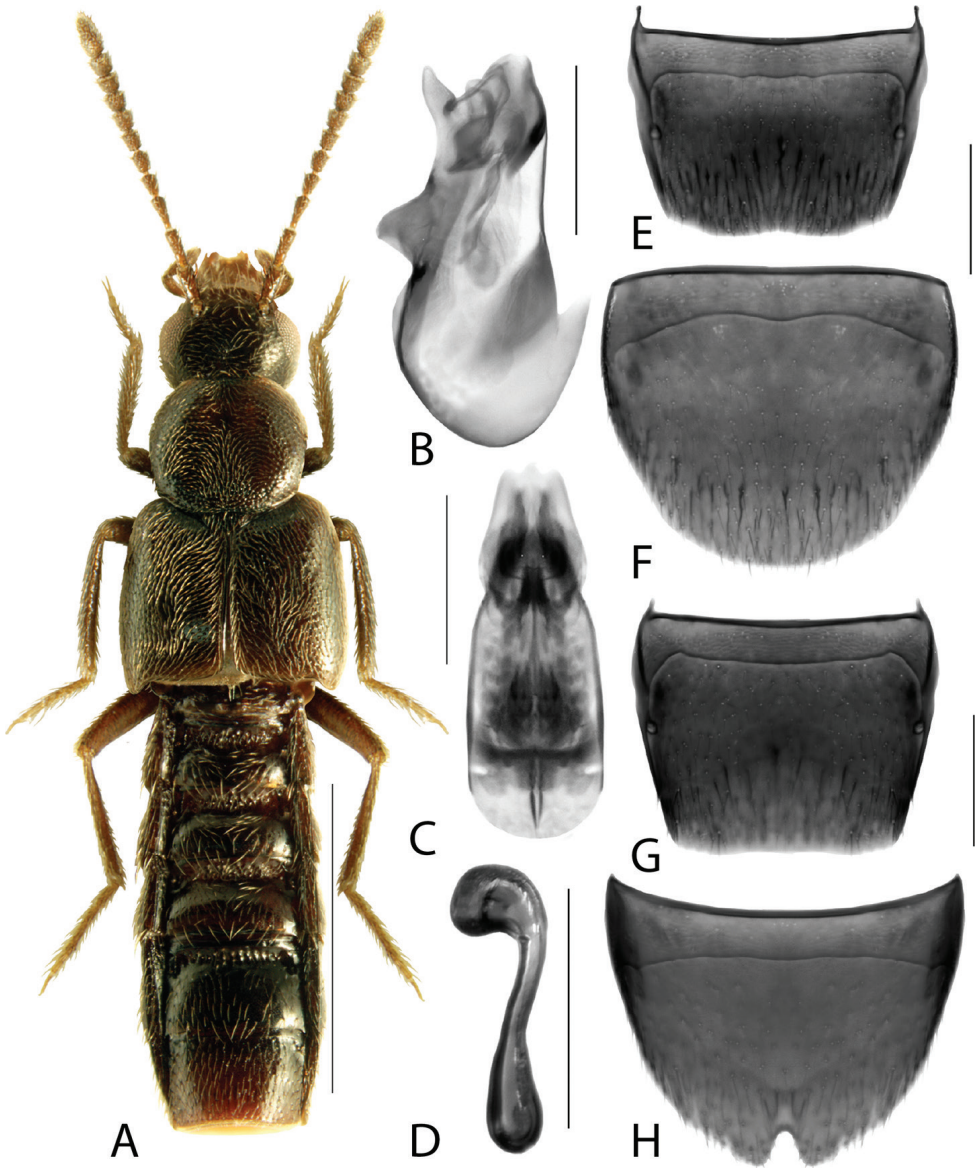
Figure 10. *Dasygnypeta baranowskii* (Klimaszewski) **A** habitus **B** median lobe of aedeagus in lateral view **C** median lobe of aedeagus in dorsal view **D** spermatheca **E** male tergite VIII **F** male sternite VIII **G** female tergite VIII **H** female sternite VIII. Scale bars: 1 mm (**A**); 0.2 mm (**B–H**). Illustrations after Klimaszewski et al. (2020), used with permission.

Material (DNA barcoded specimens). Canada: New Brunswick: York Co., Fredericton at St. John River, 45.959, -66.625, margin of river in drift (mostly maple seeds), 4.VII.2004, R.P. Webster (1, LFC).

Additional non-barcoded material. Canada: Manitoba: 5 miles SW of Shilo, 5.VI.1958, J.F. McAlpine (1, CNC); **Quebec:** Montreal, 30.VIII.1968, E.J. Kiteley
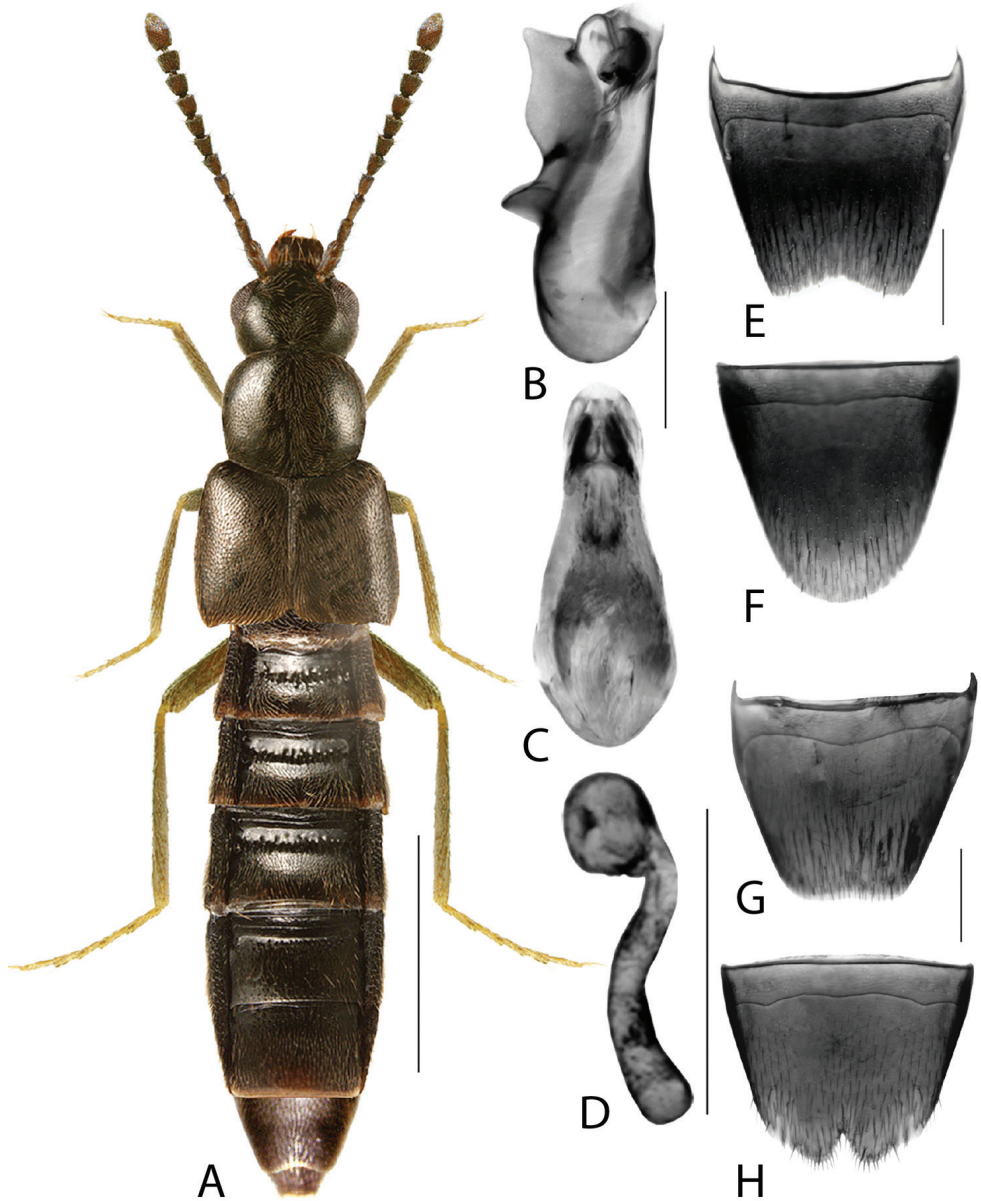
Figure 11. *Dasygnypeta nigrella* (LeConte) **A** habitus **B** median lobe of aedeagus in lateral view **C** median lobe of aedeagus in dorsal view **D** spermatheca **E** male tergite VIII **F** male sternite VIII **G** female tergite VIII **H** female sternite VIII. Scale bars: 1 mm (**A**); 0.2 mm (**B–H**). Illustrations after Klimaszewski et al. (2018), used with permission.

(1, CNC); Montreal 14.VI.1972, E.J. Kiteley (1, CNC); Berthierville, 5.VI.1976, E.J. Kiteley (3, CNC); Kazabazua, 15.VIII.1968, R.C. Lawrence (3, CNC); Wakefield, 4.VI.1930, W.J. Brown (1, CNC); Drummondville, 18.VII.1977, river mudflat, L. LeSage (5, CNC).

Distribution. Origin: Nearctic. **Canada**: MB [new record], NB, NF, ON, QC [new record]. **United States**: IL, MA, MD, NJ, NY, PA, VT, WV.

Bionomics. Collected along the edge of a variety of running and standing water-based habitats.

Comments. We here transfer this species to *Dasygnypeta* sensu nov. based on morphology and close clustering of DNA barcode sequences with *D. velata*. *Dasygnypeta nigrella* is a widespread species in eastern North America and is here newly reported from Manitoba and Quebec.

Dasygnypeta velata **(Erichson, 1837)**
BOLD:ACZ0581
Fig. 12A–H

Homalota velata Erichson, 1837
Gnypeta minuta Klimaszewski & Webster, 2008, syn. nov.

Material (DNA barcoded specimens). Germany: Thuringia, Ufergehoelze am Speicher Loessau, 50.5665, 11.894, 460 m, 1.I.2013, GBOL-Team ZFMK (1, ZFMK); Thuringia, NE, Freibad, Werraufer, 50.9768, 10.0963, 20.X.2014, GBOL-Team ZFMK (1, ZFMK). **United States: Alaska:** Selawik NWR, Kugarak River, 66.561, -158.996, mud bank, shore washing, 23.VI.2010, D.S. Sikes (3, UAM).

Additional non-barcoded material. Canada: Manitoba: 5 miles SW of Shilo, 5.VI.1958, J.F. McAlpine (2, CNC); **Northwest Territories:** Inuvik, 24.VI.1972, A. Smetana (1, CNC). **United States: Alaska:** Hess Creek, mi. 24 Wales Hwy, 1.VII.1978, J.M. Campbell and A. Smetana (1, CNC); Kenai Peninsula, Anchor River at Hwy 1, 450', 4.VI.1978, A. Smetana and E. Becker (1, CNC); mi. 1259 Alaska Hwy, 7.VII.1968, J.M. Campbell and A. Smetana (1, CNC).

Distribution. Origin: Holarctic. **Canada**: MB [new record], NB, NF, NT, SK. **United States**: AK.

Bionomics. Nearctic specimens have been collected most frequently along the margins of running water but also along the margins of a forest pool (Klimaszewski et al. 2018).

Comments. *Dasygnypeta velata* is newly reported from North America and was previously known in the Nearctic region under the synonym *Gnypeta minuta* (Klimaszewski et al. 2018). We here newly record this taxon from MB. *Dasygnypeta velata* is here considered a Holarctic species as it has a broad, transpalaearctic distribution (Europe to Siberia; Newton 2019), occurs along rivers and has been collected north of the treeline in Alaska.

This species has been collected together with *D. nigrella* in southern Manitoba (see above). The barcode sequences of the specimens from Alaska are all partial (386 to 407 bp), but the overlapping parts of the sequences are identical to the two German sequences.
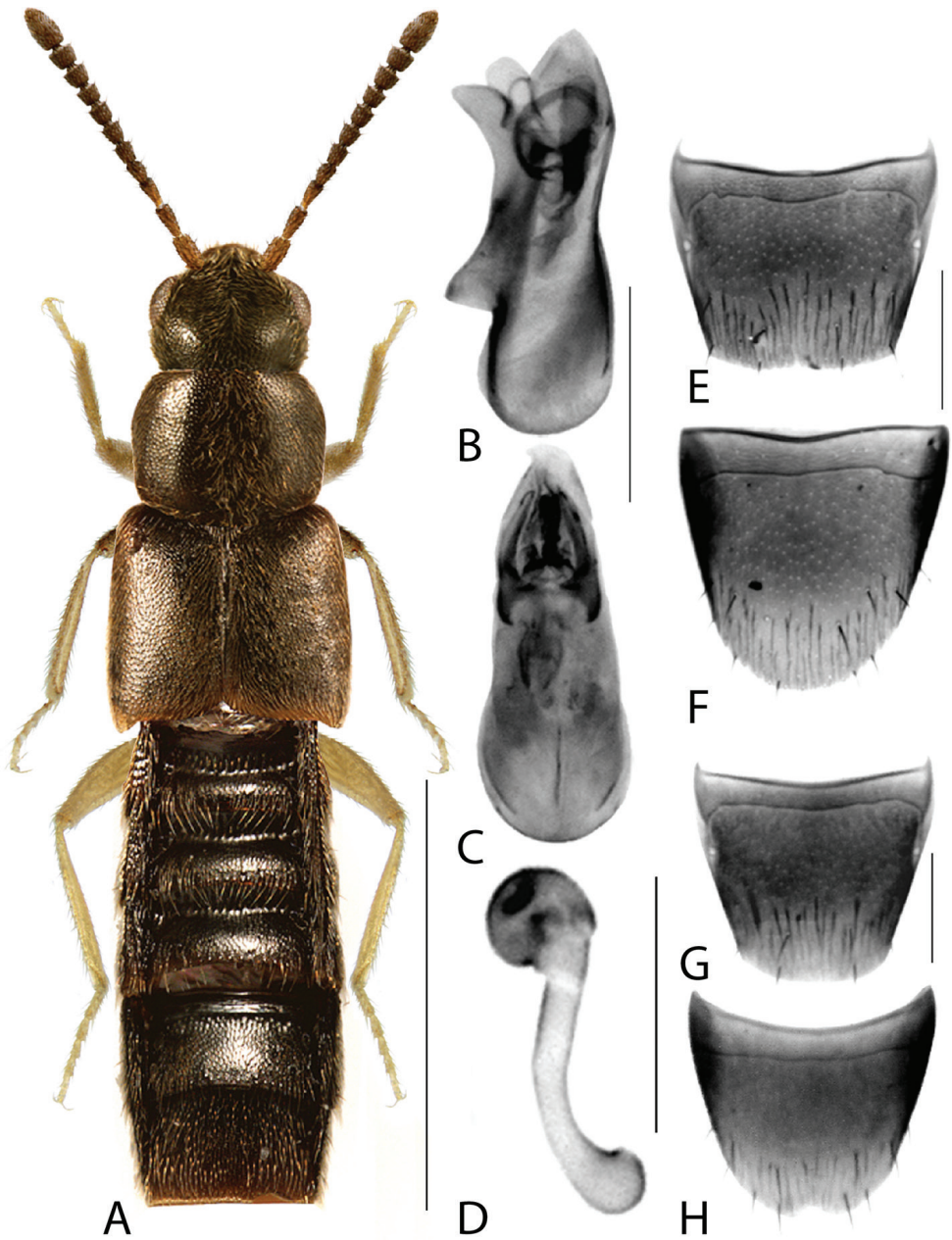
Figure 12. *Dasygnypeta velata* (Erichson) **A** habitus **B** median lobe of aedeagus in lateral view **C** median lobe of aedeagus in dorsal view **D** spermatheca **E** male tergite VIII **F** male sternite VIII **G** female tergite VIII **H** female sternite VIII. Scale bars: 1 mm (**A**); 0.2 mm (**B–H**). Illustrations after Klimaszewski et al. (2018), used with permission.

Gnypeta impressicollis Klimaszewski, Brunke & Pentinsaari, sp. nov.
http://zoobank.org/C6DC72D8-A182-43D3-9691-A352F0AF5D0E
BOLD:ADH7347
Fig. 13A–H

Type material. *Holotype.* (male, CNC): **Canada**, Ontario, Hartington, Eel Lake, South Frontenac, Paul Hebert's cottage property, 44.563°N, 76.549°W, 6.13.2017, Mikko Pentinsaari, Barcode of Life DNA voucher specimen, Sample ID: BIOUG34206-H01, Process ID: MPCAN465-17. *Paratypes* (3 CBG, 4 CNC): **Canada**, labelled as the holotype except: Sample ID: BIOUG34206-H02, Process ID: MPCAN466-17 (1 male, CBG); Sample ID: BIOUG34206-G12, Process ID: MPCAN464-17 (1 male, CBG); Sample ID: BIOUG34206-G11, Process ID: MPCAN463-17 (1 female, CBG). **United States: North Carolina:** Haywood Co., 3 mi N Dellwood, 19.VIII.1972, A. Smetana (3, CNC); **Maryland:** Patuxent Wildl. Res. Ctr., 5 km E Montpelier, treading pond vegetation, 16.VI.1982, Bousquet & Davies (1, CNC).

Etymology. The species epithet refers to the longitudinal impression on the pronotum, most strongly developed in males.

Diagnosis. *Gnypeta impressicollis* can be easily distinguished from all Nearctic species of the genus (except eastern *G. baltifera* (LeConte)) by the hexagonal pronotum with a longitudinal impression in the basal half (females) to nearly entire pronotal length (males). Males also have an impression on the vertex of the head. We have examined the female type of *G. baltifera* and it is externally similar but differs by the shorter, less angulate hexagonal pronotum, reddish and longer elytra and spermatheca with an elongate stem (C-shaped in *G. impressicollis*).

Description. Body length 3.2–3.4 mm; colour dark brown, elytra brown with irregular rust-brown patches, first two or three basal tergites rust-brown with posterior edge yellow, apex of abdomen rust-brown, legs and antennae rust-brown; integument highly glossy (Fig. 13A); pubescence yellowish grey, moderately long and moderately sparse; all antennomeres distinctly elongate; head round with short neck (visible only when head is distended from thorax), vertex in males with broad central impression, vertex of females with much smaller and narrower median impression, maximum width of head slightly less than maximum width of pronotum; pronotum hexagonal in shape, ca. as long as head, with a longitudinal impression in the basal half (females) to nearly entire pronotal length (males), pubescence on disc directed anteriad along midline and obliquely laterad elsewhere; elytra wider than either head or pronotum, at suture shorter than pronotum along midline, pubescence directed obliquely posteriad forming wavy pattern medially on each side; abdomen arcuate laterally, broadest in apical third, at base distinctly narrower than elytra; legs very long, hind tarsus with basal tarsomere ca. as long as the two following ones combined. MALE. Tergite VIII with apical margin truncate medially and arcuate laterally (Fig. 13E); sternite VIII elongate, narrowed apically, apex truncate medially and oblique laterally (Fig. 13F); median lobe of aedeagus in lateral view with tubus very short, triangular and gradually tapering to narrowly rounded apex, ventral margin broadly curved ventrad in apical half (Fig. 13B);
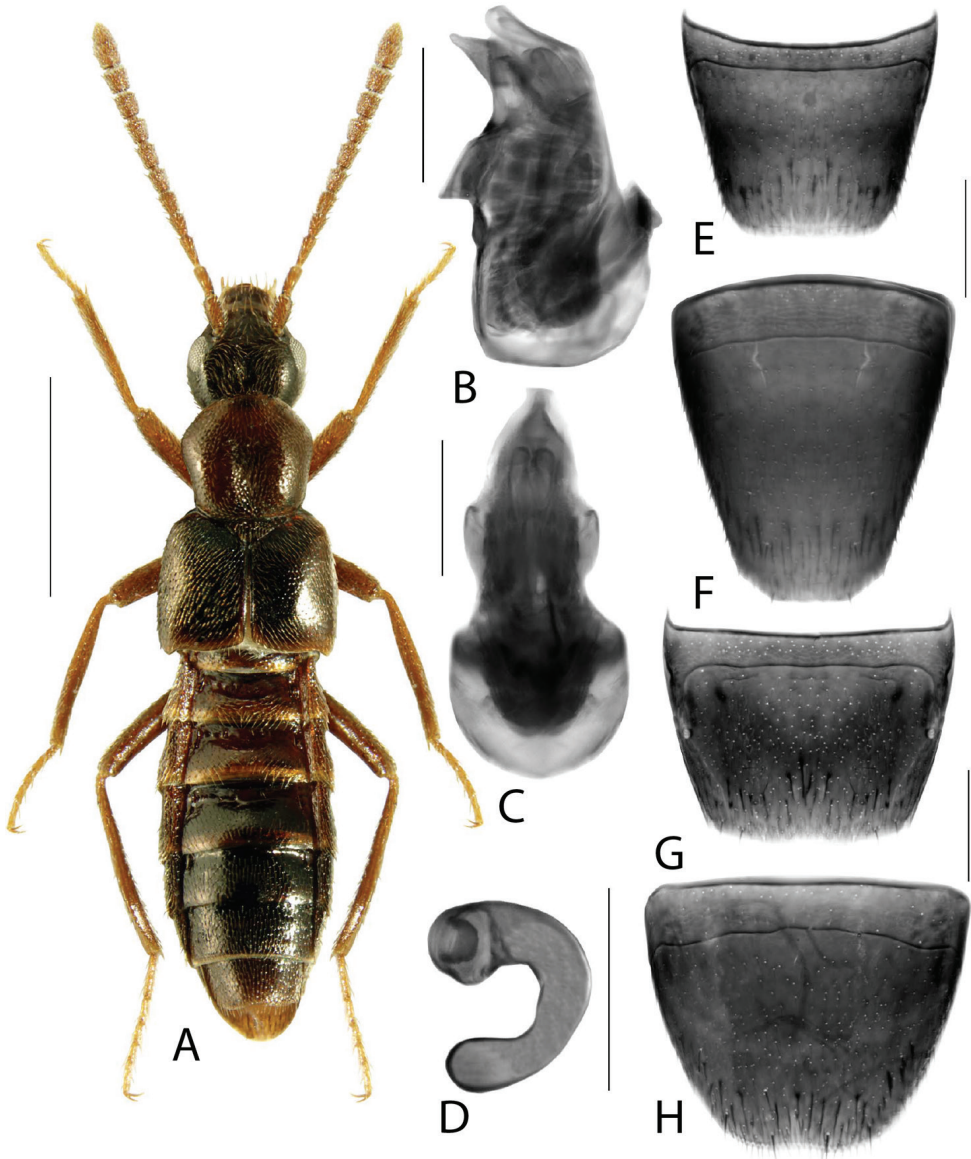
Figure 13. *Gnypeta impressicollis* Klimaszewski, Brunke & Pentinsaari, sp. nov. **A** habitus **B** median lobe of aedeagus in lateral view **C** median lobe of aedeagus in dorsal view **D** spermatheca **E** male tergite VIII **F** male sternite VIII **G** female tergite VIII **H** female sternite VIII. Scale bars: 1 mm (**A**); 0.2 mm (**B–H**).

in dorsal view bulbus moderately large and tubus swelled basally and triangular apically (Fig. 13C); internal sac with complex membranous structures (Fig. 13B,C). FEMALE. Tergite VIII broadly arcuate apically (Fig. 13G); sternite VIII rounded apically with very shallow median emargination (Fig. 13H); spermatheca C-shaped, capsule sub-spherical with broad apical invagination, stem tubular and C-shaped (Fig. 13D).

Distribution. Origin: Nearctic. **Canada**: ON. **United States**: MD, NC. *Gnypeta impressicollis* is probably broadly distributed in eastern North America.

Bionomics. Specimens were collected by sifting leaf litter along a lake margin and by treading pond vegetation.

Comments. It was challenging to place this species in either *Gnypeta* or *Ischnopoda* Stephens based on the concepts of Pašnik (2010). The extremely long legs, pronotal shape, C-shaped spermatheca and superficial punctation of the pronotum and abdomen are consistent with at least some Neotropical members of *Ischnopoda* but the ligula of *G. impressicollis* is divided to the base, which is considered to be a feature of *Gnypeta* (Pašnik 2010). The C-shaped spermatheca of *Gnypeta impressicollis* also bears some similarity to the *G. crebrepunctata* group of Klimaszewski et al. (2008) but it is rather different in external morphology. We place this species in *Gnypeta* pending future systematic research.

Tribe Hypocyphtini Laporte, 1835

Oligota parva Kraatz, 1862
BOLD:AAP9955
Fig. 14A–G

Material (DNA barcoded specimens). Germany: Bornheim-Hemmerich, Ortslage, 50.7596, 6.93151, 30.VII.2010, F. Koehler (2, ZSM); Bornheim-Hemmerich, Ortslage, 50.7596, 6.93151, 25.VIII.2013, GBOL-Team ZFMK (1, ZFMK); Wutha-Farnroda, Wartburgkreis, 50.947, 10.4214, 25.VIII.2012, GBOL-Team ZFMK (2, ZFMK). **Canada: Ontario:** Kawartha Lakes, 44.296, -78.452, farm, malaise trap, 24.VII.2015, B. McClenaghan (1, CBG); same except 19.VII.2016 (1, CBG); Guelph, Arboretum, Urban Organic Farm, 43.5381, -80.222, compost heaps and mouldy hay pile, 17.IX.2017, M. Pentinsaari (4, CBG).

Distribution. Origin: West Palaearctic (adventive in North America). **Canada**: NB, ON [new record], PE. **United States**: CA, MA, MO, NV, TX.

Bionomics. This species is generally found in anthropogenic habitats, including compost, dung, and old hay and grass (Klimaszewski et al. 2018). In Canada, it has been collected in compost and in ocean coastline drift at the top of the littoral zone (Klimaszewski et al. 2018).

Comments. *Oligota parva* is a cosmopolitan species that is adventive in Canada. Here we newly report it from Ontario.

Oligota pumilio Kiesenwetter, 1858
BOLD:AAN4271
Fig. 15A–C

Material (DNA barcoded specimens). Belgium: Blanden, BR Meerdaalboos, 50.7976, 4.71622, 8.V.2010, F. Koehler (1, ZSM). **Germany:** Neuburg, Altrheine,
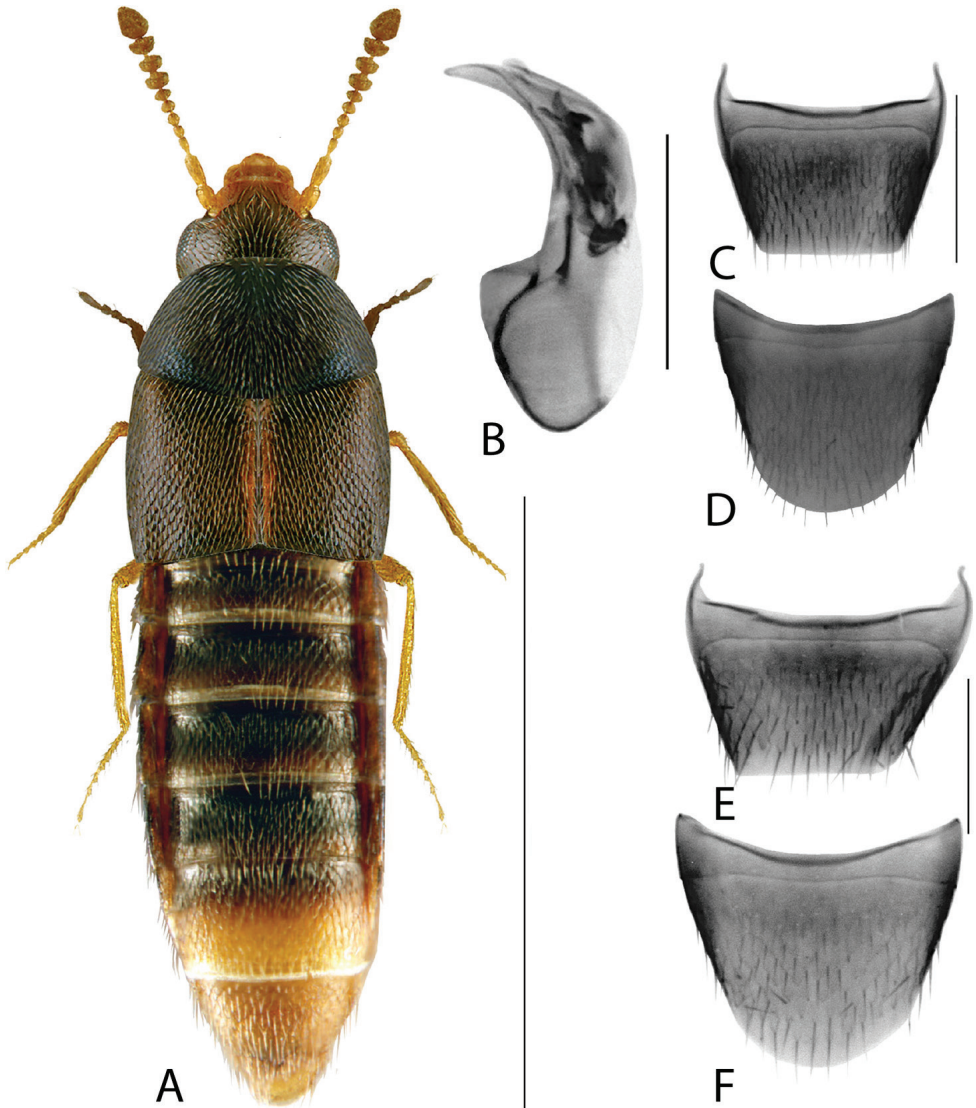
Figure 14. *Oligota parva* Kraatz **A** habitus **B** median lobe of aedeagus in lateral view **C** male tergite VIII **D** male sternite VIII **E** female tergite VIII **F** female sternite VIII. Scale bars: 1 mm (**A**); 0.2 mm (**B–F**). Illustrations after Webster et al. (2016).

48.9943, 8.24412, 29.IX.2011, F. Koehler (2, ZSM); Erftstadt-Bliesheim, NWZ Altwald Ville, 50.792, 6.844, 4.X.2010, F. Koehler (1, ZSM); Jockgrim, Sandmagerrasen, 49.0805, 8.26568, 14.XI.2010, F. Koehler (1, ZSM); Ochtendung, Michelsberg, 50.3631, 7.3889, 17.III.2012, F. Koehler (1, ZSM); Edenkoben-Rhodt, Villa Ludwigshoehe, 49.2767, 8.08991, 20.V.2012, F. Koehler (1, ZSM); Bad Muenster-Traisen, Rotenfels, 49.822, 7.832, 20.V.2012, F. Koehler & J. Koehler (1, ZSM); Osterholz bei
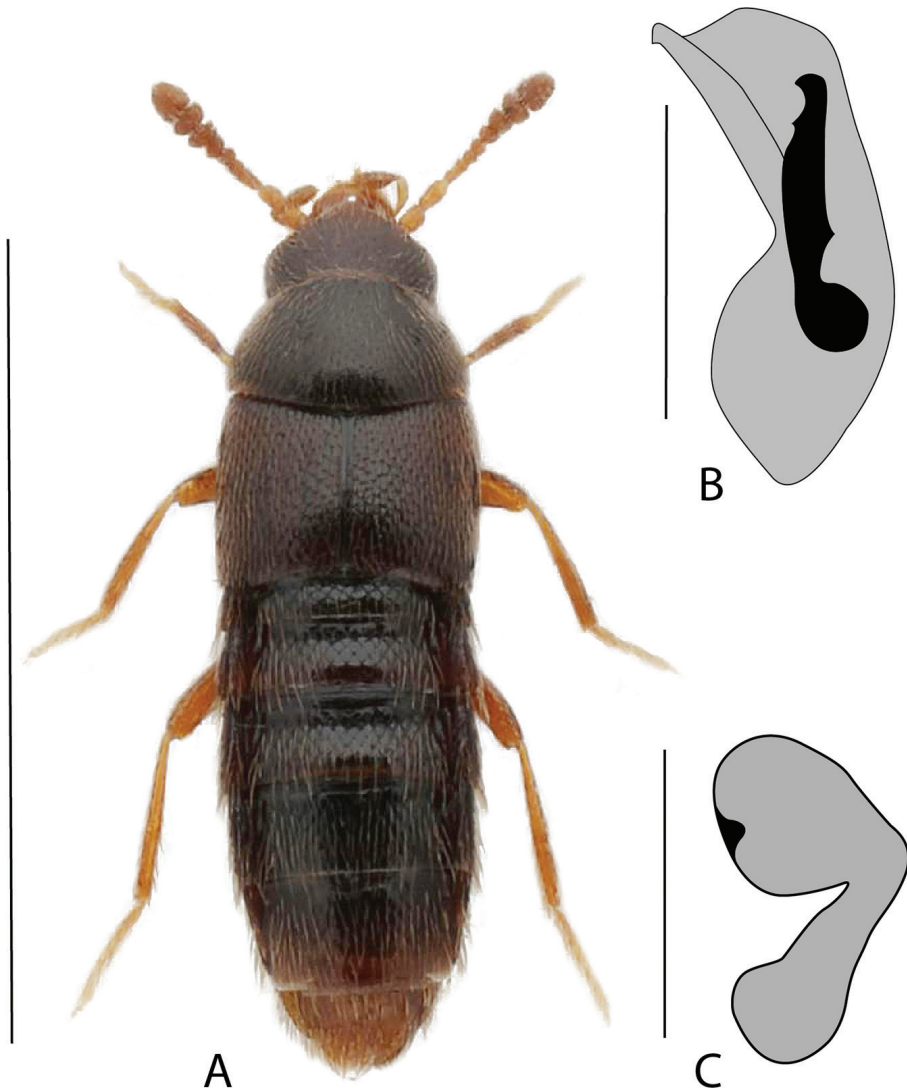
Figure 15. *Oligota pumilio* Kiesenwetter **A** habitus (image by A. Bogri – www.BilleBank.dk) **B** median lobe of aedeagus in lateral view (drawn from Kapp 2019) **C** spermatheca (drawn from Kapp 2019). Scale bars: 1 mm (**A**); 0.2 mm (**B, C**).

Blankenburg, 51.9519, 11.0526, 18.III.2015, GBOL-Team ZFMK (2, ZFMK). **Canada: Alberta:** Waterton Lakes National Park, Red Rock Parkway, 49.088, -113.883, Moraine grassland, intercept trap, 1328 m, 11.VIII.2012, BIOBus 2012 (1, CBG). **United States: Montana:** Missoula County, Florence, MPG Ranch, 46.702, -114.034, grassland, pitfall trap, 05.VI.2019, M. Seidensticker (1, CBG).

Distribution. Origin: West Palaearctic (adventive in North America). **Canada**: AB [new record]. **United States** (all except MT need verification): DC, IL, OH, MT [new record].

Diagnosis. Among Canadian species of *Oligota*, *O. pumilio* is extremely similar to *O. pusillima* in the narrow, parallel body (Fig. 15A) and in male and female genitalia (Klimaszewski et al. 2018). However, it can be distinguished by the more abruptly truncate apex of the median lobe in lateral view (Fig. 15B), differently shaped sclerites of the internal sac (Fig. 15B), medially projected apex of male sternite VIII, and the transverse capsule of the spermatheca (Fig. 15C) (Kapp 2019).

Bionomics. This species occurs in a wide variety of habitats across a broad elevational range, including hollow trees, plant debris, old hay in cattle barns, moldy substrates and in mushrooms (Kapp 2019). The barcoded Nearctic specimens were collected from grassland habitats by an intercept trap (Alberta) and a pitfall trap (Montana).

Comments. *Oligota pumilio* is a West Palaearctic species that is adventive in Canada. Although it has been previously reported from the United States (OH, IL, DC) (Newton 2019), these records need confirmation as they are in the east, some distance away from the present records. This species' presence in North America is thus verified here for the first time, from both Canada (AB) and United States (MT). It has also been reported as adventive from Argentina, Chile, and New Zealand (Newton 2019). The barcoded specimens of *O. pumilio* from Canada and the United States share the same DNA barcode haplotype, which is also shared by some of the specimens from Germany.

Oligota pusillima (Gravenhorst, 1806)
BOLD:ABW7320
Fig. 16A–G

Material (DNA barcoded specimens). Finland: Oba: Oulu, Hietasaari, 65.0225, 25.4247, 22.IV.2011, M. Pentinsaari (1, ZMUO); **Germany:** Edenkoben-Rhodt, Villa Ludwigshoehe, 49.277, 8.09, 20.V.2012, F. Koehler (2, ZSM); Edenkoben-Rhodt, Villa Ludwigshoehe, 49.277, 8.09, 23.VI.2012, F. Koehler (2, ZSM); Zweibruecken-Mauschbach, Monbijou-Wald, 49.2038, 7.39891, 16.X.2011, F. Koehler & W. Koehler (1, ZSM). **Canada: Alberta:** Two Hills, Two Hills School EQP-CLL-553, 53.7104N, 111.7437W, 613 m, Malaise trap, 21.IX.–2.X.2015, K. Warawa (2, CBG).

Additional non-barcoded material. Ontario: Ottawa, Ottawa River, Deschênes Lookout, Berlese flood debris, 1.V.1985, A. Davies (1, CNC).

Distribution. Origin: West Palaearctic (adventive in North America). **Canada**: AB [new record], NB, ON [new record]. **United States**: MA, NY.

Bionomics. This species occurs in a variety of moist to dry, decaying organic matter including rotting hay, compost, hollow trees, and ant nests (Kapp 2019). Canadian specimens were collected in compost (Webster et al. 2016), and in malaise traps and flood debris in a suburban setting (present study).

Comments. *Oligota pusillima* is a Palaearctic species that has been introduced to North America, South America, Australia, Africa, and southeast Asia (Kapp 2019, Newton 2019). It is here reported from Ontario and Alberta for the first time, the latter representing the westernmost record in North America. Specimens from Alberta
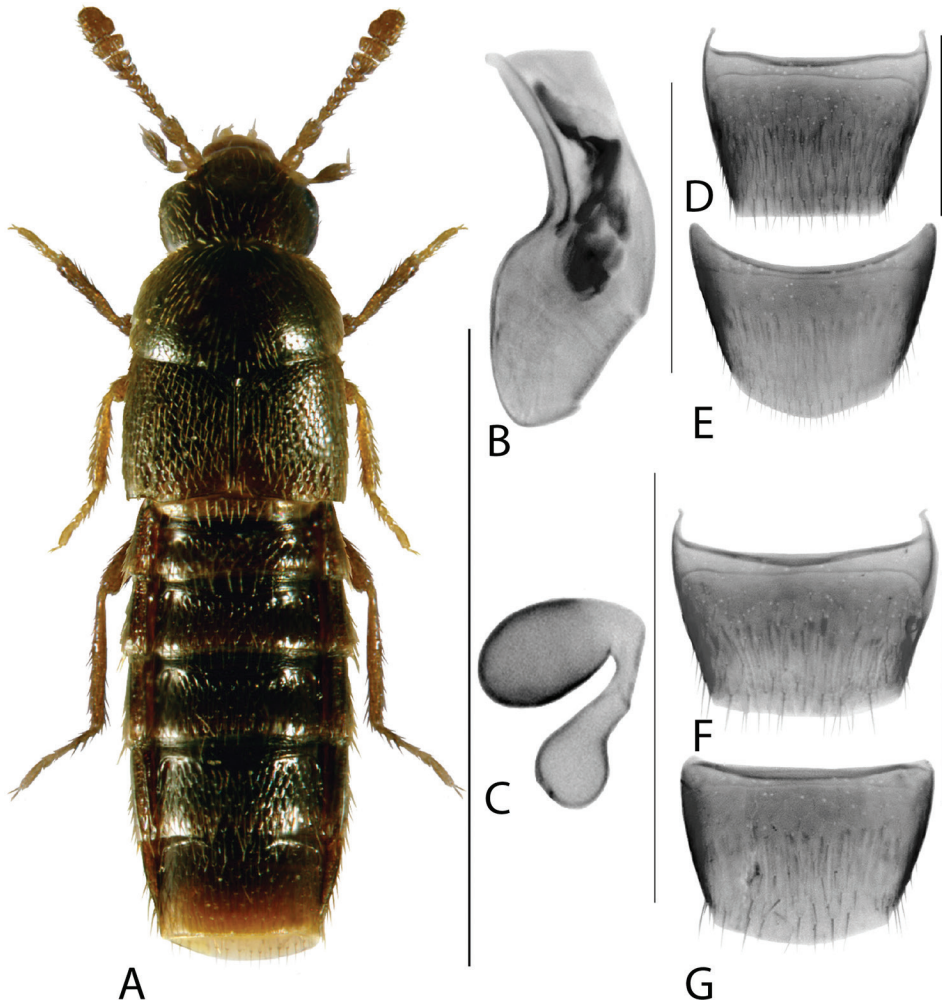
Figure 16. *Oligota pusillima* (Gravenhorst) **A** habitus **B** median lobe of aedeagus in lateral view **C** spermatheca **D** male tergite VIII **E** male sternite VIII **F** female tergite VIII **G** female sternite VIII. Scale bars: 1 mm (**A**); 0.2 mm (**B–G**).Illustrations after Webster et al. (2016).

were sequenced and their barcodes match those of Palaearctic specimens with no divergence. These specimens were also morphologically consistent with *O. pusillima*.

Homalotini Heer, 1839

Anomognathus athabascensis **Klimaszewski, Hammond & Langor, 2016**
Fig. 17A–G

Material. Non-sequenced specimens. **Canada: Manitoba:** Winnipeg, under bark of rotten 'N. aceroides' [= *Acer negundo*], 27.VIII.1918, J.B. Wallis (2, CNC).
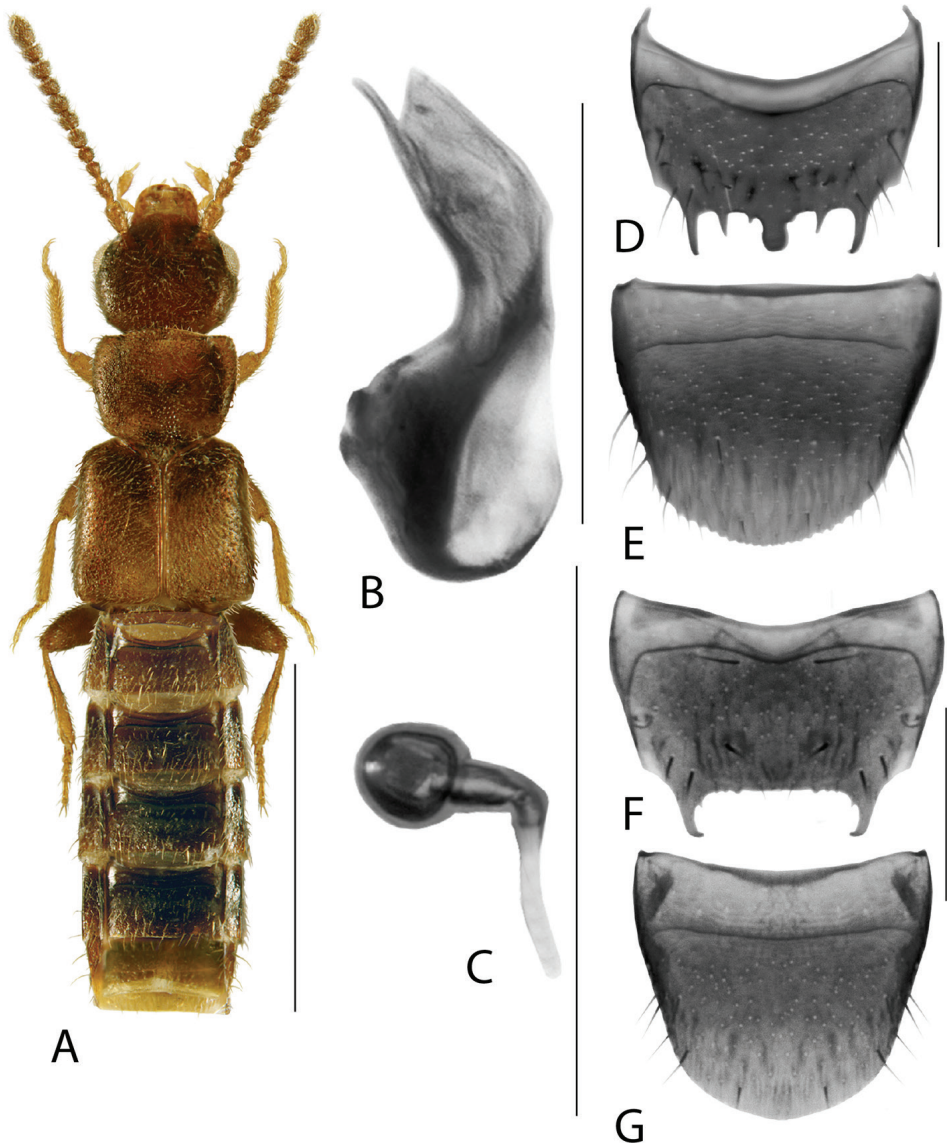
Figure 17. *Anomognathus athabascensis* Klimaszewski, Hammond & Langor **A** habitus **B** median lobe of aedeagus in lateral view **C** spermatheca **D** male tergite VIII **E** male sternite VIII **F** female tergite VIII **G** female sternite VIII. Scale bars: 1 mm (**A**); 0.2 mm (**B–G**). Illustrations after Klimaszewski et al. (2016b).

Distribution. Origin: Nearctic. **Canada**: AB, MB [new record].

Bionomics. The MB specimens were collected under bark, confirming that this species lives in a way similar to other members of the genus.

Comments. *Anomognathus athabascensis*, recently described from Alberta (Klimaszewski et al. 2016b), is newly reported from Manitoba. This native Nearctic species is likely transcontinental but rarely reported due to its small size and elusive habits.

Anomognathus cuspidatus (Erichson, 1839)
BOLD:AAO0339
Figs 18A–D, 19A–D, 20A–D.

Homalota cuspidata Erichson, 1839
Thectura americana Casey, 1893, syn. nov.
Anomognathus americanus: Seevers (1978) (as valid species)

Type material. *Homolota cuspidata* Erichson, 1839. **Lectotype**, male, here designated (ZMHB): *cuspidata* Er: [handwritten label] / 5387 [typed label] / Hist.-Coll. (Coleoptera), Nr. 5387, *Homalota cuspidata*, Erichs., Europa, Zool. Mus. Berlin [typed white label] / Lectotype *Homalota cuspidata* des. J. Klimaszewski 2019 [white printed label]. **Paralectotypes** (3, ZMHB, without original labels): Hist.-Coll., (Coleoptera), Nr. 5387, *Homolota cuspidata* Erichs., Europa, Zool. Mus. Berlin; Syntype *Homolota cuspidata* Erichson, 1837, labelled by MNHUB 2010; Paralectotype *Homalota cuspidata* des. J. Klimaszewski 2019 [white printed label] [1 female, spermatheca and terminalia dissected in Canada balsam on microslide attached to specimen]; same labels except: SYNTYPUS, *Homalota cuspidata* Erichson, 1837 [typed red label, added by MNHUB 2010] [1 female, spermatheca and terminalia dissected in Canada balsam on microslide attached to specimen]; same labels as before [1 damaged specimen, sex undetermined].

Males and females of the syntype series were morphologically consistent with the specimens forming molecular cluster BOLD:AAO0339, including those sequenced from Ontario, Canada. As the most obvious difference between *A. cuspidatus* and the potential new Central European species (see Diagnosis) was the shape of the median process on male tergite VIII (in lateral view) (Fig. 18B, D), a male syntype (see above) was designated as the lectotype of this species to fix its identity. Morphology of the aedeagus itself was difficult to study due to its small size and obvious differences between molecular clusters (see below) were not observed (Fig. 19).

Thectura americana Casey, 1893, syn. nov. Holotype (male) (NMNH): NY/ TYPE USNM 39614/ *Thectura americana* Casey (handwritten by Casey).

Casey (1893) gave numerous characters to distinguish *A. americanus* from *A. cuspidatus* but all of these were observed to be highly variable within populations in the material studied, including the shape of apical antennomeres, shape of the pronotum, position of the abdominal tubercles in the male, and the type of dorsal expansion of the median process of male tergite VIII. We could not find the depression at the base of tergite VIII on the holotype of *A. americanus* mentioned by Casey (1893). Although the aedeagus of the holotype was not studied (not extracted from partly damaged and fragile pygidium), male tergite VIII was intact and its median process in lateral view bears an apical hook, matching the present concept for *A. cuspidatus* (Fig. 20). Therefore, in corroboration with Fenyes (1918), we treat *A. americanus* as a synonym of *A. cuspidatus*.

Non-type material (sequenced specimens indicated in square brackets). Canada: Alberta: Peace River, 25 km NW Peace River, 17–23.VIII.1993, J. Hammond (2, CNC); **Ontario:** Wellington County, Guelph, Eramosa River Trail, 43.539, -80.236, deciduous forest, 14.IV.2017, M. Pentinsaari (4, CBG [4 barcoded]).

Figure 18. A, B *Anomognathus cuspidatus* (Erichson), and **C, D** *Anomognathus* sp., putative undescribed species (Europe) **A, C** habitus and **B, D** male tergite VIII in lateral view. Scale bars: 1 mm (**A, C**); 0.2 mm (**B, D**).

A photo record of this species from Ontario is available on bugguide.net (/view/1816108): Toronto, 19.V.2020, under bark, O. Strickland.

Belgium: Sint-Genesius-Rode, BR Zonienwoud, 50.7505, 4.423, 28.IV.2010, F. Koehler (1, ZSM [1 sequenced]). **Czech Republic (all CNC):** Bohemia, Poděbrady
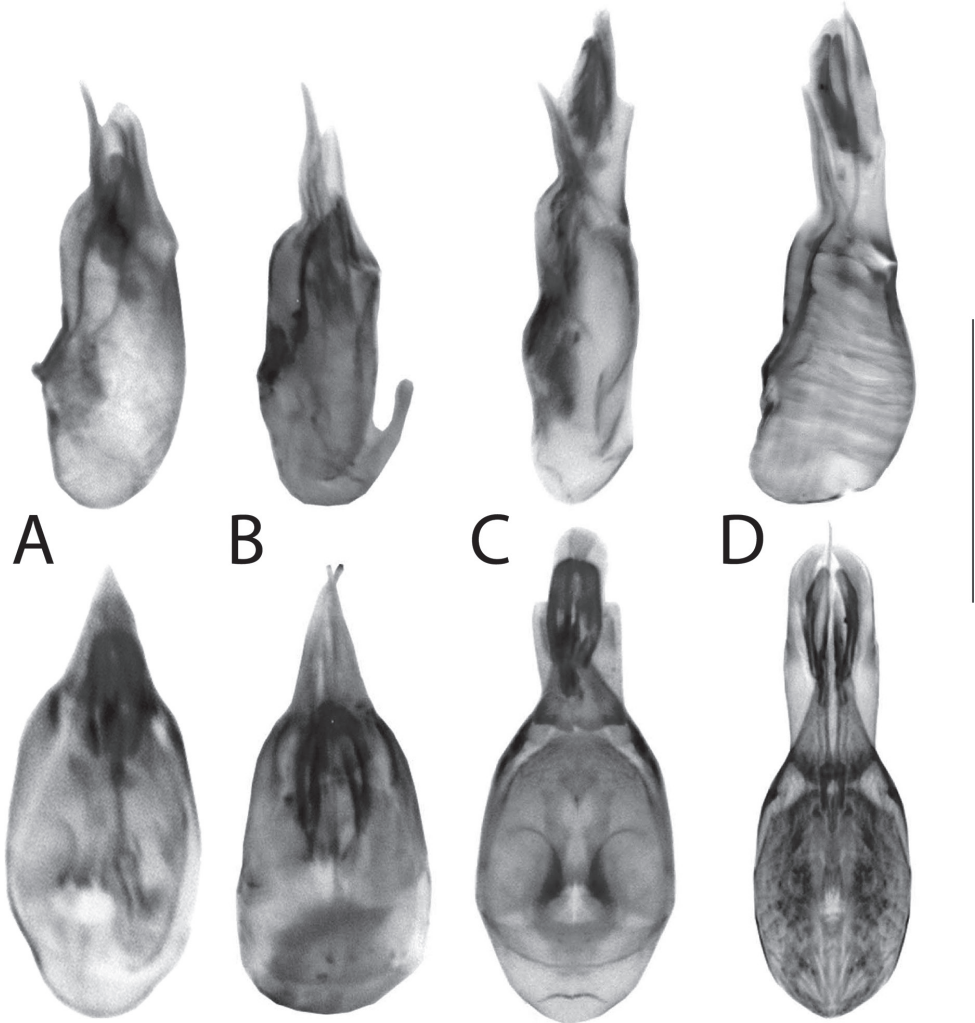
Figure 19. Aedeagi of **A–C** *Anomognathus cuspidatus* (Erichson) and **D** potential undescribed species, in lateral view (top row) and dorsal view (bottom row) **A** sequenced non-type (Ontario, Canada) **B** lectotype of *A. cuspidatus* ('Europe') **C, D** sequenced non-types (Finland). Scale bar: 0.2 mm.

50 km, Smetana, 1959, car net trap (1); Bohemia, Chvojno, Smetana (1); Moravia, Drnholec, Smetana (1). **Denmark (all NHMD):** Staksrode, EJ, 24.IX.1983 (1); Æbelø F, 18.V.1997 (1); Faested Mose, SJ, 12.IV.1986 (1); Dyrehaven, 14.4.1934 (1); same except 21.3.1923 (1); same except 21.10.1932 (1); 30.4.1922 (1); same except 19.5.1911 (1); Lyng Huse, 29.3.1997 (1).

Germany: Nationalpark Mueritz, Babke-Zartwitz-Speck-Schwarzenhof, 53.4125, 12.8463, car net, 20.VI.2015, GBOL-Team ZFMK (2, ZFMK [2 sequenced]); Hoenningen bis Insul, Ahrtal, 50.45, 6.942, 24.IV.2010, F. Koehler (1, ZSM [1 sequenced]); Oberheimbach, Franzosenkopf, 50.004, 7.805, 27.V.2012, W. Koehler (1,
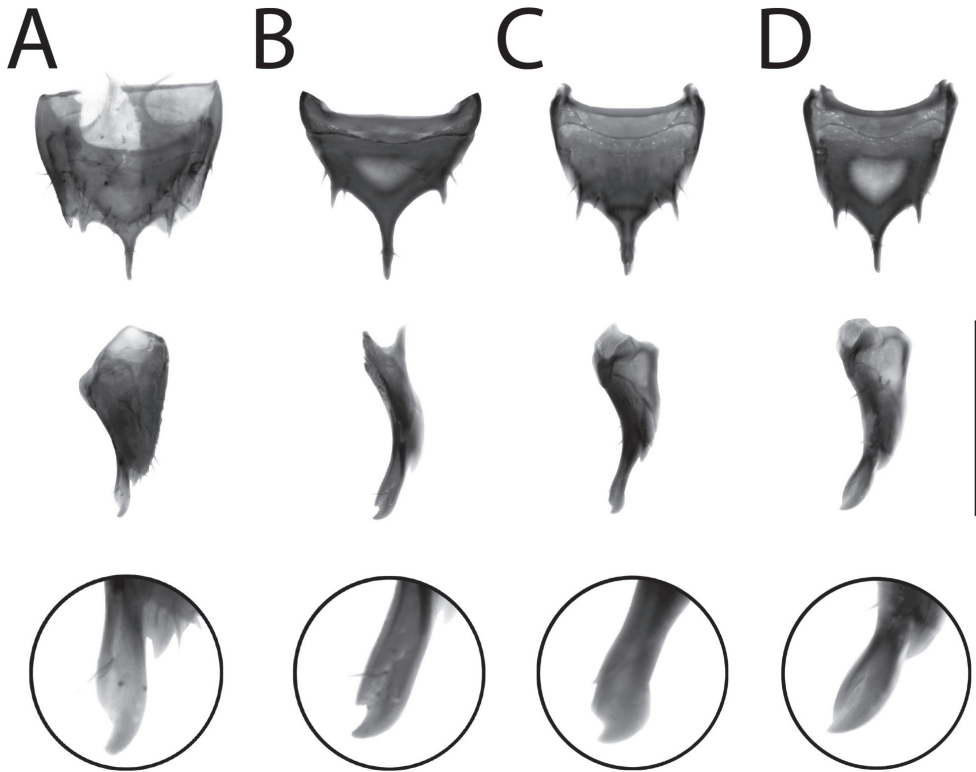
Figure 20. Male tergite VIII of **A–C** *Anomognathus cuspidatus* (Erichson) and **D** potential undescribed species, in dorsal (top row) and lateral (middle and bottom rows) **A** lectotype of *A. cuspidatus* ('Europe') **B** holotype of *A. americanus* (Casey) (= *A. cuspidatus*) **C, D** sequenced, non-types (Finland). Scale bar: 0.2 mm.

ZSM [1 sequenced]). **Finland (all ZMUO):** N: Espoo, Saunalahti, 60.1643, 24.6263, 17.IX.2012, fungusy aspen logs, E. Helve (1) [barcoded]; Al: Bjoerkoe, 59.9769, 20.1879, sifting, 24.IX.2014, M. Pentinsaari (1) [barcoded]; Ta: Lammi, R. Linnavuori leg. (1); Ab: Naantali, R. Linnavuori leg. (1); Kb: Lieksa, R. Linnavuori (1); Rynmattyla, 24.VI.1945, Karvonen (2); same except 14.VIII.1945 (2). **Slovakia (all CNC):** Cenkov, Smetana, 1963 (11); Nová Sedlica, Smetana, 1961 (2); Ruská Poruba, Smetana, 1956 (2). **United Kingdom (all CNC):** Essex (6).

Putative undescribed *Anomognathus* (corresponding to BIN BOLD:ACA9191):

Finland (all ZMUO): N: Espoo, E. Helve, 1978 (1); same except 1976 (1); same except 1977 (1); same except 1979 (1); same except 1981 (1); same except 1982 (1); Ks: Taivalkoski, 728.53 Window trap, 2003, E. Hurme (2); same except *Polyporus* trap (1); Kb, Kitee, 23.05.2016, M. Pentinsaari leg., [1 sequenced]; Obb: Rovaniemi, Rovajärvi, 16.6–8.7.2010, M. Pentinsaari and E. Kuusela [1 sequenced]. **Germany:** Schleiden-Wolfgarten, Dachsloecher, 50.6098, 6.42237, 26.VII.2012, F. Koehler (1, ZSM [1 sequenced]).

Diagnosis. *Anomognathus cuspidatus* is distinctive for its trident-shaped apex of male and female tergite VIII (Fig. 20A–C) and can be distinguished from all described

species by this feature alone. However, in the course of this study, specimens representing a remarkably divergent barcode cluster (BOLD:ACA9191; 9.63% uncorrected p-distance to *A. cuspidatus*) were investigated and found to likely represent an undescribed species of *Anomognathus* in Europe (confirmed specimens from Finland and Germany). Although most morphological characters of *A. cuspidatus* and the putative new species are highly variable, including the median lobe of the aedeagus, males can be dependably separated based on the shape of their median process of tergite VIII in lateral view: *A. cuspidatus* bears a minute to distinct hook at the apex (Fig. 20A–C), while in the undescribed species, the median process converges evenly to a single point, creating an elongate, turnip-shape (Fig. 20D). The shape of tergite VIII in females was observed to be extremely variable and no features were deemed to be diagnostic. Externally, most specimens can be recognized as either species (especially males) by the relative proportions of the head versus the pronotum, with *A. cuspidatus* generally bearing a small pronotum, narrower than the head (Fig. 18A) and the undescribed species bearing a wider, longer pronotum, wider than the head (Fig. 18C). The limits of this taxon need further investigation and should include morphological study of a much wider range of sequenced material.

Distribution. Origin: West Palaearctic (adventive in North America). **Canada**: AB, NB, ON. **United States**: NY.

Bionomics. This species occurs under the bark of dead trees. One specimen (NB) was collected from a Lindgren funnel.

Comments. *Anomognathus cuspidatus* is a widespread West Palaearctic species that is known from Europe, European Russia and Algeria (Newton 2019) and has been previously known in North America under the synonym *A. americanus*. The record from Beijing, China should be verified. The species has become introduced in North America (before 1893) and it is unclear whether the population in Alberta represents a separate introduction from Europe, a secondary introduction from eastern North America or a broad adventive distribution across Canada.

After the results of the present study, two species of *Anomognathus* are known to occur in North America: native *A. athabascensis* Klimaszewski, Hammond & Langor and the adventive *A. cuspidatus*. These are easily separated by the drastically different shapes of male and female tergites VIII (Figs 17D, 20A–C). Previously, only females of *A. cuspidatus* (as *A. americanus*) were available from Canada (Klimaszewski et al. 2016b; Webster et al. 2016). Here we demonstrate that all available Nearctic *Anomognathus* specimens with a trident-shaped tergite VIII correspond to Palaearctic *A. cuspidatus*.

Cyphea wallisi Fenyes, 1921
BOLD:ACK1459
Figs 21A–G, 22A–D

Cyphea wallisi Fenyes, 1921
Agaricomorpha vincenti Klimaszewski & Webster, 2016, syn. nov.
Agaricomorpha vincenti: Klimaszewski et al. 2018 (as synonym of *C. curtula*)
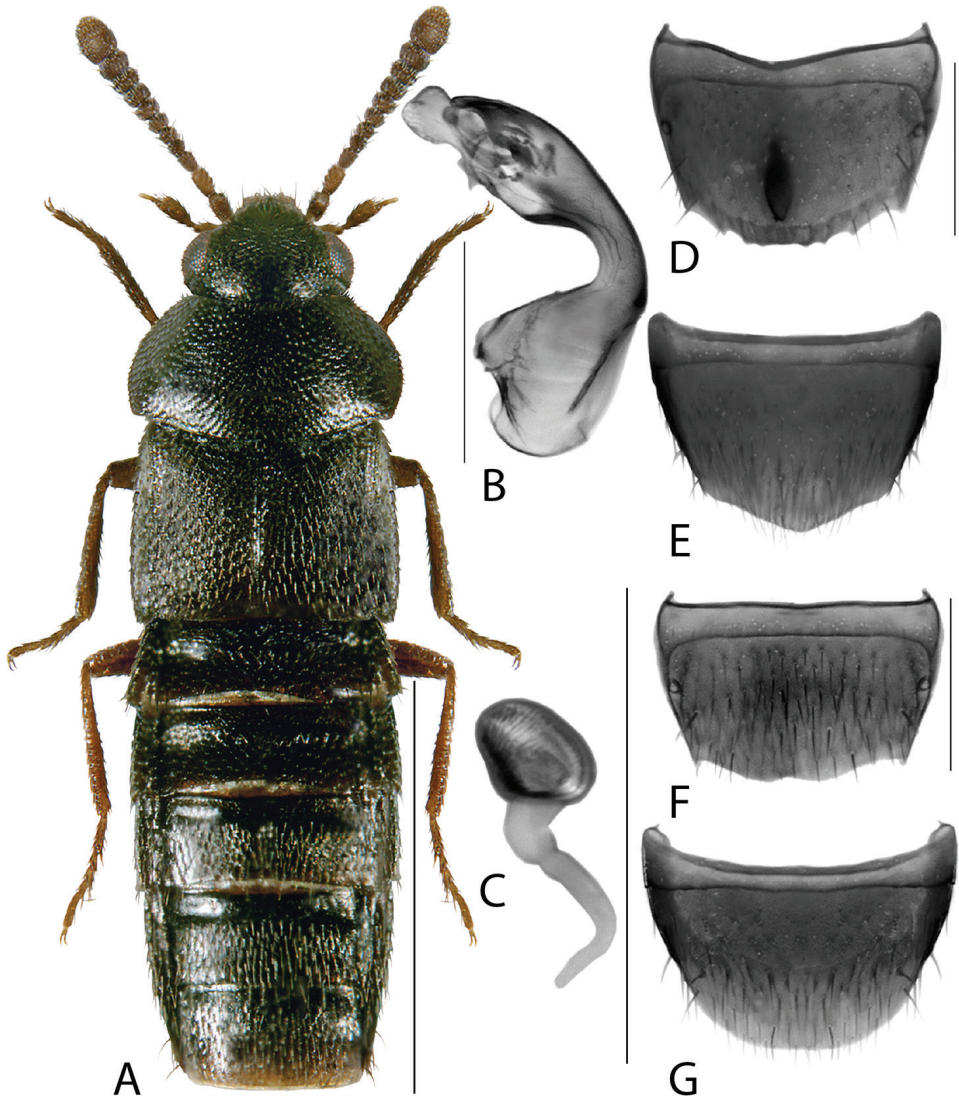
Figure 21. *Cyphea wallisi* Fenyes **A** habitus **B** median lobe of aedeagus in lateral view **C** spermatheca **D** male tergite VIII **E** male sternite VIII **F** female tergite VIII **G** female sternite VIII. Scale bars: 1 mm (**A**); 0.2 mm (**B–G**). Illustrations after Klimaszewski et al. (2018), used with permission.

Type material. *Cyphea wallisi* Fenyes, 1921. ***Paratype***, male (MCZ). Winnipeg, Man. [handwritten label] / Wallis [handwritten label] / 25490. / Cyphea, Wallisi, Feny [handwritten label] / Type., 9989, 9983 [typed red label].

Agaricomorpha vincenti Klimaszewski & Webster, 2016, syn. nov. ***Holotype***, male (LFC). Canada, New Brunswick, Carleton Co., Jackson Falls, "Bell Forest", 46.2200°N, 67.7231°W, 7–21.VI.2012, C. Alderson & V. Webster, coll. [white typed label] / Rich Appalachian hardwood forest, Lindgren funnel trap in canopy of *Fagus grandifolia* [white typed label] / Holotype *Agaricomorpha vincenti* Klimaszewski &

Webster, 2016 [red typed label] / *Cyphea curtula* (Erichson) det. Klimaszewski 2017 [white typed label] / *Cyphea wallisi* Fenyes det. A. Brunke 2020.

The aedeagi of the male paratype (holotype in collection of the California Academy of Sciences) of *C. wallisi* and holotype of *A. vincenti* are identical and both differ from that of Palaearctic *Cyphea curtula* (image by V. Assing) by the broader distal lobe in lateral view, which only slightly extends beyond the distal plate (Fig. 22A–C). Therefore, we transfer *Agaricomorpha vincenti* from synonymy with *Cyphea curtula* to synonymy with *Cyphea wallisi*.

Other material (DNA barcoded specimens). Canada: Ontario: Rouge National Urban Park, Toronto Zoo, 43.8223, -79.1897, forest, malaise trap, 25.VI.2013, L. Attard and K. Greenham (2, CBG); Hartington, Eel Lake Cottage, Lindgren funnel trap, 44.5628, -76.553, 25.VII.2017, G. Blagoev (1, CBG); **Nova Scotia:** Clyburn Valley Road, near golf course, Cape Breton National Highlands NP, forest, Malaise trap, 46.6553, -60.4285, 28.VI.2013, CBH staff (1, CBG).

Non-barcoded specimens. Canada: Quebec: Mont St. Bruno Prov Park, 45.541, -73.319, Lindgren funnel, trap 5, tree 2, beech-maple canopy, 21.VII-3.VIII.2005 (1, CNC); Oka Prov Park, Lindgren funnel, trap 3, tree 1, beech-maple canopy, 27.VII.30. VIII.2005 (1, CNC).

Distribution. Origin: Nearctic. **Canada**: AB, MB, NB, NS [new record], ON [new record], QC.

Bionomics. Specimens have been collected in Malaise traps, window traps and Lindgren funnels placed in forests. Both the closely related West Palaearctic *C. curtula* and *C. latiuscula* Sjöberg have been consistently collected under bark, where they occur in the larval burrows of various longhorn beetles (Cerambycidae), bark beetles (Curculionidae: Scolytinae) and the carpenter moth (*Cossus* L.) (Palm 1968).

Comments. *Cyphea wallisi* is a broadly distributed native Nearctic species, reported from AB east to NS. Here we treat Nearctic records of *Cyphea* as *C. wallisi* (previously treated as Palaearctic *C. curtula*, e.g., Klimaszewski et al. 2018) and newly report the genus from ON and NS. *Cyphea wallisi* is probably far more broadly distributed in North America than currently known and has been underreported due to its small size.

Sequenced Nearctic specimens of *Cyphea* from ON and NS formed a barcode cluster that was nearly 5% divergent from those of Palaearctic specimens of *C. curtula* (BOLD:AAO1175, one published sequence record from Belgium and three unpublished records from the Netherlands). Northern European *C. latiuscula*, the only other species of the genus, has a broader body outline, different male genitalia and is quite differently colored (bicolored pronotum and pale elytra). No barcode sequence data are currently available for *C. latiuscula*. Based on the study of one paratype of *C. wallisi*, described from Manitoba and not reported since, it was discovered that Nearctic specimens of *Cyphea* correspond to this species and differ from Palaearctic *C. curtula* by the broader distal lobe of the median lobe of the aedeagus in lateral view, which only slightly extends beyond the distal plate (Fig. 22A–C). The shape of the median lobe of the aedeagus in dorsal view may also be diagnostic (Fig. 22D) but a preparation in this view was unavailable for *C. curtula*. The illustration in Palm (1968) of the
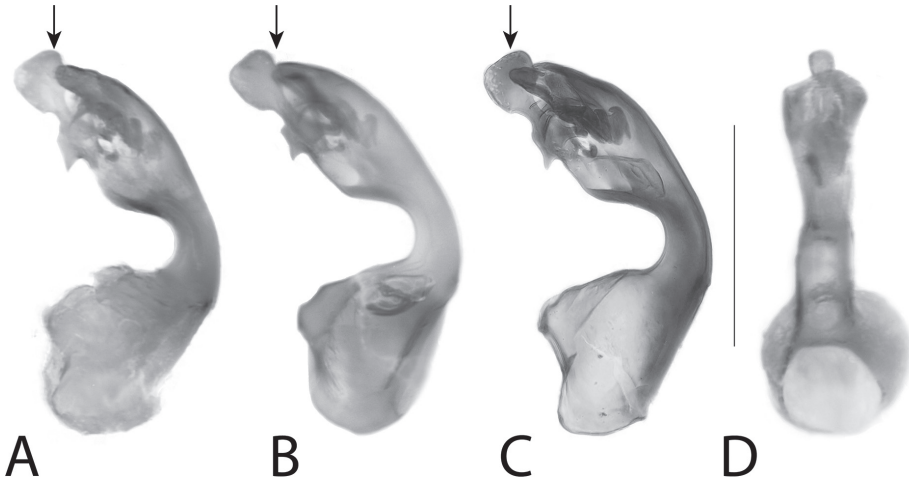
Figure 22. Aedeagi of *Cyphea wallisi* Fenyes (**A, B, D**) and *C. curtula* (Erichson) (**C**), in lateral (**A–C**) and dorsal (**D**) view. Paratype of *C. wallisi* (**A, D**); holotype of *Agaricomorpha vincenti* Klimaszewski and Webster (= *C. wallisi*) (**B**); non-type, *C. curtula* (image by V. Assing) (**C**). Scale bar: 0.2 mm.

aedeagus of *C. curtula* in dorsal view appears to be less angulate than that of *C. wallisi* but this needs verification. Based on these differences in male genitalia (Fig. 22A–C) and the COI barcodes, *Cyphea wallisi* is morphologically and genetically distinct from Palaearctic *C. curtula*, and the latter species does not occur in North America as far as known. Both of these species have a median tubercle on male tergite VII, mentioned earlier by Fenyes (1921) but this structure was omitted from the illustrations in Klimaszewski et al. (2018), though it was present in the original description of synonym *Agaricomorpha vincenti* (Webster et al. 2016). Previous differences between the two species given by Klimaszewski et al. (2018) (e.g., projecting pronotal angles, lighter/darker body) proved to be highly variable.

Gyrophaena affinis Mannerheim, 1830

BOLD:ACF7981 [Nearctic]; BOLD:ABW9049 and BOLD:AAO0291 [both Palaearctic]

Fig. 23A–G

Material (DNA barcoded specimens). Belgium: Sint-Genesius-Rode, BR Zonienwoud, 50.7505, 4.423, 135 m, 16.VI.2010, F. Koehler (1, ZSM). **Finland:** Oba: Oulu, Linnanmaa, 65.0633, 25.4712, 7.VI.2011, M. Pentinsaari (1, ZMUO); Obb: Tornio, Kalkkimaa, 65.9014, 24.4711, 10.VII.2012, M. Pentinsaari (1, ZMUO); Al: Lemland, Herrövägen, 59.9796, 20.1954, car net, 5.VII.2012, M. Pentinsaari (1, ZMUO). **Germany:** Brohl-Luetzing, Brohltal, 50.4727, 7.31272, 22.V.2010, F. Koehler (1, ZSM), Riedlhuette, Diensthuettenstrasse, 48.937, 13.412, 09.VII.2011, F. Koehler & M. Koehler (1, ZSM), Waldhaeuser, Lusen- und Boehmstrasse, 48.93,
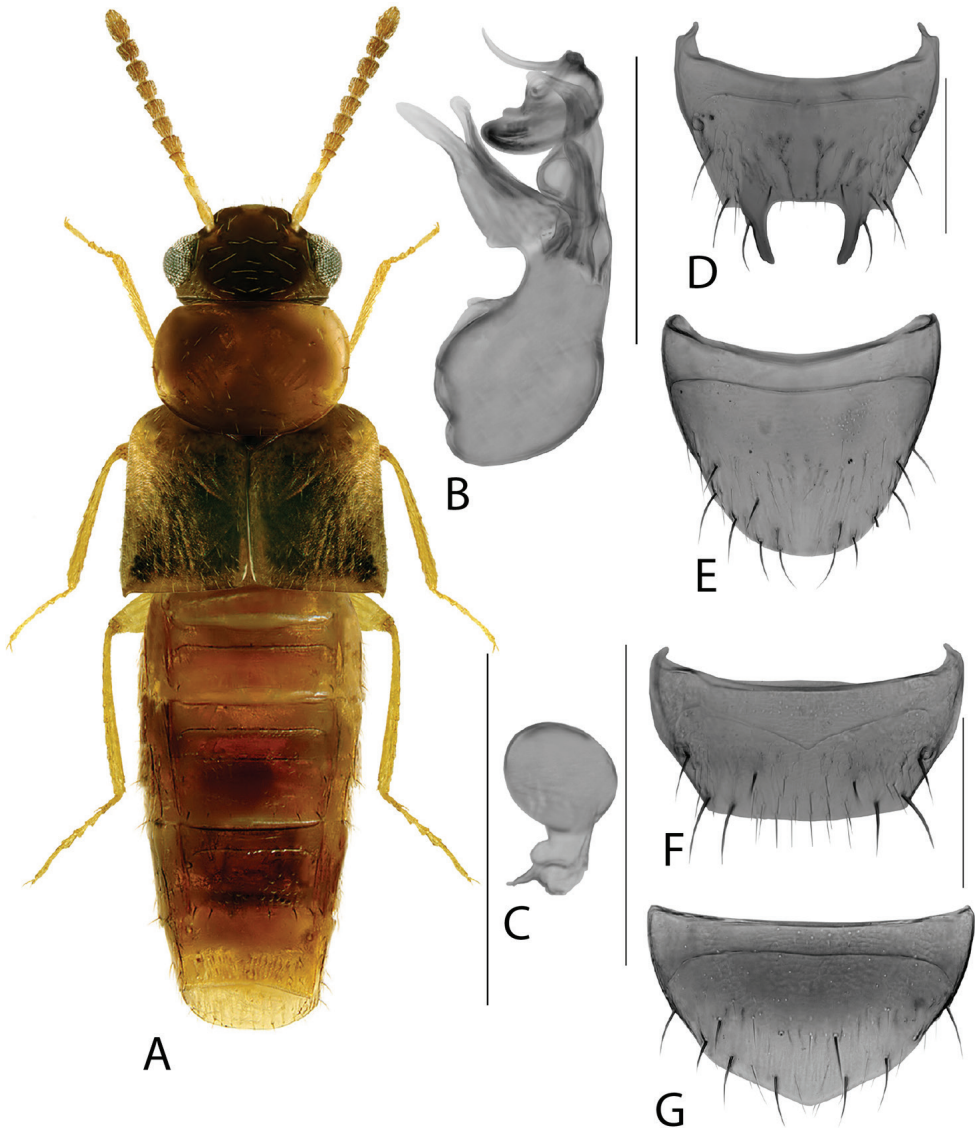
Figure 23. *Gyrophaena affinis* Mannerheim **A** habitus **B** median lobe of aedeagus in lateral view **C** spermatheca **D** male tergite VIII **E** male sternite VIII **F** female tergite VIII **G** female sternite VIII. Scale bars: 1 mm (**A**); 0.2 mm (**B–G**). Illustrations after Klimaszewski et al. (2018), used with permission.

13.492, 09.VII.2011, F. Koehler & M. Koehler (1, ZSM). **Canada: Alberta:** Waterton Lakes National Park, Highway 6 pulloff, 49.065, -113.779, 1569 m, intercept trap, montane forest, 27.VI.2012, BIOBus 2012 (2, CBG).

Distribution. Origin. Uncertain. **Canada**: AB [new record], BC, MB, NB, NF, NS, ON, QC, SK. **United States**: AZ, DC, IL, IN, IA, KY, MA, ME, MI, MN, MO, NC, NH, NJ, NM, NY, OH, PA, TN, WA, WI, WV.

Comments. *Gyrophaena affinis* is newly reported from AB based on barcoded material. Sequenced Nearctic specimens from ON, AB, NB, and QC form a distinct barcode cluster, separate from all sequenced Palearctic specimens and divergent by 4.65%. This pattern is inconsistent with a species that is adventive in North America and we remove *G. affinis* from the list of adventive species in Canada. In comparing images between those of Nearctic specimens (Fig. 23B) and those of Enushchenko and Semenov (2016) for Palaearctic specimens, there appear to be slight differences in the median lobe of the aedeagus in lateral view. In the Palaearctic illustration, the apex of the median lobe is more acute and its secondary lobe is evenly rounded at apex, while the Nearctic illustration shows a more rounded apex of the median lobe and knob-like apex of the secondary lobe (Fig. 23B). More research is needed to determine the status of the Nearctic and Palaearctic populations, though the level of genetic divergence between discrete Nearctic and Palaearctic populations suggests that two sister species are involved.

Gyrophaena gracilis Seevers, 1951
Fig. 24A–H

Material (non-sequenced material). Canada: Quebec: Gatineau Park, wolf trail, near trail start, 45.541, -75.912, hardwood forest, *Polyporus squamosus* on large beech log, 8.VI.2019, A. Brunke & J. Smith (1, CNC).

Distribution. Origin. Nearctic. **Canada**: NB, QC [new record]. **United States**: WI.

Bionomics. Specimens have been collected from a partly dried *Pleurotus* mushroom, from within the pores of a *Trametes* polypore, and from the nest contents of a Barred owl (*Strix varia* Barton) (Klimaszewski et al. 2018). The specimen from QC was collected from *Polyporus squamosus* on a beech tree.

Comments. The new record from QC, near the ON border, bridges the wide gap between previous records in NB and WI.

Gyrophaena simulans Seevers, 1951
BOLD:ACY8004
Fig. 25A–G

Material (DNA barcoded specimens). Canada: Ontario: Hartington, Eel Lake Cottage, 44.563, -76.549, deciduous forest, mushrooms, 4.X.2017, M. Pentinsaari (2, CBG).

Distribution. Origin. Nearctic. **Canada**: ON [new record]. **United States**: IL, MD, PA.

Diagnosis. *Gyrophaena simulans* is extremely similar to *G. criddlei* and *G. pseudocriddlei* but has a slightly more transverse and flatter pronotum, with straighter apical and basal margins, and differently shaped upper process of the median lobe in lateral view (Fig. 25B): longer than that of *G. pseudocriddlei* but shorter and broader than that of
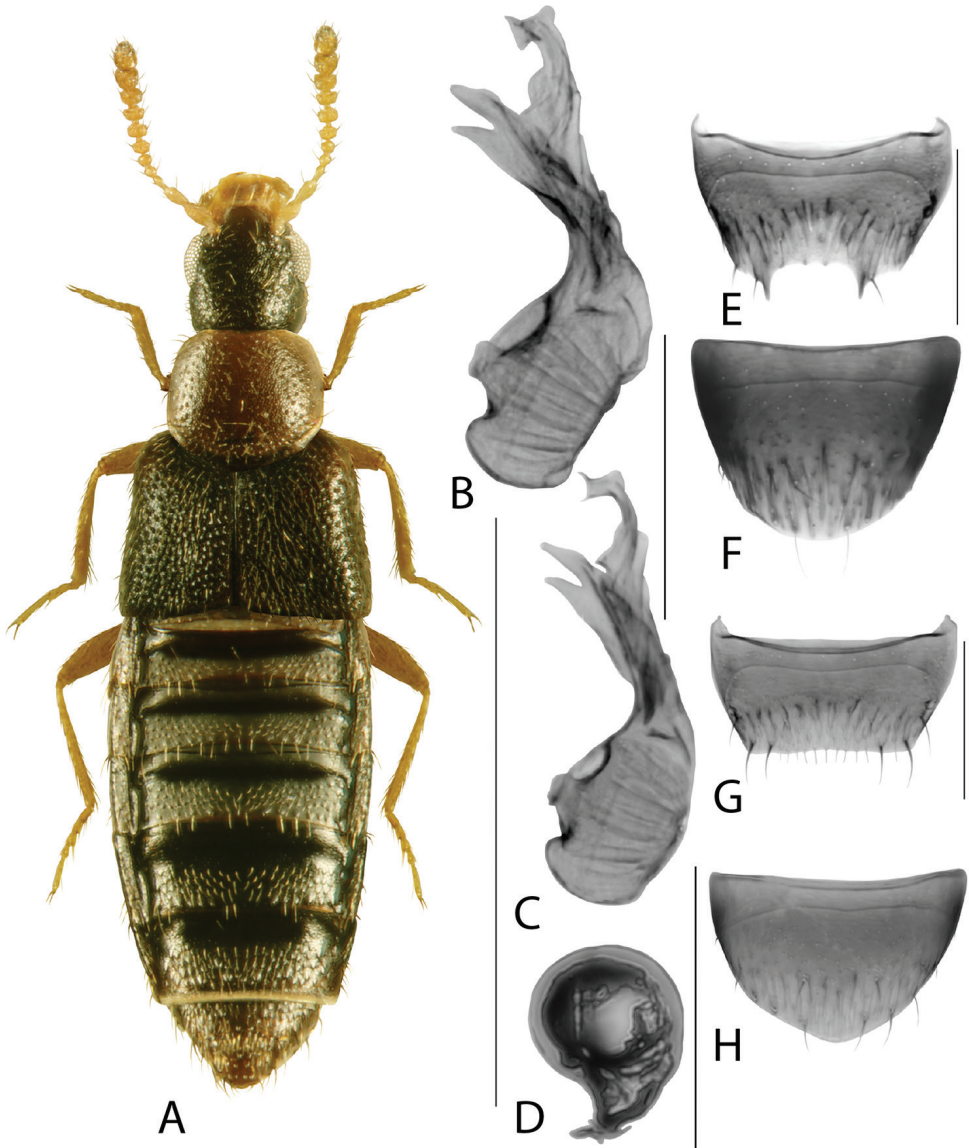
Figure 24. *Gyrophaena gracilis* Seevers **A** habitus **B, C** median lobe of aedeagus in lateral view **D** spermatheca **E** male tergite VIII **F** male sternite VIII **G** female tergite VIII **H** female sternite VIII. Scale bars: 1 mm (**A**); 0.2 (**B–H**). Illustrations after Klimaszewski et al. (2018), used with permission.

G. criddlei. The emarginated of male tergite VIII in *G. simulans* appears to be shallower and broader than that of *G. criddlei* but more specimens are needed to confirm this.

Bionomics. The Canadian specimens were collected by sifting mushrooms in a deciduous forest. No detailed data on the host fungus were recorded.

Comments. *Gyrophaena simulans* is a native Nearctic species distributed in eastern North America and is newly reported from Canada. The barcode cluster
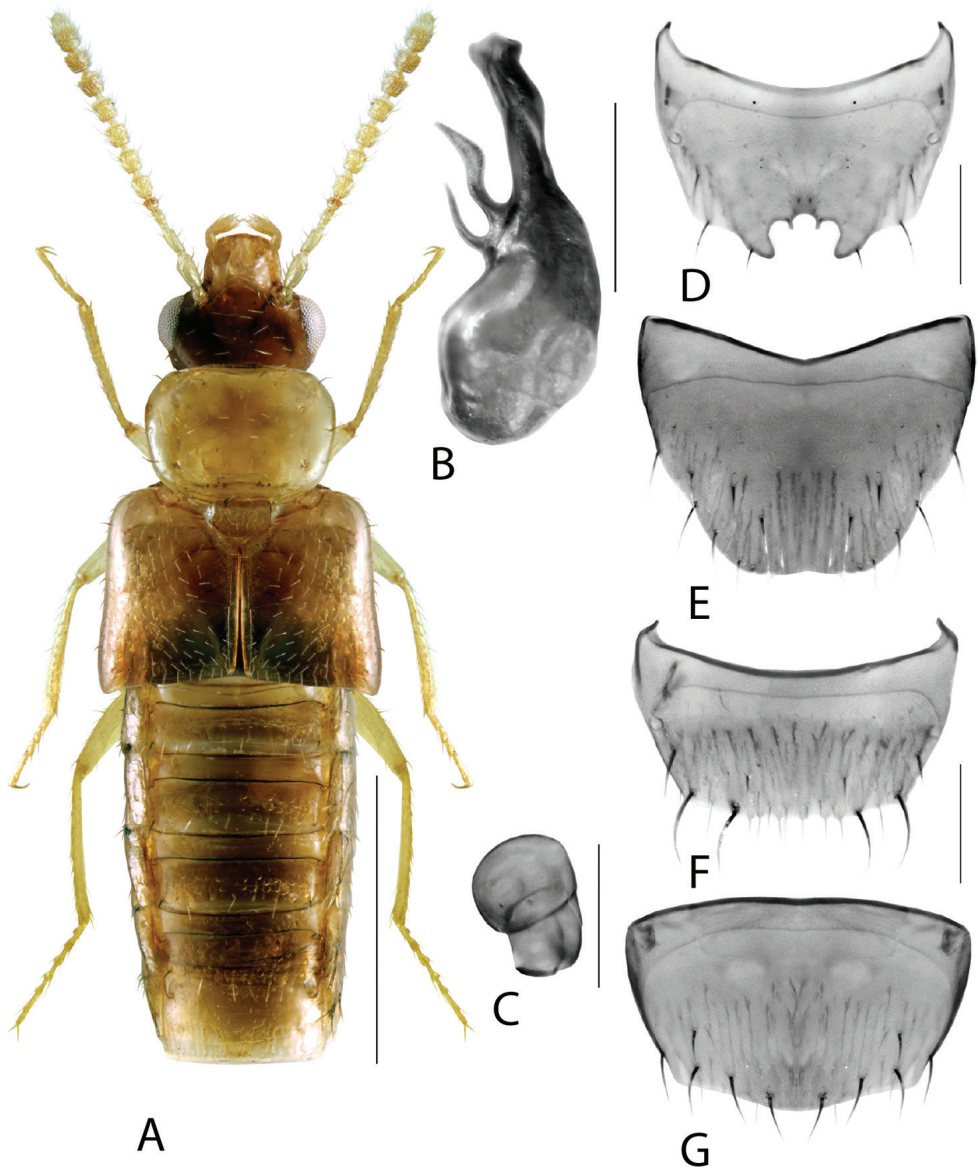
Figure 25. *Gyrophaena simulans* Seevers **A** habitus **B** median lobe of aedeagus in lateral view **C** spermatheca **D** male tergite VIII **E** male sternite VIII **F** female tergite VIII **G** female sternite VIII. Scale bars: 1 mm (**A**); 0.2 mm (**B–G**).

BOLD:ACY8004 also contains specimens identified as related species *G. criddlei* (female) and *G. pseudocriddlei* but more research, with broader sampling of sequenced, identified males, is needed to determine whether these species share a BIN or these specimens are misidentified. As we were unable to verify the identifications at this time, these records are not published here.

Homalota plana (Gyllenhal, 1810)
BOLD:ADH5714 [Nearctic]; BOLD:AAO0434 [Palaearctic]
Fig. 26A–G

Material (DNA barcoded specimens). Belgium: Sint-Genesius-Rode, BR Zonien-woud, 50.7505, 4.423, 28.IV.2010, F. Koehler (1, ZSM). **Germany:** Arnsberg-Breitenbruch, NWZ Hellerberg, 51.446, 8.135, 30.V.2011, F. Koehler (2, ZSM); Heimbach-Blens, Linkheld, 50.648, 6.468, 29.VIII.2012, F. Koehler (2, ZSM); Erftstadt-Bliesheim, NWZ Altwald Ville, 50.7917, 6.84384, 03.VI.2011, F. Koehler (1, ZSM); westl. Klein-Quenstedt, 51.9239, 11.0478, 20.III.2015, GBOL-Team ZFMK (1, ZFMK). **Finland:** Al: Finström, Norrö, 60.2458, 19.822, 5.VII.2012, M. Pentinsaari (1, ZMUO); Ka: Joutseno, Kuurmanpohja, 61.071, 28.75, 3.VIII.2012, M. Pentinsaari (1, ZMUO). **Canada: Ontario:** Guelph, Eramosa River Trail, 43.539, -80.236, deciduous forest, 14.IV.2017, M. Pentinsaari (2, CBG).

    Distribution. Origin. Uncertain. **Canada**: AB, MB, NB, NF, NS, ON. **United States**: AZ, CA, CO, IA, ID, IN, MT, NY, OH, PA, TX.

    Bionomics. Specimens occur under bark of dead trees.

    Comments. Sequenced Nearctic specimens from ON form a distinct barcode cluster, separate from all sequenced Palearctic specimens and divergent by 7.58%. This pattern is inconsistent with a species adventive in North America and we remove *H. plana* from the list of adventive species in Canada. Preliminary comparisons between images of Palaearctic and Nearctic specimens revealed that there may be some slight differences in the shape of the spermatheca. More research is needed to determine the status of the Nearctic and Palaearctic populations, though the level of genetic divergence between discrete Nearctic and Palaearctic populations suggests that two sister species are involved.

Thecturota tenuissima Casey, 1893
BOLD:AAO0406
Fig. 27A–G

Thecturota tenuissima Casey, 1893
Atheta marchii Dodero, 1922, syn. nov.
Pragensiella magnifica Machulka, 1941, syn. nov.
Thecturota marchii: Muona 1984 (as valid species)
Thecturota magnifica: Schülke and Smetana 2015 (as syn. of *T. marchii*)

Material (DNA-barcoded specimens). Germany: Kobern-Gondorf, Ortslage/Weinberge, 50.308, 7.460, 21.V.2010, F. Koehler (1, ZSM); Edenkoben-Rhodt, Villastrasse, 49.279, 8.092, 20.X.2012, F. Koehler (1, ZSM). **Finland:** Oba: Oulu, Linnanmaa, 65.0633, 25.4712, botanical garden, compost heap, flight-intercept trap, 7.VI.2011, M. Pentinsaari (1, ZMUO).
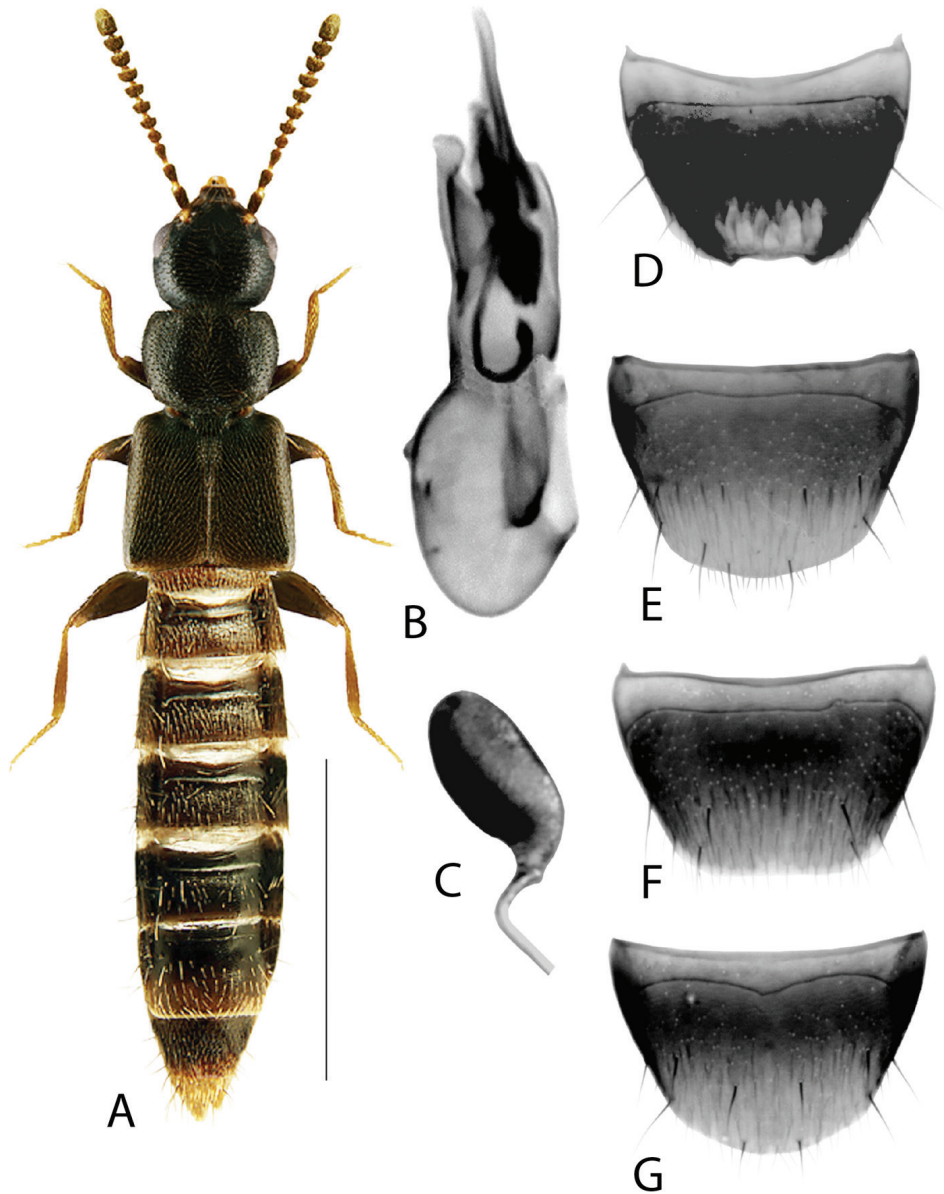
Figure 26. *Homalota plana* (Gyllenhal) **A** habitus **B** median lobe of aedeagus in lateral view **C** spermatheca **D** male tergite VIII **E** male sternite VIII **F** female tergite VIII **G** female sternite VIII. Scale bars: 1 mm (**A**); 0.2 mm (**B–G**). Illustrations after Klimaszewski et al. (2018), used with permission.

Non-sequenced material. Several males and females of *T. tenuissima* from Denmark (NMHD) were compared with illustrations from Klimaszewski et al. (2017).

Distribution. Origin. Nearctic (adventive in West Palaearctic). **Canada**: ON, QC. **United States**: RI.
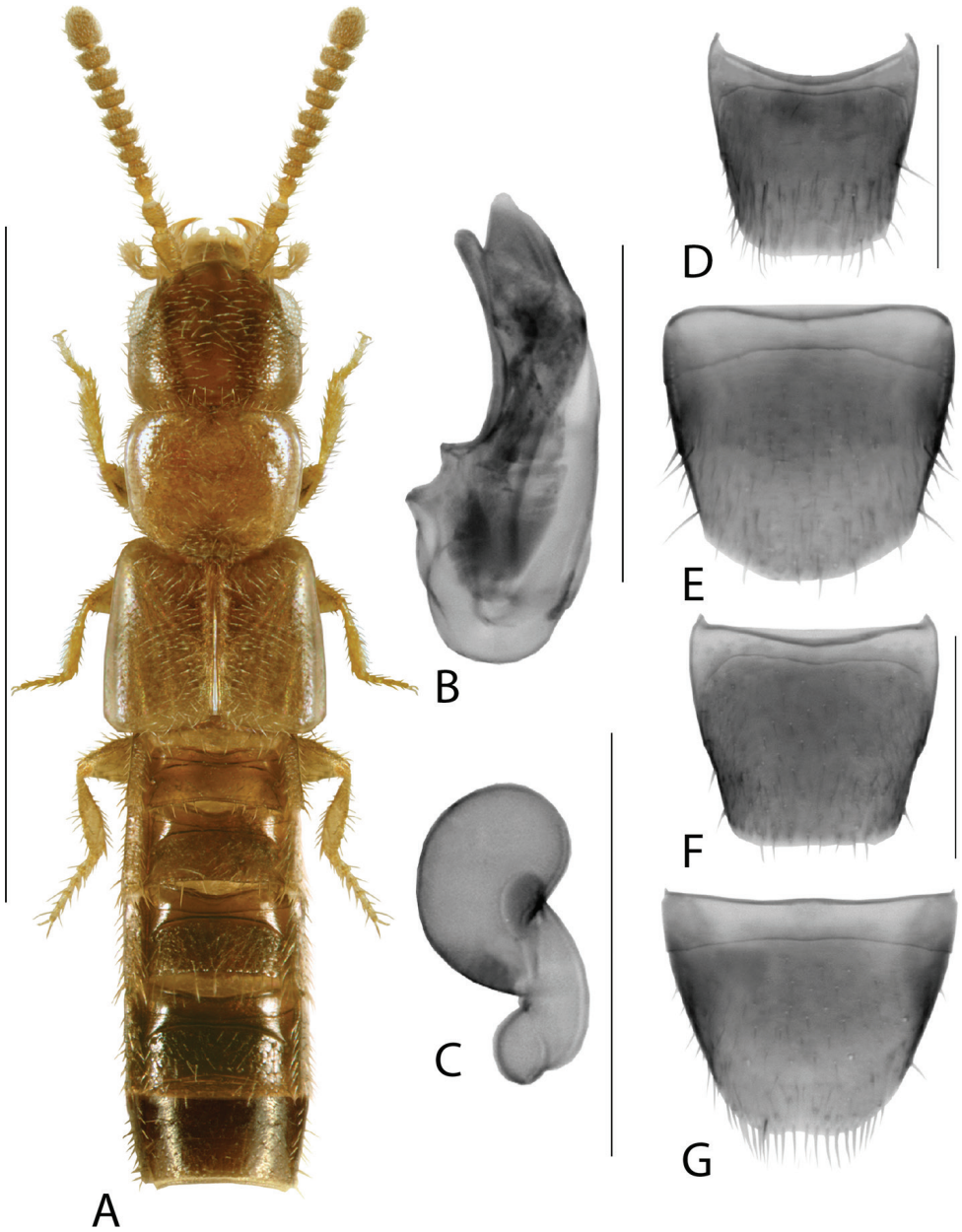
Figure 27. *Thecturota tenuissima* Casey **A** habitus **B** median lobe of aedeagus in lateral view **C** spermatheca **D** male tergite VIII **E** male sternite VIII **F** female tergite VIII **G** female sternite VIII. Scale bars: 1 mm (**A**); 0.2 mm (**B–G**). Illustrations after Klimaszewski et al. (2017).

Bionomics. Canadian specimens were collected by car-netting in mixedwood forests, while Palaearctic specimens are known from compost and other plant-based debris (Horion 1967).

Comments. *Thecturota tenuissima* is native to the Nearctic region and has become accidentally introduced to the West Palaearctic, including the Canary Islands, where it was previously known under the synonym *T. marchii* (Newton 2019). We expect this species to be broadly distributed in eastern North America and has been overlooked over much of its range because car-netting, an effective method for collecting small, obscure staphylinids, is rarely used in the Nearctic region.

Nearctic and Palaearctic populations do not differ in male and female genitalia or in external morphology. Molecular data were unavailable for the Nearctic population, which was recently reported from Canada (Klimaszewski et al. 2017) but described from Rhode Island, USA in 1893 (Casey 1893). However, we are confident that these species are synonyms. Muona (1984) stated that *T. marchii* is a 'recent' introduction to Europe but from an unknown source. *Thecturota* is primarily a New World genus, with ten described species in North and South America (Newton 2019). *Thecturota magnifica* (Machulka) is currently treated as a synonym of *T. marchii* (Newton 2019) and we simply transfer this name to synonymy with *T. tenuissima*. The only Palaearctic species remaining is poorly known *T. williamsi* (Bernhauer, 1936), known only from the type collected in Great Britain and probably a synonym of *T. tenuissima*. The characters Bernhauer (1936) gave to separate his species from *T. tenuissima* (as *T. marchii*) are slight differences in coloration and body proportions, which are both highly variable in the Palaearctic specimens of *T. tenuissima* studied. Therefore, we consider *T. tenuissima* to be a native Nearctic species that has become adventive in the West Palaearctic and suggest that genus *Thecturota* is naturally restricted to the Nearctic and Neotropical regions.

Geostibini Seevers, 1978

***Aloconota pseudogregaria* Klimaszewski, Brunke & Pentinsaari, sp. nov.**
http://zoobank.org/A72E1E63-3D1B-4CC8-882C-6921E5FC3D33
BOLD:AAY6554
Fig. 28A–G

Type material. *Holotype* (male) (CNC): **Canada: ON:** Waterloo County, Cambridge, Rare Charitable Research Reserve, 43.390, -80.374, soybean field, pitfall trap, 29.VI.2010, A. Brunke [white printed label] / HOLOTYPE *Aloconota pseudogregaria* Klimaszewski, Brunke & Pentinsaari sp. nov., des A. Brunke 2020 [red printed label]. *Paratypes* (1 NMNH, 6 DEBU, 1 CNC): **Canada: ON:** Wellington County, Eramosa, 43.616, -80.215, soybean field, pitfall trap, 13.VII.2010, A. Brunke [white printed label] / PARATYPE *Aloconota pseudogregaria* Klimaszewski, Brunke & Pentinsaari sp. nov., des A. Brunke 2020 [yellow printed label] [CNC, DEBU, 7 specimens]. **United States: VA**: Arlington County, Marcey Creek, 38.9087, -77.1083, 70 m, suburban backyard, Malaise trap, 14–21.VI.2015, S. Miller [white printed label] / Barcode of life, DNA voucher specimen, Sample ID: BIOUG42376-E12, Process ID: GMUAF1698-18 [yellow printed label] / PARATYPE *Aloconota pseudogregaria* Klimaszewski, Brunke & Pentinsaari, sp. nov., des A. Brunke 2020 [yellow printed label] [NMNH, 1 specimen].
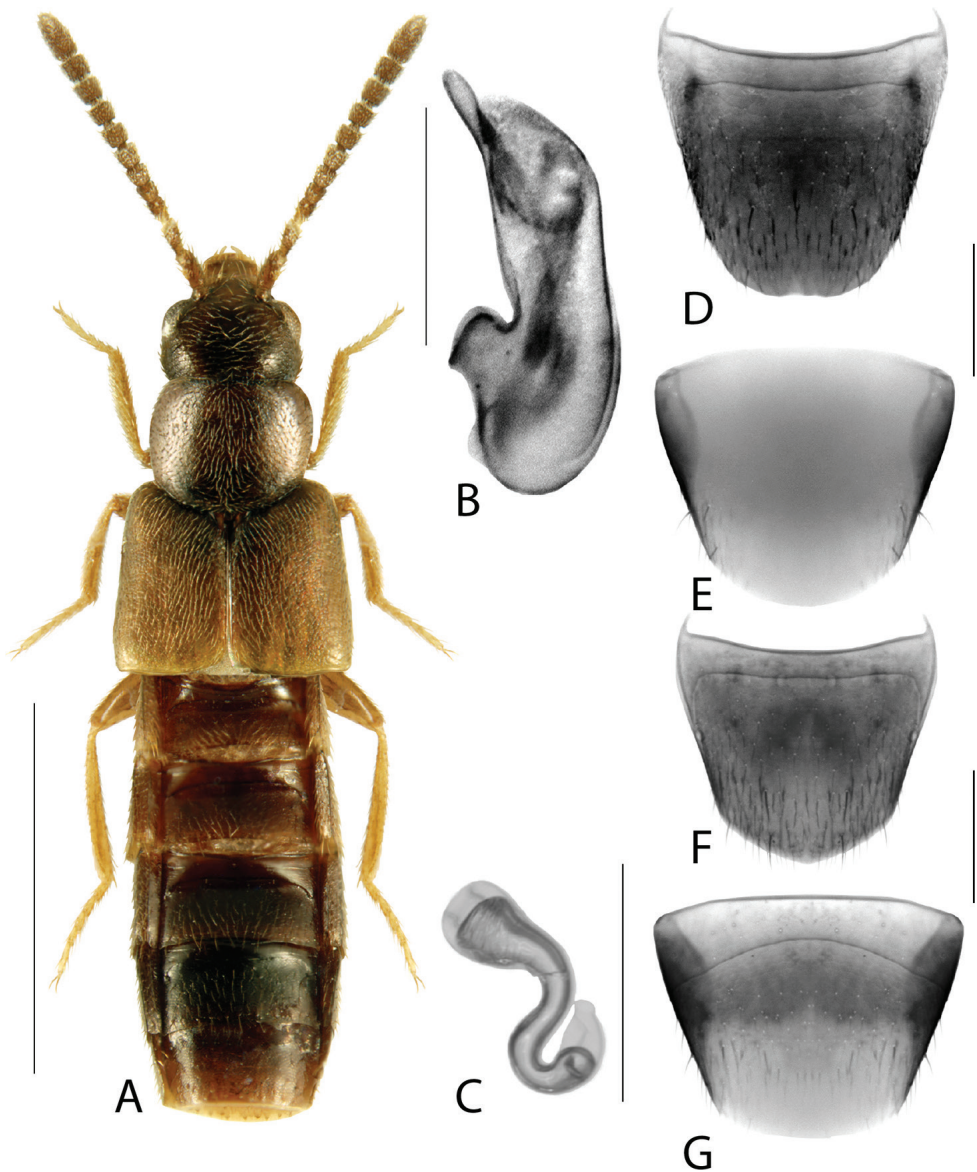
Figure 28. *Aloconota pseudogregaria* Klimaszewski, Brunke & Pentinsaari, sp. nov. **A** habitus **B** median lobe of aedeagus in lateral view **C** spermatheca **D** male tergite VIII **E** male sternite VIII (structure accidentally over-cleared in balsam preparation) **F** female tergite VIII **G** female sternite VIII. Scale bars: 1 mm (**A**); 0.2 mm (**B–G**).

Non-type material (barcoded specimens). Canada: Ontario: Guelph, 25 Division St., 43.554, -80.264, Malaise trap, 14.VII.2010, A. Smith (1, CBG); Guelph, John F. Ross CVI, 43.5621, -80.247, Malaise trap, 22.IV-03.V.2013, G. Staines (1, CBG); Milverton, Milverton Public School, 43.568, -80.928, Malaise trap, 22.IV-03.V.2013, J. Van Bakel (1, CBG); Collingwood, Collingwood Collegiate Institute,

44.489, -80.215, 188 m, Malaise trap, 22.IV-05.V.2014, A. Breton (1, CBG); Cambridge, rare Charitable Research Reserve, 43.3736, -80.3652, 304 m, 04–11.VI.2015, BIO Collections Staff (1, CBG).

Etymology. The species epithet refers to the similarity to related species *A. gregaria* (Erichson), which was originally treated separately from other *Aloconota* under subgenus *Glossola* Fowler (e.g., Benick 1954) because it lacks obvious male secondary sexual characters.

Diagnosis. *Aloconota pseudogregaria* can be easily distinguished from all other species of the genus occurring in eastern North America by the distinctly bicolored abdomen (Fig. 28A). Among Central European species, the spermatheca of *A. pseudogregaria* is most similar to that of Palaearctic *A. gregaria* but in the latter the apex is distally truncate, median lobe is distinctly sinuate and only weakly projected ventrad, the abdomen is darker and not distinctly bicolored, and the microsculpture of the forebody is much stronger, creating a dull reflection.

Description. Body length 2.4–2.7 mm, moderately flattened (stronger so on elytra), narrowly subparallel, colour of head, pronotum, scutellar region of elytra, apical part of abdomen and antennomeres 5–11 dark brown to dark reddish brown, elytra and antennomeres 1–3 paler, red-brown and legs yellow; forebody finely and densely punctate, microsculpture shallow, consisting of meshes; head slightly elongate and with small, shallow impression medially, head slightly narrower than pronotum, postocular region elongate, ca. as long as maximum diameter of eye, tempora with carinae dorsally only; antennae slender, as long as pronotum and elytra combined, basal three antennomeres strongly elongate, 4 subquadrate, 5–10 subquadrate to slightly transverse, and terminal one strongly elongate and ca. as long as two preceding antennomeres combined; pronotum slightly transverse (width/length ratio 1.3), trapezoidal in shape, flattened, pubescence directed straight posteriad in central part of disc and obliquely posteriad laterally; elytra at suture ca. as long as pronotum along midline, flat, distinctly transverse (width/length ratio 1.5), ~ 1/3 broader than pronotum, humeri angular, posterior margins slightly sinuate laterally, pubescence directed straight posteriad forming slightly arcuate lines in sutural region of disc; abdomen subparallel, tergites III–VI distinctly impressed at base; basal metatarsomere ~ 1/3 longer than the following one. MALE. Tergite VIII rounded apically with minute median emargination, lacking apical teeth (Fig. 28D); sternite VIII rounded apically (Fig. 28E); tubus of median lobe of aedeagus long, ventrally ca. straight in basal two-thirds and moderately projecting ventrad apically in lateral view (Fig. 28B). FEMALE. Tergite VIII rounded apically and slightly pointed medially (Fig. 28F); sternite VIII rounded apically (Fig. 28G); spermatheca S-shaped, capsule pitcher-shaped with short neck, stem strongly sinuate and swollen apically (Fig. 28C).

Distribution. Origin: Nearctic. **Canada**: ON. **United States**: VA.

Bionomics. This species has only been collected by passive traps, including malaise and pitfall traps. All specimens have been collected from at least partly disturbed habitats, such as forest edges, agricultural fields, and suburban environments. This species corresponds to 'Aleocharinae sp. 5' in Brunke et al. (2014), which was collected in both soybean fields and adjacent forest edges by pitfall traps.

Comments. *Aloconota pseudogregaria* is probably broadly distributed in northeastern North America. We have compared the male and female genitalia of *A. pseudogregaria* with all Central European and Nearctic species of *Aloconota*, and are confident that this taxon has not been previously described from Europe or North America, despite its occurrence in disturbed habitats in North America, which is typical for introduced species. Although *Aloconota pseudogregaria* clustered most closely with *A. gregaria* (BOLD:ABU6164) in our barcode dataset, its BIN is ~ 8% different from that of the latter. Based on morphology of the aedeagus and spermatheca, *Aloconota pseudogregaria* is probably even more closely related to East Palaearctic *Aloconota* described from Japan and Korea (e.g., Sawada 1970 [as *Tomoglossa*], Lee and Ahn 2017) rather than to *A. gregaria.* However, the described species all differ markedly in external morphology.

Athetini Casey, 1910

Atheta (*Datomicra*) *nigra* (Kraatz, 1856)
BOLD:ACO4408
Fig. 29A–G

Material (DNA-barcoded specimens). Canada: Ontario: Peterborough, 44.253N, 78.415W, farm, malaise trap, 24–30.V.2015, B. McClenaghan (1, CBG). **Germany:** Koeln-Worringen, Worringer Bruch, 51.044, 6.87427, 01.VII.2010, F. Koehler & J. Koehler (1, ZSM).

Distribution. Origin. Palaearctic (adventive in North America). **Canada**: ON [new record], SK.

Bionomics. Canadian specimens have been collected on farmland and directly from horse manure.

Comments. *Atheta nigra* is a Palaearctic species reported from across Europe, European Russia, Kazakhstan, North Korea and southern China (Newton 2019). It is adventive in North America and New Zealand (Newton 2019) and is here newly reported from Ontario. The new record from Ontario indicates that this species is far more widely distributed in North America than previously known.

Mocyta scopula (Casey, 1893), comb. nov.
BOLD:ACH8720
Fig. 30A–F

Eurypronota scopula Casey, 1893
Pancota laetabilis Casey, 1906
Dolosota abundans Casey, 1910
Dolosota flaccida Casey, 1910
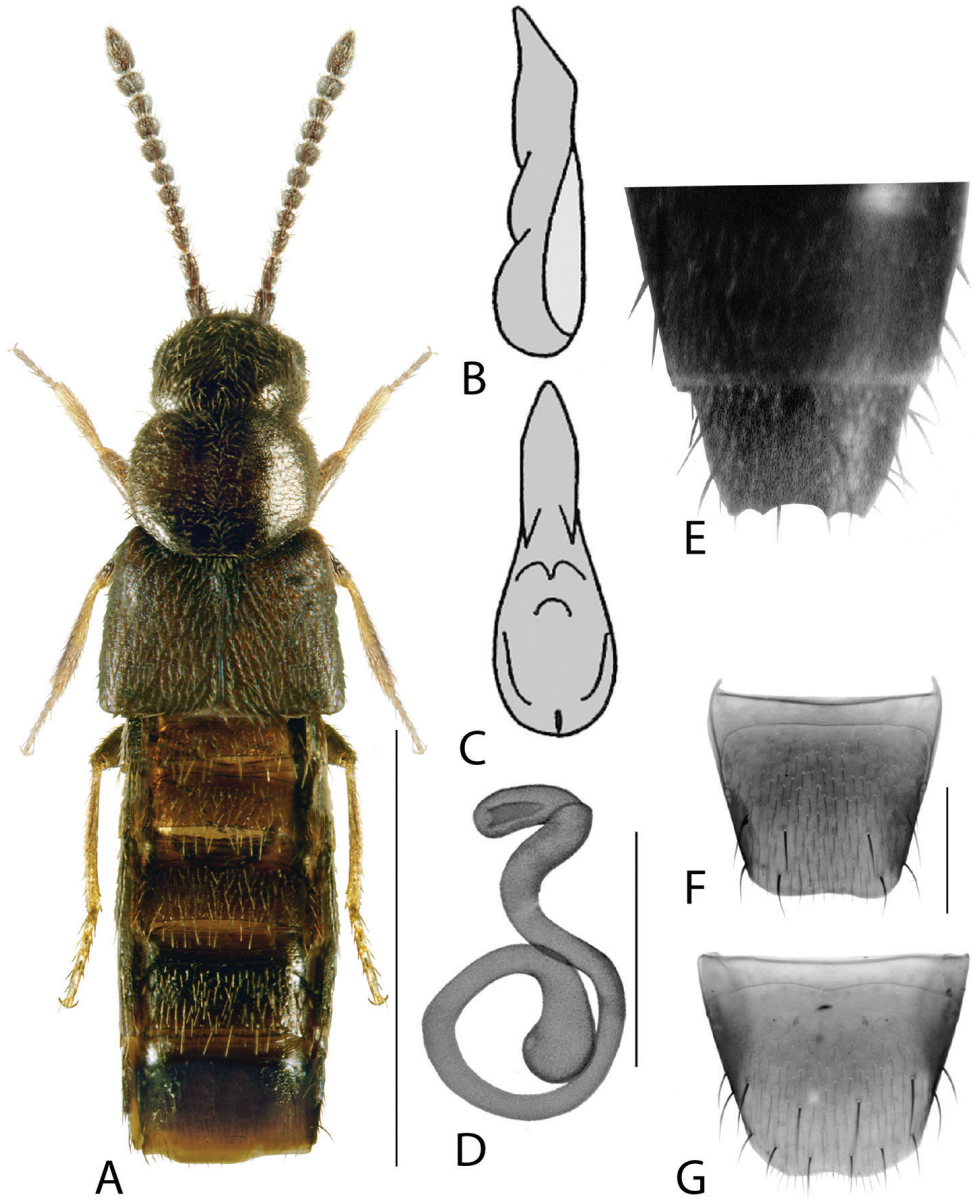
Figure 29. *Atheta* (*Datomicra*) *nigra* (Kraatz) **A** habitus **B** median lobe of aedeagus in lateral view **C** median lobe of aedeagus in ventral view **D** spermatheca **E** apical part of dorsal male abdomen showing 4 dents on tergite VIII **F** female tergite VIII **G** female sternite VIII; **A, D, F, G** after Klimaszewski et al. (2016a), based on female from Saskatchewan, Canada **B, C** after Benick and Lohse (1974) **E** after Klimaszewski et al. (2016a), based on a male from Germany. Scale bars: 1 mm (**A**); 0.2 mm (**B–G**).

Dolosota redundans tergina Casey, 1910

Dolosota scopula: Casey (1910) (as type species of *Dolosota*)

Dolosota secunda Casey, 1910

Dolosota sequax Casey, 1910

Acrotona (*Dolosota*) *abundans*: Seevers (1978) (as valid species)

Acrotona (*Dolosota*) *flaccida*: Seevers (1978) (as valid species)

Acrotona (*Dolosota*) *scopula*: Seevers (1978) (as valid species) (*Dolosota* syn. of *Acrotona*, in part; some species moved to *Pancota*)

Acrotona (*Dolosota*) *secunda*: Seevers (1978) (as valid species)

Acrotona (*Dolosota*) *sequax*: Seevers (1978) (as valid species)

Pancota laetabilis: Seevers (1978) (as valid species)

Pancota redundans tegrina: Seevers (1978) (implied, subspecies not directly mentioned)

Acrotona abundans: Majka and Sikes (2009) (syn. of *A. scopula* following Gusarov (2003b))

Acrotona flaccida: Majka and Sikes (2009) (syn. of *A. scopula* following Gusarov (2003b))

Acrotona laetabilis: Majka and Sikes (2009) (syn. of *A. scopula* following Gusarov (2003b))

Acrotona redundans tergina: Majka and Sikes (2009) (syn. of *A. scopula* following Gusarov (2003b))

Acrotona scopula: Majka and Sikes (2009) (valid species following Gusarov (2003b))

Acrotona secunda: Majka and Sikes (2009) (syn. of *A. scopula* following Gusarov (2003b))

Acrotona sequax: Majka and Sikes (2009) (syn. of *A. scopula* following Gusarov (2003b))

Material (DNA-barcoded specimens). Canada: Ontario: Georgian Bay Islands National Park, Fairy Lake, 44.8929, -79.8514, mostly conifer forest with moss, Berlese funnel, 5.VIII.2015, BIObus 2015 (1, CBG).

Distribution. Origin. Nearctic. **Canada**: ON [new record]. **United States**: IA, MO, MS, NY, PA, RI.

Diagnosis. *Mocyta scopula* can be distinguished from bicolored Canadian species and paler specimens of *M. fungi* by its finely punctate pronotum that is almost as wide as the elytra and ca. as long, and the distinctly transverse antennomeres 6–10 (Fig. 30A). The barcode sequences of *M. scopula* forms a sister cluster with *M. luteola* (BOLD:ABW2813), with a sequence divergence of ~ 7.5%. These species can be easily separated using the above diagnosis.

Bionomics. The Canadian specimen was collected from forest litter with a Berlese funnel but nothing specific is known about this species' microhabitat preferences.

Comments. *Mocyta scopula* is a native Nearctic species distributed in eastern North America. Here we newly report it from Canada based on one male specimen collected in southern Ontario. Its distribution in the United States is based on type material, including its putative synonyms, which should be verified.

Mocyta scopula is the type species of *Dolosota* Casey, which has been treated as a subgenus of *Acrotona* since Seevers (1978). However, using the generic concepts of Klimaszewski et al. (2015), this species best fits in genus *Mocyta* based on the following
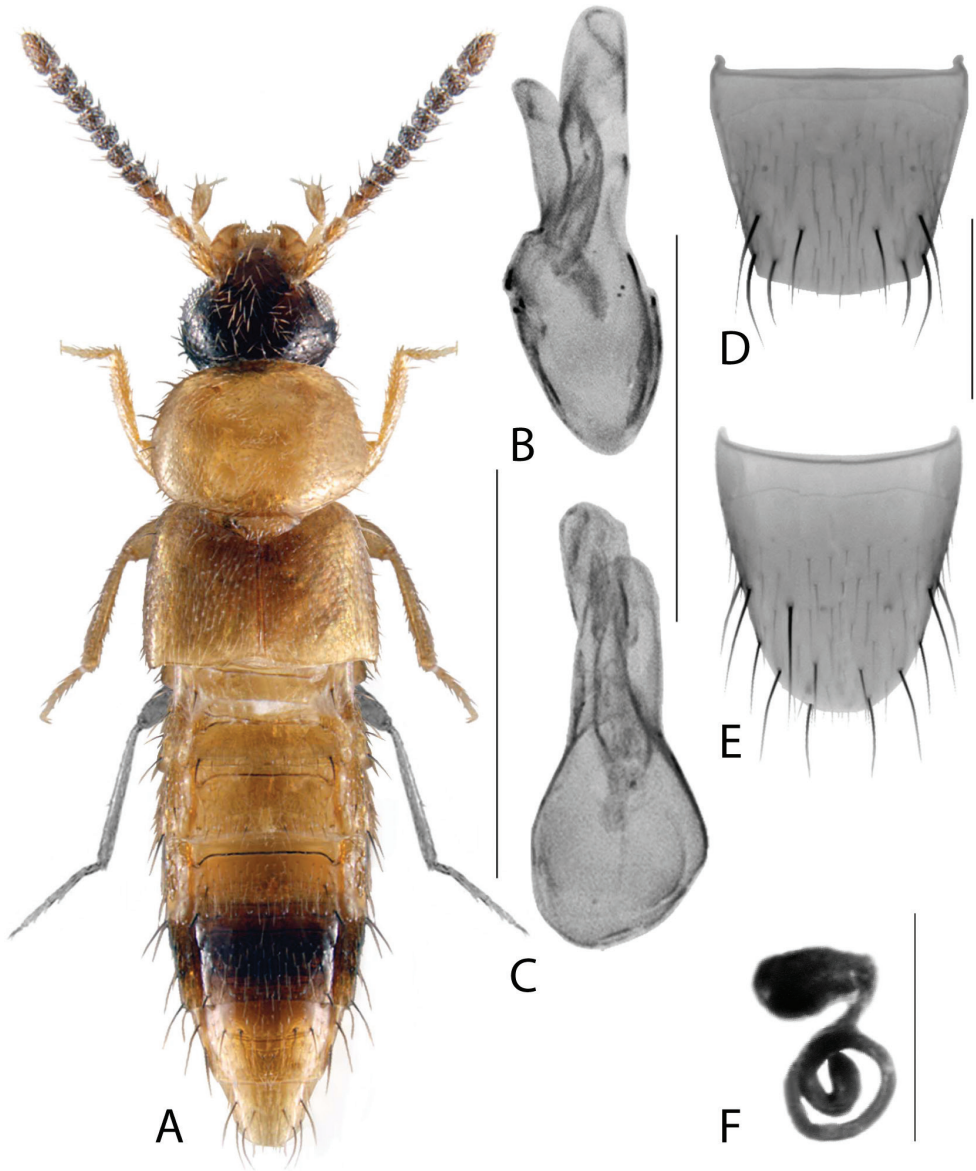
Figure 30. *Mocyta scopula* (Casey) **A** habitus (hind legs missing on specimen, taken from related species) **B** median lobe of aedeagus in lateral view **C** median lobe of aedeagus in dorsal view **D** male tergite VIII **E** male sternite VIII **F** spermatheca (female syntype). Scale bars: 1 mm (**A**); 0.2 mm (**B–F**).

character states: dorsal surface without fine white pubescence; broad tergite VIII with basal line not touching base of tergite; spermatheca with pear-shaped capsule and distinct but small invagination, and thin and irregularly shaped stem ending in a tightly deflexed apex (Fig. 30F) (based on images taken of female syntypes (NMNH). Further evidence comes from barcode sequences of this species, which cluster with the other species of *Mocyta*. Therefore, we synonymize *Dolosota* Casey syn. nov. with *Mocyta* Mulsant

and Rey. The other species included in *Dolosota* by Seevers (1978) were treated as synonyms of *M. scopula* by Majka and Sikes (2009), in addition to two other Casey names (see above synonymy), following the unpublished results of a type revision by V. Gusarov (Gusarov 2003b). These synonyms and *M. scopula* are here comb. nov. in *Mocyta*.

The aedeagus, coloration and punctation of the Canadian specimen are consistent with type material of *M. scopula*, previously examined and imaged by JK. The two other members of the BIN BOLD:ACH8720 originate from a study by Elven et al. (2010), and were mined into BOLD from GenBank. They were collected in the USA and identified verbatim as *Mocyta scopula* by V. Gusarov.

The key to Canadian *Mocyta* in Klimaszewski et al. (2015) can be modified as follows (bicolored species)

2a	Pronotum much broader than elytra; antennal articles 5–10 in specimens slightly elongate; spermatheca forming concentric circles posteriorly ....**M. discreta** (Casey)
–	Pronotum ca. as broad as elytra or slightly narrower (Fig. 30A); antennal articles 5–10 subquadrate to transverse (Fig. 30A); spermatheca forming irregular coils posteriorly **2b**
2b	Pronotum coarsely punctate and extremely transverse with weakly rounded base and apex; antennal articles 5–10 subquadrate; median lobe in lateral view strongly produced ventrad ....**M. luteola** (Erichson)
–	Pronotum finely punctate and transverse, but more rounded at base and apex (Fig. 30A); antennal articles 5–10 distinctly transverse (Fig. 30A); median lobe in lateral view only weakly produced ventrad (Fig. 30B)........................ .... **M. scopula** (Casey)

Philhygra angusticauda (Bernhauer, 1909)
BOLD:ACG2845
Fig. 31A–G

Atheta (*Metaxya*) *angusticauda* Bernhauer, 1909
Atheta (*Philhygra*) *pinegensis* Muona, 1983, syn. nov.

Material (DNA barcoded specimens). Canada: Alberta: Jasper National Park, Miette Hotsprings, 53.124, -117.7755, Malaise trap placed in valley with creek bed, sides rocky and mossy, 1439 m, 21.VII.2012, BIObus 2012 (1, CBG). **Finland:** Lkoc: Muonio, Sarvijärvi, 68.0909, 24.103, 11.VII.2012, M. Pentinsaari (2, ZMUO).

Distribution. Origin. Holarctic. **Canada**: AB[new record], BC, NB. **United States**: AK, NH.

Bionomics. As with other species of the genus, *P. angusticauda* is associated with riparian habitats.
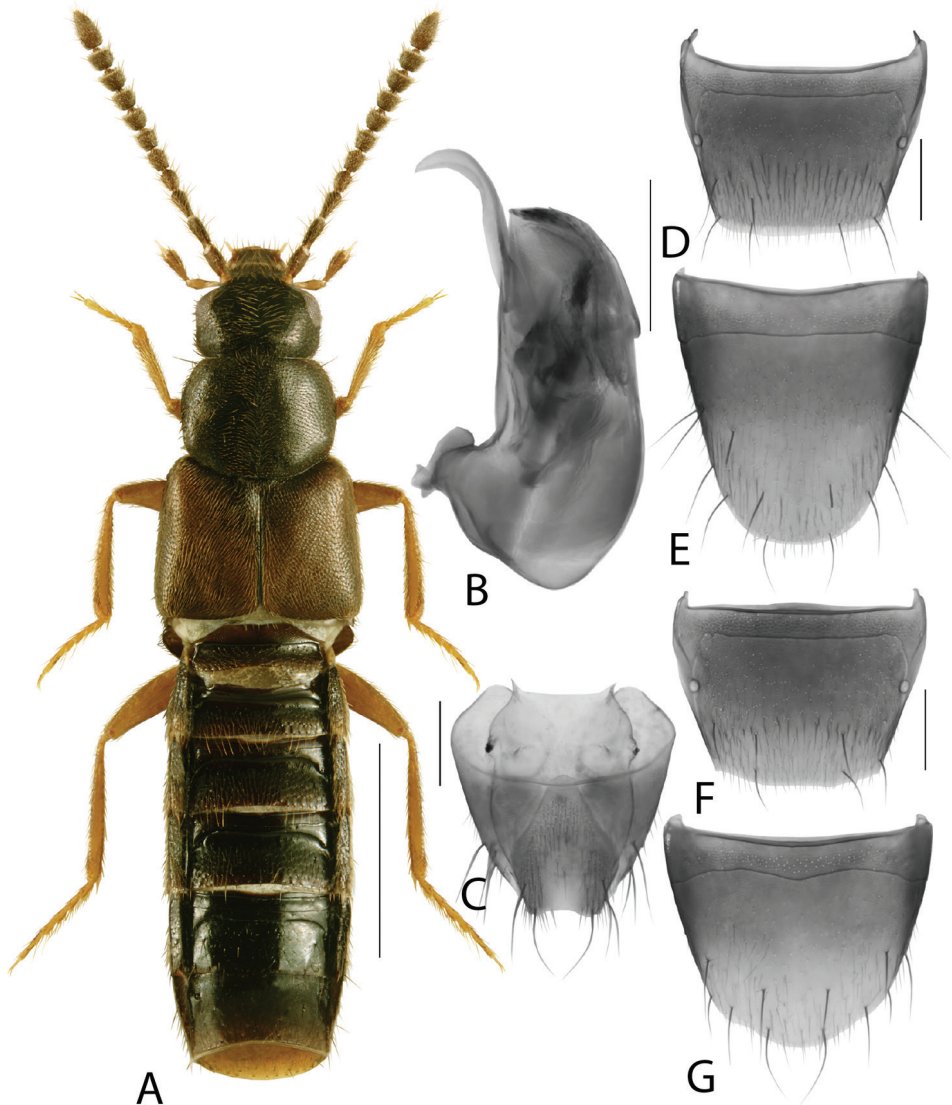
Figure 31. *Philhygra angusticauda* (Bernhauer) **A** habitus **B** median lobe of aedeagus in lateral view **C** female pygidium **D** male tergite VIII **E** male sternite VIII **F** female tergite VIII **G** female sternite VIII. Scale bars: 1 mm (**A**); 0.2 mm (**B–G**). Illustrations after Klimaszewski et al. (2018), reproduced with permission.

Comments. *Philhygra angusticauda* is a Holarctic species that was previously recognized in the Palaearctic (Finland, Norway, European Russia, Russian Far East) (Schülke and Smetana 2015; Newton 2019) under the synonym *P. pinegensis* (Muona). We newly report this species from Alberta and suggest that it broadly occurs across northern Canada. Specimens from the Nearctic and Palaearctic were found to have identical genitalia and their DNA barcodes form a cluster with only 0.3% divergence between Finnish and Canadian specimens.

Philhygra finitima **(Casey, 1910)**
Fig. 32A–H

Material (non-sequenced specimens). Canada: Ontario: Algonquin Park, ~45.87, -77.33, car net, 20.VII.2016, T. Struyve (10, CNC, LFC [4 males, 6 females])

Distribution. Origin. Nearctic. **Canada**: ON [new record]. **United States**: MA, RI.

Diagnosis. This species can be readily recognized by a combination of its small size, large eyes and relatively simple, ventrally projecting median lobe of the aedeagus in lateral view (Fig. 32B).

Bionomics. Nothing specific is known about this species' microhabitat preferences but it probably occurs near water as do other species of the genus. The series of Ontario specimens was collected using a car net, which is typically effective for collecting small staphylinids.

Comments. *Philhygra finitima* is a native Nearctic species distributed in northeastern North America. Here, we newly report it from Canada. Canadian specimens were identified based on comparison with images (Fig. 32C) of the unpublished lectotype of *P. finitima* in the Casey collection at NMNH.

Philhygra laevicollis **(Mäklin, 1852), sensu nov.**
BOLD:ACU6301
Fig. 33A–I

Material (DNA-barcoded specimens). Canada. Alberta: Waterton Lakes National Park, Highway 6 pulloff, 49.065, -113.779, 1569 m, intercept trap, montane forest, 21–27.VI.2012, BIOBus 2012 (1, CBG); same data except 06–11.VIII.2012 (1, CBG). **British Columbia:** Prince George, Nukko Lake Elementary School, EPQ-CLL-574, 54.083, -122.988, 764 m, 8.V.2015, H. Sapun (1, CBG). **United States. Alaska:** Dall Island, 54.998, -133.016, 15.VII.2011, D. S. Sikes (1, UAM); Prince of Wales Island, Luck Point, 55.98, -132.772, clear cut, berlese, 9.VIII.2011, J. Stockbridge and B. Wong (1, UAM).

Distribution. Origin. Nearctic. **Canada:** AB [new record], BC. **United States:** AK, WA.

Diagnosis. *Philhygra laevicollis* can be distinguished from most species of the genus by the general shape of the median lobe in lateral view. It is most similar to *P. pseudolaevicollis* but has a sinuate ventral face of the median lobe in lateral view and large spines in the internal sac (Fig. 33B).

Bionomics. Specimens have been collected from clear cut areas, transitional zone of a coniferous forest, seepages, and river and creek edges, from moss, leaf litter, gravel, dung, carrion and pitfall traps (Klimaszewski et al. 2020).

Comments. *Philhygra laevicollis* is a western Nearctic species that was previously considered to include eastern populations that we here treat as *Philhygra pseudolaevicollis* sp. nov. that differs in male genitalia but also by the divergent DNA barcode sequence.
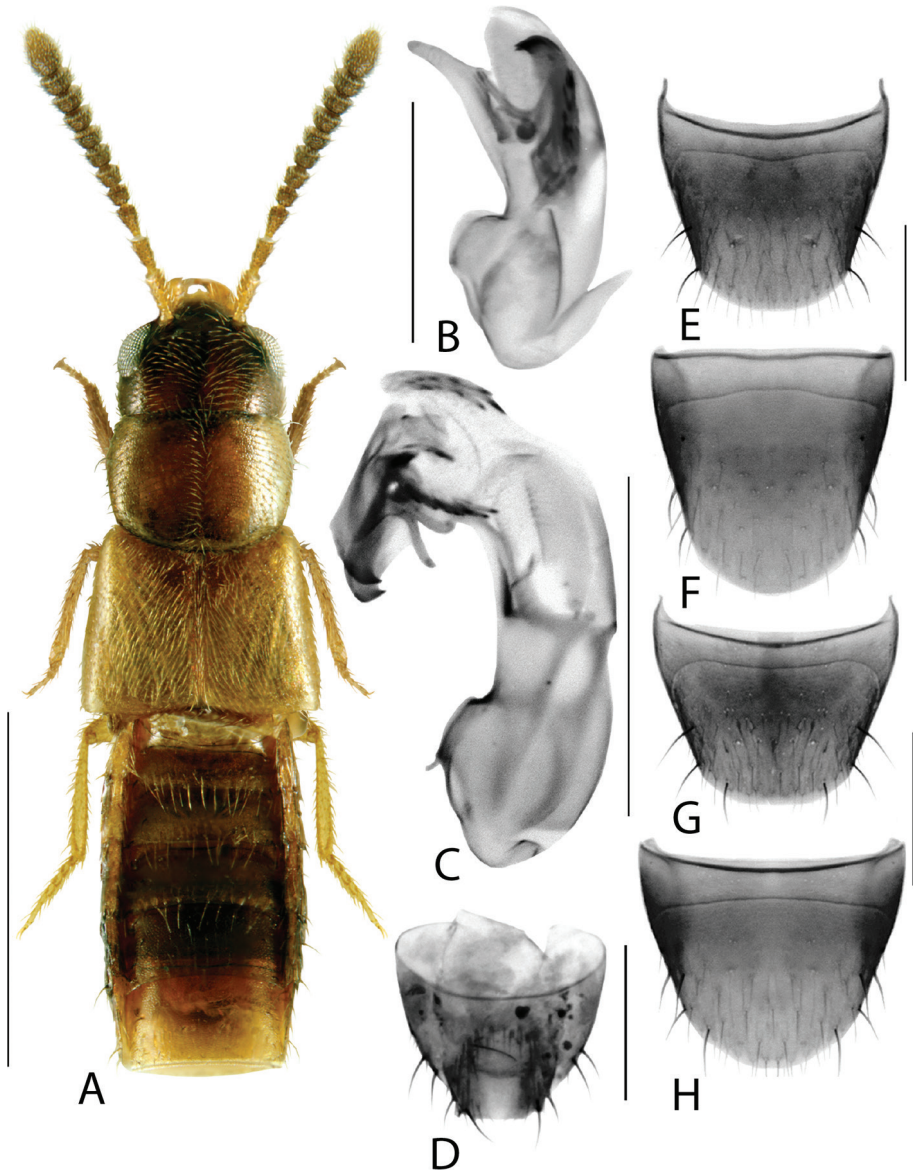
Figure 32. *Philhygra finitima* (Casey) **A** habitus **B, C** median lobe of aedeagus in lateral view **C** with internal sac everted (unpublished lectotype) **D** female pygidium **E** male tergite VIII **F** male sternite VIII **G** female tergite VIII **H** female sternite VIII. Scale bars: 1 mm (**A**); 0.2 mm (**B–H**).

Neither this species nor *P. laevicollis* are known from MB, this error was corrected by Klimaszewski et al. (2020). We have observed some variation in the shape of the sclerotized structure present on the female pygidium between specimens collected in BC, but it is not yet clear whether additional species are overlooked within the present concept of *P. laevicollis*.
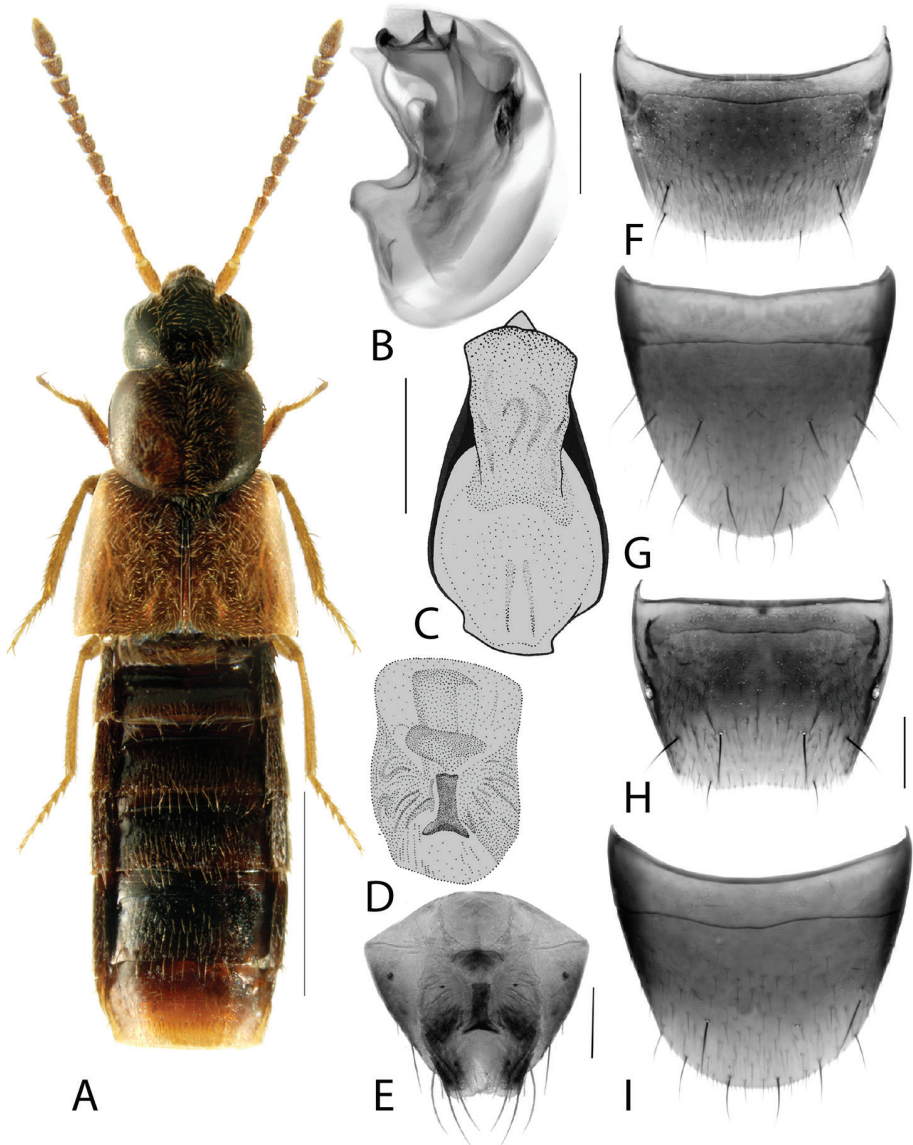
Figure 33. *Philhygra laevicollis* (Mäklin) **A** habitus **B** median lobe of aedeagus in lateral view **C** median lobe of aedeagus in ventral view **D, E** female pygidium **F** male tergite VIII **G** male sternite VIII **H** female tergite VIII **I** female sternite VIII. **A, B, E–H** after Klimaszewski et al. (2020), used with permission **C, D** after Klimaszewski and Winchester (2002). Scale bars: 1 mm (**A**); 0.2 mm (**B–I**).

Philhygra palustris (Kiesenwetter, 1844)

BOLD:AAN6150

Fig. 34A–H

Material (DNA-barcoded specimens). Canada: Ontario: Puslinch, Hanner property, 43.4464, -80.2512, Malaise trap in hardwood forest, 21.VIII.2008, T. Terzin (1,

CBG); Puslinch, concession 11/Hume Rd., 43.537, -80.134, Malaise trap in temperate mixed forest, 18–24.IV.2010, P. Hebert (1, CBG); Milverton, Milverton Public School, 43.568, -80.928, Malaise trap, 3.V.2013, J. Van Bakel (1, CBG); Cambridge, rare Charitable Research Reserve, Hogsback forest, 43.3729, -80.354, edge of hardwood forest, intercept trap, 31.V.2015, BIO collections staff (2, CBG); same except pan traps (1, CBG); Kawartha Lakes, 44.366, -78.478, farm, Malaise trap, 13.VI.2015, B. McClenaghan (2, vouchers not preserved); Guelph, Arkell Research Station, 43.5187, -80.1709, between corn and soy fields, w/ nearby pasture, Malaise trap, 8.V.2015, BIO collections staff (1, CBG); same except soy field, 43.5264, -80.1796, 4-headed SLAM trap, 17.V.2017 (1, CBG); Hamilton, Royal Botanical Gardens, Cootes Paradise, 43.281, -79.904, forest, deadwood and UV lights at night, 21.VII.2017, M. Pentinsaari (1, CBG); Markham, 43.9371, -79.2285, mixed habitat, Berlese funnel, 25.VI.2017, Rouge NUP BioBlitz Volunteers (1, CBG). **Belgium:** Sint-Genesius-Rode, BR Zonienwoud, 50.7505, 4.423, 16.VI.2010, F. Koehler (1, ZSM). **Estonia:** Piusa, 57.844, 27.466, 05.VII.2010, J. Salokannel (2, ZMUO). **Finland:** Ab: Nauvo, Sandö, 60.1747, 22.1338, 18.VI.2011, M. Pentinsaari (1, ZMUO); Ok: Vaala, Manamansalo, 64.3365, 27.0879, 21.VIII.2011, M. Pentinsaari (1, ZMUO); Ks: Kuusamo, Oulanka, 66.3686, 29.3188, 07.VIII.2011, M. Pentinsaari (1, ZMUO); Ka: Virolahti, Hailiniemi, 60.5259, 27.7366, 20.VII.2012, M. Pentinsaari (1, ZMUO). **Germany:** Riedlhuette, Diensthuettenstrasse, 48.937, 13.412, 09.VII.2011, F. Koehler and M. Koehler (2, ZSM); Spiegelau, Schwarzachstrasse, 48.9456, 13.3619, 09.VII.2011, F. Koehler and M. Koehler (2, ZSM); Waldhaeuser, Lusen- und Boehmstrasse, 48.93, 13.492, 09.VII.2011, F. Koehler and M. Koehler (2, ZSM); Arnsberg-Breitenbruch, NWZ Hellerberg, 51.4461, 8.13539, 30.V.2011, F. Koehler (2, ZSM); Bornheim-Hemmerich, Hellenmaar, 50.7402, 6.91803, 14.VIII.2012, F. Koehler (1, ZSM); Erftstadt-Bliesheim, NWZ Altwald Ville, 50.7917, 6.84384, 03.VI.2011, F. Koehler (1, ZSM); Kandel, Bienwald, 49.01, 8.103, 05.VI.2010, F. Koehler (1, ZSM); Eisenach, E, Rothenhof, Hoerselufer, 50.9643, 10.3644, 06.VII.2013, GBOL-Team ZFMK (2, ZFMK).

Distribution. Origin. Palaearctic (adventive in North America). **Canada:** MB, ON [new record]. **USA**: CT, MA, ME, NH, NY, PA, RI, SC, VT, WI.

Diagnosis. Males of this species are easily recognized among other Canadian *Philhygra* by the simple, non-projecting median lobe in lateral view (Fig. 34B).

Bionomics. Most specimens of this species were collected by passive traps in a variety of habitats. In Sweden, *P. palustris* is considered a eurytopic species that occurs in various types of decaying plant matter, including compost, seaweed and hay piles, and along muddy shores of water bodies (Palm 1970). It can be collected in very large numbers using a car net (V. Assing, *pers. comm.*).

Comments. *Philhygra palustris* is a Palaearctic species that has become adventive and widespread in eastern North America. In the Palaearctic, it is very broadly distributed and reported from Europe, North Africa (Morocco), Russia (European and Siberia), Mongolia, North and South Korea (Lee and Ahn 2012), Japan, and northern China (Newton 2019). It is also known from the Azores and the Canaries (Newton 2019), though it is likely introduced there as well.
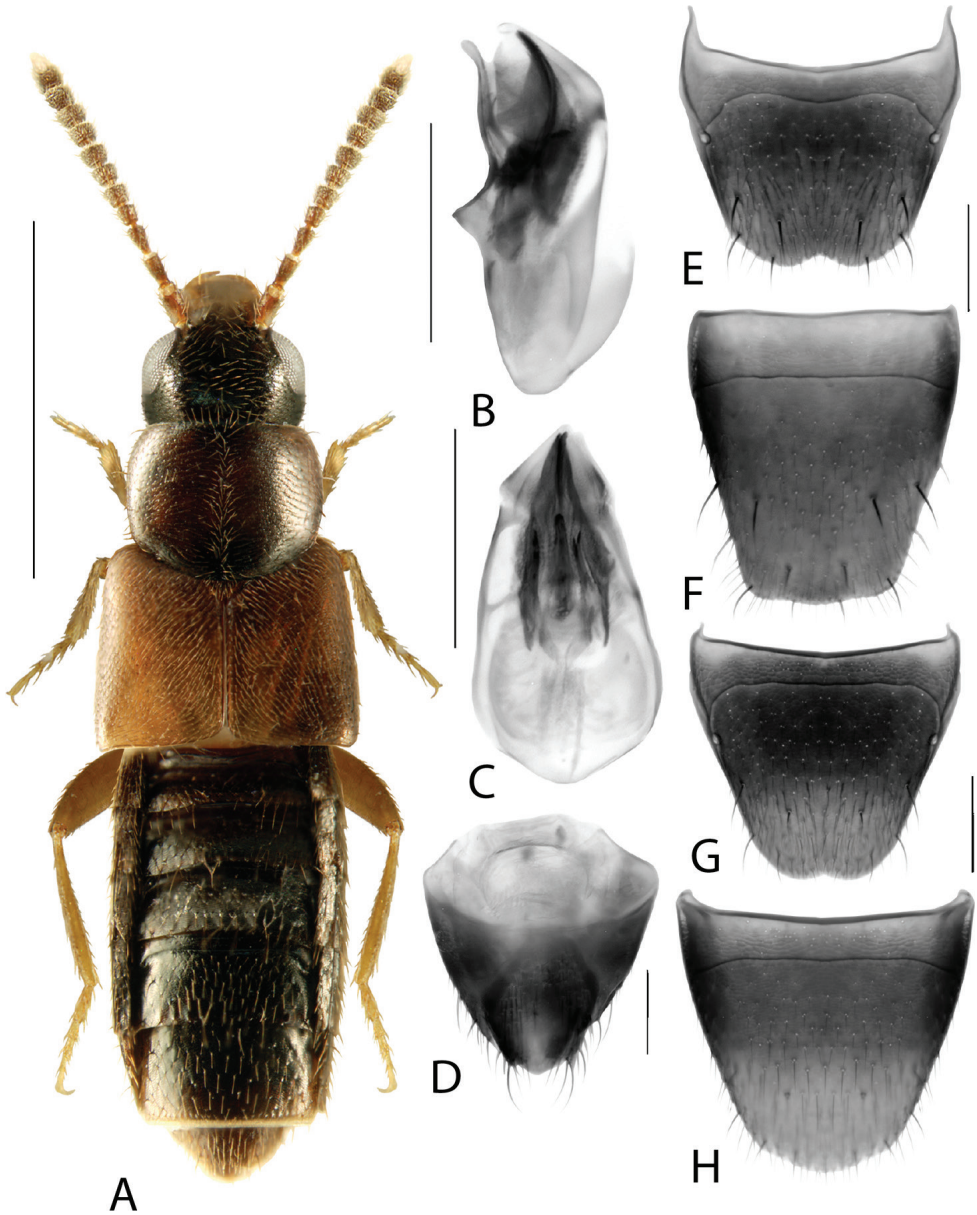
Figure 34. *Philhygra palustris* (Kiesenwetter) **A** habitus **B** median lobe of aedeagus in lateral view **C** median lobe of aedeagus in ventral view **D** female pygidium **E** male tergite VIII **F** male sternite VIII **G** female tergite VIII **H** female sternite VIII. Scale bars: 1 mm (**A**); 0.2 mm (**B–H**).

This species was reported from Canada (Manitoba) for the first time in the checklist by Bousquet et al. (2013) but no specimens could be found in the CNC to support this record. It is likely that the species *P. tenuicula* (Casey, 1911) described from Manitoba and treated as a synonym of *P. palustris* (Newton 2019), is the basis of this record.

Philhygra palustris was first recorded from North America by Muona (1984) from New York, Maine and Pennsylvania but detailed specimen level data were not provided. Several specimens from various localities in southern Ontario have been sequenced, and their barcodes cluster with European specimens, with multiple haplotypes shared between Canada and Europe. This common European species is here confirmed to be adventive in Canada and is probably broadly distributed in at least eastern North America.

Philhygra pseudolaevicollis Klimaszewski, Brunke & Pentinsaari, sp. nov.

http://zoobank.org/7D087111-AC74-4D0C-851D-801BA3206497
Fig. 35A–G

Type material. *Holotype* **(male) (CNC):** NEW BRUNSWICK. YORK CO: New Maryland, Charters Settlement, 45.8341°N, 66.7445°W, 22 April 2005, R.P. Webster coll. / mature spruce and cedar forest, seepage area, in saturated sphagnum and leaf litter / HOLOTYPE *Philhygra pseudolaevicollis* Klimaszewski, Brunke & Pentinsaari sp. nov., des. Klimaszewski 2021 [red printed label]. *Paratypes* **(12: LFC, CNC):** same data as holotype (1 male, CNC). **Canada, New Brunswick**, York Co., New Maryland, Charters Settlement, 45.8331°N, 66.7410°W, 14.04.2005, mixed forest in litter and sphagnum, R.P. Webster (1 male, LFC); York Co., New Maryland, Charters Settlement, 45.8390°N, 66.7308°W, 18.04.2005, mixed forest under bark, R.P. Webster (1 male, LFC); York Co., New Maryland, Charters Settlement, 45.8428°N, 66.7279°W, 20.04.2005, mixed forest small sedge marsh in moist grass litter and sphagnum, R.P. Webster (2 females, LFC, 1 female CNC); York Co., New Maryland, Charters Settlement, mixed forest, near small shaded brook, in leaf litter and moss, 9.05.2005, R.P. Webster (1 female, CNC); York Co., Canterbury Trail to Browns Mtn. Fen, 45.8978°N, 67.6273°W, mature cedar forest near stream, sifting leaf litter, 02.05.2005, M. Giguere and R. Webster (1 male, CNC); Northumberland Co., Goodfellow Brook Protected Area, 46.8943°N, 65.3796°W, old growth, wet eastern cedar swamp, in litter and moss on hummocks, near water, 23.05.2007, R.P. Webster (1 female, CNC). **Quebec**, Scotstown, 28.04.2008, C. Levesque, Barcode sample, BCO1 vial #X16, 26.05.2010, R. Civade (1 male, LFC). **Ontario**, Nipissing Co., Algonquin Prov. Park near Brent, 19.08.1980, R. Baranowski (1 female, LFC); same except: 21.08.1980 (1 male, LFC).

Non-types (DNA-barcoded specimens). Canada: New Brunswick: Restigouche Co., 9 km S of Saint Arthur, 47.818, -66.756, eastern white cedar swamp, in moss and litter near small ponds, 14.VI.2006, R.P. Webster (1, cRW).

Etymology. Prefix *-pseudo* meaning false/not genuine, added to the sibling species name *P. laevicollis* (Mäklin).

Diagnosis. This species is similar externally and genitally to *P. laevicollis* but may be distinguished from it by the following combination of characters: body on average narrower, antennomeres 6–7 more elongate (Fig. 35A), ventral margin of tubus of the median lobe of aedeagus straight apically (Fig. 35B) (sinuate in *P. laevicollis*, Fig. 33B), apical sclerites of internal sac without large spike-like projections (Fig. 35B).
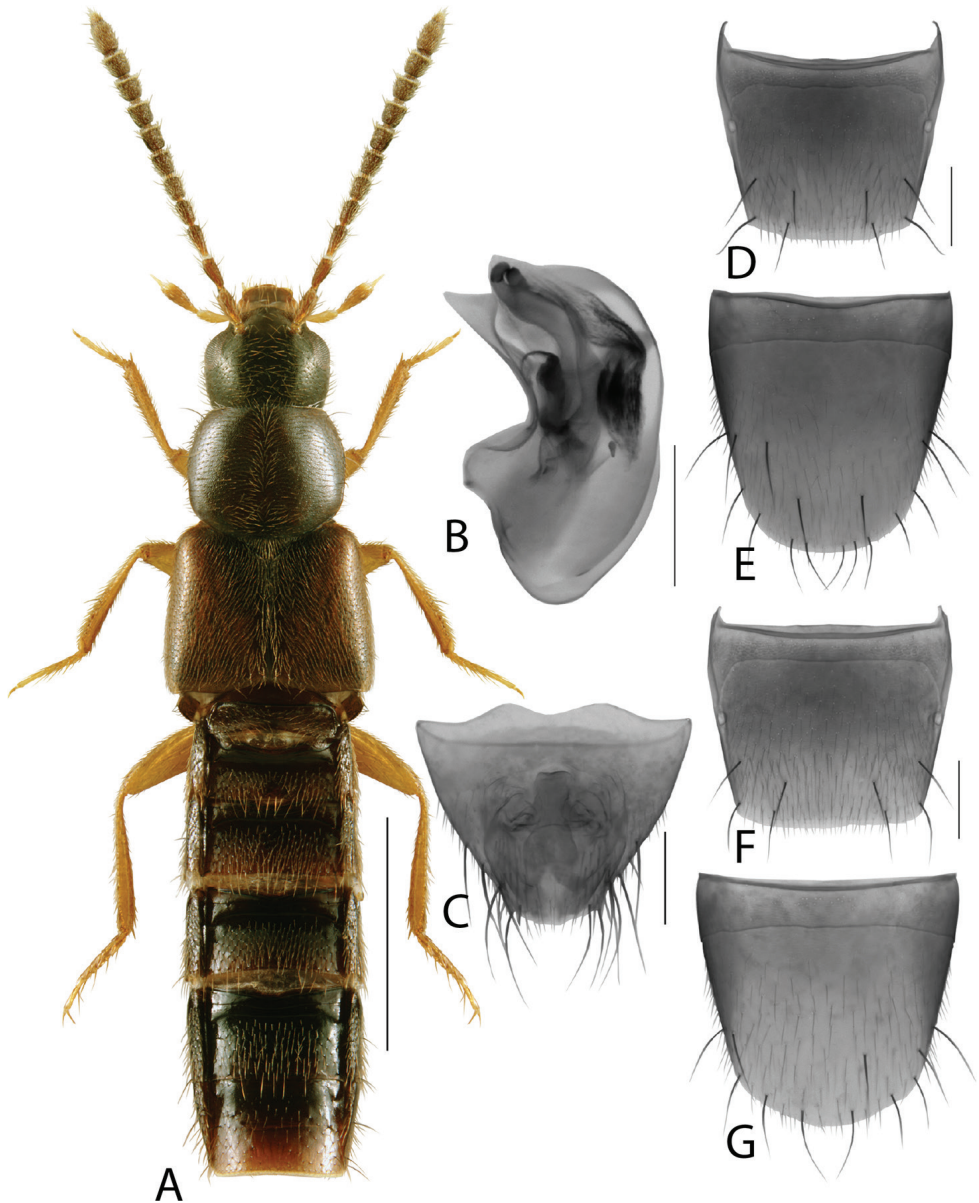
Figure 35. *Philhygra pseudolaevicollis* Klimaszewski, Brunke & Pentinsaari, sp. nov. **A** habitus **B** median lobe of aedeagus in lateral view **C** female pygidium **D** male tergite VIII **E** male sternite VIII **F** female tergite VIII **G** female sternite VIII. Scale bars: 1 mm (**A**); 0.2 mm (**B–G**). Illustrations after Klimaszewski et al. (2018), reproduced with permission.

Description. Body narrowly subparallel, moderately flattened, length 3.0–4.2 mm; colour dark brown, elytra dark brownish to brownish yellow, except for darker scutellar area and paler legs, basal antennomeres rust-brown (Fig. 35A); integument moderately glossy, forebody sparsely punctate and pubescent, with pubescence long, punctation

fine, microsculpture distinct and consisting of round and slightly convex meshes; head slightly elongate, round, ca. as wide as pronotum, eyes as long as genae in dorsal view, postocular carina strong basally, diffuse apically; antennae slender, at least as long as pronotum and elytra combined, antennomeres 1–3 strongly elongate, 6 and 7 slightly elongate, 8 and 9 slightly elongate or subquadrate, and terminal one as long as two preceding antennomeres combined; pronotum slightly transverse, impressed medially, arcuate laterally and basally, pubescence sparse, hypomeron visible almost for entire length of pronotum; elytra transverse, broader than pronotum; abdomen subparallel. MALE. Tergite VIII slightly transverse, arcuate apically (Fig. 35D); sternite VIII highly elongate, rounded apically and with wide distance between antecostal suture and base of disc (Fig. 35E); median lobe of aedeagus with moderate-sized bulbus, tubus short, ventral margin arcuate basally and straight apically, tubus narrowly triangular at apex in lateral view (Fig. 35B); internal sac sclerites without spike-like projections, complex as illustrated (Fig. 35B); in dorsal view bulbus roughly oval, tubus short, triangular apically. FEMALE. Tergite VIII transverse and truncate apically (Fig. 35F); sternite VIII rounded apically, apex slightly produced, distance between antecostal suture and base of disc wide (Fig. 35G); pygidium as illustrated, with weakly sclerotized central plate, slightly broader than in *P. laevicollis* (Fig. 35C); spermatheca not illustrated, minute with short sac-shaped capsule without apical invagination and with short narrow stem.

Distribution. Origin. Nearctic. **Canada**: NB, NS, ON, QC.

Bionomics. This species has been recorded from various wetland and riparian habitats in NB: in moss and leaf litter near brook and in litter, grasses, and moss on hummocks in old-growth eastern white cedar swamps and a wet alder swamp, in moist leaves along vernal pond margins in various mixed forests, and a red oak/red maple forest; also from pitfall traps in regenerating red spruce forests (NB) and from vernal pool litter in ON (summarized by Klimaszewski et al. 2018). **Collecting period**: IV-V, VIII. **Collecting method**: sifting leaf litter, grasses, and moss, under bark (probably overwintering).

Comments. Although they were not re-examined here, the specimens reported by Majka and Klimaszewski (2008) as *P. laevicollis*, certainly belong to *P. pseudolaevicollis*. This species is very similar externally and genitally to *P. laevicollis* occurring in western North America (AK, AB, BC, WA). Previously, it was tentatively identified as *P. laevicollis* pending additional study (e.g., Klimaszewski et al. 2005; Klimaszewski et al. 2020). The present evidence from DNA barcodes (8.5% divergence between the eastern and western specimens) and morphology of the aedeagus revealed that eastern and western populations represent two distinct, cryptic species. The single barcoded specimen of *P. pseudolaevicollis* produced a 407 bp sequence and therefore, no BIN has been generated.

***Trichiusa robustula* Casey, 1893**
BOLD:AAY6555
Fig. 36A–I

Trichiusa robustula Casey, 1893
Trichiusa immigrata Lohse, 1984, syn. nov.
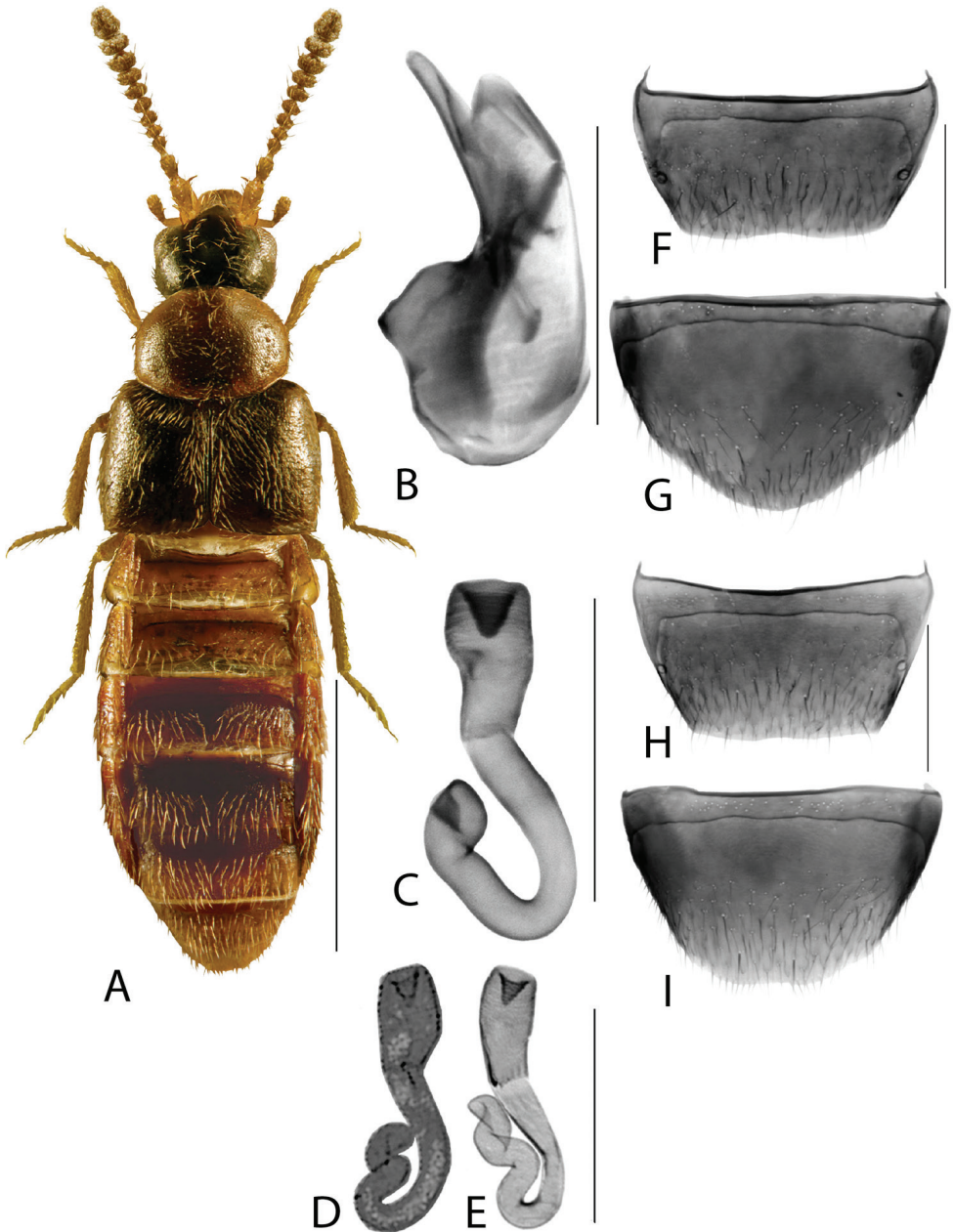
Figure 36. *Trichiusa robustula* Casey **A** habitus **B** median lobe of aedeagus in lateral view **C–E** spermatheca **F** male tergite VIII **G** male sternite VIII **H** female tergite VIII **I** female sternite VIII. **A–C, F–I** after Webster et al. (2016) **D, E** after Brunke et al. 2012. Scale bars: 1 mm (**A**); 0.2 mm (**B–I**).

Material (DNA-barcoded specimens). Austria: Innervillgraten, Arntal, 46.8362, 12.3348, mountain forest and alpine pastures, car net, 25.VIII.2013, GBOL-Team ZFMK (1, ZFMK). **Germany:** Nuernberg, N Flughafen, 49.5006, 11.0789, sifting

compost, date not provided, GBOL-Team ZFMK (1, ZFMK); Schoenau/Hoersel, W, Gewerbegebiet, 50.947, 10.4214, sifting compost, 25.VIII.2012, GBOL-Team ZFMK (2, ZFMK); Kahlenberg/Eisenach, Pferdekoppel, 50.9469, 10.4287, in horse dung, 16.IX.2013, GBOL-Team ZFMK (1, ZFMK). **Finland:** Ka: Hamina, Meltti, 60.5798, 27.2016, 12.X.2011, M. Pentinsaari (1, ZMUO); Al: Mariehamn, Dalen, 60.0703, 19.9595, 9.X.2011, M. Pentinsaari (2, ZMUO). **Canada: Ontario:** Guelph, Division Street, 43.5544, -80.2644, malaise trap, 14.VII.2010, A. Smith (1, CBG); Chelsey, Chelsey District Community School, EQP-CLL-581, 44.3028, -81.0967, 281 m, malaise trap, 22.IX–3.X.2014, A. Grieve (1, CBG); Guelph, Arboretum, Urban Organic Farm, 43.5381, -80.222, compost heaps/mouldy hay pile, 17.IX.2017, M. Pentinsaari (6, CBG).

Additional material (non-barcoded). Numerous dissected specimens from Denmark were examined in the collection of NHMD.

Distribution. Origin. Nearctic (adventive in Europe). **Canada**: ON, NB. **United States**: IA.

Bionomics. In its native range, this species has been collected in a variety of decaying plant matter, especially near water. This species was also common in compost in NB. In Europe, this species has been collected from similar microhabitats including grass clippings and compost (Denton 1998; Anderson and Bryan 2012).

Comments. *Trichiusa robustula* is a Nearctic species that is broadly distributed in eastern North America but not well collected. It was previously recognized under the synonym *T. immigrata* Lohse in the West Palaearctic (Europe, Canary Islands, Madeira; Newton 2019), where it is adventive.

When describing his new species, Lohse (1984) noted that it must have originated from North America, since *Trichiusa* is otherwise endemic to that region. Lohse (1984) stated that *T. immigrata* was compared with types of North American species described by Casey (1893), but this taxon is a morphological and molecular match to *T. robustula*. Although most of the specimens collected in North America are bicolored (reddish/dark), study of extensive material from Denmark (NMHD) revealed a grade between fully dark brown to reddish/dark bicolored. *Trichiusa robustula* is distinctive for the shape of its spermatheca, which bears a rectangular capsule, and stem that has a single 180-degree bend followed by a twisted apical portion (Fig. 36C). The figure of the spermatheca in Klimaszewski et al. (2018) is atypical (Fig. 36C) and the original illustrations in Brunke et al. (2012), reproduced here (Fig. 36D, E), better show these features.

Acknowledgements

References

Anderson R, Bryan MD (2012) *Trichiusa immigrata* Lohse (Staphylinidae) in Ireland. The Coleopterist 21: e94.

Assing V (2002) A taxonomic and phylogenetic revision of *Amarochara* Thomson. I. The species of the Holarctic region. Beiträge zur Entomologie 52: 111–204. https://doi.org/10.21248/contrib.entomol.52.1.111-204

Assing V (2021) On the taxonomy of *Parocyusa*, *Tectusa*, and miscellaneous genera of Oxypodina (Insecta: Coleoptera: Staphylinidae: Aleocharinae: Oxypodini). Annalen des Naturhistorischen Museums in Wien 123: 99–218. https://www.jstor.org/stable/26993242?seq=1

Benick G (1952) Revision der Untergattung *Aloconota* C.G. Thoms. (Gattung *Atheta*, *Staph.*). Entomologische Blatter 50: 133–174.

Bernhauer M (1936) Neuheiten der paläarktischen Staphylinidenfauna III. Koleopterologische Rundschau 22: 50–58. https://www.zobodat.at/pdf/KOR_22_1936_0050-0058.pdf

Bousquet Y, Bouchard P, Davies A, Sikes DS (2013) Checklist of Beetles (Coleoptera) of Canada and Alaska. Pensoft, Sofia, 402 pp. https://doi.org/10.3897/zookeys.360.4742

Blackwelder RE (1952) The generic names of the beetle family Staphylinidae, with an essay on genotypy. United States National Museum Bulletin 200: 1–483. https://www.biodiversitylibrary.org/part/85283

Brunke AJ, Buffam J (2018) A Review of Nearctic rove beetles (Staphylinidae) specialized on the burrows and nests of vertebrates. In: Betz O, Irmler U, Klimaszewski J (Eds) Biology of Rove Beetles (Staphylinidae), Life History, Evolution, Ecology and Distribution. Springer, Cham, Switzerland, 295 pp. [145–159.] https://doi.org/10.1007/978-3-319-70257-5_8

Brunke A, Klimaszewski J, Dorval J-A, Bourdon C, Paiero S, Marshall S (2012) New species and distributional records of Aleocharinae (Coleoptera, Staphylinidae) from Ontario, Canada, with a checklist of recorded species. ZooKeys 186: 119–206. https://doi.org/10.3897/zookeys.186.2947

Brunke AJ, Bahlai CA, Klimaszewski J, Hallett RH (2014) Rove beetles (Coleoptera: Staphylinidae) in Ontario, Canada soybean agroecosystems: assemblage diversity, composition, seasonality, and habitat use. The Canadian Entomologist 146: 652–670. https://doi.org/10.4039/tce.2014.19

Brunke AJ, Salnitska M, Hansen AK, Zmudzinska A, Smetana A, Buffam J, Solodovnikov A (2020) Are subcortical rove beetles truly Holarctic? An integrative taxonomic revision of north temperate *Quedionuchus* (Coleoptera: Staphylinidae: Staphylininae). Organisms Diversity & Evolution 20: 77–116. https://doi.org/10.1007/s13127-019-00422-2

Casey TL (1893) Coleopterological notices. V. Annals of the New York Academy of Sciences 7: 281–606. https://doi.org/10.1111/j.1749-6632.1893.tb55411.x

Casey TL (1906) Observations on the staphylinid groups Aleocharinae and Xantholinini, chiefly of America. Transactions of the Academy of Science of St. Louis 16: 125–434. https://www.biodiversitylibrary.org/page/33076327

Casey TL (1910) New Species of the Staphylinid Tribe Myrmedoniini. Memoirs on the Coleoptera 1. New Era Printing Co., Lancaster, Pennsylvania, 184 pp. https://www.biodiversitylibrary.org/page/962781

Denton, M (1998) *Trichiusa immigrata* Lohse (Staphylinidae) in Yorkshire. Coleopterist 4: 1–14.

deWaard JR, Ratnasingham S, Zakharov EV, Borisenko AV, Steinke D, Telfer AC, Perez KHJ, Sones JE, Young MR, Levesque-Beaudin V, Sobel CN, Abrahamyan A, Bessonov K, Blagoev G, deWaard SL, Ho C, Ivanova NV, Layton KKS, Lu L, Manjunath R, McKeown JTA, Milton MA, Miskie R, Monkhouse N, Naik S, Nikolova N, Pentinsaari M, Prosser SWJ, Radulovici AE, Steinke C, Warne CP, Hebert PDN (2019). A reference library for Canadian invertebrates with 1.5 million barcodes, voucher specimens, and DNA samples. Scientific Data 6: e308. https://doi.org/10.1038/s41597-019-0320-2

Elven H, Bachmann L, Gusarov VI (2010) Phylogeny of the tribe Athetini (Coleoptera: Staphylinidae) inferred from mitochondrial and nuclear sequence data. Molecular Phylogenetics and Evolution 57: 84–100. https://doi.org/10.1016/j.ympev.2010.05.023

Enushchenko IV, Semenov VB (2016) A review of the genus *Gyrophaena* Mannerheim 1830 (Coleoptera: Staphylinidae: Aleocharinae: Gyrophaenina) of the Caucasus and adjacent territories. Zootaxa 4126: 301–337. https://doi.org/10.11646/zootaxa.4126.3.1

Erichson WF (1839) Genera et species Staphylinorum insectorum coleopterorum familiae. F.H. Morin, Berlin, 400 pp. https://www.biodiversitylibrary.org/page/39356602

Fenyes A (1918) Coleoptera: Fam Staphylinidae, subfam. Aleocharinae. In: Wytsman P (Ed.) Genera Insectorum, Fasc 173 A. L. Desmet-Verteneuil, Bruxelles, 110 pp.

Fenyes A (1921) New genera and species of Aleocharinae with polytomic synopsis of the tribes. Bulletin of the Museum of Comparative Zoology 65: 17–35.

Gouix N, Klimaszewski J (2007) Catalogue of Aleocharine Rove Beetles of Canada and Alaska (Coleoptera, Staphylinidae, Aleocharinae). Pensoft Publishers, Sofia-Moscow, 168 pp.

Gusarov VI (2003a) Revision of some types of North American aleocharines (Coleoptera: Staphylinidae: Aleocharinae), with synonymic notes. Zootaxa 353: 1–134. https://doi.org/10.11646/zootaxa.353.1.1

Gusarov VI (2003b) A catalogue of the athetine species of America north of Mexico (Coleoptera: Staphylinidae: Aleocharinae: Athetini). https://web.archive.org/web/20100613213828/http://www.nhm.ku.edu/ksem/peet/catalogs/cataweb.htm

Hansen A, Bogri A, Solodovnikov A (2017) The Danish Beetle Bank. www.BilleBank.dk [last accessed on January 19, 2021]

Hendrich L, Morinière J, Haszprunar G, Hebert PDN, Hausmann A, Köhler F, Balke M (2015) A comprehensive DNA barcode database for Central European beetles with a focus on Germany: Adding more than 3,500 identified species to BOLD. Molecular Ecology Resources 15: 795–818. https://doi.org/10.1111/1755-0998.12354

Horion AD (1967) Faunistik der Mitteleuropäischen Käfer (Vol. II). Staphylinidae, part 3 Habrocerinae bis Aleocharinae (Ohne Subtribus Athetae). P.C.W. Schmidt, Überlingen-Bodensee, 4190 pp.

Kapp A (2019) Revision der westpaläarktischen Arten der Gattungen Oligota Mannerheim, 1830 und Holobus Solier, 1849 (Coleoptera, Staphylinidae, Aleocharinae, Hypocyphtini). Linzer biologische Beiträge 51: 587–698. http://doi.org/10.5281/zenodo.3754300

Klimaszewski J (1979) A revision of the Gymnusini and Deinopsini of the world (Coleoptera: Staphylinidae: Aleocharinae). Agriculture Canada Monograph 25: 1–169.

Klimaszewski J, Ashe JS (1991) The oxypodine genus *Haploglossa* Kraatz in North America (Coleoptera: Staphylinidae: Aleocharinae). Giornale Italiano di Entomologia 5: 409–416.

Klimaszewski J, Pelletier G (2004) Review of the *Ocalea* group of genera (Coleoptera, Staphylinidae, Aleocharinae) in Canada and Alaska: new taxa, bionomics and distribution. The Canadian Entomologist 136: 443–500. https://doi.org/10.4039/n03-069

Klimaszewski J, Assing V, Majka CG, Pelletier G, Webster RP, Langor DW (2007) Records of adventive aleocharine beetles (Coleoptera: Staphylinidae: Aleocharinae) found in Canada. The Canadian Entomologist 139: 54–79. https://doi.org/10.4039/n05-105

Klimaszewski J, Savard K, Pelletier G, Webster RP (2008) Species review of the genus *Gnypeta* Thomson from Canada, Alaska and Greenland (Coleoptera, Staphylinidae, Aleocharinae): systematics, bionomics and distribution. ZooKeys 2: 11–84. https://doi.org/10.3897/zookeys.2.4

Klimaszewski J, Webster RP, Bourdon C, Pelletier G, Godin B, Langor D (2015) Review of Canadian species of the genus *Mocyta* Mulsant & Rey (Coleoptera, Staphylinidae, Aleocharinae), with the description of a new species and a new synonymy. ZooKeys 487: 111–139. https://doi.org/10.3897/zookeys.487.9151

Klimaszewski J, Larson DJ, Labrecque M, Bourdon C (2016a) Twelve new species and fifty-three new provincial distribution records of Aleocharinae rove beetles of Saskatchewan, Canada (Coleoptera, Staphylinidae). ZooKeys 610: 45–112. https://doi.org/10.3897/zookeys.610.9361

Klimaszewski J, Langor D, Hammond HE, Bourdon C (2016b) A new species of *Anomognathus* and new Canadian and provincial records of aleocharine rove beetles from Alberta, Canada (Coleoptera, Staphylinidae, Aleocharinae). ZooKeys 581: 141–164. https://doi.org/10.3897/zookeys.581.8014

Klimaszewski J, Langor D, Bourdon C, Gilbert A, Labrecque M (2016c) Two new species and new provincial records of aleocharine rove beetles from Newfoundland and Labrador, Canada (Coleoptera, Staphylinidae, Aleocharinae). ZooKeys 593: 49–89. https://doi.org/10.3897/zookeys.593.8412

Klimaszewski J, Struyve T, Bourdon C, Dorval J-A (2017) First record of *Thecturota tenuissima* Casey from Canada (Coleoptera, Staphylinidae, Aleocharinae). ZooKeys 702: 19–25. https://doi.org/10.3897/zookeys.702.19963

Klimaszewski J, Webster R, Langor D, Brunke AJ, Davies A, Bourdon C, Labrecque M, Newton AF, Dorval J-A, Frank JH (2018) Aleocharine rove beetles of Eastern Canada (Coleoptera, Staphylinidae, Aleocharinae): a glimpse of megadiversity. Springer Nature, Cham, 902 pp. https://doi.org/10.1007/978-3-319-77344-5

Klimaszewski J, Sikes DS, Brunke AJ, Bourdon C (2019) Species review of the genus *Boreophilia* Benick from North America (Coleoptera, Staphylinidae, Aleocharinae, Athetini): Systematics, habitat, and distribution. ZooKeys 848: 57–102. https://doi.org/10.3897/zookeys.848.34846

Klimaszewski J, Hoebeke ER, Godin B, Davies A, Perry KI, Bourdon C, Winchester N (2020) Aleocharine rove beetles of British Columbia: a hotspot of Canadian biodiversity (Coleoptera, Staphylinidae). Springer, Cham, 631 pp. https://doi.org/10.1007/978-3-030-36174-7

Klimaszewski J, Brunke AJ, Sikes DS, Pentinsaari M, Godin B, Webster RP, Davies A, Bourdon C, Newton AF (in press) A faunal review of aleocharine rove beetles in the rapidly changing Arctic and Subarctic regions of North America (Coleoptera: Staphylinidae). Springer Nature, Cham.

LeConte JL (1863) List of the Coleoptera of North America. Prepared for the Smithsonian Institution. Smithsonian Miscellaneous Collections 6: 1–56. https://www.biodiversitylibrary.org/page/18078314

Lee S-G, Ahn KJ (2017) A taxonomic study of Korean *Aloconota* Thomson (Coleoptera: Staphylinidae: Aleocharinae) with descriptions of five new species. Journal of Natural History 51: 1–26. https://doi.org/10.1080/00222933.2017.1347298

Lohse GA (1974) Staphylinidae II (Hypocyphtinae und Aleocharinae). In: Freude H, Harde KW, Lohse GA (Eds) Die Käfer Mitteleuropas, Band 5. Goecke & Evers, Krefeld, 381 pp.

Lohse GA (1984) *Trichiusa immigrata* n. sp. eine neue Adventivart aus Mitteleuropa. Entomologische Blatter 80: 163–165.

Lohse GA, Klimaszewski J, Smetana A (1990) Revision of Arctic Aleocharinae of North America (Coleoptera: Staphylinidae). The Coleopterists Bulletin 44: 121–202. https://www.jstor.org/stable/4008713

Lundberg S (2006) Nytillkomna och strukna skalbaggsarter sedan 1995 års Catalogus Coleopterorum Sueciae [New and excluded beetle species since 1995 year's Catalogus Coleopterorum Sueciae]. Entomologisk Tidskrift 127: 101–111. http://coleoptera.se/CCS1995/ET2006%20101-111.pdf

Machulka V (1941) Einige neuen Staphyliniden aus Böhmen. I. Sborník Entomologického Oddělení při Zoologických Sbírkách Národního Musea v Praze 19: 98–102.

Majka CG, Klimaszewski J (2008) New records of Canadian Aleocharinae (Coleoptera: Staphylinidae). In: Majka CG, Klimaszewski J (Eds) Biodiversity, biosystematics, and ecology of Canadian Coleoptera. ZooKeys 2: 85–114. https://doi.org/10.3897/zookeys.2.7

Majka CG, Sikes DS (2009) Thomas L. Casey and Rhode Island's precinctive beetles: Taxonomic lessons and the utility of distributional checklists. ZooKeys 22: 267–283. https://doi.org/10.3897/zookeys.22.93

McClenaghan B, Nol E, Kerr KCR (2019) DNA metabarcoding reveals the broad and flexible diet of a declining aerial insectivore. The Auk 136: uky003. https://doi.org/10.1093/auk/uky003

Muona J (1983) Two new Palaearctic *Atheta* species (Coleoptera, Staphylinidae). Annales Entomologici Fennici 49: 57–58.

Muona J (1984) Review of the Palearctic Aleocharinae also occurring in North America (Coleoptera: Staphylinidae). Entomologica Scandinavica 15: 227–231. https://doi.org/10.1163/187631284X00190

Newton AF (2019) StaphBase: Staphyliniformia world catalog database (version Nov 2018). In: Roskov Y, Ower G, Orrell T, Nicolson D, Bailly N, Kirk PM, Bourgoin T, DeWalt RE, Decock W, Nieukerken E van, Zarucchi J, Penev L (Eds) Species 2000 & ITIS Catalogue of Life, 2019 Annual Checklist. Species 2000: Naturalis, Leiden. ISSN 2405-884X. www.catalogueoflife.org/annual-checklist/2019

Palm T (1968) Skalbaggar. Coleoptera, Kortvingar: Fam. Staphylinidae, Underfam. Aleocharinae (Deinopsis-Trichomicra). 5. Svensk Insektfauna 51: 1–113.

Palm T (1970) Skalbaggar. Coleoptera, Kortvingar: Fam. Staphylinidae, Underfam. Aleocharinae (Atheta). 6. Svensk Insektfauna 52: 117–296.

Paśnik G (2010) Phylogeny and Generic Classification of Tachyusini (Coleoptera, Staphylinidae: Aleocharinae). Institute of Systematics and Evolution of Animals, Polish Academy of Sciences, Kraków, 129 pp.

Pentinsaari M, Vos R, Mutanen M (2017) Algorithmic single-locus species delimitation: effects of sampling effort, variation and nonmonophyly in four methods and 1870 species of beetles. Molecular Ecology Resources 17: 393–404. https://doi.org/10.1111/1755-0998.12557

Pentinsaari M, Anderson R, Borowiec L, Bouchard P, Brunke AJ, Douglas H, Smith ABT, Hebert PDN (2019) DNA barcodes reveal 63 overlooked species of Canadian beetles (Insecta, Coleoptera). ZooKeys 894: 53–150. https://doi.org/10.3897/zookeys.894.37862

Ratnasingham S, Hebert PDN (2013) A DNA-based registry for all animal species: the Barcode Index Number (BIN) system. PLoS ONE 8: e66213. https://doi.org/10.1371/journal.pone.0066213

Rulik B, Eberle J, von der Mark L, Thormann J, Jung M, Köhler F, Apfel W, Weigel A, Kopetz A, Köhler J, Fritzlar F, Hartmann M, Hadulla K, Schmidt J, Hörren T, Krebs D, Theves F, Eulitz U, Skale A, Rohwedder D, Kleeberg A, Astrin JJ, Geiger MF, Wägele JW, Grobe P, Ahrens D (2017) Using taxonomic consistency with semi-automated data pre-processing for high quality DNA barcodes. Methods in Ecology and Evolution 8: 1878–1887. https://doi.org/10.1111/2041-210X.12824

Sawada K (1970) Aleocharinae (Staphylinidae, Coleoptera) of the IBP-Station in the Shiga Heights, Central Japan, II. Contributions from the Biological Laboratory of Kyoto University 23: 33–60. https://repository.kulib.kyoto-u.ac.jp/dspace/bitstream/2433/155945/1/cbl02301_033.pdf

Schülke M, Smetana A (2015) Staphylinidae. In: Löbl I, Löbl D (Eds) Catalogue of Palaearctic Coleoptera (Vol. 2). Hydrophiloidea-Staphylinoidea. Revised and updated edition. Koninklijke Brill, Leiden, 1702 pp. [304–1134.]

Seevers CH (1978) A generic and tribal revision of the North American Aleocharinae (Coleoptera: Staphylinidae) [with additions and annotations by Lee H. Herman]. Fieldiana Zoology 71: [vi +] 289 pp. https://www.biodiversitylibrary.org/page/2787293

Sikes DS, Bowser M, Morton JM, Bickford C, Meierotto S, Hildebrandt K (2017a) Building a DNA barcode library of Alaska's non-marine arthropods. Genome 60: 248–259. https://doi.org/10.1139/gen-2015-0203

Smetana A (1995) Rove beetles of the subtribe Philonthina of America north of Mexico (Coleoptera: Staphylinidae). Classification, phylogeny and taxonomic revision. Memoirs on Entomology, International 3: 1–945.

Staniec B, Pietrykowska-Tudruj E, Zagaja M (2010) Description of the larva and pupa of *Haploglossa picipennis* (Gyllenhal, 1827) and larva of *H. nidicola* (Fairmaire, 1852) (Coleoptera: Staphylinidae: Aleocharinae) with taxonomic remarks. Entomologica Fennica 21: 151–167. https://doi.org/10.33338/ef.84526

Webster R, Klimaszewski J, Bourdon C, Sweeney J, Hughes CC, Labrecque M (2016) Further contributions to the Aleocharinae (Coleoptera, Staphylinidae) fauna of New Brunswick and Canada including descriptions of 27 new species. ZooKeys 573: 85–216. https://doi.org/10.3897/zookeys.573.7016

Supplementary material 1

Specimen voucher data and corresponding DNA barcode accession numbers
Authors: Adam J. Brunke, Mikko Pentinsaari, Jan Klimaszewski
Data type: specimen data
Explanation note: All specimen data and sequence accession numbers associated with the DNA barcode dataset used in this study.
Link: https://doi.org/10.3897/zookeys.1041.64460.suppl1

RESEARCH ARTICLE

ZooKeys
A peer-reviewed open-access journal
Launched to accelerate biodiversity research

New species and records of the subgenus *Libnotes* (*Laosa*) Edwards (Diptera, Limoniidae) from China with a key to world species

Zehui Kang[1], Xiao Zhang[1]

1 *Key Lab of Integrated Crop Pest Management of Shandong Province, College of Plant Health and Medicine, Qingdao Agricultural University, Qingdao 266109, China*

Corresponding author: Xiao Zhang (xzhang_cn@163.com)

Citation: Kang Z, Zhang X (2021) New species and records of the subgenus *Libnotes* (*Laosa*) Edwards (Diptera, Limoniidae) from China with a key to world species. ZooKeys 1041: 101–112. https://doi.org/10.3897/zookeys.1041.65906

Abstract

Twenty species of *Libnotes* (*Laosa*) Edwards, 1926 are known worldwide and three are known from China so far. Here, two species of *Laosa* are added to the Chinese fauna, of which *L.* (*L.*) *baiyunensis* **sp. nov.** is described and illustrated as new to science, and *L.* (*L.*) *fuscinervis* Brunetti, 1912 is newly recorded from China. Morphologically, the new species is most similar to *L.* (*L.*) *charmosyne* (Alexander, 1958) but can be distinguished by the pleura of the thorax, the relative position of the additional cross veins in cell r_3 and r_5, and the details of the male genitalia. A key to the world species of *Laosa* is presented.

Keywords

Chinese fauna, crane flies, Limoniinae, new record, taxonomy

Introduction

Libnotes Westwood, 1876 is a species-rich Limoniidae genus with a total number of 293 species and subspecies, separated into eight subgenera: *Afrolimonia* Alexander, 1965, *Goniodineura* van der Wulp, 1895, *Gressittomyia* Alexander, 1936a, *Laosa* Edwards, 1926, *Libnotes* (s. str.), *Metalibnotes* Alexander, 1972, *Neolibnotes* Alexander,

1972 and *Paralibnotes* Alexander, 1972. The subgenus *Laosa* constitutes a small group within the genus with 20 known species from the Oriental (nine species), Australasian/Oceanian (eight species) and Palaearctic (three species) regions (Oosterbroek 2021), and here an additional new species from China is described and illustrated. It can be easily distinguished from other subgenera by the wing having two additional cross veins in cells r_3 (r-r) and r_5 (r-m, absent in some species) and Sc_1 ending far beyond the fork of Rs. Detailed features for recognition were given by Edwards (1926) and Podenas and Byun (2018).

Three species of the subgenus *Laosa* were previously recorded from China: *L.* (*L.*) *diphragma* (Alexander, 1934a), *L.* (*L.*) *regalis* Edwards, 1916 and *L.* (*L.*) *transversalis* de Meijere, 1916. In this paper, two *Laosa* species are added to the Chinese fauna, of which *L.* (*L.*) *baiyunensis* sp. nov. is described and illustrated as new to science and *L.* (*L.*) *fuscinervis* Brunetti, 1912, known previously only from India, is newly recorded from China. A key to the world species of *Laosa* based on types and non-type specimens, and on the literature is presented.

Material and methods

Specimens for this study were collected from several localities in China by different entomologists between 2002–2016. Type specimens are deposited in the Entomological Museum of China Agricultural University, Beijing, China (**CAU**). Other studied specimens are deposited in Qingdao Agricultural University, Shandong, China (**QAU**). We also examined specimens from the National Museum of Natural History, Smithsonian Institution, Washington D.C., USA (**USNM**) and the Natural History Museum, London, UK (**NHM**) (Table 1). Genitalic preparations of males were made by macerating the apical portion of the abdomen in cold 10% NaOH for 12–15 hours. Observations and illustrations were made using a ZEISS Stemi 2000-C stereomicroscope. Photographs were taken with a Canon EOS 77D digital camera through a macro lens. Details of coloration were examined in specimens immersed in 75% C_2H_5OH.

Table 1. Information of the examined specimens from USNM and NHM.

Species	Specimens examined	Collection
L. (*L.*) *charmosyne*	Holotype, male, Japan: Shikoku, Mt. Ishizachi (1800 m), 1956.VI.16, T. Yano.	USNM
L. (*L.*) *fuscinervis*	Paratype, male, India: East Himalayas, Dajiling (1829 m), 1908.IX.22, E. Brunetti.	NHM
L. (*L.*) *kariyana*	Holotype, male, Japan: Honshu, Ontake (1800 m), 1934.VII.6–10, H. Ise.	USNM
L. (*L.*) *manobo*	Holotype, male, Philippines: Mindanao, Mt. Apo (1981 m), 1930.IX.14, C. F. Clagg.	USNM
L. (*L.*) *noctipes*	Holotype, female, India: Sikkim, karponang (2469 m), 1959.VIII.22, Schmid.	USNM
L. (*L.*) *regalis*	Holotype, male?, China: Taiwan, Taihoku, T. Shiraki. Other material: 1 male, China: Taiwan, Arisan, 1917.IV.20, T. Shiraki.	NHM
L. (*L.*) *rotundifolialeos*	Paratypes, 2 males 2 females, Indonesia: Sulawesi Utara, Dumoga-Bone National Park (211 m), 1985.VIII. 19–30, Chen W. Young.	NHM
L. (*L.*) *taficola*	Holotype, female, Papua New Guinea: Mt Tafa (2591 m), 1934.III, L. E. Cheesman.	NHM
L. (*L.*) *transversalis*	1 male, China: Taiwan, Arisan, 1919.IV.25, T. Shiraki.	NHM

The morphological terminology mainly follows McAlpine (1981), and that for venation follows Alexander and Byers (1981). The following abbreviations in figures are used: **tg 9** = ninth tergite, **tg 10** = tenth tergite, **goncx** = gonocoxite, **o gonst** = outer gonostylus, **i gonst** = inner gonostylus, **aed** = aedeagus, **pm** = paramere, **cerc** = cercus, **hyp vlv** = hypogynial valve.

Taxonomy

Key to world species of *Laosa*

1	Basal 1/4 of wing with complete or broken crossband; m-m shorter than basal section of M_3 (Fig. 1a–c) **2**
–	Basal 1/4 of wing without conspicuous crossband; m-m significantly longer than basal section of M_3 (Figs 2d, 4d) **9**
2 (1)	Wing with broad and complete crossband extending from cord to distal end of cell dm (Fig. 1c) **3**
–	Wing without broad or complete crossband extending from cord to distal end of cell dm (Fig. 1a, b) **5**
3 (2)	Tip of wing narrowly falcate .... *L. (L.) falcata* **(Alexander, 1935)**
–	Tip of wing round **4**
4 (3)	Rs nearly straight or slightly curved, r-r far beyond r-m and distance between them more than twice length of r-r (Fig. 1c) .... *L. (L.) rotundifolialeos* **(Young, 1990)**
–	Rs strongly arcuated, r-r beyond r-m and distance between them about length of r-r ....*L. (L.) innuba* **(Alexander, 1941)**
5 (2)	Crossvein r-r situated before r-m, basal section of CuA_1 at fork of M (Fig. 1b)..*L. (L.) iris* **(Alexander, 1950)**
–	Crossvein r-r situated beyond r-m, basal section of CuA_1 distinctly beyond fork of M (Figs 1a, c, 2d) **6**
6 (5)	Pleura pale yellow without dark area ....*L. (L.) bipartita* **(Alexander, 1936b)**
–	Pleura with conspicuous dark area **7**
7 (6)	Basal section of CuA_1 slightly beyond fork of M and at about 1/8 of cell dm ....*L. (L.) manobo* **(Alexander, 1931)**
–	Basal section of CuA_1 far beyond fork of M and at 1/4–1/2 of cell dm (Figs 2d, 4d)...**8**
8 (7)	Coxae yellow; R_2 far before tip of Sc_2 and distance between them about twice length of R_2, tip of A_1 bent very strongly to wing margin............................... ....*L. (L.) pavo* **(Alexander, 1964)**
–	Coxae brown; R_2 before tip of Sc_2 and distance between them about length of R_2, tip of A_1 slightly curved..................*L. (L.) suffalcata* **(Alexander, 1964)**
9 (1)	Wing without additional cross vein in cell r_5 (Fig. 4d) **10**
–	Wing with additional cross vein in cell r_5 (Figs 1a–c, 2d) **15**

10 (9) Wing with stripes along veins broad and extensive, nearly covering wing tip ....*L. (L.) noctipes* (Alexander, 1967)
– Wing with stripes along veins not as broad or extensive **11**
11 (10) Crossvein m-m about four times or more as long as basal section of M_3....**12**
– Crossvein m-m less than three times as long as basal section of M_3 (Fig. 4d) **13**
12 (11) Wing with many conspicuous spots; R_2 and r-r distinct before distal end of cell dm... *L. (L.) taficola* (Alexander, 1948)
– Wing nearly unpatterned except very light brown spots at fork of Sc and over tip of Sc_2; R_2 distinct beyond distal end of cell dm, r-r aligned with distal end of cell dm..*L. (L.) transversalis* de Meijere, 1916
13 (11) Anterior scutum and pleura dark brown, without conspicuous pattern ....
....*L. (L.) dolonigra* (Alexander, 1956)
– Anterior scutum and pleura with conspicuous stripes (Fig. 4c).................**14**
14 (13) Body length of male more than 13.0 mm; r-r aligned with distal end of cell dm (Alexander 1967)............................*L. (L.) impensa* (Alexander, 1967)
– Body length of male less than 10.0 mm; r-r distinctly before distal end of cell dm (Fig. 4d) .... *L. (L.) fuscinervis* Brunetti, 1912
15 (9) R_2 far before tip of Sc_2 ....**16**
– R_2 close to tip of Sc_2 (Fig. 2d) **17**
16 (15) Antennal scape yellow, pedicel and flagellomeres dark brown; anterior scutum with four yellow stripes; Sc relatively short, end aligned with base of cell dm (Alexander 1959)..............................*L. (L.) joculator* (Alexander, 1959)
– Antenna black throughout; anterior scutum with three confluent dark brown stripes; Sc long, end aligned with middle of cell dm.......................................
....*L. (L.) kariyana* (Alexander, 1947)
17 (15) Crossvein r-r close to R_2...**18**
– Crossvein r-r far before R_2 and distance between them about or more than length of r-r (Figs 2d, 4d) **19**
18 (17) Anterior scutum with indistinct median stripe; wing length of male 10.0–15.0 mm, r-m distinctly before distal end of cell dm, tip of A_2 nearly straight or slightly curved .... *L. (L.) charmosyne* (Alexander, 1958)
– Anterior scutum with four ill-defined stripes; wing length of male about 25.0 mm, r-m aligned with distal end of cell dm, tip of A_2 bent very strongly toward margin ....*L. (L.) regalis* Edwards, 1916
19 (17) Axillary region of wing without spots (Fig. 2d) ....*L. (L.) baiyunensis* **sp. nov.**
– Axillary region of wing darkened (Fig. 4d)..**20**
20 (19) Tibiae yellow with broad, brown subbasal rings; r-r far before R_2 and distance between them about 1.5 times length of r-r ....
.... *L. (L.) riedelella* (Alexander, 1934b)
– Tibiae brownish yellow without subbasal ring; r-r before R_2 and distance between them less than length of r-r....*L. (L.) diphragma* (Alexander, 1934a)
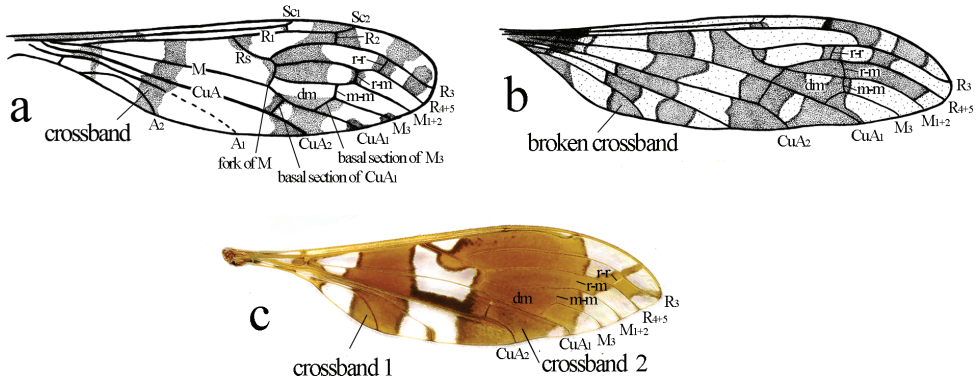
Figure 1. Wings of *Libnotes* (*Laosa*) **a** *L.* (*L.*) *bipartita* (from Alexander 1936b) **b** *L.* (*L.*) *iris* (form Edwards 1926) **c** *L.* (*L.*) *rotundifolialeos* (paratype, photo by Jinlong Ren).

Libnotes (*Laosa*) *baiyunensis* sp. nov.

http://zoobank.org/EE267965-E009-46B7-B13D-6129B6F06E2A
Figs 2, 3

Specimens examined. *Holotype*, male (CAU), China: Henan, Songxian, Mt. Baiyun, 2002.VII.22, Ding Yang. *Paratypes*: 1 male (CAU), same data as holotype. 1 male 1 female (CAU), China: Henan, Songxian, Mt. Baiyun (1500 m), 2008.VIII.14, Ding Yang.

Diagnosis. Anterior scutum brown with side edges brownish black. Pleura brownish yellow with a broad brownish black stripe extending from cervical region to base of wing. Tip of wing round. Wing nearly unpatterned except some pale brown patches around cross veins and portions of longitudinal veins, without conspicuous crossband from top to bottom. Sc long, ending near middle of cell dm. Rs slightly curved. R_2 slightly before tip of Sc_2. Two additional cross veins in cells r_3 and r_5, the former (r-r) beyond distal end of cell dm, the latter (r-m) aligned with distal end of cell dm; m-m twice as long as basal section of M_3. Basal section of CuA_1 far beyond fork of M and at about 1/3 of cell dm. Tip of A_2 nearly straight.

Description. Male. Body length 12.0–14.0 mm, wing length 19.0–22.0 mm.

Head (Fig. 2b). Brown. Hairs on head brown. Antenna length 2.9 mm, brown. Scape long cylindrical; pedicel oval, nearly as long as first flagellomere; flagellomeres oval, tapering apically, terminal flagellomere 1.5 times as long as preceding segment. Mouthparts brown with white hairs; palpus brown with brown hairs.

Thorax (Fig. 2c). Pronotum brown with sides brownish black. Prescutum brown with side edges brownish black. Anterior scutum brown with side edges brownish black; posterior scutum brown. Scutellum pale brown. Mediotergite pale brown with sides brownish black. Pleura (Fig. 2a) brownish yellow with a broad brownish black stripe extending from cervical region to base of wing. Hairs on thorax white. Coxae yellow; trochanters pale yellow; femora yellow to brownish yellow with tips dark brown;
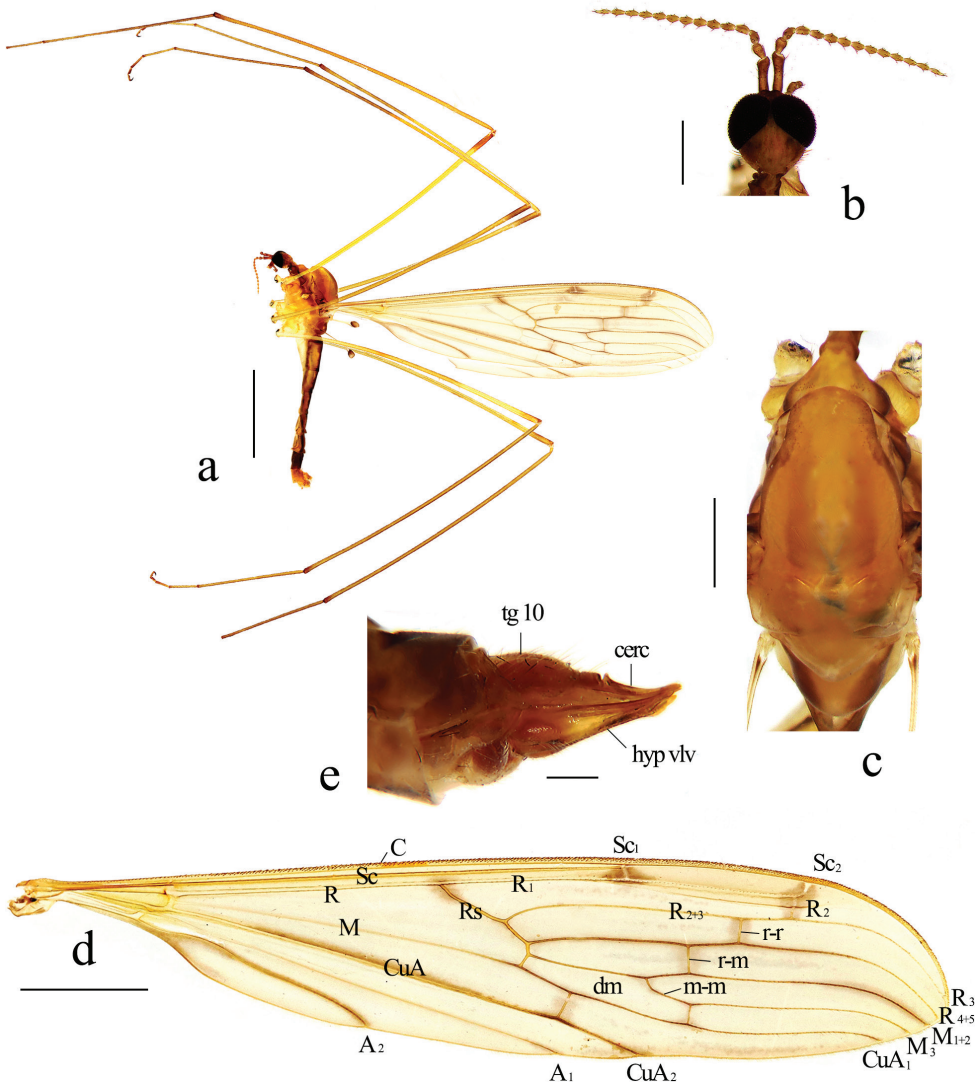
Figure 2. *Libnotes* (*Laosa*) *baiyunensis* sp. nov. **a** habitus of male, lateral view **b** head, dorsal view **c** thorax, dorsal view **d** wing **e** female ovipositor, lateral view. Scale bars: 5.0 mm (**a**); 3.0 mm (**d**); 1.0 mm (**b, c**); 0.2 mm (**e**).

tibiae brown; tarsi brown. Hairs on legs dark brown. Wing (Fig. 2d) tinged with pale brownish yellow. Darkened areas around cross veins, distal end of cell dm and CuA_1, tip of M_{1+2}, CuA and A_2; three small spots at base of Rs, at fork of Sc, and over R_2 and tip of Sc_2. Venation: Sc long, ending far beyond fork of Rs and near middle of cell dm. Basal section of Sc_2 very close to tip of Sc_1. Tip of Sc_2 nearly transverse, indistinct at wing margin. Rs very short, slightly sinuous. R_2 slightly before tip of Sc_2. Radial and medial veins distinctly curved caudally before wing margin. Two additional cross veins
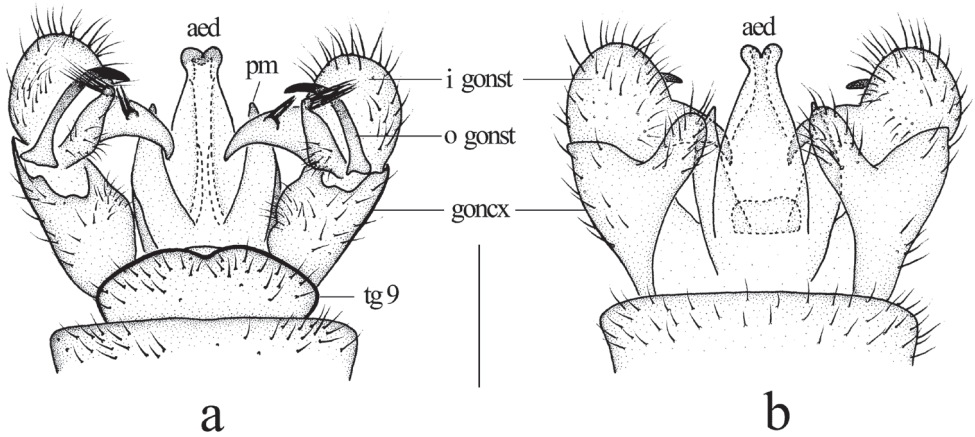
Figure 3. *Libnotes* (*Laosa*) *baiyunensis* sp. nov. **a** male hypopygium, dorsal view **b** male hypopygium, ventral view. Scale bars: 0.5 mm.

in cells r_3 and r_5, the former (r-r) at middle of cell r_3, the latter (r-m) at basal 2/5 of cell r_5 and aligned with distal end of cell dm. Cell dm elongate, more than 5 times as long as its width; m-m elongate, twice as long as basal section of M_3. Basal section of CuA_1 far beyond fork of M and at about 1/3 of cell dm. A_1 straight. A_2 slightly sinuous. Halter length 2.6 mm, yellow with knob brown.

Abdomen. Tergites brownish yellow with a brown median stripe, lateral borders brown; eighth tergite brown. Sternites brownish yellow with eighth sternite brown. Hairs on abdomen white.

Hypopygium (Fig. 3). Ninth tergite with widely rounded posterior margin and small median emargination. Gonocoxite elongate, slender with an elongate, blunt-apexed ventromesal lobe; inside edge with small setose bulge. Outer gonostylus arched at 2/3 length, tip acute. Inner gonostylus short, oval with long, arched rostral prolongation armed with two spines near base from a single tubercle; an elongate lobe arising dorsally near base with a brush of long setae at apex, at right angle to lobe and directed laterally. Paramere wide at base, elongate, triangular distally. Penis long, tip sunken in the middle.

Female. Body length 11.5 mm, wing length 17.5 mm. Similar to male, but eighth tergite brownish yellow with a broad brown median stripe. Tenth tergite brown. Cercus (Fig. 2e) brown, tip slightly exceeding tip of hypogynial valve. Hypogynial valve brownish yellow with borders darker, base slightly beyond base of tenth tergite.

Etymology. The species is named after the type locality Mt. Baiyun.

Distribution. China (Henan).

Remarks. This species is somewhat similar to *L.* (*L.*) *charmosyne* from South Korea and Japan in having similar spots on the wing, but it can be easily distinguished from the latter by the pleura of the thorax being brownish yellow with a broad brownish black stripe, the crossvein r-r being 1.5 to 2 times its length before R_2, the crossvein r-m being aligned with the distal end of cell dm, the basal section of CuA_1 being far beyond the fork of M and at about 1/3 of cell dm (Fig. 2d), and the inner gonostylus

being about 2/3 length of the gonocoxite (Fig. 3a), whereas in *L.* (*L.*) *charmosyne*, the pleura of the thorax is dark brownish gray, the crossvein r-r is near R_2, the crossvein r-m is distinctly before the distal end of cell dm, the basal section of CuA_1 is beyond the fork of M and at 1/6–1/5 of cell dm, and the inner gonostylus is half the length of the gonocoxite (Alexander 1958; Podenas and Byun 2018).

Libnotes (*Laosa*) *fuscinervis* Brunetti, 1912
Figs 4–5

Libnotes fuscinervis Brunetti, 1912: 411. Type locality: Dajiling, East Himalayas (India).

Specimens examined. *Paratype*, male (NHM), India: East Himalayas, Dajiling (1829 m), 1908.IX.22, E. Brunetti. **Other material:** 1 male (QAU), China: Yunnan, Lvchun, Yakou (1931 m), 2016.VII.7, Qilemoge.

Diagnosis. Anterior scutum brown with a broad, posteriorly subdivided, dark brown median stripe and a spot on each side of it; posterior half of median stripe with a paler division that broadens out across posterior scutum and scutellum. Pleura brownish yellow with a broad, anteriorly indistinct, brownish black stripe extending from cervical region to mediotergite. Tip of wing round. Wing with many conspicuous spots but without conspicuous crossband from top to bottom. Sc long, ending at 1/3 of cell dm. Rs slightly curved. R_2 before tip of Sc_2 and distance between them about length of R_2. Crossvein r-r before distal end of cell dm. Additional cross vein in cell r_5 absent; m-m twice as long as basal section of M_3. Basal section of CuA_1 far beyond fork of M and at about 1/4 of cell dm. Tip of A_2 slightly curved.

Description. Male. Body length 9.5 mm, wing length 14.5 mm.

Head (Fig. 4b). Brownish yellow. Hairs on head brown. Antenna length 2.0 mm, dark brownish yellow. Scape long cylindrical; pedicel oval, nearly as long as first flagellomere; flagellomeres oval, tapering apically, terminal flagellomere 1.5 times as long as preceding segment. Mouthparts brown with white hairs; palpus brown with brown hairs.

Thorax (Fig. 4c). Pronotum brownish yellow. Prescutum brown. Anterior scutum brown with a broad, posteriorly subdivided, dark brown median stripe and a spot on each side of it; posterior scutum brownish black with a broad yellow median stripe. Scutellum brownish black with a broad yellow median stripe. Mediotergite brownish black with a narrow yellow median stripe. Pleura (Fig. 4a) brownish yellow with a broad, anteriorly indistinct, brownish black stripe extending from cervical region to mediotergite. Hairs on thorax white. Coxae brownish yellow; trochanters yellow; femora brownish yellow with subtips brownish black; tibiae brownish yellow with tips narrowly brownish black; tarsi brownish yellow with tips brownish black. Hairs on legs dark brown. Wing (Fig. 4d) tinged with pale brownish yellow. Many dark patches around cross veins and portions of longitudinal veins as well as patches in cells as shown in Fig. 4d; four darker spots at base of wing, at base of Rs, at fork of Sc, and over R_2 and tip of Sc_2, the latter two spots connected by a narrow stripe along Sc_2. Venation: Sc long, ending far beyond fork of Rs and
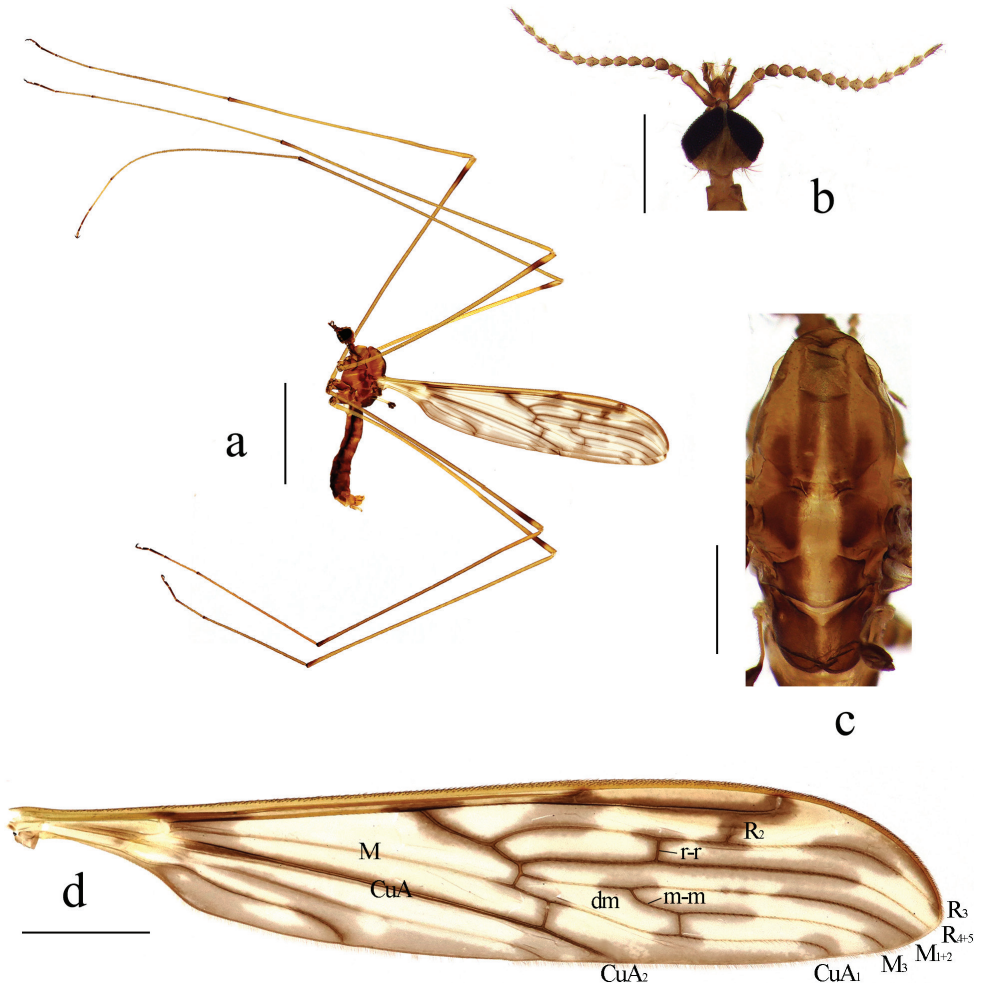
Figure 4. *Libnotes* (*Laosa*) *fuscinervis* Brunetti, 1912 **a** habitus of male, lateral view **b** head, dorsal view **c** thorax, dorsal view **d** wing. Scale bars: 5.0 mm (**a**); 2.0 mm (**d**); 1.0 mm (**b, c**).

at 1/3 of cell dm. Basal section of Sc_2 near tip of Sc_1. Tip of Sc_2 nearly transverse, indistinct at wing margin. Rs very short, slightly sinuous. R_2 before tip of Sc_2 and distance between them about length of R_2. Radial and medial veins distinctly curved caudally before wing margin. Crossvein r-r at basal 1/3 of cell r_3. Cell dm elongate, more than 5 times as long as its width; m-m elongate, twice as long as basal section of M_3. Basal section of CuA_1 far beyond fork of M and at about 1/4 of cell dm. A_1 straight, slightly curved near tip. A_2 slightly sinuous. Halter length 1.5 mm, pale yellow with knob brownish black.

Abdomen. Tergites brownish yellow with lateral borders brownish black. Sternites brownish yellow, middle of first sternite paler. Hairs on abdomen white.

Hypopygium (Fig. 5). Ninth tergite with rounded posterior margin and small median emargination. Gonocoxite stubby with an elongate, blunt-apexed ventromesal
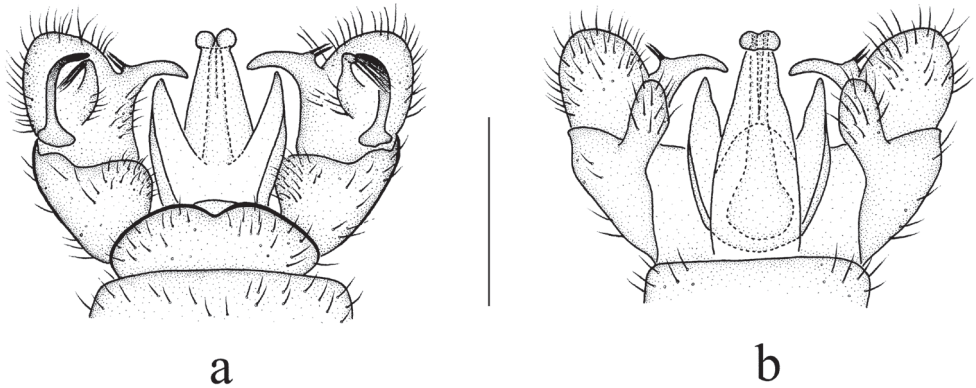
Figure 5. *Libnotes* (*Laosa*) *fuscinervis* Brunetti, 1912 **a** male hypopygium, dorsal view **b** male hypopygium, ventral view. Scale bars: 0.5 mm.

lobe; inside edge with a large setose bulge. Outer gonostylus arched at 2/3 length, tip acute. Inner gonostylus short, oval with a long arched rostral prolongation armed with two spines at base from a single tubercle; an elongate lobe arising dorsally near base with a brush of long setae at apex, at right angle to lobe and directed laterally. Paramere wide at base, elongate, triangular distally. Penis long, tip sunken in the middle.

Female. Unknown.

Distribution. China (Yunnan); India.

Remarks. This species was known previously only from India. Now it is recorded from China for the first time.

Acknowledgements

References

Alexander CP (1931) New or little-known Tipulidae from the Philippines (Diptera). XII. Philippine Journal of Science 46: 447–477.

Alexander CP (1934a) New or little-known Tipulidae from eastern Asia (Diptera). XIX. Philippine Journal of Science 54: 309–342.

Alexander CP (1934b) New or little-known Tipulidae from eastern Asia (Diptera). XX. Philippine Journal of Science 54: 433–471.

Alexander CP (1935) The Diptera of the Territory of New Guinea. II. Family Tipulidae. Proceedings of the Linnaean Society of New South Wales 60: 51–70.

Alexander CP (1936a) New or little-known Tipulidae from eastern Asia (Diptera). XXXII. Philippine Journal of Science 61: 113–149.

Alexander CP (1936b) Tipulidae. In: Curran CH (Ed.) The Templeton Crocker expedition to western Polynesian and Melanesian islands, 1933. No. 30. Diptera. Proceedings of the California Academy of Sciences 22(4): 2–11.

Alexander CP (1941) The Diptera of the Territory of New Guinea. XII. Family Tipulidae. Part IV. Proceedings of the Linnaean Society of New South Wales 66: 138–144.

Alexander CP (1947) Undescribed species of Japanese crane-flies (Diptera: Tipulidae). Part VI. Annals of the Entomological Society of America 40: 350–371. https://doi.org/10.1093/aesa/40.2.350

Alexander CP (1948) New or little-known Tipulidae (Diptera). LXXIX. Oriental-Australasian species. Annals and Magazine of Natural History 14(11): 388–414. https://doi.org/10.1080/00222934708654649

Alexander CP (1950) Notes on the tropical American species of Tipulidae (Diptera). VI. The tribe Limoniini, genus *Limonia*: subgenera *Limonia*, *Neolimnobia*, *Discobola*, and *Rhipidia*. Revista de Entomologia 21: 161–221.

Alexander CP (1956) New or little-known Tipulidae (Diptera). XCIX. Oriental-Australasian species. Annals and Magazine of Natural History 8(12): 657–674. https://doi.org/10.1080/00222935508655682

Alexander CP (1958) Undescribed species of Japanese Tipulidae (Diptera). Part I. Transactions of the Shikoku Entomological Society 6: 1–8.

Alexander CP (1959) New or little-known Tipulidae (Diptera). CVI. Oriental-Australasian species. Annals and Magazine of Natural History 1(13): 657–676. https://doi.org/10.1080/00222935808650994

Alexander CP (1964) New or little-known Tipulidae from eastern Asia (Diptera). LII. Philippine Journal of Science 92: 383–419.

Alexander CP (1965) New or little-known Tipulidae from Madagascar (Diptera). Transactions of the American Entomological Society 91: 39–83.

Alexander CP (1967) New or little-known Tipulidae from eastern Asia (Diptera). LIX. Philippine Journal of Science 95: 79–120.

Alexander CP (1972) Diptera: Tipulidae. Insects of Micronesia 12: 733–863.

Alexander CP, Byers GW (1981) Tipulidae. In: McAlpine JF, Peterson BV, Shewell GE, Teskey HJ, Vockeroth JR, Wood DM (Eds) Manual of Nearctic Diptera. Vol. I. Biosystematic Research Centre, Ottawa, 153–190.

Brunetti E (1912) Diptera Nematocera (excluding Chironomidae and Culicidae). Fauna of British India, including Ceylon and Burma 1: 1–581. https://doi.org/10.5962/bhl.title.8711

Edwards FW (1916) New and little-known Tipulidae, chiefly from Formosa. Annals and Magazine of Natural History 18(8): 245–269. https://doi.org/10.1080/00222931608693846

Edwards FW (1926) On some crane-flies from French Indo-China. Encyclopedie Entomologique, (B II), Diptera 3: 48–55.

McAlpine JF (1981) Morphology and terminology, Adults. In: McAlpine JF, Peterson BV, Shewell GE, Teskey HJ, Vockeroth JR, Wood DM (Eds) Manual of Nearctic Diptera. Vol. I. Biosystematic Research Centre, Ottawa, 9–63.

Meijere JCH de (1916) Studien uber Sudostasiatische Dipteren, 11. Zur Biologie einiger javanischen Dipteren nebst Beschreibung einiger neuen javanischen Arten. Tijdschrift voor Entomologie 59: 184–213.

Oosterbroek P (2021) Catalogue of the Craneflies of the World (Diptera, Tipuloidea: Pediciidae, Limoniidae, Cylindrotomidae, Tipulidae). http://ccw.naturalis.nl/ [accessed 10 March 2021]

Podenas S, Byun HW (2018) *Libnotes* crane flies (Diptera: Limoniidae) from Jeju Island (South Korea). Zootaxa 4483: 375–384. https://doi.org/10.11646/zootaxa.4483.2.9

Ribeiro GC (2006) Homology of the gonostylus in crane flies, with emphasis on the families Tipulidae and Limoniidae (Diptera, Tipulomorpha). Zootaxa 1110: 47–57. https://doi.org/10.11646/zootaxa.1110.1.5

Westwood JO (1876) Notae Dipterologicae. No. 2. – Descriptions of some new exotic species of Tipulidae. Transactions of the Entomological Society of London 1876: 501–506. https://doi.org/10.1111/j.1365-2311.1876.tb01926.x

Wulp FM van der (1895) Eenige Javaansche Diptera. Tijdschrift voor Entomologie 38: 35–48.

Young CW (1990) A new *Limonia* (subgenus *Laosa*) species from Sulawesi (Dipt., Tipulidae) and its resting behaviour. Entomologists Monthly Magazine 126: 239–244.

RESEARCH ARTICLE

New species and records of *Venturia* Schrottky (Hymenoptera, Ichneumonidae, Campopleginae) from China and Nepal

Yuan-Yuan Han[1,4], Kees van Achterberg[1,4], Xue-Xin Chen[1,2,3,4]

1 *State Key Lab of Rice Biology, Zhejiang University, Hangzhou 310058, China* **2** *Ministry of Agriculture Key Lab of Molecular Biology of Crop Pathogens and Insects, Zhejiang University, Hangzhou 310058, China* **3** *Zhejiang Provincial Key Laboratory of Biology of Crop Pathogens and Insects, Zhejiang University, Hangzhou 310058, China* **4** *Institute of Insect Sciences, College of Agriculture and Biotechnology, Zhejiang University, Hangzhou 310058, China*

Corresponding author: Xue-Xin Chen (xxchen@zju.edu.cn)

Citation: Han Y-Y, van Achterberg K, Chen X-X (2021) New species and records of *Venturia* Schrottky (Hymenoptera, Ichneumonidae, Campopleginae) from China and Nepal. ZooKeys 1041: 113–136. https://doi.org/10.3897/zookeys.1041.64238

Abstract

Four new species of *Venturia* Schrottky, 1902 (Hymenoptera, Ichneumonidae, Campopleginae) from Oriental China and Nepal are described (*V. contiguus* **sp. nov.** and *V. yunnanensis* **sp. nov.** from China; *V. liuae* **sp. nov.** and *V. levocarinata* **sp. nov.** from Nepal). In addition, two species are reported from China (*V. serpentina* Maheshwary, 1977 and *V. inclyta* (Morley, 1923)) for the first time and all listed species are illustrated. A key to all species from China and Nepal is provided.

Keywords

Lepidoptera, Oriental region, parasitoid, Pyralidae

Introduction

The genus *Venturia* Schrottky, 1902 (Ichneumonidae, Campopleginae) is a moderately large genus with 144 valid species worldwide, but predominantly from the Neotropical, Nearctic, and Oriental regions (Gupta and Maheshwary 1977; Wahl 1987; Yu et

al. 2016; Vas 2019a, b, 2020; Vas and Di Giovanni 2020). Nine species are known from China and two from Nepal (Yu et al. 2016).

Members of *Venturia* are solitary koinobiont endoparasitoids (Hemerik and Harvey 1999; Jervis et al. 2008; Biddinger et al. 2014). They mainly parasitize the larvae of microlepidoptera that feed in a concealed situation (Wahl 1987), most commonly of the family Pyralidae (He et al. 1996; Eliopoulos et al. 2002; Shaw et al. 2016), and several species were reared indirectly from Vespidae (Sonan 1937) because the caterpillars used for their offspring were parasitized.

Up to now, 36 species of *Venturia* have been recorded from the Oriental area prior to this study (Yu et al. 2016). Two new species are described from southern China, and two species are newly recorded in China in this paper. In addition, two new species are described from Nepal. A key to all species from China and Nepal is provided.

Material and methods

This study is based on specimens preserved in the Parasitoid Hymenoptera Collection of the Institute of Insect Sciences, Zhejiang University (**ZJUH**) which contains about 0.6 million pinned specimens and about same number of specimens in alcohol collected from all over the China.

The terminology and measurements used follow Broad (2018). All description and measurements were made under ZEISS Stemi 305 microscopes, and all figures were made by digital microscope (VHX-2000C, KEYENCE, Osaka, Japan). Type specimens and other materials are deposited in the Parasitic Hymenoptera Collection of ZJUH.

Results

Key to female species of *Venturia* Schrottky from China and Nepal

1	Face either punctate (sometimes rugose-punctate) or strongly rugose; frons usually rugose, in a few species granulose-punctate **2**
–	Face granulose or granulose-rugose; frons granulose..................................**12**
2	Apical half of antenna reddish brown; fore and mid legs from coxae on yellow; hind leg from trochantellus on yellow; mandible and tegula yellow; areolet present, emitting 2m-cu vein a little beyond its middle; anterior transverse carina away from base of propodeum............***V. mongolica* (Kokujev, 1915)**
–	Antenna entirely black or with a white band medially (*V. inclyta*); fore and mid legs from coxae on not wholly yellow; hind leg from trochantellus on not wholly yellow; mandible yellow or blackish brown, tegula yellow or black; areolet present or absent, **if** present, emitting 2m-cu vein a little beyond its middle or its apical part; anterior transverse carina not away from base of propodeum **3**

3 Mesopleuron with sparse and shallow punctures, and shiny; interocellar distance almost equal to or a little less than ocello-ocular distance; metapleuron shiny....**4**
– Mesopleuron closely to densely punctate or rugose-punctate, and matte; interocellar distance 1.0–2.5× ocello-ocular distance; metapleuron matte.......**5**
4 Fore wing with areolet; malar space matte, 0.6× basal width of mandible; occipital carina beak-like medially; interocellar distance 1.8× distance between median and lateral ocelli .... *V. taiwana* (**Sonan, 1937**)
– Fore wing without areolet (Fig. 7A); malar space shiny, 0.2× basal width of mandible (Fig. 7F); occipital carina not beak-like medially; interocellar distance 2.5× distance between median and lateral ocelli (Fig. 7H) ....
.... *V. levocarinata* **sp. nov.**
5 Lateral longitudinal carina of propodeum absent (Fig. 9D); lateromedian longitudinal carina absent below anterior transverse carina (Fig. 9D)............
.... *V. liuae* **sp. nov.**
– Lateral longitudinal carina of propodeum present; lateromedian longitudinal carina present below anterior transverse carina **6**
6 Interocellar distance equal to ocello-ocular distance; hind leg entirely black; propodeum long, extending to 0.7 of hind coxa; areolet small with a long stalk .... *V. longipropodeum* (**Uchida, 1942**)
– Interocellar distance 1.5–2.5× distance ocello-ocular distance; hind leg usually partly pale, **if** entirely black, then fore wing without areolet; propodeum short to long; areolet absent, or if present then areolet relatively large with a short stalk **7**
7 Mesopleuron strongly and closely rugose-punctate; mesopleuron, metapleuron and propodeum more or less similar in sculpture..................................**8**
– Mesopleuron distinctly punctate, punctures well separated; metapleuron and propodeum punctate to rugose-punctate..**9**
8 Female antenna without a white band; interocellar distance 1.5× ocello-ocular distance (Fig. 14G); metanotum rugose-reticulate; lateromedian longitudinal carina relatively weak below anterior transverse carina (Fig. 14D); face and frons rugose-punctate (Fig. 14F) .... *V. yunnanensis* **sp. nov.**
– Female antenna with a white band (Fig. 3); interocellar distance 2.0–2.2× ocello-ocular distance (Fig. 5G); metanotum rugose; lateromedian longitudinal carina strong below anterior transverse carina (Fig. 5D); face rugose and frons punctate (Fig. 5F) .... *V. inclyta* (**Morley, 1923**)
9 Fore wing with areolet **10**
– Fore wing without areolet **11**
10 Lateromedian longitudinal carina of propodeum weak below anterior transverse carina; area superomedia pentagonal; fore wing areolet not triangular.. *V. canescens* (**Gravenhorst, 1829**)
– lateromedian longitudinal carina of propodeum strong below anterior transverse carina; area superomedia triangular; fore wing areolet triangular...........
.... *V. himachala* **Maheshwary, 1977**

11   Malar space 0.2× basal width of mandible (Fig. 2F); propodeal area basalis not confluent with area superomedia (Fig. 2D); second tergite 2.0× longer than third tergite; 2rs-m vein very close to 2m-cu vein (Fig. 2A)...................... .... ***V. contiguus* sp. nov.**
–   Malar space 0.5–0.6× basal width of mandible; propodeal area basalis confluent with area superomedia; second tergite a little longer than third tergite; 2rs-m vein not distinctly removed from 2m-cu vein ......***V. oditesi* (Sonan, 1939)**
12   Tegula dark brown; trochanters and trochantellus dark brown; mesosoma sculpture superimposed on a granulose surface; hind tibia reddish .... ***V. roborowskii* (Kokujev, 1915)**
–   Tegula yellow; trochanters and trochantellus not wholly dark brown; mesosoma sculpture superimposed on a granulose surface or not; hind tibia yellow or yellowish brown..**13**
13   Interocellar distance 1.7–2.0× ocello-ocular distance; head not conspicuously swollen and vertex excavate behind; lateromedian longitudinal carina of propodeum angulate and strong below anterior transverse carina **14**
–   Interocellar distance equal to ocello-ocular distance; head usually swollen and vertex not excavate behind; lateromedian longitudinal carina of propodeum parallel-sided and weak below anterior transverse carina **15**
14   Area superomedia of propodeum elongated and closed; propodeal carinae strong; apex of propodeum produced and reaching up to 0.7 of hind coxa ... . ***V. hexados* Maheshwary, 1977**
–   Area superomedia of propodeum squarish and open; propodeal carinae weak; propodeum short, not produced apically....***V. quadrata* Maheshwary, 1977**
15   Metasoma smooth and shiny (Fig. 10); petiole rounded and without a distinct postpetiole; thyridium after basal 0.3 of tergite; second tergite 0.7× as long as first tergite.................................... ***V. serpentina* Maheshwary, 1977**
–   Metasoma matte; postpetiole swollen and distinctly differentiated from petiole; thyridium in basal 0.3 of tergite; second tergite as long as first tergite..... .... ***V. minuta* Maheshwary, 1977**

Species account

Subfamily Campopleginae Förster, 1869

Genus *Venturia* Schrottky, 1902

Type species. *Venturia argentina* Schrottky, 1902; by original designation.

Diagnosis. Eye not indented to weakly indented opposite antennal socket; frons with or without a lateromedian longitudinal carina; propodeum long, reaching beyond middle of hind coxa, sometimes extending to apex of hind coxa; area superomedia and area petiolaris usually confluent; lateromedian longitudinal carina close together and

more or less parallel to each other; propodeal spiracle round to oval; areolet present to absent; CU&cu-a of hind wing intercepted or not intercepted; claws not pectinate to strongly pectinate; metasoma petiole slender, first metasomal segment round in cross-section of basal 0.3, the suture separating tergite from its sternite lies in the middle or above the middle; ovipositor long, straight to strongly upcurved; male genital paramere weakly to strongly notched apically.

Venturia contiguus sp. nov.
http://zoobank.org/111B1B1D-ECF6-4D6C-BA77-4A5853C9DEB5
Figures 1, 2

Materia examined. *Holotype***:** CHINA • ♀; Fujian, Nanping; 21.IX.2002; Xiao-Xia Yu leg.; No. 20025513. *Paratype***:** CHINA • 1♀; Zhejiang, Songyang; 7.VII.1982; Han-Lin Chen leg.; No. 924532.

Comparative diagnosis. In the key by Gupta and Maheshwary (1977), this species keys out as *V. oditesi* (Sonan, 1939) from China and Myanmar because of the missing areolet on the fore wing. It can be easily distinguished from *V. oditesi* by the following: malar space approximately 0.2× basal width of mandible, propodeal area basalis not confluent with area superomedia, second tergite 2.0× longer than third tergite, 2rs-m vein very close to 2m-cu vein, hind femur blackish brown, hind tibia blackish brown medially, and metasoma wholly blackish with apical segments blackish brown.

This species is also similar to *V. oblongata* Gupta & Maheshwary, 1977 from Singapore, but differs from it by having the following: face rugulose-punctate, malar space 0.2× basal width of mandible, pronotum rugose-punctate dorsally, mesoscutum punctate and punctate-reticulate apically, propodeal area lateralis rugose-punctate, area basalis not confluent with area superomedia, area external punctate, hind femur blackish brown, and metasoma wholly blackish with apical segments blackish brown.

Description. Female holotype (Fig. 1). Body length 7.2 mm, fore wing length 3.9 mm.

Head. Antenna with 37 flagellomeres; first flagellomere 1.2× longer than second flagellomere. Face (Fig. 2F) rugulose-punctate, somewhat less pronounced laterally. Clypeus matte, weakly punctate. Malar space finely granulate, 0.2× basal width of mandible. Mandible with lamella more prominent in the basal 0.5. Frons granulate-punctate, median carina indistinct. Vertex granulate. Interocellar distance (Fig. 2G) 2.1× ocello-ocular distance and 2.0× distance between median and lateral ocelli. Temple subpolished, ca 0.4× length of the eye in dorsal view. Occipital carina evenly arched, joining hypostomal carina at mandible base.

Mesosoma. Pronotum (Fig. 2I) rugose-punctate dorsally, trans-striate laterally. Mesoscutum (Fig. 2H) punctate, rugulose-punctate in notaulic area, punctate-reticulate apically. Scutellum punctate anteriorly, rugose-punctate posteriorly. Metanotum rugose-punctate. Mesopleuron (Fig. 2C) punctate, trans-striate below tegula, speculum smooth. Propodeum (Fig. 2D) with area basalis trapezoid; area superomedia long and

Figure 1. *Venturia contiguus* sp. nov., female, habitus, lateral view.

narrow with rugosity, not confluent with area basalis but confluent with area petiolaris; area petiolaris trans-striate; area external punctate; area dentipara rugose-punctate; area lateralis rugose-punctate; lateromedian longitudinal carina almost parallel; propodeal spiracle small, oval. Propodeum extending to 0.7 of hind coxa.

Wing. Fore wing (Fig. 2A) areolet absent. 2rs-m slightly in front of the 2m-cu by only 0.2× of its length. RS ca 1.6× longer than 2r&RS. 1cu-a opposite M&RS, inclivous. External angles of second discal cell acute (70°). Hind wing (Fig. 2B) with CU&cu-a intercepted at lower 0.3 of its length. Distal abscissa of CU connected to CU&cu-a, spectral.

Legs. Hind femur 5.3× longer than wide. Inner spur ca 0.6× as long as first tarsomere of hind tarsus. Tarsal claws pectinate (Fig. 2K).

Metasoma. Apical tergites from third on compressed. First segment (Fig. 2E) long and slender, ca 3.1× longer than its apical width, without glymma; dorsolateral carina of first tergite missing; petiole ca 6.0× width; suture separating first tergite from
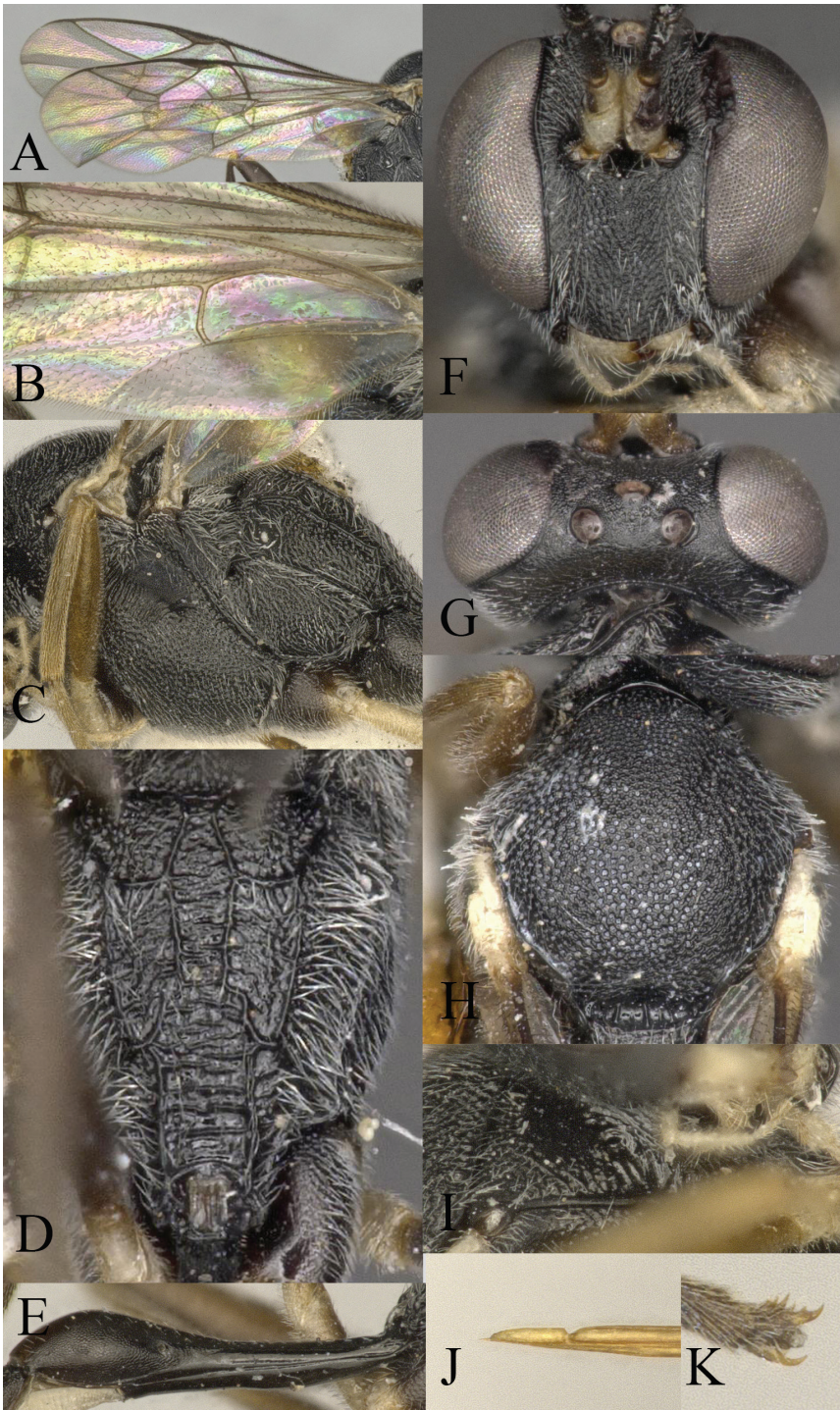
Figure 2. *Venturia contiguus* sp. nov., female **A** fore wing **B** hind wing **C** mesosoma, lateral view **D** propodeum, dorsal view **E** first metasomal segment, lateral view **F** head, anterior view **G** head, dorsal view **H** mesoscutum, dorsal view **I** pronotum, lateral view **J** tip of ovipositor, lateral view **K** hind tarsal claw.

sternite situated mid height at basal third of first metasomal segment. Second tergite finely granulate, relatively long and slender, 0.8× first tergite, 2.0× third tergite, 3.4× its apical width; thyridium oval, located at basal 0.4 length of second tergite. Posterior margins of sixth and seventh tergites medially concave. Ovipositor sheath ca 1.5× longer than hind femur, ovipositor ca 2.5× longer than hind femur. Ovipositor upcurved apically, dorsal preapical notch strong, tip acute (Fig. 2J).

Colour. Black. Mandible except teeth, scape and pedicel except laterally, palpi, tegula, fore and mid coxae in apical half and all trochanters, yellow. Coxae ventrally blackish brown. Rest of fore and mid legs yellowish brown to blackish brown, with apical tarsal segment blackish brown. Hind coxa in apical half and trochanter, yellow. Remainder of hind leg blackish brown with tibia basally and apically darker. Metasoma wholly blackish with apical segments blackish brown.

Distribution. China (Fujian, Zhejiang).

Etymology. Name derived from "contiguus" (Latin for "near"), because 2rs-m vein situated close to 2m-cu vein.

Venturia inclyta (Morley, 1923)
Figures 3–5

Cymodusa inclyta Morley, 1923: 8; Townes and Gupta 1961: 234.
Venturia inclyta Gupta and Maheshwary 1977: 93–95.

Materia examined. China • 1♀; Fujian, Shaowu; 5.XII.1981; Jian-Hong Qiu leg.; No. 816433 • 5♀4♂; Guangxi, Lingchuan; 1983; Gui-Yu Li leg.; No. 835369(9) • 1♀1♂; Guangxi, Nanning; 17.III.1986; Wei-Bao Huang leg.; No. 860822.

Figure 3. *Venturia inclyta*, female, habitus, lateral view.

Figure 4. *Venturia inclyta*, male, habitus, lateral view.

Male (Fig. 4). Antenna without a white band, face rugose-punctate, propodeal carinae strong, metasoma strongly compressed apically, otherwise similar to female.

Variation. Antenna with 41–43 flagellomeres, first flagellomere 1.4–1.6× second flagellomere, malar space 0.3–0.5× basal width of mandible, ovipositor 2.4–2.8× the length of hind femur, ovipositor sheath 2.1–2.6× the length of hind femur.

Distribution. China (Fujian, Guangxi), India, Nepal, Sri Lanka. New record for China.
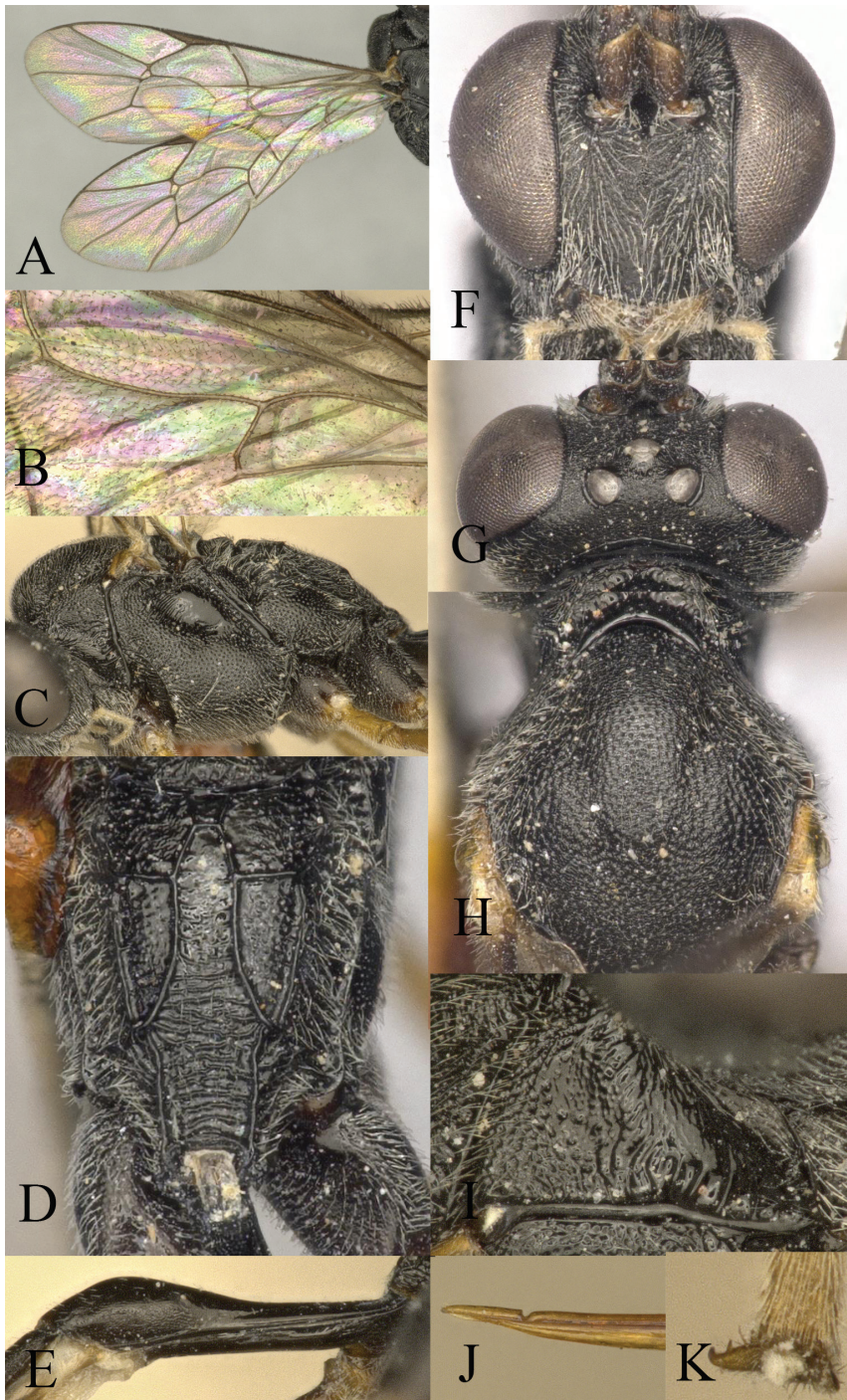
Figure 5. *Venturia inclyta*, female **A** fore wing **B** hind wing **C** mesosoma, lateral view **D** propodeum, dorsal view **E** first metasomal segment **F** head, anterior view **G** head, dorsal view **H** mesoscutum, dorsal view **I** pronotum, lateral view **J** tip of ovipositor, lateral view **K** hind tarsal claw.

Venturia levocarinata sp. nov.

http://zoobank.org/4FAC75BD-5F83-4DE7-B391-50D7C7577CD0
Figures 6, 7

Materia examined. *Holotype*: Nepal • ♀; Nepal, Tansen; 12.VII.2014; Bin-Bin Xu leg.; No. 201502137.

Comparative diagnosis. In the key by Gupta and Maheshwary (1977), this species keys out to *V. inquinata* (Morley, 1913) from India, but differs from *V. inquinata* by the following: face rugose-punctate, teeth with an elevated carina, malar space 0.2× basal width of mandible, mandible without lamella, mandible blackish brown, and postpetiole reddish brown.

This species is also similar to *V. taiwana* (Sonan, 1937) from Taiwan province of China, but differs from it by the following: clypeus without a median apical tooth, teeth with an elevated carina, malar space smooth and shiny, 0.2× basal width of mandible, temple not strongly swollen, fore wing without areolet, tegula black, mid trochanter and femur except apex blackish, hind femur black, and metasoma from third tergite on lateral surface reddish brown with a black dorsal stripe.

This species is similar to *V. prolixa* Wahl, 1987 from America, but differs from latter by having teeth with an elevated carina, propodeal median area not granulate, area external rugose-punctate, area dentipara rugose-reticulate and not on a granulate surface, hind femur ca 11.0× longer than wide, tegula black, hind leg black except extreme base of first tarsomere yellowish brown, and metasoma with second tergite black, laterally brownish, from third tergite on lateral surface reddish brown with a black dorsal stripe.

Description. Female holotype (Fig. 6). Body length 15.0 mm, fore wing length 9.0 mm.

Head. Antenna at least with 48 flagellomeres (apex missing); first flagellomere 1.4× longer than second flagellomere. Face (Fig. 7F) rugose-punctate, laterally more superficial. Clypeus smooth and shiny, punctate. Malar space smooth and shiny, partly granulate, 0.2× basal width of mandible. Mandible (Fig. 7G) without lamella, with an elevated carina on outer surface. Frons rugose-punctate, median carina distinct. Vertex shallowly to deeply punctate. Ocellar region small. Interocellar distance (Fig. 7H) 0.9× ocello-ocular distance and 2.5× distance between median and lateral ocelli. Temple subpolished, densely punctate below, ca 0.5× length of the eye. Occipital carina evenly arched, joining hypostomal carina far before mandible base.

Mesosoma. Pronotum (Fig. 7J) punctate dorsally, smooth and shiny medially, short striate laterally. Mesoscutum (Fig. 7I) punctate, rugose in notaulic area, rugose-reticulate apically. Scutellum punctate anteriorly, rugose-punctate posteriorly. Metanotum rugose-reticulate. Mesopleuron (Fig. 7C) rugose-punctate above, punctate below, weakly trans-striate below tegula; speculum smooth and shiny. Metapleuron rugose-punctate above, punctate below. Propodeum (Fig. 7D) with area basalis trapezoid; area superomedia small and narrow, confluent with area petiolaris, trans-striate; area external rugose-punctate; area dentipara rugose-reticulate; area lateralis

Figure 6. *Venturia levocarinata* sp. nov., female, habitus, lateral view.

rugose-punctate; all carinae distinct; propodeal spiracle oval. Propodeum extending to 0.9 of hind coxa.

Wing. Fore wing (Fig. 7A) without areolet, and distance between 2rs-m and 2m-cu ca 0.6× length of 2rs-m. RS ca 1.4× longer than 2r&RS. 1cu-a opposite M&RS. External angles of second discal cell acute (75°). Hind wing (Fig. 7B) with CU&cu-a slightly inclivous and not intercepted. Distal abscissa of CU not connected to CU&cu-a.

Legs. Coxae weakly punctate. Hind femur ca 11.0× longer than wide. Inner spur ca. 0.5 as long as first tarsomere of hind tarsus. Tarsal claws strongly pectinate (Fig. 7L).
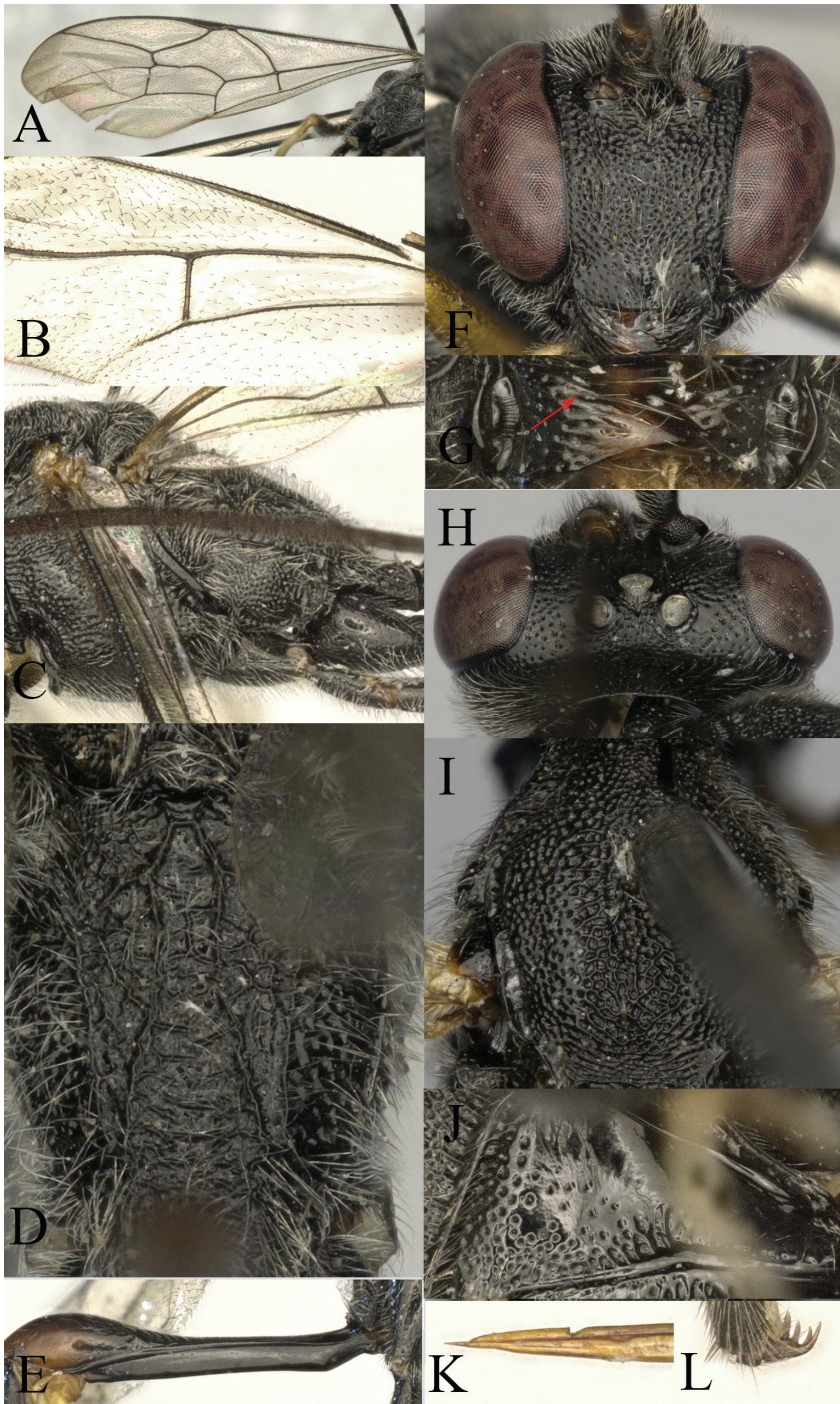
Figure 7. *Venturia levocarinata* sp. nov., female **A** fore wing **B** hind wing **C** mesosoma, lateral view **D** propodeum, dorsal view **E** first metasomal segment **F** head, anterior view **G** mandible, anterior view **H** head, dorsal view **I** mesoscutum, dorsal view **J** pronotum, lateral view **K** tip of ovipositor, lateral view **L** hind tarsal claw.

Metasoma. Apical tergites from third on slightly compressed. First segment (Fig. 7E) long and slender, ca 6.3× longer than apical width, without glymma; dorsolateral carina of first tergite missing; petiole ca 6.5× longer than wide. Suture separating first tergite from sternite situated above the mid-height at basal third of first metasomal segment. Second tergite finely granulate, long and slender, 0.9× first tergite, 1.8× third tergite, 5.0× its apical width; thyridium oval, located at basal 0.4 length of second tergite. Third tergite 2.8× longer than its apical width. Posterior margins of sixth and seventh tergites medially concave. Ovipositor sheath ca 1.8× longer than hind femur, ovipositor ca 2.4× longer than hind femur. Ovipositor nearly straight, dorsal preapical notch strong, tip acute (Fig. 7K).

Colour. Mandible blackish brown, subapically brownish. Tegula black. All coxae black. Fore legs missing. Mid trochanter and femur except apex blackish, remainder of leg yellowish brown. Hind leg black except extreme base of first tarsomere yellowish brown. Petiole black and postpetiole reddish brown, second tergite black, laterally brownish, from third tergite on lateral surface reddish brown with a black dorsal stripe.

Distribution. Nepal.

Etymology. Name derived from "levo" (Latin for "raised") and "carinata" (Latin for "carina"), because teeth with elevated carina on outer surface.

Venturia liuae sp. nov.

http://zoobank.org/7E2F1CB3-B112-4A32-B2EE-117B10E979D5
Figures 8, 9

Materia examined. *Holotype*: Nepal • ♀; Nepal, Kathmandu Nagarkot; 24.VII.2013; Zhen Liu leg.; No. 201406299.

Comparative diagnosis. In the key by Gupta and Maheshwary (1977) this species keys out as *V. ahlensis* Maheshwary, 1977 from India, because the propodeal lateromedian longitudinal carina and lateral longitudinal carina are absent, but it can be easily distinguished from *V. ahlensis* by the following: areolet small with a long stalk, malar space ca 0.45× basal width of mandible, and area superomedia region rugulose.

This species is also similar to *V. himachala* Gupta & Maheshwary, 1977 from Indian and Nepal, but differs from latter by the following: frons rugulose with median carina absent, interocellar distance 1.3× ocello-ocular distance, anterior part of median lobe of mesoscutum with indistinct punctures, and propodeal lateromedian carina absent below anterior transverse carina.

Description. Female holotype (Fig. 8). Body length 6.5 mm, fore wing length 4.0 mm.

Head. Antenna with at least 33 flagellomeres (apex missing), length of first flagellomere ca 1.3× longer than second flagellomere; face (Fig. 9F) rugose-punctate, punctures stronger and coalescent centrally, and shallow laterally; malar space granulate, ca 0.45× basal width of mandible; mandible with a weak lamella; frons rugulose, median carina absent; vertex rugulose-punctate; temple shallowly punctate, ca 0.5× length of the eye; ocellar region punctate; interocellar distance (Fig. 9G) 1.3× ocello-ocular distance and 2.0× distance between median and lateral ocelli; occipital carina evenly arched, joining hypostomal carina before mandible base.

Figure 8. *Venturia liuae* sp. nov., female, habitus, lateral view.

Mesosoma. Pronotum (Fig. 9I) trans-striate laterally, closely punctate dorsally; mesoscutum (Fig. 9H) punctate, matte, anterior part of median lobe with indistinct punctures; scutellum punctate; metanotum rugose-punctate; mesopleuron (Fig. 9C) densely punctate, punctures separated by less than their diameter, weakly striate below subtegular ridge; metapleuron similar to mesopleuron except that the punctures little denser. Propodeum (Fig. 9D) with area superomedia rugulose, area petiolaris rugose-striate; lateral longitudinal carina absent; lateromedian longitudinal carina absent below anterior transverse carina; propodeal spiracle oval; propodeum projecting at 0.5 of hind coxa.

Wing. Fore wing (Fig. 9A) areolet small with a long stalk, the height of areolet ca 0.7× as long as stalk, emitting 2m-cu vein from its apical part. RS ca 1.8× longer than 2r&RS. 1cu-a opposite M&RS. External angles of second discal cell acute (70°). Hind wing (Fig. 9B) with CU&cu-a intercepted at lower 0.35 of its length.

Legs. Hind femur 5.0× longer than wide. Inner spur of hind tibia ca 0.45× as long as first tarsomere of hind tarsus. Tarsal claws pectinate (Fig. 9K).

Metasoma. Apical tergites from third on slightly compressed. First segment (Fig. 9E) long and slender, ca 3.8× longer than its apical width, without glymma; dorsolateral carina of first tergite missing; petiole ca 5.0× longer than high. Suture separating first tergite from sternite situated mid-height at basal third of first metasomal segment. Second tergite granulate, long and slender, 0.9× first tergite, 2.6× its apical width; thyridium oval, small, its distance from basal margin of tergite ca 3.0× its length. Third tergite 1.3× longer than its apical width. Posterior margins of sixth and seventh tergites medially concave. Ovipositor sheath ca 1.8× longer than hind femur, ovipositor ca 3.0× longer than hind femur, ovipositor gradually upcurved, dorsal preapical notch strong, tip acute (Fig. 9J).
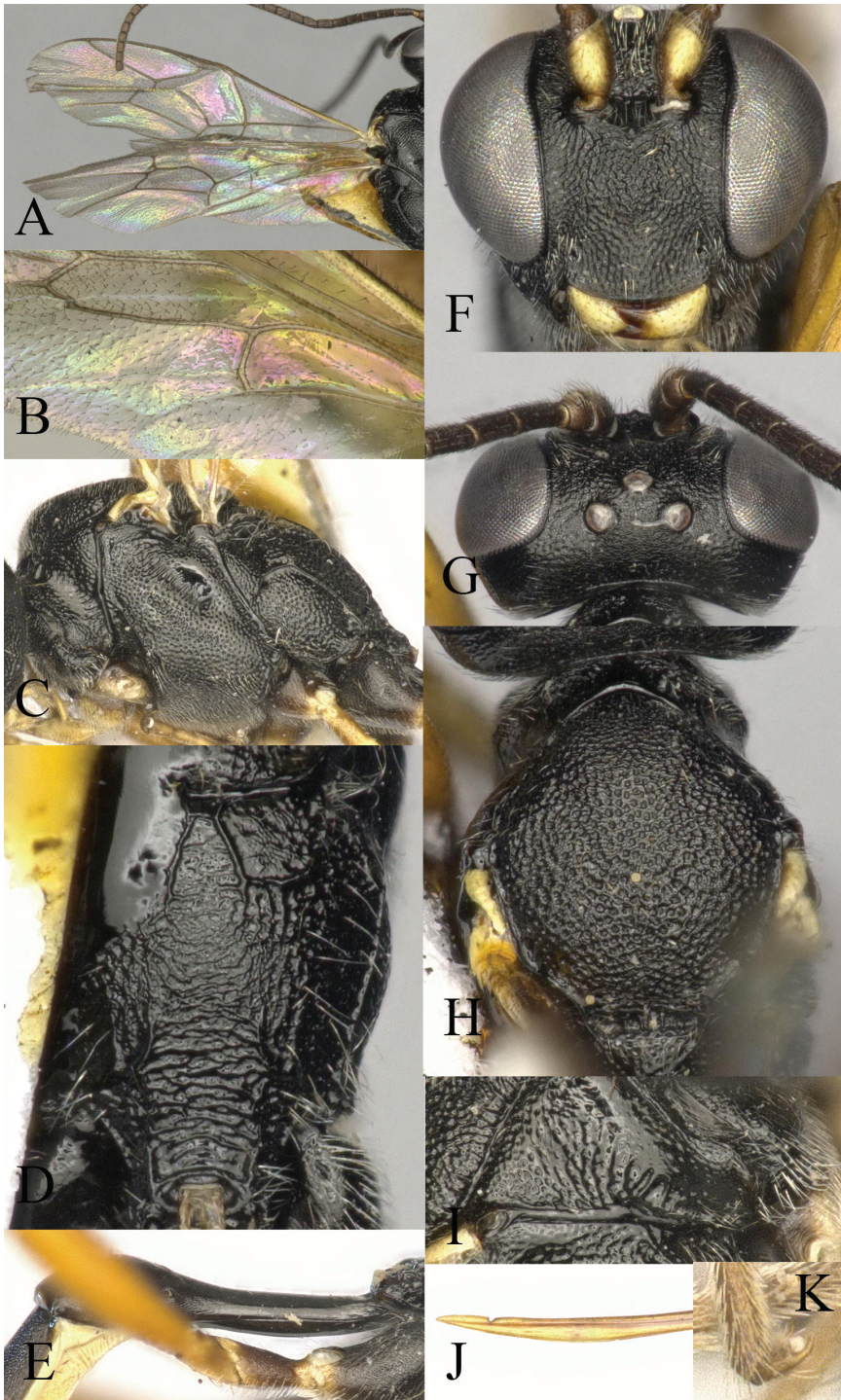
Figure 9. *Venturia liuae* sp. nov., female **A** fore wing **B** hind wing **C** mesosoma, lateral view **D** propodeum, dorsal view **E** fisrt metasomal segment, lateral view **F** head, anterior view **G** head, dorsal view **H** mesoscutum, dorsal view **I** pronotum, lateral view **J** tip of ovipositor, lateral view **K** hind tarsal claw.

Colour. Black. Scape narrowly in front, mandible except teeth, palpi, tegula, extreme apices of fore and mid coxae, fore trochanter and trochantellus of mid trochanter, yellow; remainder of fore leg yellowish brown with apical segment dark brown and remainder of mid leg yellowish brown with tarsus blackish brown; hind leg with trochanter blackish brown, trochantellus yellowish brown with externally more brownish, femur yellowish brown but apically blackish, tibia brownish with base and apex blackish, tarsus blackish brown; metasoma with first and second segment wholly black, dorsal surface from third segment on black but laterally reddish brown.

Distribution. Nepal.

Etymology. This species is named in honor of Dr Zhen Liu, the collector of the holotype.

Venturia serpentina **Maheshwary, 1977**
Figures 10–12

Venturia serpentina Maheshwary in Gupta and Maheshwary 1977: 114–115.

Materia examined. China • 1♀; Guangdong, Shixing; 25.V.2002; Zai-Fu Xu leg.; No. 201806114 • 1♂; Zhejiang, Hangzhou; 8.VIII.1981; Jun-Hua He leg.; No. 815229.

Figure 10. *Venturia serpentina*, female, habitus, lateral view.

Figure 11. *Venturia serpentina*, male, habitus, lateral view.

Male (Fig. 11). Interocellar distance 1.7× ocello-ocular distance and 2.5× distance between median and lateral ocelli. Fore wing 1cu-a distad of M&RS by 0.3 its length. Metasoma not snake-like. Hind coxa yellow, hind tibia wholly yellow.

Distribution. China (Guangdong, Zhejiang), Myanmar. New record for China.

Venturia yunnanensis sp. nov.
http://zoobank.org/31AF3FED-3F01-433A-BB4E-83D5E11DDD2C
Figures 13, 14

Materia examined. *Holotype*: Сhina • ♀; Yunnan, Xishuangbanna; 20.VI.2018; 21°44.75'N, 100°26.00'E; 1610 m; Malaise trap; No. 20180823.
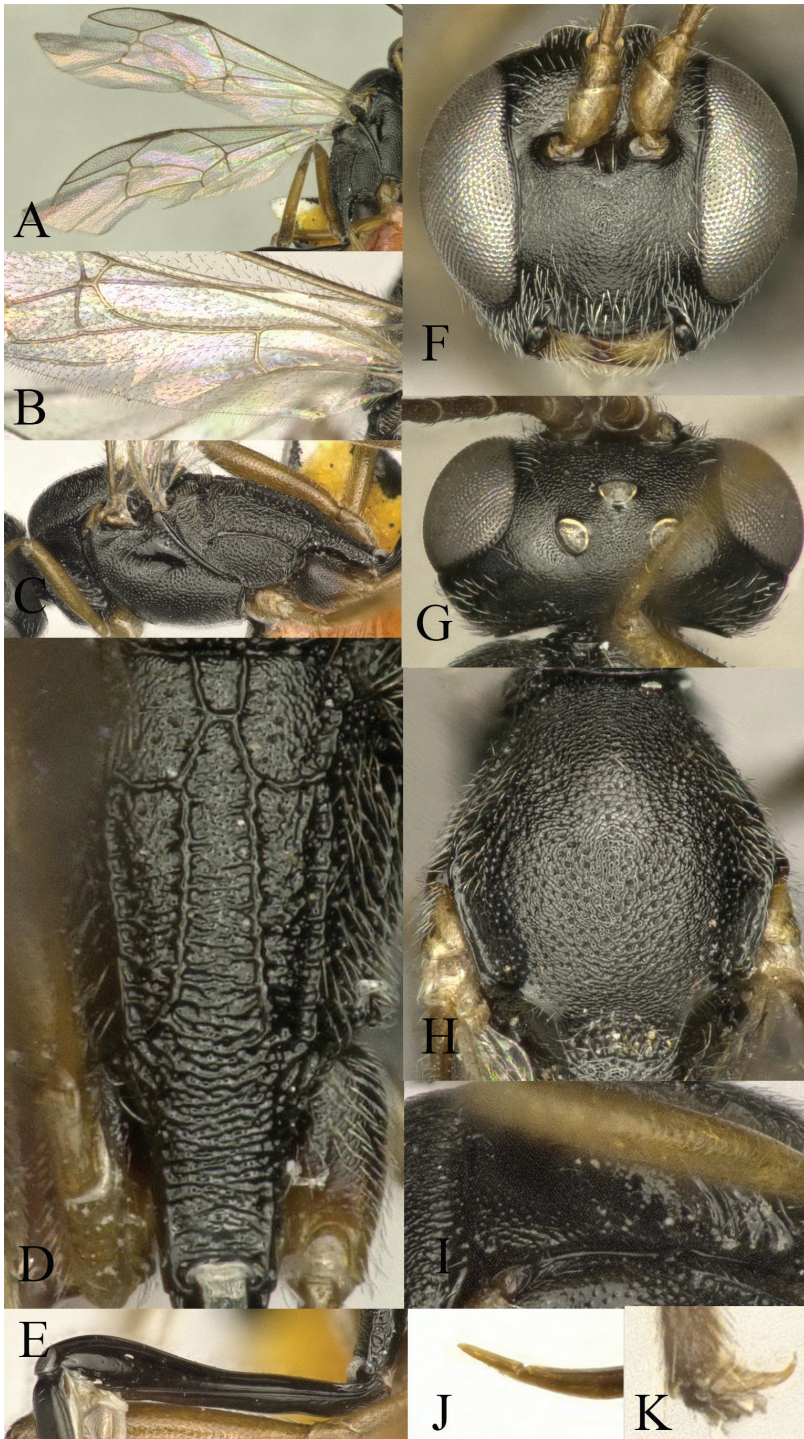
Figure 12. *Venturia serpentina*, female **A** fore wing **B** hind wing **C** mesosoma, lateral view **D** propodeum, dorsal view **E** first metasomal segment **F** head, anterior view **G** head, dorsal view **H** mesoscutum, dorsal view **I** pronotum, lateral view **J** tip of ovipositor, lateral view **K** hind tarsal claw.

Figure 13. *Venturia yunnanensis* sp. nov., female, habitus, lateral view.

Comparative diagnosis. In the key by Gupta and Maheshwary (1977), this species keys out to *V. tectonae* (Perkins, 1936) from Myanmar, but differs from it by the following: interocellar distance 1.2× ocello-ocular distance, second tergite 1.5× third tergite, malar space weakly punctate, tegula yellowish brown, and differently coloured metasoma.

This species is also similar to *V. anchisteus* Wahl, 1987 from Mexico, but differs from it by the following: propodeal area external punctate, area dentipara rugose-reticulate, the height of areolet ca equal to the length of stalk, second metasomal tergite ca 1.7× its apical width, and hind tibia except base and apex yellowish brown.

Description. Female holotype (Fig. 13). Body length 13.0 mm, fore wing length 8.8 mm.

Head. Antenna a little shorter than fore wing, with 42 flagellomeres; first flagellomere ca 1.5× longer than second flagellomere. Face (Fig. 14F) densely rugose-punctate. Clypeus punctate, punctures sparser than on face. Malar space weakly punctate, 0.35× basal width of mandible. Frons rugose-punctate, punctate on sides; with median carina. Vertex matte, shallowly punctate. Ocellar region punctate. Interocellar distance (Fig. 14G) 1.5× ocello-ocular distance and 2.4× distance between median and lateral ocelli. Temple shallowly punctate, ca 0.4× length of the eye. Occipital carina evenly arched, joining hypostomal carina at mandible base.
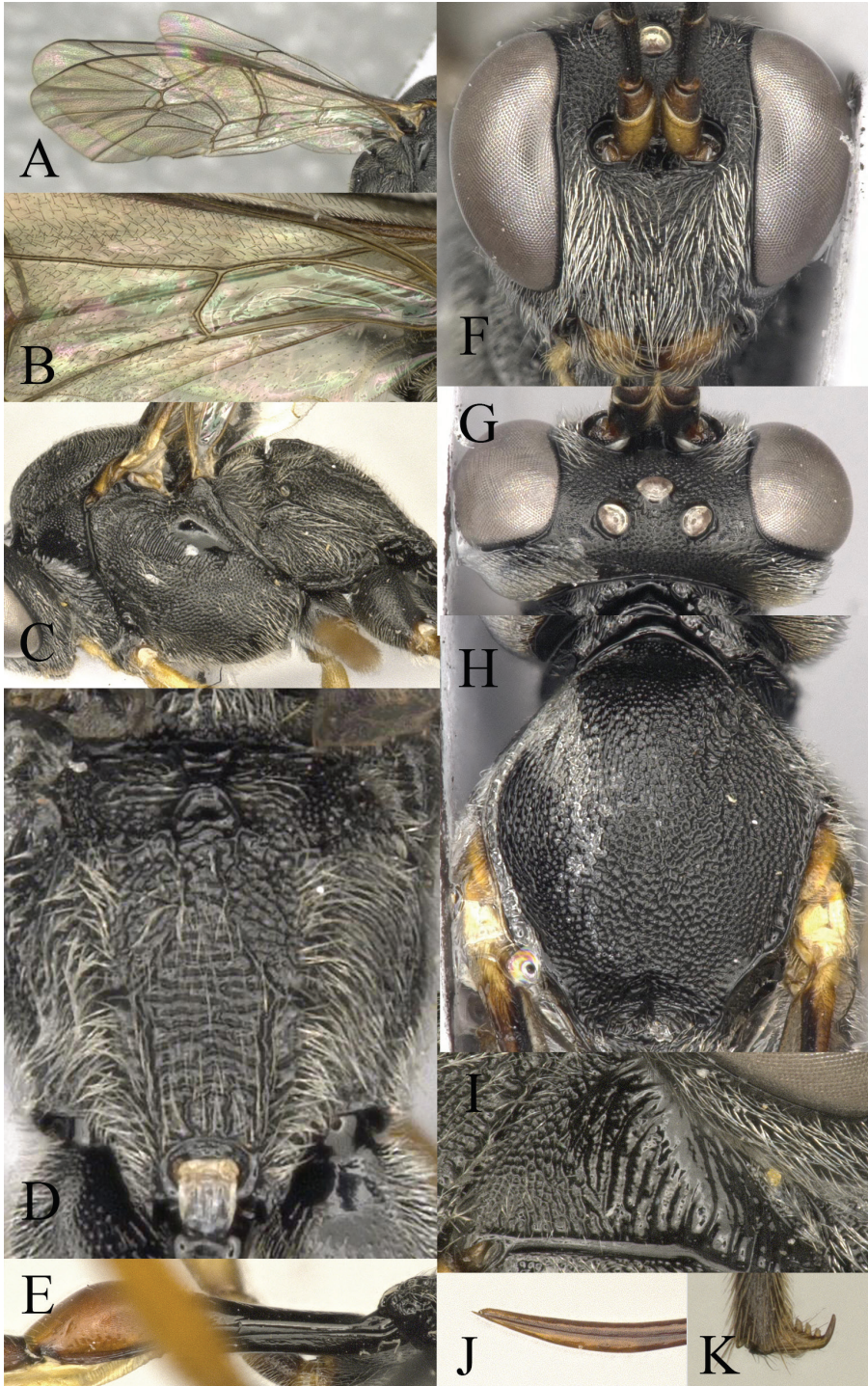
Figure 14. *Venturia yunnanensis* sp. nov., female **A** fore wing **B** hind wing **C** mesosoma, lateral view **D** propodeum, dorsal view **E** first metasomal segment, lateral view **F** head, anterior view **G** head, dorsal view **H** mesoscutum, dorsal view **I** pronotum, lateral view **J** tip of ovipositor, lateral view **K** hind tarsal claw.

Mesosoma. Pronotum (Fig. 14I) rugose-punctate dorsally, trans-striate laterally. Mesoscutum (Fig. 14H) punctate, rugose in notaulic region. Scutellum punctate anteriorly, rugose-punctate posteriorly. Metanotum rugose-reticulate. Mesopleuron (Fig. 14C) rugose-punctate above, punctate below, trans-striate below tegula. Metapleuron rugose-punctate above, rugose-reticulate below. Propodeum (Fig. 14D) with area basalis trapezoid; area superomedia region small, rugose and confluent with area petiolaris; area petiolaris trans-striate; area external punctate; area dentipara rugose-reticulate; area lateralis rugose-punctate; lateromedian longitudinal carina relatively weak below anterior transverse carina, and narrow posteriorly; propodeal spiracle oval. Propodeum extending to 0.5 of hind coxa.

Wing. Fore wing (Fig. 14A) with relatively small, petiolate areolet, height of areolet ca equal to the length of stalk, emitting 2m-cu vein from its apical part. RS ca 1.8× longer than 2r&RS. 1cu-a opposite M&RS. External angles of second discal cell acute (75°). Hind wing (Fig. 14B) with CU&cu-a intercepted at lower 0.35× of its length. Distal abscissa of CU connected to CU&cu-a, spectral.

Legs. Coxae weakly punctate. Hind femur ca 5.3× longer than wide. Inner spur ca 0.45× first tarsomere of hind tarsus. Tarsal claws pectinate (Fig. 14K).

Metasoma. Apical tergites from third on slightly compressed. First segment (Fig. 14E) long and slender, ca 3.9× longer than its apical width, without glymma; dorsolateral carina of first tergite missing; petiole ca 5.5× longer than wide. Suture separating first tergite from sternite situated mid-height at basal third of first metasomal segment. Second tergite finely granulate, relatively long and slender, 0.7× first tergite, 1.5× third tergite, 1.7× its apical width; thyridium oval, its distance from basal margin of tergite ca 2.5× its length. Third tergite 1.15× longer than its apical width. Posterior margins of sixth and seventh tergites medially concave. Ovipositor sheath ca 1.8× longer than hind femur, ovipositor ca 2.6× longer than hind femur. Ovipositor upcurved apically, dorsal preapical notch absent, tip acute (Fig. 14J).

Colour. Mandible except teeth, palpi, tegula, scape and pedicel in front, fore and middle legs from the apices of coxae onward, yellowish brown, femora and tarsus darker. Hind leg with tarsus, base and apex of tibia, base of trochanter, blackish brown; remainder of the hind leg yellowish brown. First metasomal segment black with postpetiole reddish brown, second segment reddish brown with apically lighter, remainder of the tergites light reddish orange.

Distribution. China (Yunnan).

Etymology. Name derived from the name of type locality of species.

Acknowledgements

References

Biddinger DJ, Leslie TW (2014) Observation on the biological control agents of the American plum borer (Lepidoptera: Pyralidae) in Michigan cherry and plum orchards. Great Lakes Entomologist 47(1–2): 51–65.

Broad GR, Shaw MR, Fitton MG (2018) Ichneumonid wasps (Hymenoptera: Ichneumonidae): their classification and biology. Handbooks for the Identification of British Insects 7(12): 1–418.

Eliopoulos PA, Athanasiou CG, Buchelos CH (2002) Occurrence of hymenopterous parasitoids of stored product pests in Greece. Bulletin Olib Srop 25(3): 127–139.

Gupta VK, Maheshwary S (1977) Ichneumonologia Orientalis, Part IV. The tribe Porizontini (=Campoplegini) (Hymenoptera: Ichneumonidae). Oriental Insects Monograph 5: 1–267.

He JH, Chen XX, Ma Y (1996) Hymenoptera: Ichneumonidae. Economic Insect Fauna of China, Science Press, Beijing, 697 pp. [in Chinese]

Hemerik L, Harvey JA (1999) Flexible larval development and the timing of destructive feeding by a solitary endoparasitoid: an optimal foraging problem in evolutionary perspective. Ecological Entomology 24(3): 308–315. https://doi.org/10.1046/j.1365-2311.1999.00203.x

Jervis MA, Ellers J, Harvey JA (2008) Resource acquisition, allocation, and utilization in parasitoid reproductive strategies. Annual Review of Entomology 53: 361–385. https://doi.org/10.1146/annurev.ento.53.103106.093433

Shaw MR, Horstmann K, Whiffin AL (2016) Two hundred and twenty-five species of reared western Palaearctic Campopleginae (Hymenoptera: Ichneumonidae) in the National Museums of Scotland, with descriptions of new species of *Campoplex* and *Diadegma*, and records of fifty-five species new to Britain. Entomologist's Gazette 67: 177–222.

Sonan J (1937) Two new species and one new genus of Hymenoptera. Transactions of the Natural History Society of Formosa 27(166): 169–174.

Vas Z (2019a) Contributions to the taxonomy, identification, and biogeography of *Casinaria* Holmgren and *Venturia* Schrottky (Hymenoptera: Ichneumonidae: Campopleginae). Zootaxa 4664(3): 351–364. https://doi.org/10.11646/zootaxa.4664.3.3

Vas Z (2019b) New species and new records of Campopleginae from the Palaearctic region (Hymenoptera: Ichneumonidae). Folia Entomologica Hungarica 80: 247–271. https://doi.org/10.17112/FoliaEntHung.2019.80.247

Vas Z (2020) New species and records of Afrotropical, Oriental and Palaearctic *Venturia* Schrottky, 1902 (Hymenoptera: Ichneumonidae: Campopleginae). Opuscula Zoologica Instituti Zoosystematici et Oecologici Universitatis Budapestinensis 51(2): 97–114. https://doi.org/10.18348/opzool.2020.2.97

Vas Z, Di Giovanni F (2020) New species and records of Afrotropical Campopleginae (Hymenoptera: Ichneumonidae). Folia Entomologica Hungarica 81: 105–114.

Wahl DB (1987) A revision of *Venturia* north of Central America (Hymenoptera: Ichneumonidae). The University of Kansas Science Bulletin 53(6): 275–356.

Yu DS, van Achterberg C, Horstmann K (2016) World Ichneumonoidea 2015. Taxonomy, Biology, Morphology and Distribution. Flash drive. Taxapad, Vancouver.

REVIEW ARTICLE

A peer-reviewed open-access journal

ZooKeys

Launched to accelerate biodiversity research

A review of the spider-attacking *Polysphincta dizardi* species-group (Hymenoptera, Ichneumonidae, Pimplinae), with descriptions of seven new species from South America

Diego G. Pádua[1], Ilari E. Sääksjärvi[2], Tamara Spasojevic[3], Kari M. Kaunisto[2], Ricardo F. Monteiro[4], Marcio L. Oliveira[1]

I *Programa de Pós-Graduação em Entomologia, Instituto Nacional de Pesquisas da Amazônia (INPA), Manaus, Brazil* **2** *Biodiversity Unit, Zoological Museum, University of Turku, Turku, Finland* **3** *Department of Entomology, National Museum of Natural History, Washington, DC, USA* **4** *Laboratório de Ecologia de Insetos, Depto. de Ecologia, Universidade Federal do Rio de Janeiro (UFRJ), Rio de Janeiro, Brazil*

Corresponding author: Diego G. Pádua (paduadg@gmail.com)

Citation: Pádua DG, Sääksjärvi IE, Spasojevic T, Kaunisto KM, Monteiro RF, Oliveira ML (2021) A review of the spider-attacking *Polysphincta dizardi* species-group (Hymenoptera, Ichneumonidae, Pimplinae), with descriptions of seven new species from South America. ZooKeys 1041: 137–165. https://doi.org/10.3897/zookeys.1041.65407

Abstract

The Neotropical *Polysphincta dizardi* species-group is revised. We describe seven new species from South America: *P. bonita* **sp. nov.**, *P. cosnipata* **sp. nov.**, *P. inca* **sp. nov.**, *P. macroepomia* **sp. nov.**, *P. organensis* **sp. nov.**, *P. pichincha* **sp. nov.**, and *P. teresa* **sp. nov.** In addition, we provide a diagnosis and an identification key to all species of the group.

Introduction

Polysphincta Gravenhorst, 1829 is a Neotropical and Holarctic Darwin wasp genus with 30 valid species (Yu et al. 2016; Kloss et al. 2018; Higa and Penteado-Dias 2020). The genus belongs to the *Polysphincta* genus-group (*sensu* Gauld and Dubois 2006) which exclusively comprises koinobiont ectoparasitoids of spiders (Matsumoto 2016; Yu et al. 2016; Kloss et al. 2018).

The revision of the Neotropical species of *Polysphincta* was started by Gauld (1991) and Gauld et al. (1998) who described several new species from Central America and divided the genus into three species-groups based on morphological characters: *P. dizardi*, *P. gutfreundi*, and *P. purceli* species-groups. Gauld (1991) also reported that several undescribed species occur throughout tropical America.

The species of the *P. dizardi* species-group are somewhat intermediate between the "more typical" *Polysphincta* species and the species of *Hymenoepimecis* Viereck (Gauld 1991). The *P. dizardi* species-group is normally characterized by the following two characters: a shelf-like projection (pronotal shelf) in the mediodorsal part of the pronotum and epomia absent.

The morphological phylogenetic analysis of the *Polysphincta* genus-group by Gauld and Dubois (2006) placed a single included representative of *P. dizardi* species-group, *P. shabui* Gauld, into the clade "F" as a sister group of genera *Ticapimpla* Gauld, *Acrotaphus* Townes and *Hymenoepimecis*. This suggests that the *P. dizardi* species-group could be a new genus. The status of *Polysphincta* should be revised after the tropical fauna of the genus is better known.

During the last two decades, we have found several new species of *Polysphincta* from various parts of South America (tropical Andes, Amazonia, Brazilian coastal rain forests and Chilean temperate rain forests), which calls for the revision of Neotropical species of the genus. The review of the *P. dizardi* species-group, studied here, is the first part of this larger work.

Materials and methods

The specimens studied in this review are deposited in the following collections:

BMNH   The Natural History Museum, London, United Kingdom;
DCBU   Departamento de Ecologia e Biologia Evolutiva, São Carlos, São Paulo, Brazil;
INPA   Invertebrate Collection of the Instituto Nacional de Pesquisas da Amazônia, Manaus, Amazonas, Brazil;
MUSM   Universidad Nacional de San Marcos, Lima, Peru;
MZUSP Zoological Museum of the Universidade de São Paulo, São Paulo, São Paulo, Brazil;
RBINS Royal Belgian Institute of Natural Sciences, Brussels, Belgium;
UEFS   Universidade Estadual de Feira de Santana, Feira de Santana, Bahia, Brazil;

UFMG Universidade Federal de Minas Gerais, Belo Horizonte, Minas Gerais, Brazil;
ZMUT Biodiversity Unit, Zoological Museum of the University of Turku, Turku, Finland.

The morphological terminology follows Broad et al. (2018) and style of the descriptions follow those of Gauld (1991). However, we add two new characters to the descriptions: the shape of the tarsal claws and the shape of the pronotal shelf. We also add the following proportions to the descriptions: (a) margin of gena/length of eye; (b) length of the epomia/length of the proximal mandibular width; and (c) length/posterior width of tergite II.

The measures and proportions between the structures are given as the value of the holotypes or paratypes [in brackets], followed by the minimum and maximum number of variations. The [brackets] were also used to add, supplement or correct information on the specimen labels.

Specimens were examined using OLYMPUS SZ61 and SZX10 (at ZMUT) and the ZEISS Stemi 2000 (at INPA) stereomicroscopes. Measurements were obtained using millimetric oculars attached to the stereomicroscope, calibrated with a precision ruler. Digital images were taken using a CANON DS126461 digital camera attached to an OLYMPUS SZX16 stereomicroscope and combined by using the software Zerene Stacker (v. 1.04 Build T201706041920) (at ZMUT) and a LEICA DMC4500 digital camera attached to a LEICA M205A stereomicroscope and combined by using the software Helicon Focus v. 5.3 Pro. (at INPA).

The distributional maps were created using SimpleMappr online software (Shorthouse 2010).

Taxonomy

The *Polysphincta dizardi* species-group

Diagnosis. The *P. dizardi* species-group can be distinguished from all other species-groups of the genus by the combination of two characters: (1) pronotum with a strong shelf-like projection mediodorsally and (2) submetapleural carina absent.

Remarks. According to Gauld (1991) and our new discoveries, this species group is known to occur only in the Neotropical region.

Key to the species of the *P. dizardi* species-group

[Obs. Only the males of *P. shabui* Gauld, *P. sinearanea* Pádua, and *P. organensis* sp. nov. are known].

1   Epomia present (Figs 5B, 9B, 10B) **2**
–   Epomia absent (Figs 1B, 2B, 3B, 4B, 6B, 7B, 8B)..**4**

2 Epomia 1.5 times the length of the proximal mandibular width (Fig. 5B)...........
....*P. macroepomia* **sp. nov.**
– Epomia <1.0 times the length of the proximal mandibular width (Figs 9B, 10B)
....**3**
3 Metasoma orange, with posterior margins of tergites II–IV narrowly black, posterior half of tergite V black, and tergites VI+ black (Fig. 9A, C); ovipositor robust (Fig. 9A) ....*P. sinearanea* **Pádua, 2018**
– Metasoma darkish brown, with posterior margins of tergites II–V narrowly black (Fig. 10A, C); ovipositor slender (Fig. 10A) ....*P. teresa* **sp. nov.**
4 Metasoma orange with posterior margins of tergites II–IV narrowly black, tergites V+ or VI+ black (Figs 4A, 7A); fore wing yellowish hyaline with or without apex slightly blackish (Figs 4A, 7A); mesosoma entirely orange (Figs 4A, 7A).............**5**
– Metasoma entirely darkish brown (some specimens with tergites I–III reddish orange with posterior margin blackish) or blackish with anterior parts whitish (Figs 1A, 2A, 3A, 6A, 8A); fore wing hyaline (Figs 1A, 2A, 3A, 6A, 8A); mesosoma entirely orange or reddish brown, or orange or reddish brown with black parts (Figs 1A, 2A, 3A, 6A, 8A) **6**
5 Malar space >0.6 times as long as proximal mandibular width; hind coxa black (Fig. 4A) ....*P. inca* **sp. nov.**
– Malar space 0.4 times as long as proximal mandibular width; hind coxa orange (Fig. 7A) ....*P. pichincha* **sp. nov.**
6 Mesosoma reddish brown or orange with some blackish or brownish markings (Figs 2A, 3A)..**7**
– Mesosoma entirely reddish brown or orange without blackish or brownish markings (Figs 6A, 8A) **8**
7 Mesosoma reddish brown with anterior part of pronotum, propleuron, metapleuron and propodeum blackish (Fig. 3A); metasoma entirely darkish brown (Fig. 3A, C)...*P. dizardi* **Gauld, 1991**
– Mesosoma orange with metapleuron and propodeum brown (Fig. 2A); metasoma brownish with anterior and anterolateral margins of tergites III–V whitish (Fig. 2A, C)..*P. cosnipata* **sp. nov.**
8 Metasoma entirely darkish brown (Fig. 8A, C) or darkish brown with tergites I–III reddish orange with posterior margin blackish; malar space 0.6 times as long as proximal mandibular width...*P. shabui* **Gauld, 1991**
– Metasoma blackish with tergites II–IV or II–VI with anterior and anterolateral margins whitish (Figs 1A, 6A, C); malar space <0.5 times as long as proximal mandibular width **9**
9 Metasoma blackish with tergites II–VI with anterior and anterolateral margins whitish (Fig. 6A, C); ovipositor 1.2–1.3 times as long as hind tibia....................
....*P. organensis* **sp. nov.**
– Metasoma with tergite I orange with posterior margin black, tergites II–IV brownish with anterior and anterolateral margins whitish and posterior margin black, and tergites V+ brownish (Fig. 1A, E); ovipositor 1.0 times as long as hind tibia ....*P. bonita* **sp. nov.**

The species of *Polysphincta dizardi* species-group

Polysphincta bonita Pádua & Sääksjärvi, sp. nov.
http://zoobank.org/29EA486A-7AD0-4C27-BB9A-F54C4B55E11A
Fig. 1A–E

Diagnosis. *Polysphincta bonita* sp. nov. can be distinguished from other species of the *P. dizardi* species-group by the combination of the following characters: (1) epomia absent (Fig. 1B); (2) malar space 0.5 times as long as proximal mandibular width (Fig. 1B); (3) fore wing vein 1*cu-a* interstitial relative to *M&RS*; (4) mesosoma orange (Fig. 1A); (5) wing hyaline, slightly infuscate (Fig. 1A); (6) hind leg brownish, except coxa orange and middle inner and outer region whitish (Fig. 1A); (7) metasoma with tergite I orange with posterior margin black, tergites II–IV brownish with anterior and anterolateral margins whitish and posterior margin black, and tergites V+ brownish (Fig. 1A, E); (8) ovipositor slightly slender, 1.0 times as long as hind tibia.

   Description. Female. Body about [9.5] mm. ***Head.*** Clypeus weakly convex, the posterior margin thin and straight centrally; malar space [0.5] times as long as proximal mandibular width; lower face [1.1] times as broad as high, weakly convex centrally, polished, with fine sparse setiferous punctures; head in dorsal view with margin of the gena weakly convex behind the eyes, and its margin about [0.5] times length of eye in dorsal view; ocelli moderately large, the lateral one separated from compound eyes by [1.1] times their own maximum diameter. ***Mesosoma.*** Pronotum without epomia; shelf-like projection, in dorsal view, with the apex bilobed, and in lateral view, with anterolateral part posteriorly rounded and weakly decurved; mesoscutum more or less robust, in dorsal view, smooth and polished, with notauli weakly impressed anteriorly; scutellum convex, not laterally carinate; mesopleuron highly polished, virtually impunctate; epicnemial carina reaching almost to the level of the lower corner of pronotum; epicnemium with a vestigial vertical carina near lower corner of pronotum; metapleuron convex, smooth and polished, with sparse, fine bristles evenly spaced, without a discernible submetapleural carina. Propodeum mediodorsally smooth and polished, with longitudinal carinae present only posteriorly and with scattered fine bristles. Fore wing length about [8.0] mm; 1*cu-a* interstitial relative to *M&RS*; base of 1*m-cu&M* separated from *CU* by about length of 2*cu-a*; hind wing with distal abscissa of *CU* present and complete, well pigmented; first abscissa of *RS* subequal to *rs-m*. Tarsal claw with proximal lobe quadrangular, with claw apex slightly overtaking the distal margin of lobe. ***Metasoma.*** Tergite I [1.25] times as long as posteriorly broad, dorsally with lateromedian longitudinal carinae only discernible at the extreme anterior part; sternite I with a weak swelling near the hind rim, and with a weak median longitudinal ridge anteriorly; tergite II about [1.25] times as long as posteriorly broad, highly polished, at most with only fine setiferous punctures laterally; tergite III about [1.1] times as long as posteriorly broad, highly polished, at most with only fine setiferous punctures; subgenital plate subquadrate. Ovipositor slightly slender, about [1.0] times as long as hind tibia, posteriorly evenly tapered to a sharp point.
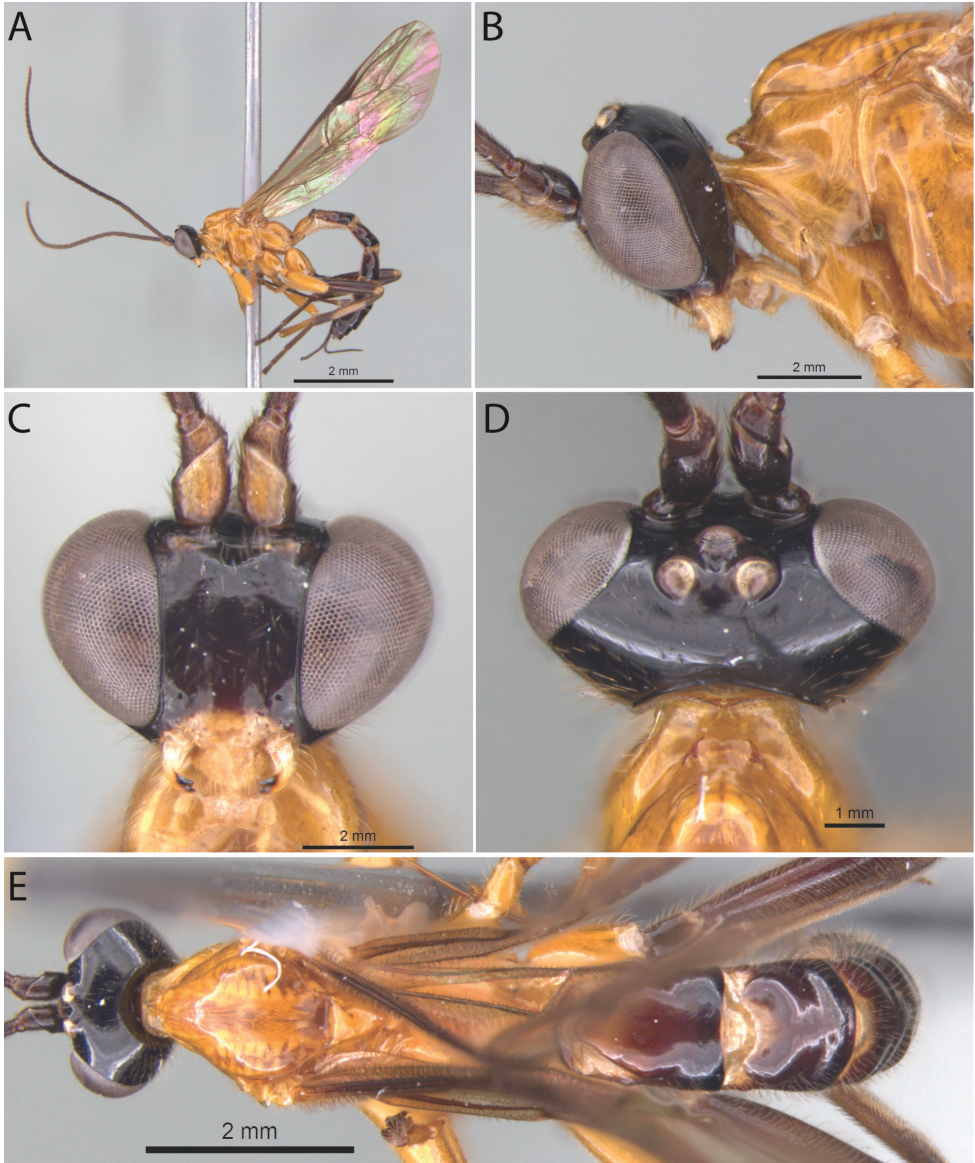
Figure 1. *Polysphincta bonita* sp. nov., ♀, holotype **A** habitus, lateral view **B** head and pronotum, lateral view **C** face, anterior view **D** head and shelf-like projection, dorsal view **E** habitus, dorsal view.

Color. Head black except posterior 0.8 of clypeus yellowish; antennae brownish with scape and pedicel ventrally yellowish; mouthparts whitish, except apex of mandible blackish. Mesosoma orange. Metasoma with tergite I orange with posterior margin black, tergites II–IV brownish with anterior and anterolateral margins whitish and posterior margin black, and tergites V+ brownish. Fore and mid leg orange, hind leg brownish, except coxa orange and a medium inner and outer region whitish. Wings are

hyaline, slightly infuscate, pterostigma brown. Ovipositor brown, with posterior and anterior part whitish.

Male. Unknown.

Type material. *Holotype* ♀. BRAZIL, BA [= Bahia], Camacan, PPPN [sic] [= RPPN, Reserva Particular do Patrimônio Natural], Serra Bonita, IX.2010, Malaise trap 3 (without collector), UEFS.

Distribution. Brazil (Fig. 13).

Biological note. Host unknown.

Etymology. The specific name (in apposition) refers to the type locality of this species, RPPN Serra Bonita, Bahia state, Brazil, and also to the beauty of this new species.

Remarks. *Polysphincta bonita* sp. nov. closely resembles *P. organensis* sp. nov. mainly by the coloration, with mesosoma entirely orange and metasoma brownish with tergites II–IV or II–VI whitish in anterior and anterolateral margins. It clearly differs from *P. organensis* sp. nov. by having ovipositor 1.0 times as long as hind tibia and fore and mid leg orange, hind leg brownish, except coxa orange and a medium inner and outer region whitish (ovipositor >1.2 times as long as hind tibia and fore leg orange, mid leg orange with coxa, trochanter and trochantellus whitish and tarsus brownish, hind leg whitish with coxa inner region, trochanter proximally, trochantellus distal, femur proximally and distally, tibia proximally and distally, first tarsal segment distally, and remaining tarsal segments entirely blackish brown in *P. organensis* sp. nov.).

Polysphincta cosnipata Pádua & Sääksjärvi, sp. nov.

http://zoobank.org/1D4251B0-17C6-4220-AF11-9B2D2E7FB721
Fig. 2A–F

Diagnosis. *Polysphincta cosnipata* sp. nov. can be distinguished from other species of the *P. dizardi* species-group by the combination of the following characters: (1) epomia absent (Fig. 2B); (2) malar space 0.4 times as long as proximal mandibular width (Fig. 2B); (3) fore wing vein 1*cu-a* more or less interstitial relative to *M&RS* (Fig. 2A); (4) mesosoma orange with metapleuron and propodeum brown (Fig. 2A); (5) wings hyaline (Fig. 2A); (6) hind leg whitish with inner part of coxa, trochanter proximally, trochantellus distally, femur proximally and distally, tibia proximally and distally, first tarsal segment distally, and remaining tarsal segments entirely blackish brown (Fig. 2A); (7) metasoma brownish with anterior and anterolateral margins of tergites III–V whitish (Fig. 2A, C); (8) ovipositor slightly slender, 1.2 times as long as hind tibia.

Description. Female. Body [8.0] mm. ***Head.*** Clypeus weakly convex, posterior margin thin and flat centrally; malar space [0.4] times as long as proximal mandibular width; lower face [0.9] times as broad as high, weakly convex centrally, polished, with fine sparse setiferous punctures; head in dorsal view with margin of the gena weakly convex behind eyes and its margin about [0.5] times length of eye; ocelli moderately large, lateral ones separated from compound eyes by about [0.8] times their own maximum diameter. ***Mesosoma.*** Pronotum without epomia; shelf-like projection, in
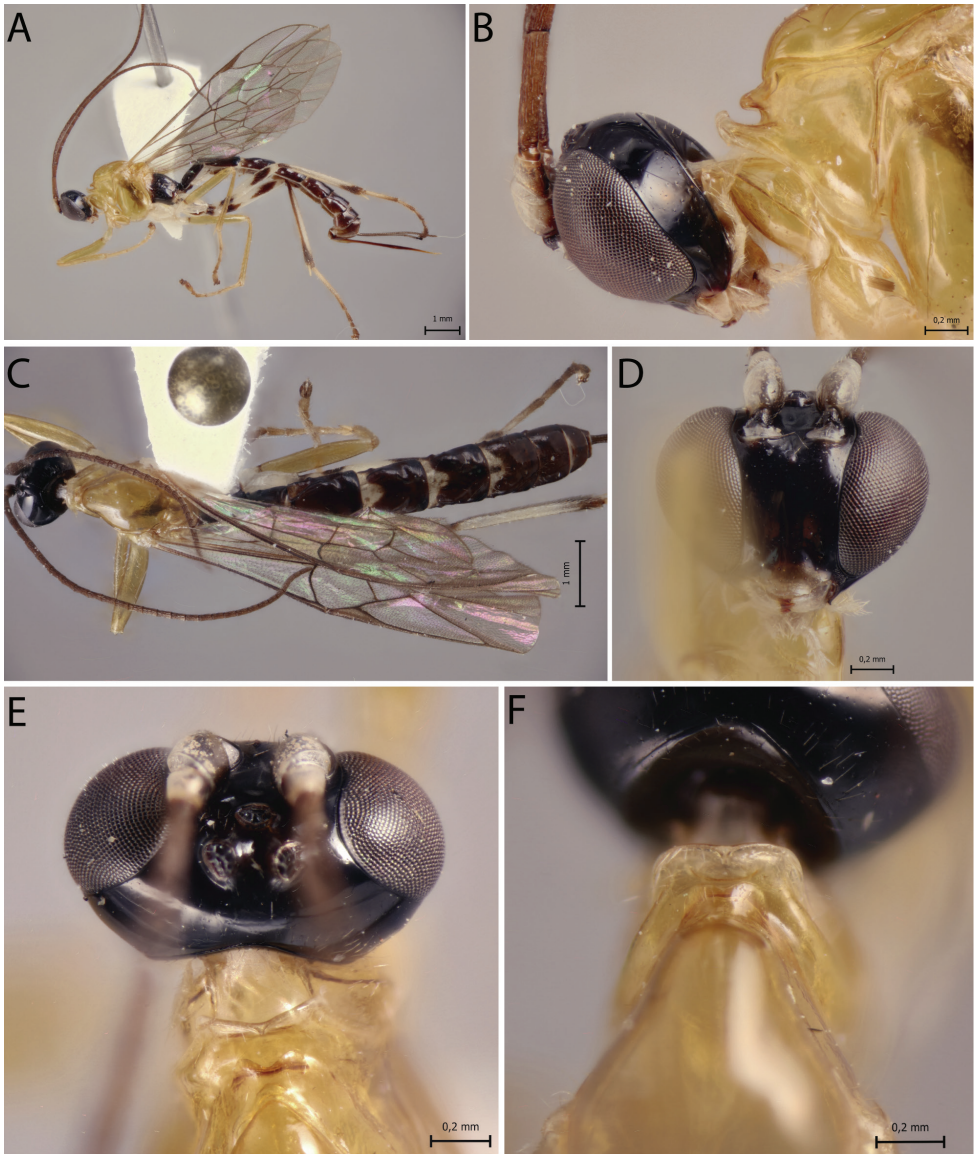
Figure 2. *Polysphincta cosnipata* sp. nov., ♀, holotype **A** habitus, lateral view **B** head and pronotum, lateral view **C** habitus, dorsal view **D** face, anterior view **E** head, dorsal view **F** shelf-like projection, dorsal view.

dorsal view, bilobed, subquadrangular, and in lateral view, slender, with anterolateral corners weakly decurved; mesoscutum more or less robust, in dorsal view, smooth and polished, with notauli weakly impressed anteriorly; scutellum convex, not laterally carinate; mesopleuron highly polished, virtually impunctate; epicnemial carina reaching almost to level of lower corner of pronotum; epicnemium with vestigial vertical carina near lower corner of pronotum; metapleuron convex, smooth and polished, with sparse, fine bristles evenly spaced, without discernible submetapleural carina.

Propodeum mediodorsally smooth and polished, with longitudinal carinae present only posteriorly and with scattered fine bristles. Fore wing length about [7.0] mm; 1*cu-a* more or less interstitial relative to *M&RS*; base of 1*m-cu&M* separated from *CU* by about length of 2*cu-a*; hind wing with distal abscissa of *CU* present and complete but weakly pigmented; first abscissa of *RS* subequal to *rs-m*. Tarsal claw with proximal lobe quadrangular, with claw apex slightly overtaking distal margin of lobe. **Metasoma.** Tergite I about [1.5] times as long as posteriorly broad, dorsally with lateromedian longitudinal carinae only discernible at extreme anterior part; sternite I with weak swelling near hind rim, and with weak median longitudinal ridge anteriorly; tergite II about [1.5] times as long as posteriorly broad, highly polished, at most with only fine setiferous punctures laterally; tergite III about [1.3] times as long as posteriorly broad, highly polished, at most with only fine setiferous punctures; subgenital plate subquadrate. Ovipositor slightly slender, [1.2] times as long as hind tibia, posteriorly evenly tapered to sharp point.

Color. Head black except 0.8 of clypeus yellowish; antennae brownish with scape and pedicel ventrally whitish; mouthparts whitish, except apex of mandible brownish. Mesosoma orange with metapleuron and propodeum brown. Metasoma brownish with anterior and anterolateral margins of tergites III–V whitish. Fore leg orange, mid leg orange with coxa, trochanter and trochantellus whitish and tarsus distally brownish, hind leg whitish with coxa inner region, trochanter proximal, trochantellus distally, femur proximally and distally, tibia proximally and distally, first tarsal segment distally, and remaining tarsal segments entirely blackish brown. Wings hyaline, pterostigma brown. Ovipositor brown, with posterior and anterior parts whitish.

Male. Unknown.

Type material. *Holotype* ♀. Peru, CU [= Cusco], Cosñipata valley, San Pedro, 13°03'23"S, 71°32'55"W, 1520 m, 12.XII.2007, Malaise trap (C. Castillo leg.), MUSM.

Distribution. Peru (Fig. 11).

Biological note. Host unknown.

Etymology. The specific name (in apposition) refers to type locality of this species, Cosñipata valley, Cusco, Peru.

Remarks. *Polysphincta cosnipata* sp. nov. closely resembles *P. dizardi* Gauld, 1991 and *P. macroepomia* sp. nov. mainly by coloration, with mesosoma orange and propodeum blackish or brownish. However, it differs from *P. dizardi* by having pronotum orange and metasomal tergites II–VI with anterior and anterolateral margins whitish (anterior part of pronotum brownish and metasomal tergites entirely darkish brown in *P. dizardi*), and from *P. macroepomia* sp. nov. by having epomia absent (present in *P. macroepomia* sp. nov.).

Polysphincta dizardi Gauld, 1991
Fig. 3A–F

Polysphincta dizardi Gauld, 1991: 313. Holotype ♀, Costa Rica (MNCR).
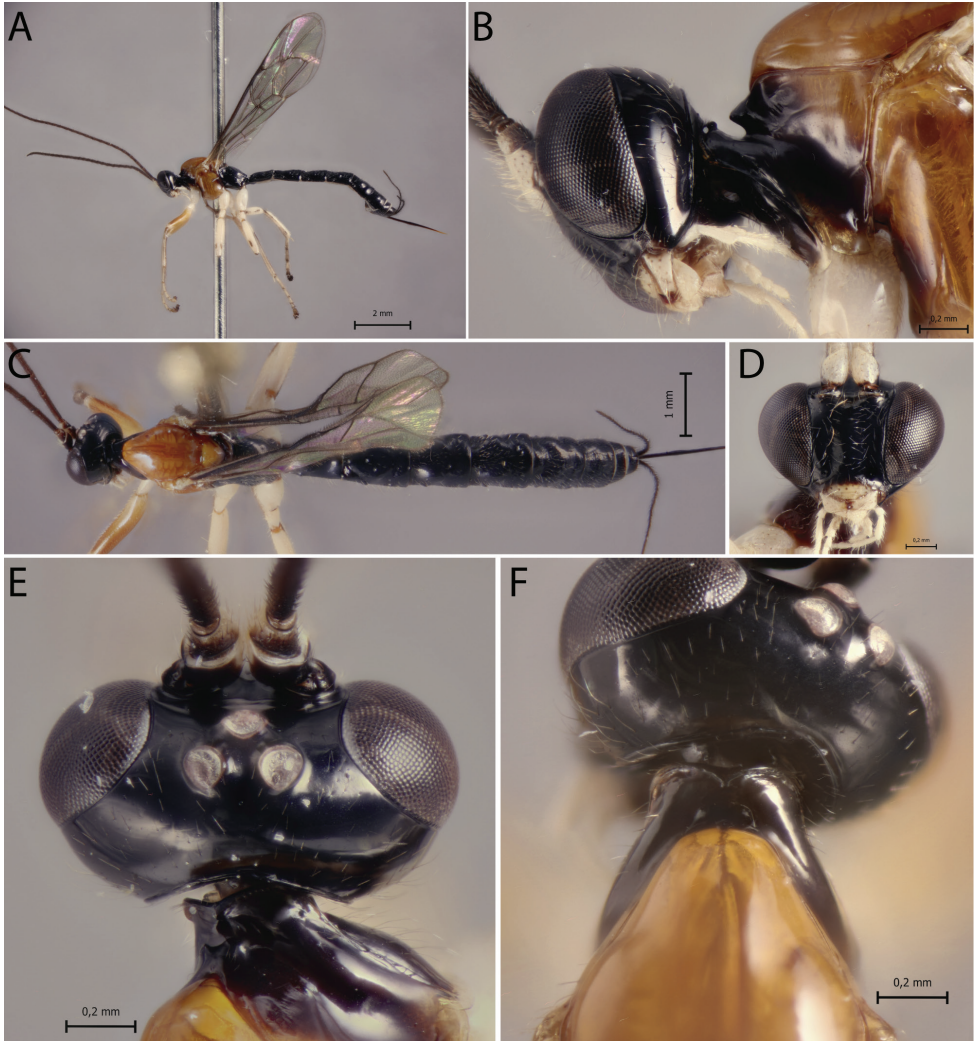
Figure 3. *Polysphincta dizardi* Gauld, 1991, ♀, paratype **A** habitus, lateral view **B** head and pronotum, lateral view **C** habitus, dorsal view **D** face, anterior view **E** head, dorsal view **F** shelf-like projection, dorsal view.

Diagnosis. *Polysphincta dizardi* can be distinguished from other species of the *P. dizardi* species-group by the combination of the following characters: (1) epomia absent (Fig. 3B); (2) malar space 0.45–0.5 times as long as proximal mandibular width (Fig. 3B); (3) fore wing vein 1*cu-a* interstitial relative to *M&RS* (Fig. 3A); (4) mesosoma reddish brown with anterior part of pronotum, propleuron, metapleuron and propodeum blackish (Fig. 3A); (5) wings hyaline (Fig. 3A); (6) hind leg whitish with femur laterally, tibia proximally and distally, and tarsus distally brownish (Fig. 3A); (7) metasoma entirely darkish brown (Fig. 3A, C); (8) ovipositor slender, 1.1–1.3 times as long as hind tibia.

Comments. Additional characters to the original description (♀) are as follows: body about [7.7–8.3] 7.5–8.5; head in dorsal view with margin of the gena convex behind the eyes, and its margin [0.5–0.55] 0.45–0.55 times length of eye; shelf-like projection, in dorsal view, more or less developed anterolaterally, apex very weakly bilobed, and in lateral view, with anterolateral part of apex rounded and very weakly decurved; mesoscutum robust, in dorsal view; tarsal claw with proximal lobe quadrangular, with claw apex slightly overtaking distal margin of lobe.

Distribution. Costa Rica (Fig. 11).

Biological notes. Host unknown.

Materials examined. *Paratypes*: Costa Rica, Sn. José Pv., Zurqui de Moravis, 1600 m., nr. to Braulio Carrillo, I–II.1990 (Gauld leg.), 1♀, BMNH; idem, but Heredia Pv., 9.5 km., E. of El Tunel, 1000 m., IV.1989, 1♀, BMNH. **Costa Rica:** Sn. José Pv., Zurqui de Moravia, 1600 m. near to Braulio Carrillo, I.1991 (Gauld leg.), 1♀, BMNH; idem, but VI.1992, 1♀, BMNH.

Polysphincta inca **Pádua, Sääksjärvi & Spasojevic, sp. nov.**
http://zoobank.org/8B54350E-46CE-4911-B8D6-4CC386F01AF6
Fig. 4A–F

Diagnosis. *Polysphincta inca* sp. nov. can be distinguished from other species of the *P. dizardi* species-group by the combination of the following characters: (1) epomia absent (Fig. 4B); (2) malar space 0.6–0.7 times as long as proximal mandibular width (Fig. 4B); (3) fore wing vein 1*cu-a* interstitial relative to *M&RS* (Fig. 4A); (4) mesosoma orange, except posterior carinae of propodeum darkish brown (Fig. 4A); (5) wings yellowish hyaline with apex weakly blackish (Fig. 4A); (6) hind leg entirely darkish brown or darkish brown, with median region of tibia pale (Fig. 4A); (7) metasoma orange, with posterior margins (or only laterally) of tergites II–V narrowly black, tergites VI+ black (Fig. 4A, C); (8) ovipositor slender, 1.1–1.3 times as long as hind tibia.

Description. Female. Body [13.0] 12.0–14.0 mm. ***Head.*** Clypeus weakly convex, posterior margin thin and flat centrally; malar space [0.7] 0.6–0.7 times as long as proximal mandibular width; lower face about [1.2] 1.0–1.4 times as broad as high, weakly convex centrally, polished, with fine sparse setiferous punctures; head in dorsal view with margin of gena flat behind the eyes, and its margin about [0.6] 0.4–0.6 times length of eye; ocelli moderately large, the lateral ones separated from compound eyes by [1.1] 1.0–1.3 times their own maximum diameter. ***Mesosoma.*** Pronotum without epomia; shelf-like projection, in dorsal view, more or less bilobed, subquadrangular, and in lateral view, slender with anterolateral corners weakly decurved; mesoscutum more or less slender, in dorsal view, smooth and polished, with notauli weakly impressed anteriorly; scutellum convex, not laterally carinate; mesopleuron highly polished, virtually impunctate; epicnemial carina reaching almost level of lower corner of pronotum; epicnemium with vestigial vertical carina near lower corner of pronotum; metapleuron convex, smooth and polished, with few sparse, fine bristles evenly
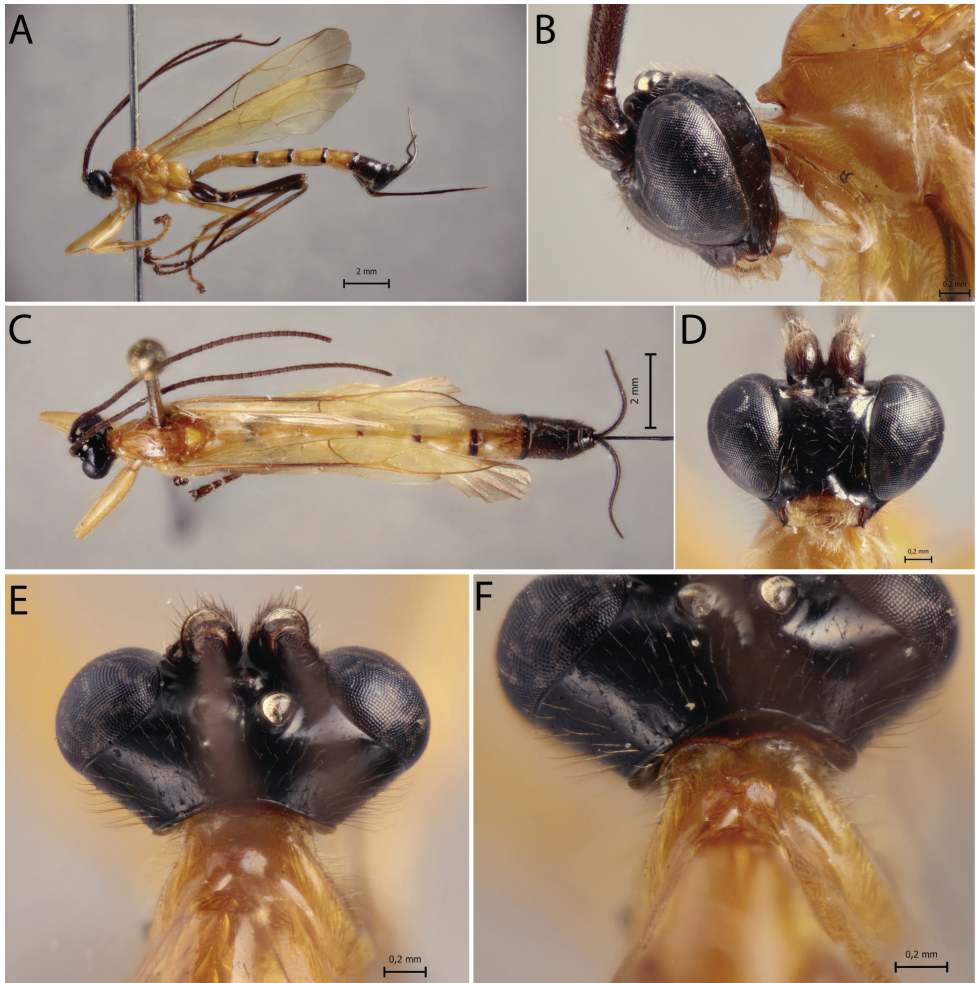
Figure 4. *Polysphincta inca* sp. nov., ♀, holotype **A** habitus, lateral view **B** head and pronotum, lateral view **C** habitus, dorsal view **D** face, anterior view **E** head, dorsal view **F** shelf-like projection, dorsal view.

spaced, without discernible submetapleural carina. Propodeum mediodorsally smooth and polished, with longitudinal carinae present only posteriorly and laterally with scattered fine bristles. Fore wing length [10.0] 10.0–11.0 mm; 1*cu-a* interstitial relative to *M&RS*; base of 1*m-cu&M* separated from *CU* by about length of 2*cu-a*; hind wing with distal abscissa of *CU* present and complete but weakly pigmented; first abscissa of *RS* subequal to *rs-m*. Tarsal claw with proximal lobe quadrangular, with claw apex slightly overtaking the distal margin of lobe. ***Metasoma.*** Tergite I about [1.4] 1.4–1.8 times as long as posteriorly broad, dorsally with lateromedian longitudinal carinae only discernible at extreme anterior part; sternite I with weak swelling near hind rim, and with weak median longitudinal ridge anteriorly; tergite II about [1.4] 1.4–1.7 times as long as posteriorly broad, highly polished, at most with only fine setiferous

punctures laterally; tergite III about [1.3] 1.3–1.4 times as long as posteriorly broad, highly polished, at most with only fine setiferous punctures laterally; subgenital plate subquadrate. Ovipositor slightly slender, about [1.2] 1.1–1.3 times as long as hind tibia, posteriorly evenly tapered to sharp point.

Color. Head black except 0.8 distal of clypeus yellowish; antennae brown; mouthparts pale, except apex of mandible brownish. Mesosoma orange, except posterior carinae of propodeum darkish brown. Metasoma orange, with posterior margins of tergites II–V narrowly black, tergites VI+ black. Fore leg orange, mid leg orange with tarsus brownish, hind leg darkish brown, with median region of tibia pale. Wings yellowish hyaline with apex weakly blackish, pterostigma yellow. Ovipositor darkish brown, with posterior and anterior parts pale.

Variation. Some specimens present hind leg entirely darkish brown; metasoma orange with posterior margins of tergites II–V narrowly black only laterally and tergite VI orange with posterior margin black.

Male. Unknown.

Type material. *Holotype* ♀. Peru, CU [= Cusco], Cosñipata valley, Rocotal 13°07'00"S, 71°34'20"W, 2075 m., 23.X.2007, Malaise trap (C. Castillo leg.), MUSM. *Paratypes:* idem holotype, but San Pedro, 13°03'22"S, 71°32'55"W, 1520 m., 1♀, ZMUT. Ecuador: R. Biol. San Francisco, 03°58'30"S, 79°04'25"W, 2000 m., 13.II–03.III.2009, Malaise trap (M. Pollet & A. Braekeleer leg.), EC/2009-36/MP&ADB-017 [code?], 2♀♀, RBINS.

Distribution. Ecuador and Peru (Fig. 12).

Biological note. Host unknown.

Etymology. This species is named in honour of the Andean Inca empire.

Remarks. *Polysphincta inca* sp. nov. closely resembles *A. sinearanea* Pádua, 2018 and *P. pichincha* sp. nov. mainly by color pattern, body orange with last metasomal tergites black. It differs from *P. sinearanea* by having epomia absent (present in *P. sinearanea*), and from *P. pichincha* sp. nov. by having malar space > 0.6 times as long as proximal mandibular width (malar space 0.4 times as long as proximal mandibular width in *P. pichincha* sp. nov.).

Polysphincta macroepomia **Pádua & Sääksjärvi, sp. nov.**
http://zoobank.org/67A518F3-413E-4233-B77A-135CEDF17743
Fig. 5A–E

Diagnose. *Polysphincta macroepomia* sp. nov. can be distinguished from other species of the *P. dizardi* species-group by the combination of the following characters: (1) epomia present, 1.5 times length of proximal mandibular width (Fig. 5B); (2) malar space 0.6 times as long as proximal mandibular width (Fig. 5B); (3) fore wing vein 1*cu-a* interstitial relative to *M&RS* (Fig. 5A); (4) mesosoma orange, except metapleuron and propodeum darkish brown (Fig. 5A); (5) fore wing hyaline (Fig. 5A); (6) hind leg whitish with spot in proximal region of coxa, base of trochanter, longitudinal spot in
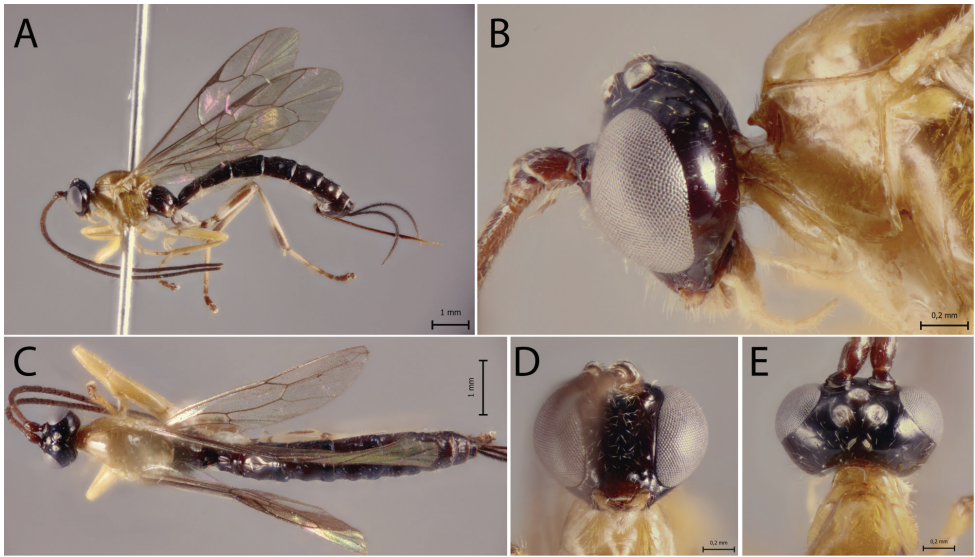
Figure 5. *Polysphincta macroepomia* sp. nov., ♀, holotype **A** habitus, lateral view **B** head and pronotum, lateral view **C** habitus, dorsal view **D** face, anterior view **E** head and shelf-like projection, dorsal view.

subdistal region of inner and outer margin of femur, distal part of tibia and distal part of tarsus brownish (Fig. 5A); (7) metasoma darkish brown, with posterior margins of tergites II–V narrowly black (Fig. 5A, C); (8) ovipositor slightly slender, 1.7 times as long as hind tibia.

Description. Female. Body about [7.0] mm. ***Head.*** Clypeus very weakly convex, posterior margin thin and flat centrally; malar space [0.6] times as long as proximal mandibular width; lower face about [1.1] times as broad as high, weakly convex centrally, polished, with fine sparse setiferous punctures; head in dorsal view with margin of gena very weakly convex behind the eyes, and its margin about [0.6] times length of eye; ocelli moderately large, the lateral ones separated from compound eyes by [1.0] times their own maximum diameter. ***Mesosoma.*** Pronotum with epomia distinct, about [1.5] times length of proximal mandibular width; shelf-like projection, in dorsal view, more or less straight, broader than long, and in lateral view, slender and slightly decurved in apex; mesoscutum robust, in dorsal view, smooth and polished, with notauli weakly impressed anteriorly; scutellum convex, not laterally carinate; mesopleuron highly polished, virtually impunctate; epicnemial carina reaching almost the level of lower corner of pronotum; epicnemium with vestigial vertical carina near lower corner of pronotum; metapleuron weakly convex, smooth and polished, with few sparse fine bristles, without discernible submetapleural carina. Propodeum mediodorsally smooth and polished, with longitudinal carinae present only posteriorly and with scattered fine bristles. Fore wing length [6.0] mm; 1*cu-a* interstitial relative to *M&RS*; base of 1*m-cu&M* separated from *CU* by about length of 2*cu-a*; hind wing with distal abscissa of *CU* present and complete but weakly pigmented; first abscissa

of *RS* subequal to *rs-m*. Tarsal claw with proximal lobe quadrangular, with claw apex slightly overtaking distal margin of lobe. ***Metasoma.*** Tergite I about [1.4] times as long as posteriorly broad, dorsally with lateromedian longitudinal carinae only discernible at extreme anterior part; sternite I with weak swelling near hind rim, and with weak median longitudinal ridge anteriorly; tergite II [1.3] times as long as posteriorly broad, highly polished, at most with only fine setiferous punctures laterally; tergite III about [1.2] times as long as posteriorly broad, highly polished, at most with only fine setiferous punctures; subgenital plate subquadrate. Ovipositor slightly slender, [1.7] times as long as hind tibia, posteriorly evenly tapered to sharp point.

Color. Head darkish brown except clypeus brownish; antennae brown; mouthparts white, except apex of mandible black. Mesosoma orange, except metapleuron and propodeum darkish brown. Metasoma entirely darkish brown, with posterior margins of tergites II–V narrowly black. Legs whitish, fore leg with femur, tibia and tarsus weakly yellowish; mid leg with femur and tibia and tarsus weakly yellowish, except final distal of tarsus brownish; hind leg with spot in proximal region of coxa, base of trochanter, longitudinal spot in subdistal region of inner and outer margin of femur, distal part of tibia and final distal of tarsus brownish. Wings hyaline, pterostigma brown. Ovipositor brown, with posterior portion whitish.

Male. Unknown.

Type material. *Holotype* ♀. Peru, CU [= Cusco], San Pedro, 1520 m., 13°03'22"S, 71°32'55"W, 22.IX.2007, Malaise trap 11 (C. Castillo leg.), MUSM.

Distribution. Peru (Fig. 13).

Biological notes. Host unknown.

Etymology. The specific name refers to the long epomia, main characteristic of this species.

Remarks. *Polysphincta macroepomia* sp. nov. closely resembles *P. dizardi* Gauld, 1991 and *P. cosnipata* sp. nov. mainly by the coloration, mesosoma orange with metapleuron and propodeum blackish and metasoma brownish or blackish. However, it differs from both species by having epomia present (absent in *P. dizardi* and *P. cosnipata* sp. nov.).

Polysphincta organensis Pádua & Sääksjärvi, sp. nov.

http://zoobank.org/B43CD278-FD39-44F7-B453-5940E400CAA8

Fig. 6A–G

Diagnosis. *Polysphincta organensis* sp. nov. can be distinguished from other species of the *P. dizardi* species-group by the combination of the following characters: (1) epomia absent (Fig. 6B); (2) malar space 0.4 times as long as proximal mandibular width (Fig. 6B); (3) fore wing vein 1*cu-a* interstitial relative to *M&RS* (Fig. 6A); (4) mesosoma orange with weak spot posteriorly in metapleuron and posterior carinae of propodeum brown (Fig. 6A); (5) wings hyaline (Fig. 6A); (6) hind leg whitish with inner region of coxa, trochanter proximally, trochantellus distally, femur proximally and distally, tibia proximally and distally, first tarsal segment distally, and remaining tarsal segments
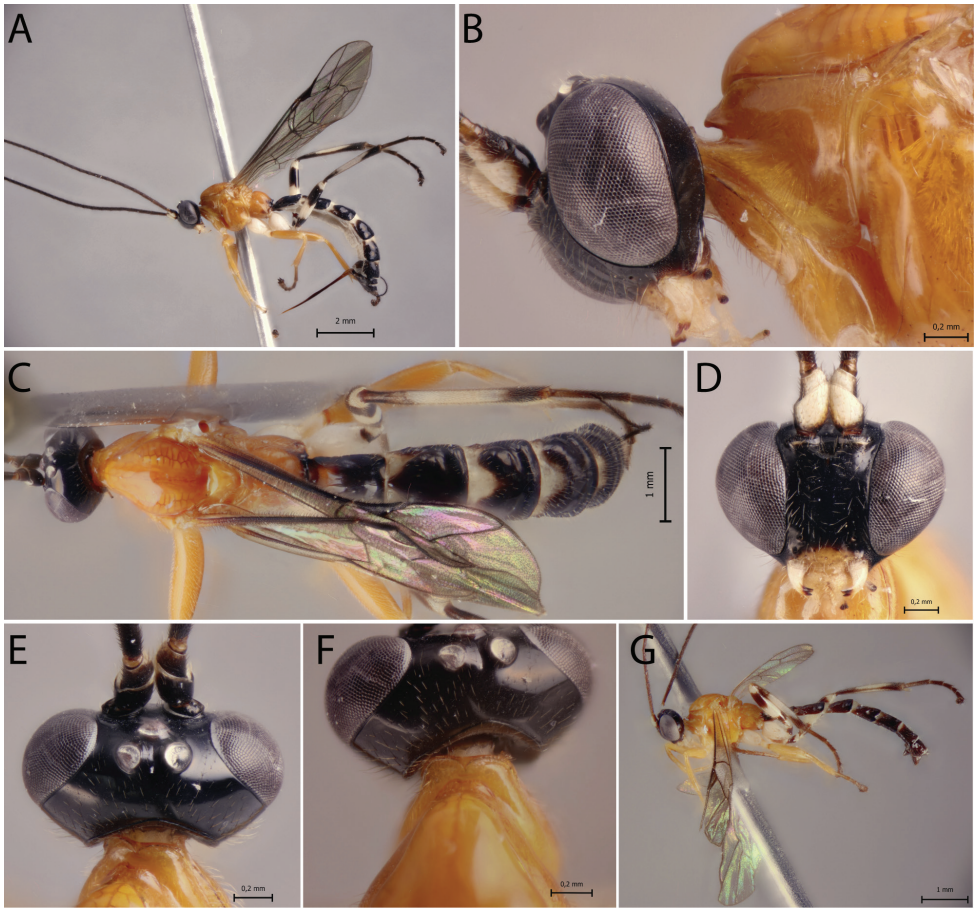
Figure 6. *Polysphincta organensis* sp. nov. **A** habitus, lateral view, ♀ (holotype) **B** head and pronotum, lateral view, ♀ (holotype) **C** habitus, dorsal view, ♀ (holotype) **D** face, anterior view, ♀ (holotype) **E** head, dorsal view, ♀ (holotype) **F** shelf-like projection, dorsal view, ♀ (holotype) **G** habitus, ♂ (paratype).

entirely blackish brown (Fig. 6A); (7) metasoma blackish with anterior margin centrally orange in tergite I, tergites II–VI with anterior and anterolateral margins whitish (Fig. 6A, C, G); (8) ovipositor slightly slender, 1.2–1.3 times as long as hind tibia.

Description. Female. Body [8.5] 7.0–8.5 mm. *Head.* Clypeus weakly convex, posterior margin thin and straight centrally; malar space [0.4] times as long as proximal mandibular width; lower face about [0.9] 0.9–1.0 times as broad as high, weakly convex centrally, polished, with fine sparse setiferous punctures; head in dorsal view with margin of gena weakly convex behind the eyes, and its margin about [0.5] 0.45–0.5 times length of eye; ocelli moderately large, lateral ones separated from compound eyes by about [0.9] 0.9–1.0 times their own maximum diameter. *Mesosoma.* Pronotum without epomia; shelf-like projection, in dorsal view, more or less bilobed, subquadrangular, and in lateral view, slender and with anterolateral corners weakly decurved;

mesoscutum robust, in dorsal view, smooth and polished, with notauli weakly impressed anteriorly; scutellum convex, not laterally carinate; mesopleuron highly polished, virtually impunctate; epicnemial carina reaching almost level of lower corner of pronotum; epicnemium with vestigial vertical carina near lower corner of pronotum; metapleuron convex, smooth and polished, with few sparse, fine bristles evenly spaced, without discernible submetapleural carina. Propodeum mediodorsally smooth and polished, with longitudinal carinae present only posteriorly and with scattered fine bristles. Fore wing length about [7.0] 5.0–7.0 mm; 1*cu-a* interstitial relative to *M&RS*; base of 1*m-cu&M* separated from *CU* by about length of 2*cu-a*; hind wing with distal abscissa of *CU* present and complete; first abscissa of *RS* subequal to *rs-m*. Tarsal claw with proximal lobe quadrangular, with claw apex slightly overtaking the distal margin of lobe. ***Metasoma.*** Tergite I about [1.5] times as long as posteriorly broad, dorsally with lateromedian longitudinal carinae only discernible at extreme anterior part; sternite I with weak swelling near hind rim, and with weak median longitudinal ridge anteriorly; tergite II about [1.2] 1.0–1.2 times as long as posteriorly broad, highly polished, at most with only fine setiferous punctures laterally; tergite III about [0.9] 0.9–1.1 times as long as posteriorly broad, highly polished, at most with only fine setiferous punctures; subgenital plate subquadrate. Ovipositor slender, about [1.3] 1.2–1.3 times as long as hind tibia, distally evenly tapered to sharp point.

Color. Head black except 0.8 distal of clypeus yellowish; antennae brownish with scape and pedicel ventrally whitish; mouthparts whitish, except apex of mandible brownish. Mesosoma orange with weak spot posteriorly of metapleuron and posterior carinae of propodeum brown. Metasoma blackish with anterior margin centrally orange in tergite I, tergites II–VI with anterior and anterolateral margins whitish. Fore leg orange, mid leg orange with coxa, trochanter and trochantellus whitish and tarsus brownish, hind leg whitish with coxa inner region, trochanter proximal, trochantellus distal, femur proximally and distally, tibia proximally and distally, first tarsal segment distally, and remaining tarsal segments entirely blackish brown. Wings hyaline, pterostigma brown. Ovipositor darkish brown, with posterior and anterior part whitish.

Male. (Fig. 6G). Similar to female in structure and coloration, but body about 5.0 mm; malar space 0.3 times as long as proximal mandibular width; lower face about 1.15 times as broad as high; lateral ocelli separated from compound eyes by about 0.75 times their own maximum diameter; fore wing length about 4.0 mm.

Type materials. *Holotype* ♀. Brazil, RJ [= Rio de Janeiro], Teresópolis, PARNASO [= Parque Nacional Serra dos Órgãos], Pto. 6A, 868 m, 22°28'11.8"S, 43°00'05.3"W, I.2015, [Malaise trap] (R.F. Monteiro et al. leg.), DCBU. ***Paratypes*:** idem holotype, but 1♀ and 1♂, MZUSP; idem, but 1♀ and 1♂, DCBU; idem, but 2♂♂, INPA; idem, but 1♂, INPA; idem but Pto. 8B, 1068 m, 22°27'09.0"S, 42°59'30.8"W, I.2015, 1♀, MZUSP; idem, but Pto. 9B, 1246 m, 22°26'55.1"S, 43°00'16.4"W, III.2015, 1♀, DCBU; idem, but Pto. 6B, 877 m, 22°28'11.5"S, 43°00'06.0"W, X.2015, 2♀♀, INPA; idem, but 1♀, MZUSP; idem, but Guapimirim, Pto. 4B, 540 m, 22°28'36.4"S, 42°59'30.7"W, XII.2014, 1♂, DCBU; idem, but Pto. 4A, 549 m, 22°28'36.5"S, 42°59'30.8"W, I.2015, 1♀, DCBU; idem, but 1♀, MZUSP.

Distribution. Brazil (Fig. 11).

Biological note. Host unknown.

Etymology. The specific name refers to the type locality of this species Serra dos Órgãos, Rio de Janeiro state, Brazil.

Remarks. *Polysphincta organensis* sp. nov. closely resembles *P. bonita* sp. nov. mainly by coloration: mesosoma entirely orange and propodeum brownish with some whitish in anterior part on tergites. It differs from *P. bonita* sp. nov. by having ovipositor >1.2 times as long as hind tibia and fore leg orange, mid leg orange with coxa, trochanter and trochantellus whitish and tarsus brownish, hind leg whitish with inner region of coxa, trochanter proximally, trochantellus distally, femur proximally and distally, tibia proximally and distally, first tarsal segment distally, and remaining tarsal segments entirely blackish brown (ovipositor 1.0 times as long as hind tibia and fore and mid leg orange, hind leg brownish, except coxa orange and a medium inner and outer region whitish in *P. bonita* sp. nov.).

Polysphincta pichincha Pádua, Sääksjärvi & Spasojevic, sp. nov.

http://zoobank.org/30D68683-592D-44E2-90EA-7E801DDAE203
Fig. 7A–E

Diagnosis. *Polysphincta pichincha* sp. nov. can be distinguished from other species of the *P. dizardi* species-group by the combination of the following characters: (1) epomia absent (Fig. 7B); (2) malar space 0.4 times as long as proximal mandibular width (Fig. 7B); (3) fore wing vein 1*cu-a* more or less interstitial relative to *M&RS* (Fig. 7A); (4) mesosoma entirely orange (Fig. 7A); (5) wings yellowish hyaline (Fig. 7A); (6) hind leg orange with trochanter, apex distal and proximal of femur, tibia, except longitudinal spot pale in subdistal region of inner and outer margin and tarsus brownish (Fig. 7A); (7) metasoma orange, with posterior margins of tergites II–IV narrowly black, tergites V+ black (Fig. 7A, C); (8) ovipositor slender, 1.2 times as long as hind tibia.

Description. Female. Body [13.5] mm. *Head.* Clypeus weakly convex, posterior margin thin and flat centrally; malar space [0.4] times as long as proximal mandibular width; lower face about [1.0] times as broad as high, weakly convex centrally, polished, with fine sparse setiferous punctures; head in dorsal view with margin of gena flat behind eyes, and its margin about [0.5] times length of eye; ocelli moderately large, lateral ones separated from compound eyes by [0.85] times their own maximum diameter. *Mesosoma.* Pronotum without epomia; shelf-like projection, in dorsal view, more or less bilobed, broader than long, and, in lateral view, slender and with anterolateral corners weakly decurved; mesoscutum slender, in dorsal view, smooth and polished, with notauli weakly impressed anteriorly; scutellum convex, not laterally carinate; mesopleuron highly polished, virtually impunctate; epicnemial carina reaching almost level of lower corner of pronotum; epicnemium with vestigial vertical carina near lower corner of pronotum; metapleuron convex, smooth and polished, with few sparse, fine bristles evenly spaced, without discernible submeta-
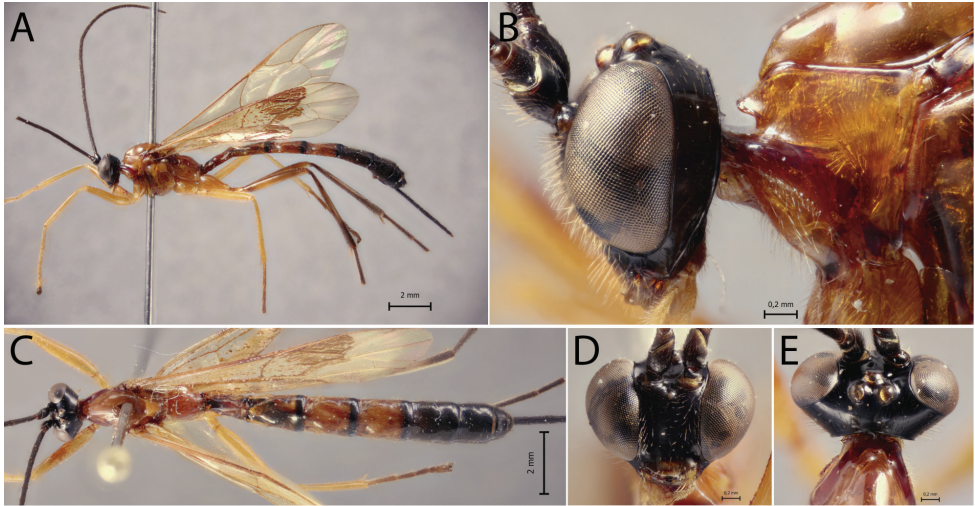
Figure 7. *Polysphincta pichincha* sp. nov., ♀, holotype **A** habitus, lateral view **B** head and pronotum, lateral view **C** habitus, dorsal view **D** face, anterior view **E** head and shelf-like projection, dorsal view.

pleural carina. Propodeum mediodorsally smooth and polished, with longitudinal carinae present only posteriorly and laterally with scattered fine bristles. Fore wing length [10.0] mm; 1*cu-a* more or less interstitial relative to *M&RS*; base of 1*m-cu&M* separated from *CU* by more than length of 2*cu-a*; hind wing with distal abscissa of *CU* present and complete; first abscissa of *RS* subequal to *rs-m*. Tarsal claw with proximal lobe quadrangular, with claw apex slightly overtaking the distal margin of lobe. ***Metasoma.*** Tergite I about [1.8] times as long as posteriorly broad, dorsally with lateromedian longitudinal carinae only discernible at extreme anterior part; sternite I with weak swelling near hind rim, and with weak median longitudinal ridge anteriorly; tergite II about [1.6] times as long as posteriorly broad, highly polished, at most with only fine setiferous punctures laterally; tergite III [1.4] times as long as posteriorly broad, highly polished, at most with only fine setiferous punctures laterally; subgenital plate subquadrate. Ovipositor slightly slender, about [1.2] times as long as hind tibia [without apex].

Color. Head black, except posterior margin of clypeus whitish; antennae brown; mouthparts pale, except apex of mandible brownish. Mesosoma orange. Metasoma orange, with posterior margins of tergites II–IV narrowly black, tergites V+ black. Legs orange, the mid leg with tarsus brownish, hind leg with trochanter, apex distal and proximal of femur, tibia, except longitudinal spot pale in subdistal region of inner and outer margin and tarsus brownish. Wings yellowish hyaline, pterostigma yellow.

Male. Unknown.

Type material. *Holotype* ♀. Ecuador, Pichincha, Nambillo Valley near Mindo, 1450 m, 26.VI.1987 (M. Cooper leg.), #2005-152, BMNH.

Distribution. Ecuador (Fig. 11).

Biological note. Host unknown.

Etymology. The specific name (in apposition) refers to type locality of this species, Pichincha province, Ecuador.

Remarks. *Polysphincta pichincha* sp. nov. closely resembles *A. sinearanea* Pádua, 2018 and *P. inca* sp. nov. mainly by coloration with body orange and the last tergites black. It differs from *P. sinearanea* by having epomia absent (present in *P. sinearanea*), and from *P. inca* sp. nov. by having malar space 0.4 times as long as proximal mandibular width (malar space >0.6 times as long as proximal mandibular width in *P. inca* sp. nov.).

Polysphincta shabui **Gauld, 1991**
Fig. 8A–F

Polysphincta shabui Gauld, 1991: 314. Holotype ♀, Costa Rica (MNCR).

Diagnosis. *Polysphincta shabui* can be distinguished from other species of the *P. dizardi* species-group by the combination of the following characteristics: (1) epomia absent (Fig. 8B); (2) malar space 0.6 times as long as proximal mandibular width (Fig. 8B); (3) fore wing vein 1*cu-a* more or less interstitial relative to *M&RS* (Fig. 8A); (4) mesosoma entirely reddish brown (Fig. 8A); (5) wings hyaline (Fig. 8A); (6) hind leg orange with femur, tibia and tarsus darkish brown (or femur reddish orange) (Fig. 8A); (7) metasoma entirely darkish brown or darkish brown with tergites I–III reddish orange with posterior margins narrowly black (Fig. 8A, C); (8) ovipositor slender, 1.2–1.4 times as long as hind tibia.

Comments. Additional characters to the original description (♀) are as follows: body about [10.5–11.0] 10.5–14.0; head in dorsal view with margin of the gena flat behind the eyes, and its margin [0.5] 0.5–0.6 times length of eye; shelf-like projection, in dorsal view, developed anterolaterally in apex, the apex bilobed, and in lateral view, with anterolateral part in apex rounded and weakly decurved; mesoscutum robust, in dorsal view; tarsal claw with proximal lobe quadrangular, with claw apex slightly overtaking the distal margin of lobe.

Distribution. Costa Rica and Brazil (Fig. 12).

Biological notes. Host unknown.

Materials examined. *Paratypes*: Costa Rica, Limón Pv., 16 km, W. Guápiles, 400 m, V.1989 (without collector), 1♀, BMNH; idem, but Heredia Pv., Braulio Carrillo, 9.5 km, E. of El Tunel, 1000 m, X–XI.1989, 1♀, BMNH. **Costa Rica:** Cartago Pv., Cachí, 1200 m, II.1996 (Chaves leg.), 1♀, BMNH; Ptas Pv., San Vito, Las Alturas, 1500 m, V.1992 (K. Gaston leg.), 1♀, BMNH.

Polysphincta sinearanea **Pádua, 2018**
Fig. 9A–E

Polysphincta sinearanea Pádua, 2018 *in* Kloss et al. 2018: 102. Holotype ♀, Brazil (INPA).
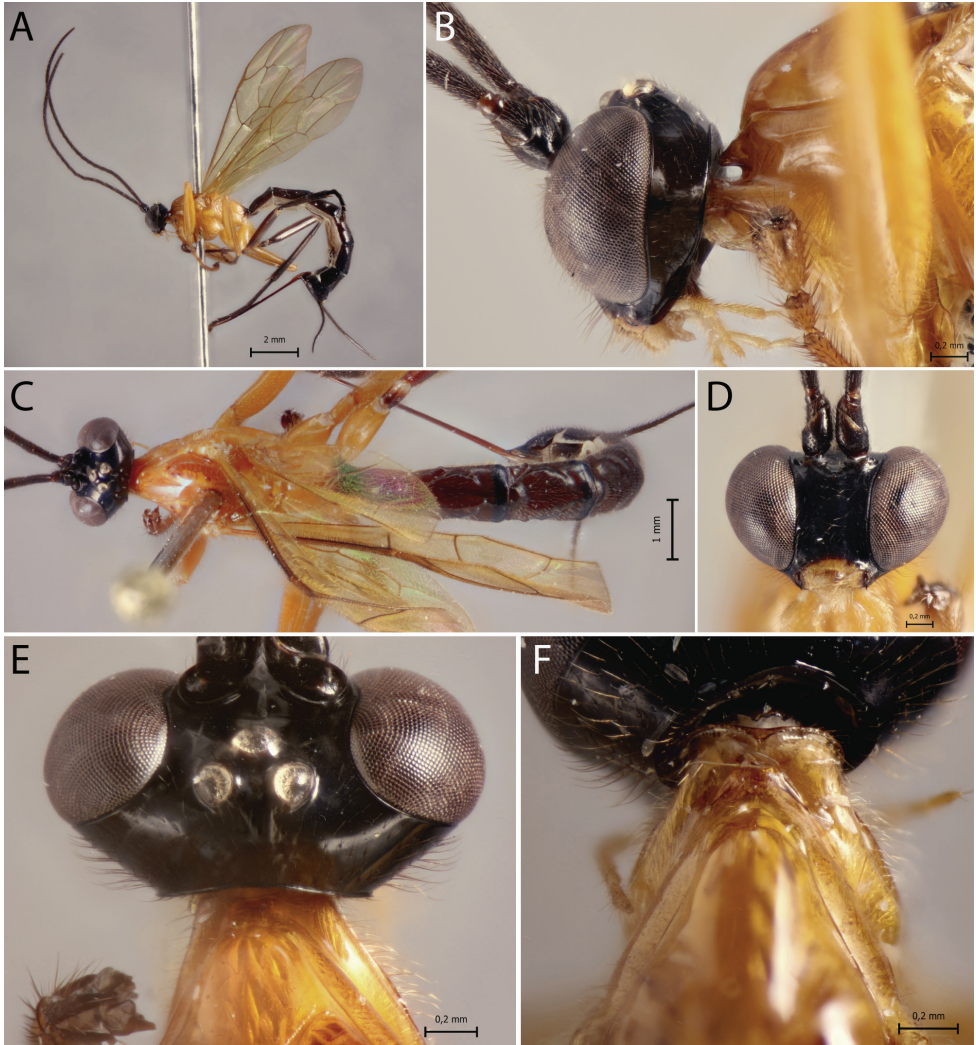
Figure 8. *Polysphincta shabui* Gauld, 1991, ♀, paratype **A** habitus, lateral view **B** head and pronotum, lateral view **C** habitus, dorsal view **D** face, anterior view **E** head, dorsal view **F** shelf-like projection, dorsal view.

Diagnosis. *Polysphincta sinearanea* can be distinguished from other species of the *P. dizardi* species-group by the combination of the following characters: (1) epomia present, about 0.9 times length of proximal mandibular width (Fig. 9B); (2) malar space 0.5–0.6 times as long as proximal mandibular width (Fig. 9B); (3) fore wing vein 1*cu-a* more or less interstitial relative to *M&RS* (Fig. 9A); (4) mesosoma entirely orange (Fig. 9A); (5) fore wing very slightly yellowish hyaline (Fig. 9A); (6) hind leg orange with femur, tibia and tarsus brownish (Fig. 9A); (7) metasoma orange, with posterior margins of tergites II–IV narrowly black, posterior half of tergite V black, and tergites VI+ black (Fig. 9A, C); (8) ovipositor robust, 1.5 times as long as hind tibia.
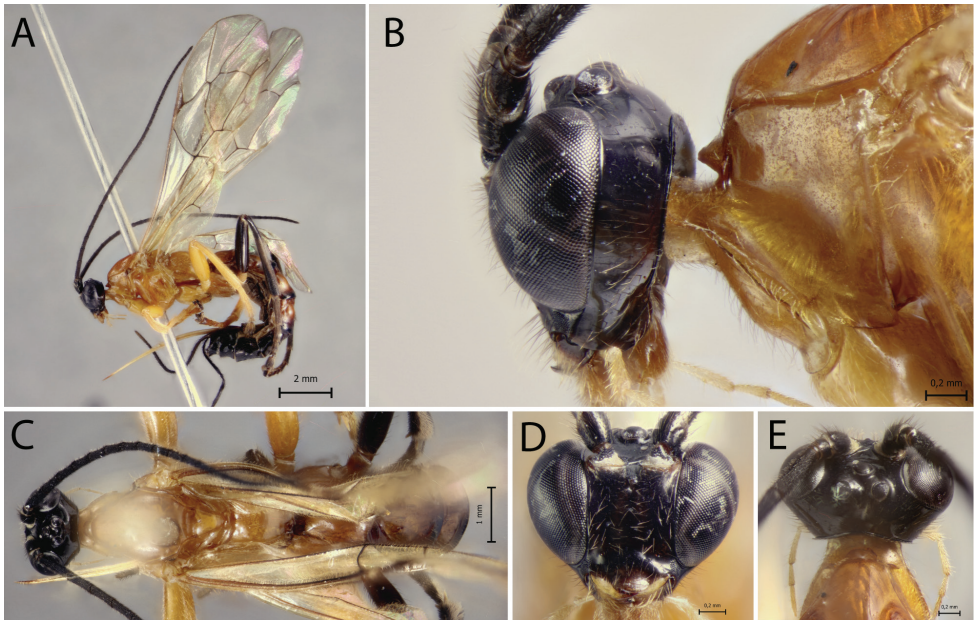
Figure 9. *Polysphincta sinearanea* Pádua, 2018, ♀, paratype **A** habitus, lateral view **B** head and pronotum, lateral view **C** habitus, dorsal view **D** face, anterior view **E** head and shelf-like projection, dorsal view.

Comments. Additional characters to the original description (♀) are as follows: head in dorsal view with margin of the gena flat behind the eyes, and its margin [0.7] times length of eye; shelf-like projection, in dorsal view, weakly developed in the anterolateral part of apex, the apex more or less straight, not bilobed, and in lateral view, with anterolateral part in apex more or less rounded and not decurved; mesoscutum robust, in dorsal view; tarsal claw with proximal lobe quadrangular, with claw apex slightly overtaking the distal margin of lobe; ovipositor robust.

Distribution. Brazil (Fig. 12).

Biological notes. Parasitoid of the spider species *Metazygia laticeps* (O. Pickard-Cambridge, 1889) (Kloss et al. 2018).

Materials examined. *Holotype*: Brazil, Espírito Santo, Cariacica, Res. [= Reserva] Biológica de Duas Bocas, 26.I.2017, parasitizing *M. laticeps* (T.G. Kloss leg.), INPA. *Paratypes*: same data of holotype, 1♀ and 2♂♂ (one with the last metasomal segments extracted), INPA; Minas Gerais, Viçosa, Mata do Prof. Chaves (Silvestre), V.2017, parasitizing *M. laticeps* (T.G. Kloss leg.), 1♀ and 1♂, INPA.

Polysphincta teresa **Pádua & Sääksjärvi, sp. nov.**
http://zoobank.org/E22AD4A9-CB81-467A-83F5-A0BB902659B6
Fig. 10A–F

Diagnose. *Polysphincta teresa* sp. nov. can be distinguished from other species of the *P. dizardi* species-group by the combination of the following characters: (1) epomia
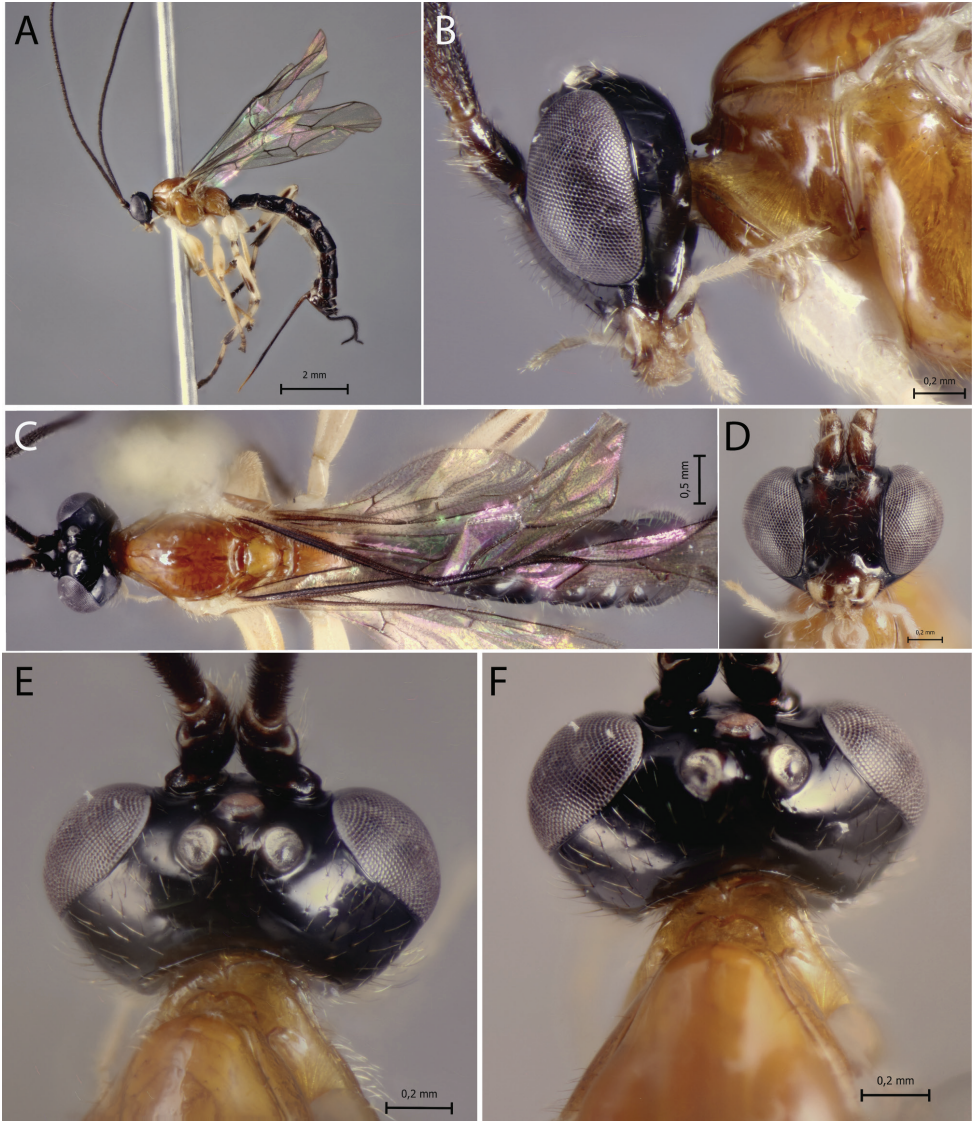
Figure 10. *Polysphincta teresa* sp. nov., ♀, holotype **A** habitus, lateral view **B** head and pronotum, lateral view **C** habitus, dorsal view **D** face, anterior view **E** head, dorsal view **F** shelf-like projection, dorsal view.

present, about 0.9–1.0 times length of proximal mandibular width (Fig. 10B); (2) malar space 0.4–0.6 times as long as proximal mandibular width (Fig. 10B); (3) fore wing with vein 1*cu-a* postfurcal relative to *M&RS* (0.25–0.35 times its own length) or 1*cu-a* more or less interstitial relative to *M&RS* (Fig. 10A); (4) mesosoma orange, except posterior carinae of propodeum darkish brown (Fig. 10A); (5) fore wing hyaline (Fig. 10A); (6) hind leg whitish with proximal region of trochanter, longitudinal spot in subdistal region of inner and outer margin of femur, distal part of tibia and first tarsal segment distally and remaining tarsal segments brownish (Fig. 10A); (7) metasoma

Figure 11. Distribution of *Polysphincta dizardi* group in the Neotropical Region.

darkish brown, with posterior margins of tergites II–V narrowly black (Fig. 10A, C); (8) ovipositor slightly slender, [1.7] 1.4–1.7 times as long as hind tibia.

Description. Female. Body [7.75] 7.0–9.0 mm. *Head.* Clypeus weakly convex, posterior margin thin and straight centrally; malar space [0.4] 0.4–0.6 times as long as proximal mandibular width; lower face about [1.1] 0.9–1.1 times as broad as high, weakly convex centrally, polished, with fine sparse setiferous punctures; head in dorsal view with margin of gena very weakly convex behind eyes, and its margin [0.55] 0.4–0.6 times length of eye; ocelli moderately large, lateral ones separated from compound eyes by [0.9] 0.75–1.0 times their own maximum diameter. *Mesosoma.* Pronotum with epomia distinct, about [0.9] 0.9–1.3 times length of proximal mandibular width; shelf-like projection, in dorsal view, developed in anterolateral part of apex, apex bilobed, and in lateral view, with anterolateral part in apex rounded and weakly decurved; mesoscutum robust, in dorsal view, smooth and polished, with notauli weakly impressed anteriorly; scutellum convex, not laterally carinate; mesopleuron highly polished, virtually impunctate; epicnemial carina reaching almost level of lower corner of pronotum; epicnemium with vestigial vertical carina near lower corner of pronotum; metapleuron convex, smooth and polished, with sparse, fine bristles evenly
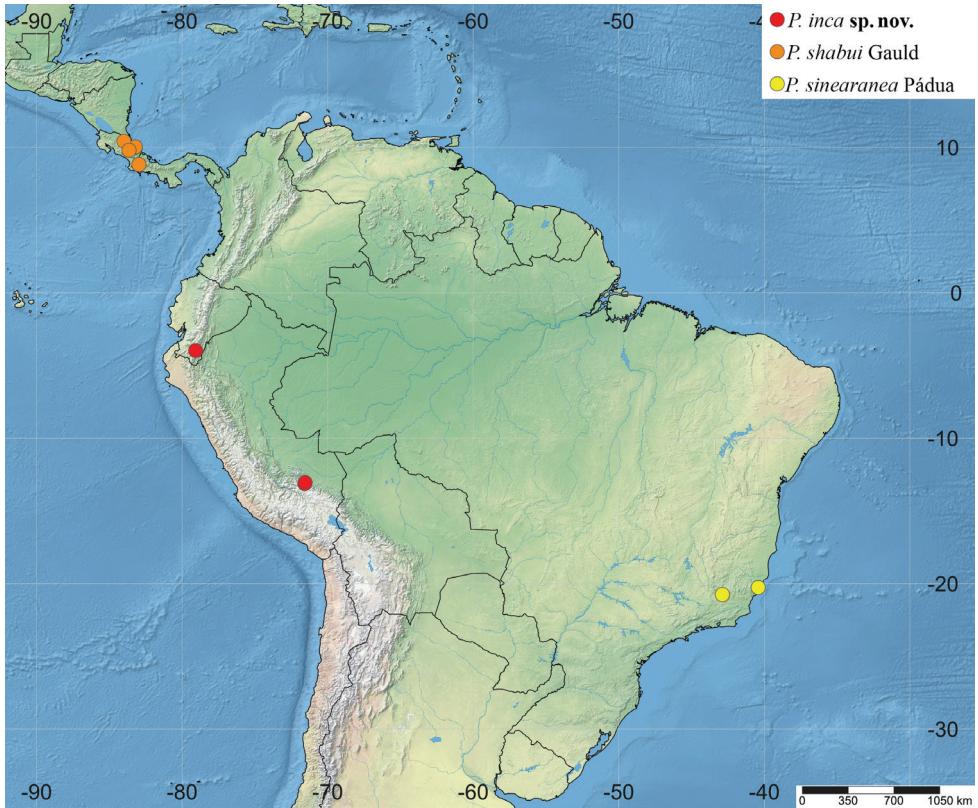
Figure 12. Distribution of *Polysphincta dizardi* group in the Neotropical Region.

spaced, without discernible submetapleural carina. Propodeum mediodorsally smooth and polished, with longitudinal carinae present only posteriorly and laterally with scattered fine bristles. Fore wing length [6.0] 5.0–7.0 mm; $1cu$-a postfurcal relative to *M&RS* by [0.35] 0.25–0.35 times its own length; base of $1m$-$cu&M$ separated from *CU* by more than length of $2cu$-a; hind wing with distal abscissa of *CU* present and complete but weakly pigmented; first abscissa of *RS* subequal to *rs-m*. Tarsal claw with proximal lobe quadrangular, with claw apex slightly overtaking distal margin of lobe. ***Metasoma.*** Tergite I [1.1] 1.1–1.7 times as long as posteriorly broad, dorsally with lateromedian longitudinal carinae only discernible at extreme anterior part; sternite I with weak swelling near hind rim, and with weak median longitudinal ridge anteriorly; tergite II about [1.3] 1.1–1.3 times as long as posteriorly broad, highly polished, at most with only fine setiferous punctures laterally; tergite III [1.0] 1.0–1.3 times as long as posteriorly broad, highly polished, at most with only fine setiferous punctures laterally; subgenital plate subquadrate. Ovipositor slightly slender, [1.7] 1.4–1.7 times as long as hind tibia, posteriorly evenly tapered to sharp point.

Color. Head black except lower face and clypeus brownish; antennae brown, except apex of scape and pedicel whitish; mouthparts white, except apex of mandible
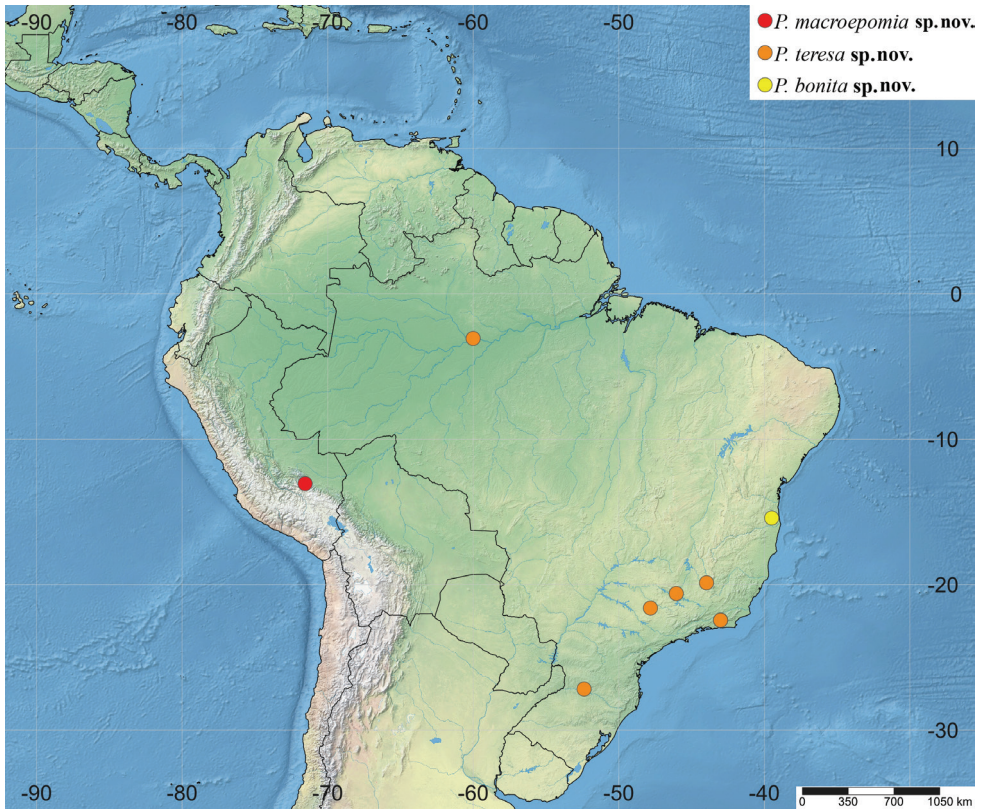
Figure 13. Distribution of *Polysphincta dizardi* group in the Neotropical Region.

black. Mesosoma orange, except posterior carinae of propodeum darkish brown. Metasoma entirely darkish brown, with posterior margins of tergites II–V narrowly black. Legs whitish, fore leg with 0.7 distal of femur, tibia and tarsus weakly rufescent; mid leg with 0.3 distal of femur and tibia weakly rufescent, 0.2 distal of tarsomere I, distal half of tarsomere II, 0.8 distal tarsomere III and tarsomeres IV+ brownish; hind leg with proximal region of trochanter, longitudinal spot in subdistal region of inner and outer margin of femur, distal part of tibia and first tarsal segment distally and remaining tarsal segments brownish. Wings hyaline, pterostigma brown. Ovipositor brown, with anterior and posterior portions slightly whitish.

Male. Unknown.

Variation. Some specimens with clypeus whitish and fore and mid legs with femur and tibia whitish, others have the fore leg entirely orange; the mid leg orange with tarsomeres brownish; the hind leg whitish, with inner margin of coxa, trochanter, trochantellus, proximal region and longitudinal spot in subdistal region of inner and outer margin of femur, proximal and distal part of tibia and all tarsus darkish brown.

Type materials. *Holotype* ♀. Brazil, RJ [= Rio de Janeiro], Teresópolis, PARNASO [= Parque Nacional Serra dos Órgãos], Pto. 9A, 1236 m, 22°26'57.8"S, 43°00'13.7"W, I.2015, [Malaise trap] (R.F. Monteiro et al. leg.), DCBU. *Paratypes*: same data of

holotype, 2♀♀, DCBU; idem, but Pto. 11A, 1681 m, 22°27'07.9"S, 43°00'53.8"W, I.2015, 2♀♀, MZUSP; Pto. 11B, 1649 m, 22°27'03.7"W, 43°00'54.0"W, I.2015, 1♀, DCBU; idem, but Pto. 7A, 952 m, 22°27'24.8"S, 42°59'07.2"W, IX.2015, 1♀, MZUSP; idem, but Pto. 10A, 1444 m, 22°26'51.0"S, 43°00'46.4"W, XI.2015, 1♀, INPA; idem, but Pto. 12A, 1812 m, 22°27'18.2"W, 43°00'58.9"W, 1♀, INPA; idem, but Guapimirim, Pto. 3A, 332 m, 22°29'40.5"S, 42°59'52.6"W, 1♀, DCBU; SP [= São Paulo], Luiz Antônio, Est. Ecológica de Jataí, Mata ciliar, Point 1, 21°36'47.00"S, 47°49'49.04"W, 30.I.2008, Light trap (Lara and team leg.), INPA; Amazonas, Manaus, WWF, Reserve 1208, Rede Central Norte, 12.XII.1984, Malaise trap (Bert Klein leg.) 1♀, INPA; MG [= Minas Gerais], Belo Horizonte, Estação Ecológica, 19°52'30"S, 43°58'20"W, 842 m, 02.VI.1999 (A.F. Kumagai leg.), 1♀, IHY 1500544, UFMG; idem, but Capitólio, Trilha do Sol, Ponto III, 01.VI.2012, Malaise trap (J.F. Nunes and team leg.), 1♀, INPA; [Santa Catarina], Nova Teutônia, 27°11'S, 52°23'W, 30.VIII.1938 (Fritz Plaumann leg.), 1♀ [without hind legs], BMNH.

Distribution. Brazil (Fig. 13).

Biological note. Host unknown.

Etymology. The specific name (in apposition) refers to the "Cidade de Teresa", informal name of the type locality, Teresópolis, Rio de Janeiro state, Brazil.

Remarks. *Polysphincta teresa* sp. nov. closely resembles *P. shabui* Gauld, 1991 mainly by coloration, with mesosoma entirely orange and propodeum blackish with anterior parts whitish. It differs from *P. shabui* by having epomia present (absent in *P. shabui*).

Discussion

Gauld (1991) characterized the *P. dizardi* species-group mainly by the shelf-like projection present mediodorsally on the pronotum. He also observed that the epomia was absent in most of the species (but present in one undescribed Brazilian species).

Pádua in Kloss et al. (2018) recently described a new species from Brazil (*P. sinearanea*) which is characterized by a strong epomia (Fig. 5B). In the present work, we described two additional new species which both have the epomia present (*P. macroepomia* sp. nov. and *P. teresa* sp. nov.). Thus, the *P. dizardi* species-group may no longer be defined by the absence of epomia.

We also studied the shape of the pronotal shelf and noted that it may be used in separating the species from each other. The shelf-like structure of the pronotum in *P. dizardi* species-group is a strong projection in the anterolateral part of the pronotal apex. We have also studied some undescribed species of *Polysphincta* from southeastern Brazil that possess a strong prominence in the same region of the pronotum. However, this structure is not developed into a strong shelf-like projection in those species. Therefore, we have not included those species in the present work, but we will describe them in a separate study in the future.

Gauld and Dubois (2006) proposed that the *P. dizardi* species-group could be a new polysphinctine genus that could be described when the tropical diversity of the group becomes better known. Given the non-declining rates of discovery and descrip-

tion of new polysphinctine species in the Neotropics (Kloss et al. 2018; Pádua et al. 2019, 2020a, b; Sobczak et al. 2019), we refrain at present from splitting the genus *Polysphincta*. We will firstly continue filling in the gap in biodiversity knowledge of *Polysphincta* of South America.

Acknowledgements

References

Broad GR, Shaw MR, Fitton MG (2018) Ichneumonid Wasps (Hymenoptera: Ichneumonoidea): their Classification and Biology. RES Handbooks for the Identification of British Insects, 7(12). Field Studies Council, Shrewsbury, 418 pp.

Gauld ID (1991) The Ichneumonidae of Costa Rica I. Memoirs of the American Entomological Institute 47: 1–589.

Gauld ID, Ugalde-Gómez IA, Hanson P (1998) Guía de los Pimplinae de Costa Rica (Hymenoptera: Ichneumonidae). Revista de Biologia Tropical 46 (supplement 1): 1–189. https://doi.org/10.15517/rbt.v46i1

Gauld ID, Dubois J (2006) Phylogeny of the *Polysphincta* group of genera (Hymenoptera: Ichneumonidae; Pimplinae): a taxonomic revision of spider ectoparasitoids. Systematic Entomology 31: 529–564. https://doi.org/10.1111/j.1365-3113.2006.00334.x

Higa PT, Penteado-Dias AM (2020) Altitudinal effects on diversity of Pimplinae (Hymenoptera, Ichneumonidae) from Southeast Brazil and description of new species. Brazilian Journal of Biology 80(2): 377–385. https://doi.org/10.1590/1519-6984.210438

Kloss TG, Pádua DG, Lacerda FG, Oliveira LS, Cossolin JFS, Serrão JE, Gonzaga MO (2018) Suppression of orb-web building behavior of the spider *Metazygia laticeps* (O. Pickard-Cambridge, 1889) (Araneae: Araneidae) by a new parasitoid wasp. Zoologischer Anzeiger 276: 100–106. https://doi.org/10.1016/j.jcz.2018.06.005

Matsumoto R (2016) Molecular phylogeny and systematics of the Polysphincta group of genera (Hymenoptera, Ichneumonidae, Pimplinae). Systematic Entomology 41(4): 854–864. https://doi.org/10.1111/syen.12196

Pádua DG, Sääksjärvi IE, Monteiro RF, Oliveira ML (2019) New records of *Ticapimpla* Gauld, 1991 (Hymenoptera: Ichneumonidae: Pimplinae) from Brazil and French Guiana, with taxonomic notes. Biodiversity Data Journal 7: e38141. https://doi.org/10.3897/BDJ.7.e38141

Pádua DG, Sääksjärvi IE, Monteiro RF, Oliveira ML (2020a) Review of the New World genus *Acrotaphus* Townes, 1960 (Hymenoptera: Ichneumonidae: Pimplinae), with descriptions of fifteen new species. Zootaxa 4719(1): 001–062. https://doi.org/10.11646/zootaxa.4719.1.1

Pádua DG, Sääksjärvi IE, Monteiro RF, Oliveira ML (2020b) Seven new species of spider-attacking *Hymenoepimecis* Viereck (Hymenoptera, Ichneumonidae, Pimplinae) from Ecuador, French Guiana, and Peru, with an identification key to the world species. ZooKeys 935: 57–92. https://doi.org/10.3897/zookeys.935.50492

Shorthouse DP (2010) SimpleMappr, an online tool to produce publication-quality point maps. http://www.simplemappr.net/ [accessed 09 September 2020]

Sobczak JF, Pádua DG, Villanueva-Bonilla GA, Sousa FA, Messas YF (2019) Two new species of *Zatypota* (Hymenoptera: Ichneumonidae, Pimplinae) sharing the same host spider in Northeast Brazil. Zootaxa 4609(1): 169–177. https://doi.org/10.11646/zootaxa.4609.1.9

Yu DS, van Achterberg C, Horstmann K (2016) World Ichneumonoidea 2015: Taxonomy, Biology, Morphology and Distribution. Taxapad 2016. [Database on flash-drive]

RESEARCH ARTICLE

The mitochondrial genome and phylogenetic characteristics of the Thick-billed Green-Pigeon, *Treron curvirostra*: the first sequence for the genus

Nan Xu[1*], Jiayu Ding[1*], Ziting Que[1], Wei Xu[1], Wentao Ye[1], Hongyi Liu[1]

1 *College of Biology and the Environment, Nanjing Forestry University, Nanjing 210037, China*

Corresponding author: Hongyi Liu (hongyi_liu@njfu.edu.cn)

Citation: Xu N, Ding J, Que Z, Xu W, Ye W, Liu H (2021) The mitochondrial genome and phylogenetic characteristics of the Thick-billed Green-Pigeon, *Treron curvirostra*: the first sequence for the genus. ZooKeys 1041: 167–182. https://doi.org/10.3897/zookeys.1041.60150

Abstract

Members of the genus *Treron* (Columbidae) are widely distributed in southern Asia and the Indo-Malayan Region but their relationships are poorly understood. Better knowledge of the systematic status of this genus may help studies of historical biogeography and taxonomy. The complete mitochondrial genome of *T. curvirostra* was characterized, a first for the genus. It is 17,414 base pairs in length, containing two rRNAs, 22 tRNAs, 13 protein coding genes (PCGs), and one D-loop with a primary structure that is similar to that found in most members of Columbidae. Most PCGs start with the common ATG codon but are terminated by different codons. The highest value of the Ka/Ks ratio within 13 PCGs was found in ATP8 with 0.1937, suggesting that PCGs of the mitochondrial genome tend to be conservative in Columbidae. Moreover, the phylogenetic relationships within Columbidae, which was based on sequences of 13 PCGs, showed that (*T. curvirostra* + *Hemiphaga novaeseelandiae*) were clustered in one clade, suggesting a potentially close relationship between *Treron* and *Hemiphaga*. However, the monophyly of the subfamilies of Columbidae recognized by the Interagency Taxonomic Information System could not be corroborated. Hence, the position of the genus *Treron* in the classification of Columbidae may have to be revised.

Keywords

---

* Authors contributed equally to this work.

Introduction

Mitochondrial DNA sequences can be reliable markers for studying the origin and phylogenetic relationships of species owing to its fast evolution rate, simple structure, light molecular weight, and maternal inheritance (Nabholz et al. 2016; Martins et al. 2019). Mitochondrial genomes of birds have a closed loop structure with lengths of 15,500–23,000 base pairs (bp) (Sammler et al. 2011; Xu et al. 2019; Wang et al. 2020). They typically contain 13 protein coding genes (PCGs), 22 transfer RNA genes (tRNAs), two ribosomal RNA genes (rRNAs), and one D-loop (Bensch and Härlid 2000; Sun et al. 2020), while some species were found to have duplicate regions (Eberhard and Wright 2016).

The pigeons and doves (family Columbidae) are widely distributed on all continents except Antarctica, ranging from tropical to temperate regions (Gibbs et al. 2001). The number of subfamilies of Columbidae differs among taxonomic authorities. Dickinson and Remsen (2013) recognize three subfamilies (Columbinae, Peristerinae, and Raphinae), whereas the Interagency Taxonomic Information System (ITIS) recognizes five subfamilies (Columbinae, Didunculinae, Gourinae, Otidiphabinae, and Treroninae), as well as 49 genera and more than 300 extant species (Integrated Taxonomic Information System 2020).

All species of green-pigeons (*Treron*) are listed as second-class national protected animals under China's Catalog of Wildlife of the Key State Protection. Most species in the genus are declining (Birdlife International 2018); however, only a few genetic resources are available for the genus *Treron* (e.g., Sorenson et al. 2003; Pereira et al. 2007; Hackett et al. 2008; Price et al. 2014; Claramunt and Cracraft 2015).

The Thick-billed Green-Pigeon *Treron curvirostra* (Gmelin, 1789) is mainly distributed in virgin, evergreen, broad-leaved, and secondary forests of the tropical and subtropical hilly zone in Southeast Asia and South Asia (Gibbs et al. 2001). Like most species of Columbidae, *T. curvirostra* feeds on seeds and fruits (Korzun et al. 2008). Members of this species have a medium-sized body and a colorful plumage (Korzun et al. 2008) distinguished by their grey head and green neck. The lower body is yellowish green, while the wing is nearly black, with a yellow feather margin and a distinct yellow wing spot. The central tail feathers are green, while the remaining feathers are gray with black secondary end spots (Korzun et al. 2008; Nair 2010). At present, only few studies have focused on *T. curvirostra*: Nair (2010) discussed the zoogeography.

To understand the systematic position of the genus *Treron* among Columbidae, we sequenced and characterized the first complete mitochondrial genome sequence of *T. curvirostra*. We compared the complete mitochondrial genome of *T. curvirostra* with that of 33 other pigeons and doves and determined its genetic structural characteristics. In addition, we used 13 protein-coding genes (PCGs) to reconstruct a phylogenetic tree, which we use to infer the taxonomic position of the species and illuminate the phylogenetic relationships among species of Columbidae.

Materials and methods

Sample collection and DNA extraction

This study was authorized by Nanjing Forestry University. The youngest tail feathers of a male Thick-billed Green-Pigeon *T. curvirostra* were collected from an individual rescued from a net that was used to prevent birds from stealing fruit at the Xieyang peak of Dali City, Yunnan Province, China. The bird was identified as *T. curvirostra* based on its morphological characters (Gibbs et al. 2001). After sample collection, the bird was released. The tail feather samples were transported to the Laboratory of Animal Molecular Evolution at the Nanjing Forestry University and stored at -80 °C. The tubules were cut and the pulp was removed for genomic DNA extraction using the FastPure Cell/Tissue Isolation Mini kit (Vazyme Biotechnology Co., Ltd., Nanjing, China) and stored at -20 °C for later use.

PCR amplification and sequencing

Primers were designed based on the mitochondrial gene sequences of *Streptopelia decaocto*, *Hemiphaga novaeseelandiae*, and *Columba hodgsonii* (GenBank accession numbers KY827036, EU725864, and MN919176,respectively) using DNASTAR software (DNASTAR, USA; Burland 2000). Primer sequences are listed in Table 1. The PCR reaction volume was 25 μL, which included 1 μL of template DNA, 12.5 μL of the 2×Rapid Taq Master Mix (Vazyme Biotech Co., Ltd, Nanjing, China), 1 μL per primer, and 9.5 μL double-distilled (dd)H_2O. The PCR reaction procedure consisted of a pre-denaturation at 95 °C for 3 min, a denaturation at 95 °C for 15 s, an annealing at 50 °C to 60 °C for 15 s, which was adjusted according to the primers' own conditions, an extension at 72 °C for 2 min, cycling 35 times, and a final extension at 72 °C for

Table 1. Primers used for amplification of the *T. curvirostra* mitogenome.

Fragment	Region	Primer pair	Primer sequence (5' - 3')
DG 1	COI-COII	DG 1F	CACTCAGCCATCTTACCT
		DG 1R	ACAGATTTCTGAGCATTGGC
DG 2	COII-ND4	DG 2F	CCAATCCGCATCATCGTC
		DG 2R	GGTTTCCTCATCGTGTGA
DG 3	ND4-ND5	DG 3F	CAGCCTCCTAATTGCCAC
		DG 3R	GTAGGGCGGAGACTGGAG
DG 4	ND5-Cyt b	DG 4F	ACAGGGCCGAGCAGAAGC
		DG 4R	TAGGAAGTATCACTCTGG
DG 5	Cyt b-12S rRNA	DG 5F	GCAGGCCTCACCATTATCC
		DG 5R	GTTAATTACTGCTGAGTACC
DG 6	12S rRNA-16S rRNA	DG 6F	GCTGGCATCAGGCACGCC
		DG 6R	TGGGTCTGGTTACTGTTA
DG 7	16S rRNA-ND2	DG 7F	CGGTTGGGGCGACCTTGGAG
		DG 7R	AGAGTGGGAGGAGTAGGGC
DG 8	ND2-COI	DG 8F	AGCAGCCACAATCATGGC
		DG 8R	ATAGATTTGGTCATCTCC

5 min. The PCR products were detected by a 1% agarose gel electrophoresis, and then sent to Tsingke Biotech Co., Ltd. (Nanjing, China), where the original primers were used for the bidirectional sequencing.

Sequence analysis

By comparing and identifying the DNA sequence of each mitochondrial gene in other pigeon families, the range and location of *T. curvirostra*'s mitochondrial genes were annotated. Hence, the complete mitochondrial genome sequence was used to predict the transcriptional direction of each gene component using the Improved de novo Metazoan Mitochondrial Genome Annotation (MITOS) platform (Bernt et al. 2013). The annotated mitochondrial genome sequence of *T. curvirostra* was submitted to GenBank (accession number MT535857). The mitochondrial ring structure was plotted, and 22 tRNA clover two-dimensional structures were predicted using programs, such as the comparative genomics (CG) View Server and the tRNAscan-Se (Stothard and Wishart 2005; Lowe and Chan 2016). Composition skew was calculated according to the following formulae: AT-skew = $(A-T)/(A+T)$ and GC-skew = $(G-C)/(G+C)$ (Perna and Kocher 1995). Moreover, the relative synonymous codon usage (RSCU) frequency and the ratio of the number of nonsynonymous substitutions per nonsynonymous site to the number of synonymous substitutions per synonymous site (Ka/Ks) of 13 PCGs of Columbidae were calculated using MEGA7 (Kumar et al. 2016), while the RSCU comparison graph was drawn by PhyloSuite (Zhang et al. 2020).

Phylogenetic analysis

We used a concatenated set of base sequences of the 13 PCGs from 34 pigeons and doves to investigate the phylogenetic position of *T. curvirostra* (Table 2). Yellow-throated Sandgrouse (*Pterocles gutturalis* Smith, 1836) was used as an outgroup. All operations were performed in the PhyloSuite software package (Zhang et al. 2020). The sequences were aligned in batches using MAFFT software (Katoh et al. 2002). ModelFinder was used to partition the codons and identify the best substitution model for the phylogenetic analyses (Kalyaanamoorthy et al. 2017). Phylogenetic trees were constructed with Bayesian inference (BI) and maximum-likelihood (ML) (Yang 1994; Huelsenbeck and Ronquist 2001). The best substitution model of BI was selected according to codon 1, 2 and 3, while the model of ML was determined by the automatic partitioning (Table 3). For the BI tree, Markov chains were run for one million generations and were sampled every 100 generations. The majority-rule consensus trees were estimated by combining the results from duplicated analyses, while discarding the first 25% of generations. Besides, we checked for nuclear copies of mitochondrial sequences (numts) and possible chimerism (Sangster et al. 2016; Sangster and Luksenburg 2020).

Table 2. Summary of the mitogenomes used in the analyses.

Family	Subfamily	Genus	Species	Accession
Columbidae	Columbinae	*Geopelia*	*Geopelia cuneata*	MN930521.1
			Geopelia striata	MG590276.1
		Trugon	*Trugon terrestris*	MG590263.1
		Caloenas	*Caloenas maculata*	KX902249.1
			Caloenas nicobarica	MG590264.1
		Streptopelia	*Streptopelia tranquebarica*	MT535858
			Streptopelia orientalis	KY827037.1
			Streptopelia decaocto	KY827036.1
			Streptopelia chinensis	KP273832.1
		Columba	*Columba hodgsonii*	MN919176.1
			Columba janthina	LC541479.1
			Columba jouyi	KX902247.1
			Columba livia	KP319029.1
			Columba rupestris	KX902246.1
		Ectopistes	*Ectopistes migratorius*	KC489473.1
		Patagioenas	*Patagioenas fasciata*	KX902240.1
		Leptotila	*Leptotila verreauxi*	HM640214.1
		Zenaida	*Zenaida macroura*	KX902235.1
			Zenaida auriculata	HM640211.1
		Geotrygon	*Geotrygon violacea*	HM640213.1
		Turtur	*Turtur tympanistria*	HM746793.1
		Columbina	*Columbina picui*	MN356335.1
		Chalcophaps	*Chalcophaps indica*	HM746789.1
	Treroninae	*Alopecoenas*	*Alopecoenas salamonis*	KX902250.1
		Hemiphaga	*Hemiphaga novaeseelandiae*	EU725864.1
	Gourinae	*Goura*	*Goura cristata*	MG590273.1
			Goura sclaterii	MG590285.1
			Goura scheepmakeri	MG590282.1
			Goura victoria	MG590299.1
		Pezophaps	*Pezophaps solitaria*	KX902238.1
		Raphus	*Raphus cucullatus*	KX902236.1
	Otidiphabinae	*Otidiphaps*	*Otidiphaps nobilis*	MG590265.1
	Didunculinae	*Didunculus*	*Didunculus strigirostris*	MG590266.1
Pteroclidae		*Pterocles*	*Pterocles gutturalis*	MN356147.1

Results and discussion

Mitochondrial genome structure and organization

The mitochondrial genome of the Thick-billed Green-Pigeon was found to be 17,414 bp in length, which agrees with the length of most of the other sequenced species of pigeons and doves (Table 4, Table 5, Table 6) (Pereira et al. 2007; Zhang et al. 2015). In addition, the base composition of *T. curvirostra* was found to be A = 30.32%, G = 13.61%, T = 24.83%, and C = 31.24%), where the A+T content (55.15%) was higher than the G+C content (44.85%) and is similar to other birds in Columbidae (Table 5 and Table 6) (Huang et al. 2016; Jang et al. 2016). Moreover, the genome had a closed circular ring structure, containing 22 tRNAs, 2 rRNAs, 13 PCGs, and one D-loop. The ND6 gene and the other 8 tRNAs (tRNA-Gln, tRNA-Ala, tRNA-

Table 3. The best substitution models for Bayesian inference (BI) and maximum-likelihood (ML) analyses.

		ND1	ND2	COI	COII	ATP6	ATP8	COIII	ND3	ND4L	ND4	ND5	Cyt b	ND6
BI	Codon 1	SYM + I + G4	GTR + F + I + G4	SYM + I + G4	SYM + I + G4	GTR + F + I + G4	GTR + F + G4	SYM + I + G4	SYM + I + G4	GTR + F + I + G4	GTR + F + I + G4	GTR + F + I + G4	SYM + I + G4	GTR + F + G4
	Codon 2	GTR + F + I + G4	GTR + F + I + G4	GTR + F + I + G4	GTR + F + I + G4	GTR + F + I + G4	GTR + F + I + G4	GTR + F + I + G4	GTR + F + I + G4	GTR + F + I + G4	GTR + F + I + G4	GTR + F + I + G4	GTR + F + I + G4	HKY + F + I + G4
	Codon 3	GTR + F + I + G4	GTR + F + I + G4	GTR + F + I + G4	GTR + F + I + G4	GTR + F + I + G4	GTR + F + I + G4	GTR + F + I + G4	GTR + F + I + G4	GTR + F + I + G4	GTR + F + I + G4	GTR + F + I + G4	GTR + F + I + G4	GTR + F + G4
ML		TVM + F + R4	TVM + F + R4	TIM2 + F + I + G4	TIM2 + F + I + G4	TVM + F + R4	TN + F + I + G4	TIM2 + F + I + G4	TIM2 + F + I + G4	TIM2 + F + I + G4	TVM + F + R4	TVM + F + R4	TIM2 + F + I + G4	TIM2 + F + I + G4

Table 4. Mitochondrial genetic composition of *T. curvirostra*.

Gene	Strand	Position	Anticodon	Size (bp)	Start codon		Intergenic length
tRNA-Phe	H	1–68	GAA	68			0
12S rRNA	H	69–1041		973			0
tRNA-Val	H	1042–1114	UAC	73			0
16S rRNA	H	1115–2703		1589			0
tRNA-Leu	H	2704–2777	UAA	74			12
ND1	H	2790–3755		966	ATG	AGA	17
tRNA-Ile	H	3773–3844	GAU	72			5
tRNA-Gln	L	3850–3920	UUG	71			0
tRNA-Met	H	3921–3988	CAU	68			0
ND2	H	3989–5027		1039	ATG	T	0
tRNA-Trp	H	5028–5098	UCA	71			1
tRNA-Ala	L	5100–5168	UGC	69			2
tRNA-Asn	L	5171–5243	GUU	73			2
tRNA-Cys	L	5246–5313	GCA	68			0
tRNA-Tyr	L	5314–5384	GUA	71			1
COI	H	5386–6936		1551	ATG	AGG	0
tRNA-Ser	L	6937–7001	UGA	65			2
tRNA-Asp	H	7004–7072	GUC	69			1
COII	H	7074–7757		684	ATG	TAA	1
tRNA-Lys	H	7759–7828	UUU	70			1
ATP8	H	7830–7997		168	ATG	TAA	0
ATP6	H	7988–8671		684	ATG	TAA	-1
COIII	H	8671–9454		784	ATG	T	0
tRNA-Gly	H	9455–9523	UCC	69			0
ND3	H	9524–9875		352	ATT	TAA	1
tRNA-Arg	H	9877–9945	UCG	69			1
ND4L	H	9947–10243		297	ATG	TAA	-7
ND4	H	10237–11614		1378	ATG	T	0
tRNA-His	H	11615–11683	GUG	69			0
tRNA-Ser	H	11684–11749	GCU	66			0
tRNA-Leu	H	11750–11819	UAG	70			0
ND5	H	11820–13637		1818	ATG	AGA	8
Cyt b	H	13646–14788		1143	ATG	TAA	0
tRNA-Thr	H	14789–14856	UGU	68			6
tRNA-Pro	L	14863–14932	UGG	70			4
ND6	L	14937–15458		522	ATG	TAG	3
tRNA-Glu	L	15462–15532	UUC	71			0
D-loop		15553–17414		1862			0

Table 5. Composition and skewness in mitochondrial genome of *T. curvirostra*.

Region	A%	T%	AT-skew	G%	C%	GC-skew
whole mitogenome	30.32	24.83	0.100	13.61	31.24	-0.393
PCGs	29.46	24.56	0.091	12.23	33.76	-0.468
rRNAs	32.75	21.19	0.214	19.05	27.01	-0.173
tRNAs	32.33	25.16	0.125	16.95	25.55	-0.203
D-loop	30.45	31.31	-0.014	11.92	26.32	-0.376

Table 6. Nucleotide composition indices in different regions of mitogenomes of Columbidae.

Species	GenBank no	Whole mitogenome		Protein coding genes		Ribosomal RNA	
		Length (bp)	AT (%)	Length (bp)	AT (%)	Length (bp)	AT (%)
Goura sclaterii	MG590285.1	18242	54.13	11386	52.99	2571	53.21
Treron curvirostra	MT535857	17414	55.16	11386	54.02	2562	53.94
Columba hodgsonii	MN919176.1	17477	54.55	11385	53.82	2557	53.23
Trugon terrestris	MG590263.1	17405	55.62	11395	54.94	2569	55.86
Didunculus strigirostris	MG590266.1	17389	54.94	11390	54.32	2569	55
Geopelia striata	MG590276.1	17354	54.83	11383	53.78	2565	54.07
Otidiphaps nobilis	MG590265.1	17346	55.83	11382	55.2	2581	54.75
Hemiphaga novaeseelandiae	EU725864.1	17264	54.89	11386	54.1	2575	54.52
Caloenas nicobarica	MG590264.1	17178	55.13	11386	54.83	2567	53.64
Leptotila verreauxi	HM640214.1	17176	54.1	11383	53.34	2556	53.4
Alopecoenas salamonis	KX902250.1	17141	55.18	11381	54.78	2569	54.81
Streptopelia orientalis	KY827037.1	17102	53.41	11386	52.86	2561	53.58
Raphus cucullatus	KX902236.1	17092	56.08	11385	55.87	2566	54.6
Ectopistes migratorius	KC489473.1	17026	54.52	11383	54.3	2596	52.97
Patagioenas fasciata	KX902239.1	16970	54.51	11384	54.02	2550	53.8
Geotrygon violacea	HM640213.1	16864	55.04	11383	54.27	2561	53.85
Zenaida auriculata	HM640211.1	16781	53.29	11380	52.71	2567	52.83

Asn, tRNA-Cys, tRNA-Tyr, tRNA-Ser (UGA), tRNA-Pro, and tRNA-Glu) were transcribed from the light (L)-strand, while the other genes were transcribed from the heavy (H)-strand (Fig. 1, Table 4). In addition, two pairs of overlapping regions among the ATP6/COIII and ND4L/ND4 were found, with an overlapping region of ATP6/COIII being one bp and the overlapping region of ND4L/ND4 being seven bp. Furthermore, 18 intergenic spacers were observed between the mitochondrial regions with lengths between -7 and 17 bp. Among all these intergenic spacers, the shortest was -7 bp (found between ND4L and ND4), while the longest was 17 bp (found between ND1 and tRNA-Ile).

The PCGs

The total length of the PCGs was 11,386 bp, which is consistent with the average length of PCGs found in Columbidae (Table 5). The base composition of PCGs was A = 29.46%, G = 12.23%, T = 24.56%, and C = 33.76%, while the A+T content (54.01%) was slightly higher than the G+C content (45.99%). The AT-skew of *T. curvirostra* was positive, while the GC-skew was negative (Table 5). Furthermore, the PCG regions of *T. curvirostra* contained genes coding for cytochrome b (Cytb), two

Figure 1. Circular map of the *T. curvirostra* mitochondrial genome.

ATPases (ATP6 and ATP8), three cytochrome c oxidases (COI, COII, and COIII), and seven NADH dehydrogenases (ND1-6 and ND4L). With the exception of ND3 (which had ATT as its start codon), all the other PCGs had ATG as a start codon. Six PCGs had the complete stop codon of TAA, while four PCGs had the other complete stop codons of AGA (ND1 and ND5), AGG (COI), and TAG (ND6). ND2, ND4, and COIII had the incomplete stop codon of T (Table 4). The RSCU of *T. curvirostra* is illustrated in Fig. 2, where Leu1 had the highest concentration and Cys had the lowest. In addition, Met only had AUG, while the other seven regions had four codons. With *T. curvirostra* as a baseline, the Ka/Ks ratio (Hurst 2002) of the 13 PCGs in 17 species of doves were all less than 1, with the highest Ka/Ks ratio (0.1937) in ATP8 and the lowest ratio (0.0243) in COI (Fig. 3). Hence, it seems that evolution tended to be conservative and maintained the generated protein (Hanada et al. 2007).

Figure 2. Codon distribution and relative synonymous codon usage in *T. curvirostra* mitogenome.
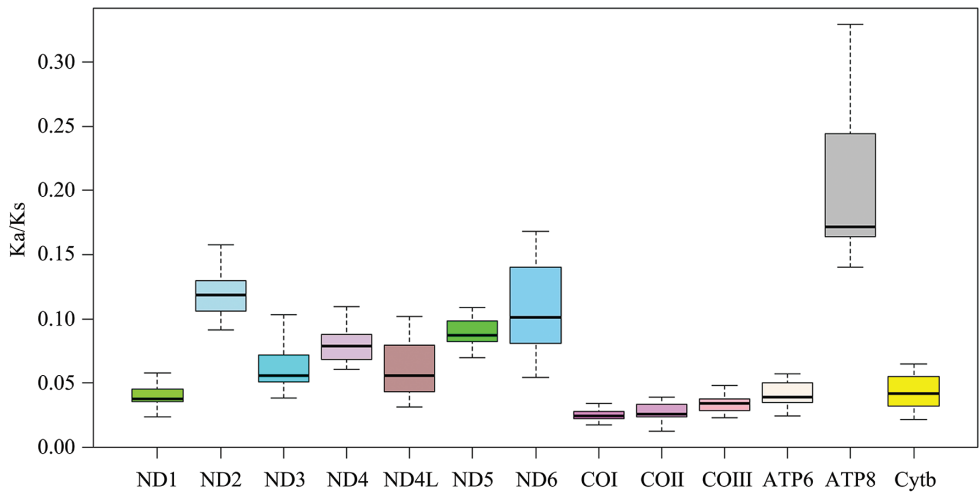
Figure 3. The ratio of the number of nonsynonymous substitutions per nonsynonymous site to the number of synonymous substitutions per synonymous site of 13 PCGs among 17 species of pigeons and doves. *T. curvirostra* was set as a baseline.

Transfer RNAs, ribosomal RNAs, and the D-loop

The mitogenome of *T. curvirostra* contained 22 tRNAs with lengths ranging from 65 bp (tRNA-Ser (UGA)) to 74 bp (tRNA-Leu (UAA)), which is similar to that in the mitogenomes of other pigeons and doves (Zhang et al. 2015). Moreover, the total length of the tRNAs was 1,534 bp, with an A+T content of 57.50%, a G+C content of 42.50%, an AT-skew of 0.1247, and a GC-skew of -0.2025 (Table 5). Among all the secondary structures of the 22 tRNA genes from the *T. curvirostra* mitochondrial genome, with the exception of tRNA-Ser (GCU), all had a typical cloverleaf structure (Fig. 4).

The total size of the two rRNAs was 2,562 bp, with an A+T content of 53.94%, an AT-skew of 0.2142, and a GC-skew of -0.1729 (Table 5). The 12S rRNA was 973 bp in length and was located between tRNA-Phe and tRNA-Val, while the 16S rRNA was 1,589 bp in length and was located between tRNA-Val and tRNA-Leu (UAA).

A D-loop was found between tRNA-Glu and tRNA-Phe, and was 1,862 bp in length, with a A+T content of 61.76%, an AT-skew of -0.0139, and a GC-skew of -0.3764 (Table 5). Duplication and rearrangement of the avian mitochondrial genomes is common, but *T. curvirostra* had only one D-loop, which is similar to that present in other known mitogenomes of Columbidae (Pacheco et al. 2011; Eberhard and Wright 2016; Bruxaux et al. 2018).

Phylogenetic analysis

Although the topology of ML tree and BI tree were similar to each other, they differed with respect to the phylogenetic position of *T. curvirostra*. *Treron curvirostra* clustered with *Hemiphaga novaeseelandiae* (Gmelin, 1789) in the BI tree, whereas it did not cluster with any species in the ML tree (Fig. 5). Therefore, we tested for the presence of the numts and chimerism. All these tests were negative, indicating the validity of *T. curvirostra* mitogenome. The phylogenetic trees also highlighted the stable relationships among the same genera within Columbidae, which was consistent with previous studies from analyses of mitochondrial and nuclear genes (Kan et al. 2010; Pacheco et al. 2011; Hung et al. 2013; Mlíkovský 2016; Soares et al. 2016; Kretschmer et al. 2020; Liu et al. 2020) (Fig. 5). However, the phylogenetic analysis did not support the arrangement of pigeons into five subfamilies (Columbinae, Didunculinae, Gourinae, Otidiphabinae, and Treroninae) as recognized by ITIS. *Caloenas*, *Geopelia*, and *Trugon terrestris* (which were placed in Columbinae by ITIS) clustered with species from other subfamilies in our phylogenies (Fig, 5). The most likely cause might be that the original classification system was based mainly on patterns of overall similarity in morphology which may not accurately reflect phylogenetic relationships. Similar contradictions between overall similarity and phylogeny have also been found in other groups of birds, including terns (Bridge et al. 2005), rails (Sangster et al. 2015), nightjars (Han et al. 2010), eagles (Lerner and Mindell 2005), laughing thrushes (Luo et al. 2008), and chats and flycatchers (Sangster et al. 2010). Our results indicate that
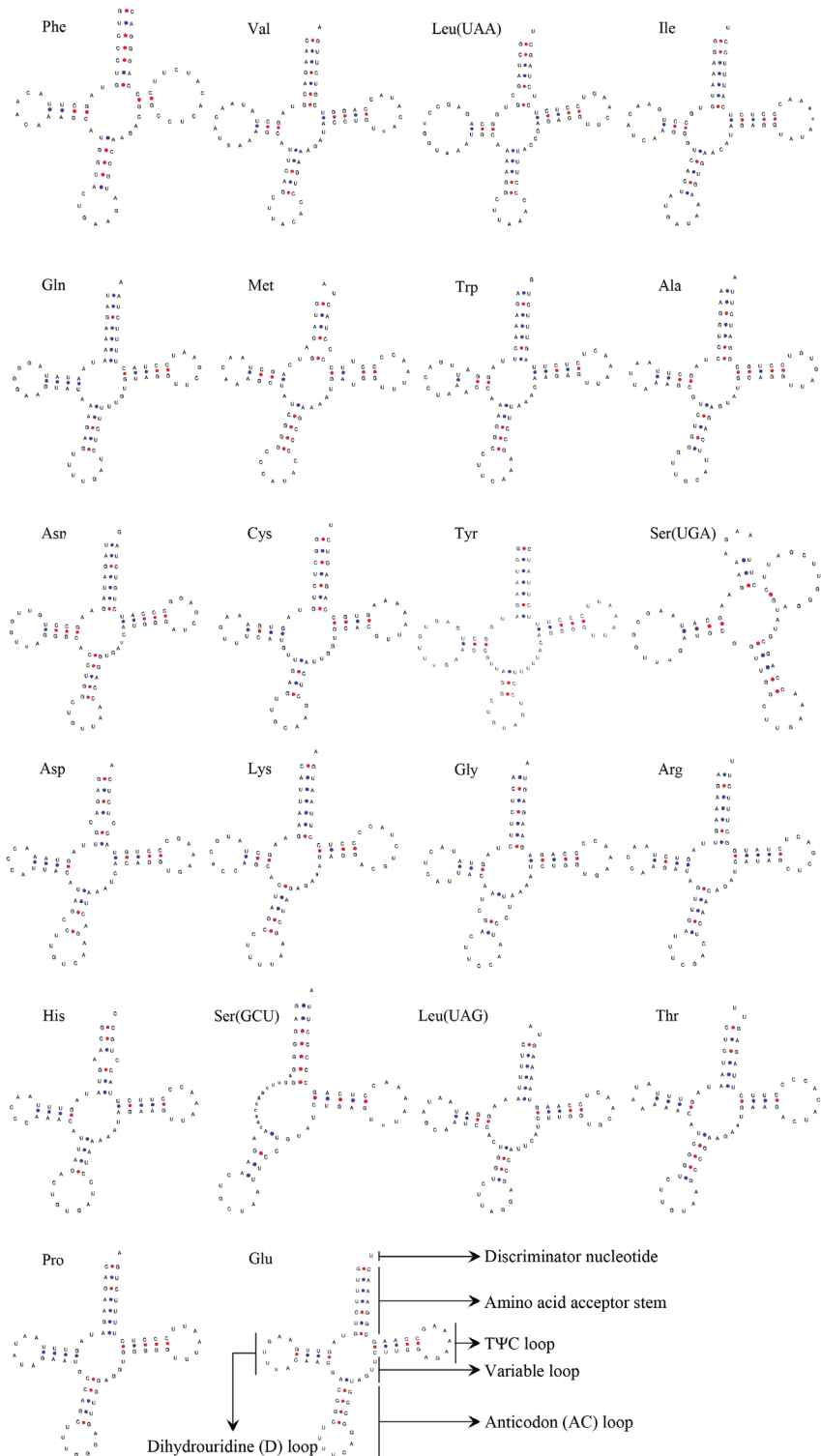
Figure 4. Secondary structure of 22 tRNA genes from the *T. curvirostra* mitochondrial genome.
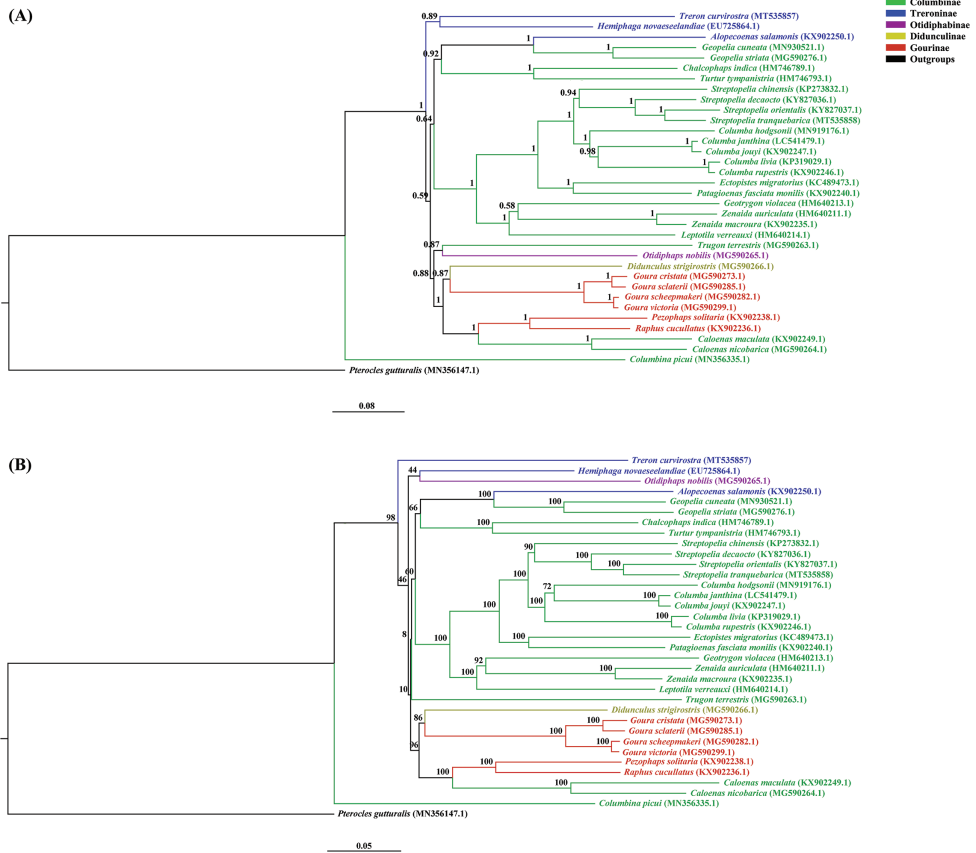
Figure 5. Mitogenomic phylogeny of 34 Columbidae species and an outgroup (*Pterocles gutturalis*) based on 13 PCGs using the Bayesian inference (**A**) and maximum likelihood (**B**) methods. Different colors indicated different subfamilies.

the subfamily classification of Columbidae may not accurately reflect historical relationships and may need to be revised. However, the poor branch support of basal clades of Columbidae precludes such a revision at present. Clearly, future attempts to resolve the phylogeny of Columbidae with confidence should include a suitable set of nuclear markers.

Acknowledgements

References

Bensch S, Härlid A (2000) Mitochondrial genomic rearrangements in songbirds. Molecular Biology and Evolution 17: 107–113. https://doi.org/10.1093/oxfordjournals.molbev.a026223

Bernt M, Donath A, Jühling F, Externbrink F, Florentz C, Fritzsch G, Pütz J, Middendorf M, Stadler PF (2013) MITOS: improved de novo metazoan mitochondrial genome annotation. Molecular Phylogenetics and Evolution 69: 313–319. https://doi.org/10.1016/j.ympev.2012.08.023

BirdLife International (2018) *Treron curvirostra*. The IUCN Red List of Threatened Species 2018: e.T22691160A130177198. https://doi.org/10.2305/IUCN.UK.2018-2.RLTS.T22691160A130177198.en [accessed 18 January 2021]

Bridge ES, Jones AW, Baker AJ (2005) A phylogenetic framework for the terns (Sternini) inferred from mtDNA sequences: implications for taxonomy and plumage evolution. Molecular Phylogenetics and Evolution 35: 459–469. https://doi.org/10.1016/j.ympev.2004.12.010

Bruxaux J, Gabrielli M, Ashari H, Prŷs-Jones R, Joseph L, Milá B, Besnard G, Thébaud C (2018) Recovering the evolutionary history of crowned pigeons (Columbidae: *Goura*): Implications for the biogeography and conservation of New Guinean lowland birds. Molecular Phylogenetics and Evolution 120: 248–258. https://doi.org/10.1016/j.ympev.2017.11.022

Burland TG (2000) DNASTAR's Lasergene sequence analysis software. Methods in Molecular Biology 132: 71–91. https://doi.org/10.1385/1-59259-192-2:71

Claramunt S, Cracraft J (2015) A new time tree reveals Earth history's imprint on the evolution of modern birds. Science Advances 1: e1501005. https://doi.org/10.1126/sciadv.1501005

Eberhard JR, Wright TF (2016) Rearrangement and evolution of mitochondrial genomes in parrots. Molecular Phylogenetics and Evolution 94: 34–46. https://doi.org/10.1016/j.ympev.2015.08.011

Gibbs D, Barnes E, Cox J (2001) Pigeons and doves: a guide to the pigeons and doves of the world. Pica Press, Robertsbridge.

Hackett SJ, Kimball RT, Reddy S, Bowie RCK, Braun EL, Braun MJ, Chojnowski JL, Cox WA, Han K-L, Harshman J, Huddleston CJ, Marks BD, Miglia KJ, Moore WS, Sheldon FH, Steadman DW, Witt CC, Yuri T (2008). A phylogenomic study of birds reveals their evolutionary history. Science 320: 1763–1768. https://doi.org/10.1126/science.1157704

Han K-L, Robbins MB, Braun MJ (2010) A multi-gene estimate of phylogeny in the nightjars and nighthawks (Caprimulgidae). Molecular Phylogenetics and Evolution 55: 443–453. https://doi.org/10.1016/j.ympev.2010.01.023

Hanada K, Shiu SH, Li WH (2007) The nonsynonymous/synonymous substitution rate ratio versus the radical/conservative replacement rate ratio in the evolution of mammalian genes. Molecular Biology and Evolution 24: 2235–2241. https://doi.org/10.1093/molbev/msm152

Huang ZH, Tu FY, Liu XH (2016) Determination of the complete mitogenome of Spotted Dove, *Spilopelia chinensis* (Columbiformes: Columbidae). Mitochondrial DNA Part A 27: 4224–4225. https://doi.org/10.3109/19401736.2015.1022750

Huelsenbeck JP, Ronquist F (2001) MRBAYES: Bayesian inference of phylogenetic trees. Bioinformatics 17: 754–755. https://doi.org/10.1093/bioinformatics/17.8.754

Hung CM, Lin RC, Chu JH, Yeh CF, Yao CJ, Li SH (2013) The de novo assembly of mitochondrial genomes of the extinct Passenger Pigeon (*Ectopistes migratorius*) with next generation sequencing. PLoS ONE 8: e56301. https://doi.org/10.1371/journal.pone.0056301

Hurst LD (2002) The Ka/Ks ratio: diagnosing the form of sequence evolution. Trends in Genetics 18: 486–487. https://doi.org/10.1016/S0168-9525(02)02722-1

Integrated Taxonomic Information System [ITIS] (2020) Columbidae. Taxonomic Serial No.: 177061. http://www.itis.gov

Jang KH, Ryu SH, Kang SG, Hwang UW (2016) Complete mitochondrial genome of the Japanese Wood Pigeon, *Columba janthina* (Columbiformes, Columbidae). Mitochondrial DNA Part A 27: 2165–2166. https://doi.org/10.3109/19401736.2014.982608

Kalyaanamoorthy S, Minh BQ, Wong TKF, von Haeseler A, Jermiin LS (2017) Modelfinder: fast model selection for accurate phylogenetic estimates. Nature Methods 14: 587–589. https://doi.org/10.1038/nmeth.4285

Kan XZ, Li XF, Zhang LQ, Chen L, Qian CJ, Zhang XW, Wang L (2010) Characterization of the complete mitochondrial genome of the Rock Pigeon, *Columba livia* (Columbiformes: Columbidae). Genetics and Molecular Research 9: 1234–1249. https://doi.org/10.4238/vol9-2gmr853

Katoh K, Misawa K, Kuma K, Miyata T (2002) MAFFT: a novel method for rapid multiple sequence alignment based on fast Fourier transform. Nucleic Acids Research 30: 3059–3066. https://doi.org/10.1093/nar/gkf436

Korzun LP, Erard C, Gasc JP, Dzerzhinsky FJ (2008) Bill and hyoid apparatus of pigeons (Columbidae) and sandgrouse (Pteroclididae): a common adaptation to vegetarian feeding? Comptes Rendus Biologies 331: 64–87. https://doi.org/10.1016/j.crvi.2007.10.003

Kretschmer R, Furo IO, Gomes AJB, Kiazim LG, Gunski RJ, Del Valle Garnero A, Pereira JC, Ferguson-Smith MA, Corrêa de Oliveira EH, Griffin DK, Freitas TRO, O'Connor RE (2020) A comprehensive cytogenetic analysis of several members of the family Columbidae (Aves, Columbiformes). Genes 11(6): e632. https://doi.org/10.3390/genes11060632

Kumar S, Stecher G, Tamura K (2016) MEGA7: molecular evolutionary genetics analysis version 7.0 for bigger datasets. Molecular Biology and Evolution 33: 1870–1874. https://doi.org/10.1093/molbev/msw054

Lerner HRL, Mindell DP (2005) Phylogeny of eagles, Old World vultures, and other Accipitridae based on nuclear and mitochondrial DNA. Molecular Phylogenetics and Evolution 37: 327–346. https://doi.org/10.1016/j.ympev.2005.04.010

Liu HY, Sun CH, Zhu Y, Zhang QZ (2020) Complete mitogenomic and phylogenetic characteristics of the Speckled Wood-pigeon (*Columba hodgsonii*). Molecular Biology Reports 47: 3567–3576. https://doi.org/10.1007/s11033-020-05448-w

Lowe TM, Chan PP (2016) tRNAscan–SE on–line: search and contextual analysis of transfer RNA genes. Nucleic Acids Research 44: W54–W57. https://doi.org/10.1093/nar/gkw413

Luo X, Qu YH, Han LX, Li SH, Lei FM (2008) A phylogenetic analysis of laughing thrushes (Timaliidae: *Garrulax*) and allies based on mitochondrial and nuclear DNA sequences. Zoologica Scripta 38: 9–22. https://doi.org/10.1111/j.1463-6409.2008.00355.x

Martins G, Balbino E, Marques A, Almeida C (2019) Complete mitochondrial genomes of the *Spondias tuberosa* Arr. Cam and *Spondias mombin* L. reveal highly repetitive DNA sequences. Gene 720: 144026. https://doi.org/10.1016/j.gene.2019.144026

Mlíkovský J (2016) The type species of the genus *Geotrygon* Gosse, 1847 (Aves: Columbidae). Zootaxa 4126: 138–140. https://doi.org/10.11646/zootaxa.4126.1.8

Nabholz B, Lanfear R, Fuchs J (2016) Body mass-corrected molecular rate for bird mitochondrial DNA. Molecular Ecology 25: 4438–4449. https://doi.org/10.1111/mec.13780

Nair MV (2010) Thick-billed Green-Pigeon *Treron curvirostra* in Similipal Hills, Orissa: an addition to the avifauna of peninsular India. Indian Birds 6: 19–20. http://www.indianbirds.in/pdfs/Nair_ThickbilledGreenPigeon.pdf

Pacheco MA, Battistuzzi FU, Lentino M, Aguilar RF, Kumar S, Escalante AA (2011) Evolution of modern birds revealed by mitogenomics: timing the radiation and origin of major orders. Molecular Biology and Evolution 28: 1927–1942. https://doi.org/10.1093/molbev/msr014

Pereira SL, Johnson KP, Clayton DH, Baker AJ (2007) Mitochondrial and nuclear DNA sequences support a Cretaceous origin of Columbiformes and a dispersal-driven radiation in the Paleogene. Systematic Biology 56: 656–672. https://doi.org/10.1080/10635150701549672

Perna NT, Kocher TD (1995) Patterns of nucleotide composition at fourfold degenerate sites of animal mitochondrial genomes. Journal of Molecular Evolution 41: 353–358. https://doi.org/10.1007/BF01215182

Reddy S, Kimball RT, Pandey A, Hosner PA, Braun MJ, Hackett SJ, Han KL, Harshman J, Huddleston CJ, Kingston S, Marks BD, Miglia KJ, Moore WS, Sheldon FH, Witt CC, Yuri T, Braun EL (2017) Why do phylogenomic data sets yield conflicting trees? Data type influences the avian tree of life more than taxon sampling. Systematic Biology 66: 857–879. https://doi.org/10.1093/sysbio/syx041

Sammler S, Bleidorn C, Tiedemann R (2011) Full mitochondrial genome sequences of two endemic Philippine hornbill species (Aves: Bucerotidae) provide evidence for pervasive mitochondrial DNA recombination. BMC Genomics 12: e35. https://doi.org/10.1186/1471-2164-12-35

Sangster G, Alström P, Forsmark E, Olsson U (2010) Multi-locus phylogenetic analysis of Old World chats and flycatchers reveals extensive paraphyly at family, subfamily and genus level (Aves: Muscicapidae). Molecular Phylogenetics and Evolution 57: 380–392. https://doi.org/10.1016/j.ympev.2010.07.008

Sangster G, García-R JC, Trewick SA (2015) A new genus for the Lesser Moorhen *Gallinula angulata* Sundevall, 1850 (Aves, Rallidae). European Journal of Taxonomy 153: 1–8. https://doi.org/10.5852/ejt.2015.153

Sangster G, Luksenburg JA (2020) Chimeric mitochondrial genomes: a hazard for phylogenetics and environmental DNA identification of fishes. Authorea (Online). https://doi.org/10.22541/au.160205226.65255244/v1

Sangster G, Roselaar CS, Irestedt M, Ericson PGP (2016) Sillem's Mountain Finch *Leucosticte sillemi* is a valid species of rosefinch (*Carpodacus*, Fringillidae). Ibis 158: 184–189. https://doi.org/10.1111/ibi.12323

Soares AER, Novak BJ, Haile J, Heupink TH, Fjeldså J, Gilbert MTP, Poinar H, Church GM, Shapiro B (2016) Complete mitochondrial genomes of living and extinct pigeons revise the timing of the columbiform radiation. BMC Evolutionary Biology 16: e230. https://doi.org/10.1186/s12862-016-0800-3

Sorenson MD, Oneal E, García-Moreno J, Mindell DP (2003) More taxa, more characters: the Hoatzin problem is still unresolved. Molecular Biology and Evolution 20: 1484–1498. https://doi.org/10.1093/molbev/msg157

Stothard P, Wishart DS (2005) Circular genome visualization and exploration using CGView. Bioinformatics 21: 537–539. https://doi.org/10.1093/bioinformatics/bti054

Sun CH, Liu HY, Lu CH (2020) Five new mitogenomes of *Phylloscopus* (Passeriformes, Phylloscopidae): Sequence, structure, and phylogenetic analyses. International Journal of Biological Macromolecules 146: 638–647. https://doi.org/10.1016/j.ijbiomac.2019.12.253

Wang E, Zhang D, Braun MS, Hotz-Wagenblatt A, Pärt T, Arlt D, Schmaljohann H, Bairlein F, Lei F, Wink M (2020) Can mitogenomes of the Northern Wheatear (*Oenanthe oenanthe*) reconstruct its phylogeography and reveal the origin of migrant birds? Scientific Reports 10: e9290. https://doi.org/10.1038/s41598-020-66287-0

Xu N, Zhang QZ, Chen R, Liu HY (2019) The complete mitogenome of Red-collared Lorikeet (*Trichoglossus rubritorquis*) and its phylogenetic analysis. Mitochondrial DNA Part B 4: 3116–3117. https://doi.org/10.1080/23802359.2019.1667917

Yang Z (1994) Maximum likelihood phylogenetic estimation from DNA sequences with variable rates over sites: approximate methods. Journal of Molecular Evolution 39: 306–314. https://doi.org/10.1007/BF00160154

Zhang D, Gao FL, Jakovlić I, Zou H, Zhang J, Li WX, Wang GT (2020) PhyloSuite: An integrated and scalable desktop platform for streamlined molecular sequence data management and evolutionary phylogenetics studies. Molecular Ecology Resources 20: 348–355. https://doi.org/10.1111/1755-0998.13096

Zhang RH, Xu MJ, Wang CL, Xu T, Wei D, Liu BJ, Wang GH (2015) The complete mitochondrial genome of the Fancy Pigeon, *Columba livia* (Columbiformes: Columbidae). Mitochondrial DNA 26: 162–163. https://doi.org/10.3109/19401736.2014.1003851

Ichthyofauna in the last free-flowing river of the Lower Iguaçu basin: the importance of tributaries for conservation of endemic species

Suelen Fernanda Ranucci Pini[1,2], Maristela Cavicchioli Makrakis[2],
Mayara Pereira Neves[3], Sergio Makrakis[2],
Oscar Akio Shibatta[4], Elaine Antoniassi Luiz Kashiwaqui[2,5]

1 *Instituto Federal de Mato Grosso do Sul (IFMS), Rua Salime Tanure s/n, Santa Tereza, 79.400-000 Coxim, MS, Brazil* **2** *Grupo de Pesquisa em Tecnologia em Ecohidráulica e Conservação de Recursos Pesqueiros e Hídricos (GETECH), Programa de Pós-graduação em Engenharia de Pesca, Universidade Estadual do Oeste do Paraná (UNIOESTE), Rua da Faculdade, 645, Jardim La Salle, 85903-000 Toledo, PR, Brazil* **3** *Programa de Pós-Graduação em Biologia Animal, Laboratório de Ictiologia, Departamento de Zoologia, Instituto de Biociências, Universidade Federal do Rio Grande do Sul (UFRGS), Avenida Bento Gonçalves, 9500, Agronomia, 90650-001, Porto Alegre, RS, Brazil* **4** *Departamento de Biologia Animal e Vegetal, Universidade Estadual de Londrina, Rod. Celso Garcia Cid PR 445 km 380, 86057-970, Londrina, PR, Brazil* **5** *Grupo de Estudos em Ciências Ambientais e Educação (GEAMBE), Universidade Estadual de Mato Grosso do Sul (UEMS), Br 163, KM 20.7, 79980-000 Mundo Novo, MS, Brazil*

Corresponding author: Suelen F. R. Pini (suelen.pini@hotmail.com)

Abstract

The fish fauna from the Lower Iguaçu River and tributaries upstream of the Iguaçu Falls, the last free-flowing river stretch, were investigated. Twenty five sites in tributaries and the main channel were sampled between 2010 and 2016 using several kinds of fishing gear. The species were categorized according to their size, origin, and conservation status. Species richness and abundance in the main channel and tributaries were compared. In total, 87,702 specimens were recorded, comprising 76 species, 25 families, 53 genera, and eight orders. Characiformes and Siluriformes were the richest orders, representing 92% of the total specimens; Characidae, Cichlidae, Pimelodidae, and Loricariidae were the richest families. The fish fauna was composed of small and medium-sized species and included endemic (42%), autochthonous (24%), allochthonous (21%), and exotic (9%) species, as well as hybrids (4%). Significant differences in the relative numerical abundance of species were found among sites. *Ancistrus mullerae* and *Rhamdia branneri*

(endemic) were indicator species for tributaries inside of Iguaçu National Park (INP), while *Phalloceros harpagos* (autochthonous) and *Ictalurus punctatus* (exotic) for tributaries outside of INP and *Odontesthes bonariensis* (allochthonous) for the main channel. The last dam-free stretch of the Lower Iguaçu River and tributaries upstream the Iguaçu Falls exhibits a rich endemic fish fauna, including some rare, endangered species (*Steindachneridion melanodermatum*, *Gymnogeophagus taroba*, and *Psalidodon gymnogenys*). These findings are essential to predict and understand the effects caused by the new Baixo Iguaçu Hydroelectric Power Plant and highlight the importance of tributaries and Iguaçu National Park for conservation of endemic species.

Introduction

The high diversity of species in the Neotropical region is recognized worldwide. This region currently has more than 5,160 species of freshwater fish and may have as many as 9,000 species (Reis et al. 2016). Three large freshwater basins dominate the South American continent: Amazon, Orinoco, and Paraná-Paraguay (Reis et al. 2016). The Paraná-Paraguay basin represents the third most diverse freshwater basin in South America (Reis et al. 2016), and within it, the Iguaçu River is renowned for its peculiar geomorphological and ichthyofaunal characteristics (Baumgartner et al. 2012).

Endemism is a well-recognized feature of the Iguaçu river basin (Baumgartner et al. 2012), which has led to its classification as a distinct ecoregion for freshwater fish conservation (Abell et al. 2008). This unique fauna arose from the isolation of this basin caused by the formation of the Iguaçu Falls some 22 million years ago (Oligo-Miocene period) (Severi and Cordeiro 1994). Currently, approximately 127 species of fish are known from the Iguaçu river basin (Reis et al. 2020). Many of these species have been described in the last decade, although taxonomic problems remain (Baumgartner et al. 2012), indicating that the diversity may be underestimated.

The main anthropogenic threats to fish fauna are habitat loss and environmental degradation. Specifically, damming rivers for hydroelectric power generation and water diversion for irrigation, as well as extensive changes in land use for agriculture and urbanization, are the main drivers of habitat loss (Reis et al. 2016) and the leading causes of the loss of biodiversity (Carvalho et al. 2019; Teresa and Casatti 2017). Therefore, it is essential to identify species, understand their distribution, and mitigate threats.

The topographic relief of the Iguaçu river basin has been a major attraction for hydroelectric projects. There are now five large reservoirs and several small ones, which have changed the natural landscape and stream habitats in the basin (Baumgartner et al. 2012). The last dam-free stretch of the Iguaçu River is 190 km in length and extends downstream from Salto Caxias dam to the Iguaçu Falls and encompasses Iguaçu National Park (INP), a world heritage site. However, in 2013, construction began on the sixth hydroelectric power plant, the Baixo Iguaçu Hydroelectric Power Plant (HPP)

about 30 km downstream of the Salto Caxias dam and 500 m upstream from the mouth of the Gonçalves Dias River, which forms the boundary of INP. INP is one of the few remaining areas of Atlantic Forest protected by law. Although this hydroelectric plant project is very controversial due to its possible impacts on the region and particularly on INP, its operation started in 2019. Worryingly, the Baixo Iguaçu HPP potentially could be source of threats to the fish fauna, especially endemic species both inside and outside the INP (UNESCO 2012; Assumpção et al. 2017; Delariva et al. 2018).

The demand for electricity has grown in recent decades. To supply this demand in Brazil, most of needed electricity comes from hydroelectric plants (Kliemann and Delariva 2015; Makrakis et al. 2019). The extensive water network favors the implementation of hydroelectric projects, from small and medium-sized plants to large ones, but these projects directly change the physical and abiotic characteristics of aquatic ecosystems (Barbosa et al. 1999; Pelicice et al. 2018) and their fauna. Among the adverse effects is the profound change in river hydrology, which alters the structure of the fish fauna by fragmenting habitat, restricting dispersal of fish, decreasing the diversity of microhabitats and the supply of resources, and preventing movements of migratory species (e.g., Agostinho et al. 2007). Effects on the trophic structure of fish are already known on the Iguaçu River at the Salto Caxias HPP (Delariva et al. 2013) and Salto Segredo HPP (Mise et al. 2013). Although these effects are recognized, cascade hydroelectric projects have become increasingly common in Brazilian rivers (Santos et al. 2018).

Changes in land use have also negatively affected the biodiversity of fish in the Lower Iguaçu river basin (Larentis et al. 2016; Delariva et al. 2018), and the Iguaçu River is also recognized as the second most polluted river in Brazil (Bueno-Krawczyk et al. 2015; IBGE 2015). This pollution originates mainly from industrial and domestic sewage of urban areas in the Higher Iguaçu region (Bueno-Krawczyk et al. 2015) and from contamination by pesticides using in agriculture in the middle and lower portions of the basin (Nimet et al. 2017; Neves et al. 2018). These threats can lead to species extinctions and changes in the distinct structure of the fish fauna, whose evolutionary and biogeographic history is still not well understood. Therefore, it is essential to study the fish fauna prior to additional anthropogenic threats to assess the state of this ecosystem's conservation.

This study provides an ichthyofaunistic inventory of the last free-flowing river stretch of the Lower Iguaçu River. This area is poorly studied and may be affected by the construction of a new hydroelectric power plant near Iguaçu National Park. While a previous inventory has been carried out in the river mostly upstream of the Salto Caxias Dam (Baumgartner et al. 2012), our study was based on a wider spatial-temporal scale, and intense sampling efforts include areas not yet sampled downstream of this dam. The 190 km stretch of the Iguaçu River and its tributaries exhibits a diverse landscape, and includes the area protected within INP, including a pristine river, areas at the INP border, and anthropogenic areas. We compare the composition, richness, frequency, and numerical abundance of species in tributaries and the main river channel. We describe the relative numerical abundance of species according to their biogeographic origins among the sites. We determine fish species indicative for the main

channel, as well as tributaries inside and outside of INP. The results contribute to the knowledge of the basin's fish fauna, including important information on the biogeographic origins and conservation status of the species. Our new data are an important contribution to the conservation and sustainable management of the last free-flowing stretch of the Lower Iguaçu River and mitigate future anthropogenic threats to this river's fish fauna.

Material and methods

Study area

The Iguaçu River is considered one of the most important tributaries of the Paraná river basin, having 1,320 km in length (Bartozek et al. 2016). This river rises in the Serra do Mar and flows through a geological fault in the three plateaus in Paraná. The river flows through three regions: the upper Iguaçu on the first plateau; the middle Iguaçu on the second plateau, and the Lower Iguaçu on third plateau (Maack 1981). Before joining the Paraná River near the city of Foz do Iguaçu, the river passes over the Iguaçu Falls (Maack 1981). The falls are within INP and are the most important feature of the park. The Iguaçu Falls form a natural barrier in the Iguaçu river basin that has isolated the ichthyofauna of the Iguaçu basin from Paraná river for millions of years (Agostinho et al. 2003). This isolation has resulted in speciation and high endemism of the fish fauna in the Iguaçu basin (Garavello et al. 1997; Agostinho et al. 1999), which is estimated at 70% (Baumgartner et al. 2012).

The study area comprises the Lower Iguaçu River, including its tributaries and the main channel, extending from the Salto Caxias dam downstream to the mouth of the Santo Antônio mouth, which is in INP (Fig. 1) at the Brazil–Argentina boundary. In this region, 25 sites were sampled: five in the main channel and 20 in tributaries. The sampled tributaries were: Cotejipe, Sarandi, Andrada, Capanema, Monteiro (outside INP), Santo Antônio, Gonçalves Dias (boundary of INP), Floriano, and Silva Jardim rivers (within INP; Table 1).

The Baixo Iguaçu HPP (25°30'S, 53°40'W), the last hydroelectric power plant on the Iguaçu River downstream from Salto Caxias HPP, is approximately 500 meters from the mouth of the Gonçalves Dias River, at the INP boundary. On its right bank is the municipality of Capanema, and on its left bank is the municipality of Capitão Leonidas Marques (Paraná, Brazil).

Data collection

Fish samples were collected (Fig. 1) using several types of fishing gear: gill nets (mesh sizes 2.5–14.0 cm), trammel nets (6.0, 7.0, and 8.0 cm), and longlines. The gear was installed and remained in position for 24 h and inspected every 6 h. Samplings were taken monthly in two periods: during the fish faunal survey from January to December
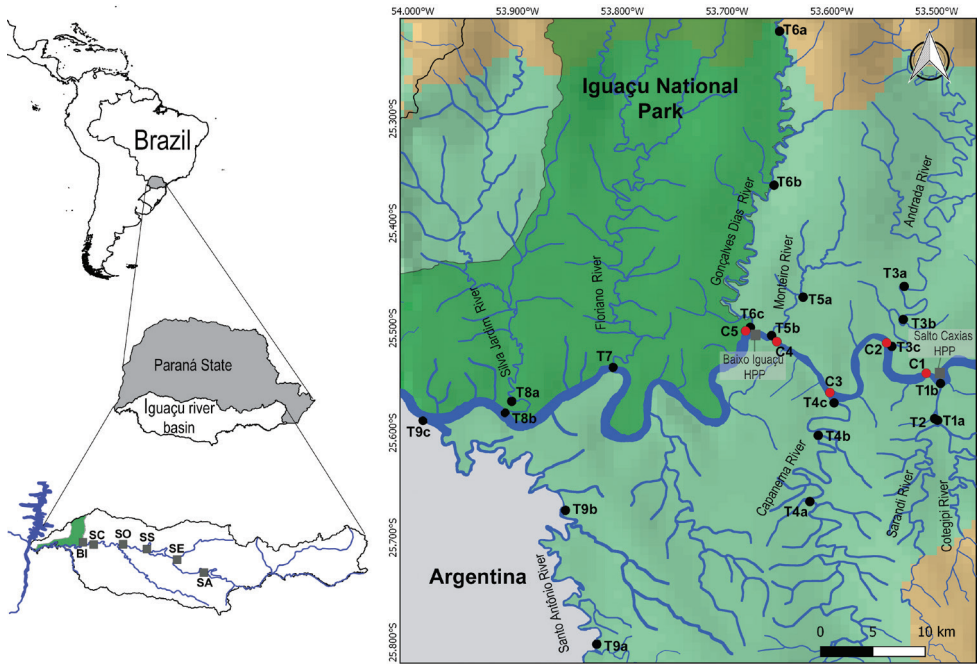
Figure 1. Study area: Lower Iguaçu river basin highlighting the existing hydroelectric dams (SA: Foz do Areia; SE: Segredo; SS Salto Santiago; SO: Salto Osório; SC: Salto Caxias; and BI: Baixo Iguaçu) and the Iguaçu National Park (left). Sampling sites are located in tributaries (black dots) and the main channel (red dots) of the Iguaçu River (right). Sampling sites in tributaries were indicated considering their upstream (a), intermediate (b), and downstream location (c).

2010, and during four years of monitoring from September 2013 to March 2015, August 2015 to March 2016, and August to December 2016 (44 samplings in total).

After capture, the fish were euthanized with 250 mg/L benzocaine, fixed in 10% formaldehyde, and preserved in 70% ethanol. Fish were collected under license from the Instituto Ambiental do Paraná (IAP) (licenses no. 37788 and 43394) and Instituto Chico Mendes de Conservação da Biodiversidade (ICMBio) (no. 003/2014 and 63/2016-DIBIO/ICMBio). The protocols of the Ethics Committee on Animal Use (CEUA, no. 62/09) of the Universidade Estadual Oeste do Paraná were followed.

The specimens identified according to Baumgartner et al. (2012), Garavello et al. (2012), Garavello and Sampaio (2010), and Graça and Pavanelli (2007), and total and standard lengths (in cm) were measured. Taxonomic classification and species names mainly follow Fricke et al. (2020). Voucher specimens were deposited at the fish collection of the Museum of Zoology (MZUEL) at the Universidade Estadual de Londrina.

The species were classified according to body size, origin, and conservation status. Using standard length (measured and reported in the literature), the species were classified as small (S = <20 cm), medium (M = 20–40 cm), and large (L = >40 cm) following Baumgartner et al. (2012). For their biogeographic origins, the species were

Table 1. Characteristics of the sampled sites in the Lower Iguaçu river basin, Brazil. INP = Iguacu National Park; T = tributary; C = main channel.

Sites	Sub sites	Latitude and longitude	Altitude (m)	river width (m)	Description
T1	a	25°35'17.04"S, 53°29'56.58"W	257	39	Cotejipe River, tributary of Iguaçu. Located just downstream of Salto Caxias HPP.
	b	25°33'9.54"S, 53°29'46.92"W	270		
T2		25°35'10.74"S, 53°30'7.44"W	278	12	Sarandi River, tributary of Cotejipe River.
C1		25°32'30.18"S, 53°30'37.98"W	268	348	Iguaçu River, just downstream of the Salto Caxias.
T3	a	25°27'36.18"S, 53°31'51.69"W	291	24	Andrada River, tributary of Iguaçu River.
	b	25°29'29.70"S, 53°31'55.08"W	263	37	
	c	25°31'2.28"S, 53°32'34.44"W	309	62	
C2		25°30'48.00"S, 53°32'40.62"W	246	652	Iguaçu River.
T4	a	25°39'54.84"S, 53°37'15.66"W	268	25	Capanema River, tributary of Iguaçu River.
	b	25°36'8.40"S, 53°36'46.98"W	275	38	
	c	25°34'16.26"S, 53°35'52.68"W	256	72	
C3		25°33'49.14"S, 53°36'16.92"W	284	592	Iguaçu River.
C4		25°30'42.58"S, 53°39'5.76"W	262	287	Iguaçu River, just upstream of Baixo Iguaçu HPP (current reservoir).
T5	a	25°28'12.96"S, 53°37'39.00"W	269	9	Monteiro River, tributary of Iguaçu River.
	b	25°30'25.38"S, 53°39'27.24"W	279	17	
T6	a	25°12'58.98"S, 53°39'0.06"W	460	17	Gonçalves Dias River, tributary of Iguaçu River. Located at the limit of the INP (right margin). Its mouth with Iguaçu is approximately 500 meters from the Baixo Iguaçu HPP.
	b	25°21'48.12"S, 53°39'18.00"W	293	36	
	c	25°29'57.06"S, 53°40'40.50"W	241	38	
C5		25°29'57.54"S, 53°40'53.52"W	249	747	Iguaçu River, just downstream of the Baixo Iguaçu HPP reservoir, right bank in the INP.
T7		25°32'14.82"S, 53°48'31.98"W	225	39	Floriano River, a tributary of Iguaçu River. Fully inserted in the INP.
T8	a	25°34'11.09"S, 53°54'20.36"W	250	31	Silva Jardim River, a tributary of Iguaçu River. Fully inserted in the INP.
	b	25°34'51.24"S, 53°54'43.68"W	229	20	
T9	a	25°48'6.28"S, 53°49'28.35"W	265	40	Santo Antônio River, a tributary of Iguaçu River. It is the border between Brazil and Argentina.
	b	25°40'25.80"S, 53°51'15.90"W	233	15	
	c	25°35'17.16"S, 53°59'25.20"W	215	57	

categorized following Langeani et al. (2007): autochthonous (native species that occur in other river basins), allochthonous (introduced species belonging to the Neotropical region), endemic (species restricted to the Iguaçu river basin above the Iguaçu Falls), exotic (introduced species from other continents), and hybrids (crosses of species). The origins of each species were determined according to Reis et al. (2003), Langeani et al. (2007), Baumgartner et al. (2012), and Casciotta et al. (2016).

The conservation status of species was based on the Red Book of Endangered Brazilian Fauna (ICMBio 2018), which classifies the risk of extinction of species following the International Union for Conservation of Nature (IUCN) criteria; the categories are: Extinct in the wild (EW), Critically endangered (CR), Endangered (EN), Vulnerable (VU), Near Threatened (NT), Data Deficient (DD), and Least Concern (LC).

Data analysis

The generalized linear mixed models (GLMMs) were used to verify differences in the relative numerical abundance of species according to their origins (allochthonous, autochthonous, endemic, exotic, and hybrid) among sites. GLMMs were constructed using Gaussian family distribution, including sites as response variables (fixed fac-
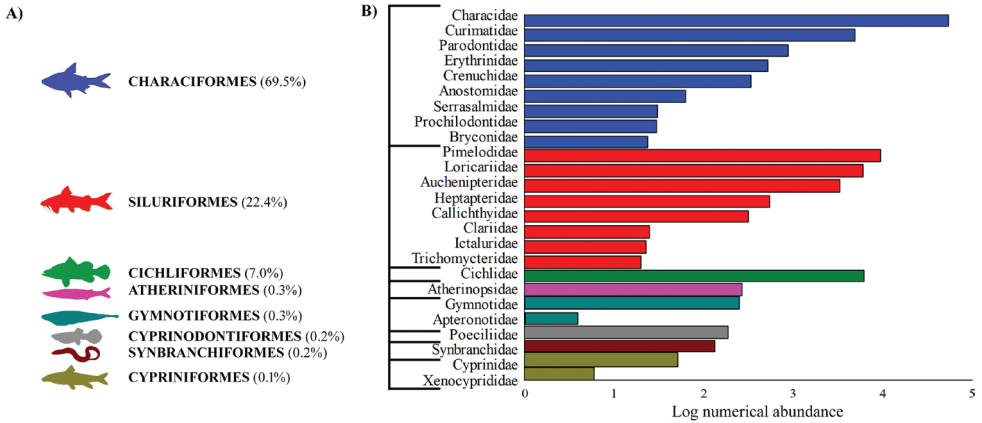
Figure 2. Relative numerical abundance of fish orders (**A**) and fish families (**B**) recorded between 2010 and 2016 in the Lower Iguaçu river basin, Brazil.

tor), and the time (sampling years) as random factor. GLMMs were ran using the following packages: "nlme" (Pinheiro et al. 2021), "lme4" (Bates et al. 2015), "lmerTest" (Kuznetsova et al. 2017), "stats" (R Core Team 2021), and "car" (Fox and Weisberg 2019). When the result was significant for the categorical factor (sites), we performed a post-hoc test using the *difflsmeans* function.

To determine fish species indicative for each site category (main channel: C1–C5; tributaries outside of INP: T1-T5 and T9, and tributaries inside or in the border of INP: T6–T8), the indicator value analysis (IndVal; Dufrêne and Legendre 1997) was applied based on the relative numerical abundance of fish species using the *multipatt* function, with 999 permutations, in the "indicspecies" package v. 1.7.8 (Caceres and Legendre 2009). Indicator values reflect specificity (the probability of a taxon occurring in a group) and fidelity (the relative abundance of the taxon in that group). IndVal produces an indicator species value (ISV) that ranges from 0 (absent) to 1 (present in all samples of a particular group). Species considered the "best" indicators of a group are those with scores closest to 1, meaning they are found within their group only and do not occur anywhere else. All statistical analyses were performed in R version 3.5.2 (R Core Team 2021), considering the confidence interval of $p < 0.05$.

Results

A total of 87,702 specimens were recorded, comprising 76 species, 25 families, 53 genera, and eight orders (Fig. 2; Table 2). The richest orders were Siluriformes and Characiformes, with 28 and 27 species, respectively (Table 2). Together these two orders represent approximately 92% of all species collected (Fig. 2a). Characidae (13 species), Cichlidae (11 species), and Loricariidae (nine species) were the families with the greatest richness (Table 2). However, Characidae, Cichlidae, and Pimelodidae are the

Table 2. Fish species recorded and their respective occurrence at the sampling sites in the Lower Iguaçu River basin, Brazil. %N: abundance in numerical percentage; SL: standard lengths (minimum-maximum; cm); Size: the reported size that the species can reach: Small (S)= fish less than 20 cm; Medium (M)= 20-40 cm; and Large (L)= more than 40 cm; Origin refers to species classified in Autochthonous (AU), Endemic (END), Allochthonous (AL), Exotic (EX), and Hybrid (HY) to the Lower Iguaçu River; Threat level= Brazilian Red List of Threatened Species: Extinct in the wild (EW), Critically endangered (CR), Endangered (EN), Vulnerable (VU), Near Threatened (NT), Data Deficient (DD), and Least Concern (LC) (ICMBio 2018); Voucher specimens: individuals deposited in the Zoology Museum at the Universidade Estadual de Londrina (MZUEL). T = tributary; C = main channel.

Taxonomic position/Species	% N	SL (cm) / Size	Origin/ Threat level	T1	T2	C1	T3	C2	T4	C3	C4	T5	T6	C5	T7	T8	T9	Voucher specimens
CYPRINIFORMES																		
Cyprinidae																		
Cyprinus carpio Linnaeus, 1758	0.06	16.0/74.0/L	EX	x			x		x		x	x	x			x	x	MZUEL13303
Xenocyprididae																		
Ctenopharyngodon idella (Valenciennes, 1844)	0.01	23.0/48.8/L	EX	x			x									x		
Hypophthalmichthys nobilis (Richardson, 1845)	*	26.0/M	EX														x	MZUEL15861
CHARACIFORMES																		
Parodontidae																		
Apareiodon vittatus Garavello, 1977	1.00	1.4/15.5/S	END/LC	x	x	x	x	x	x	x	x	x	x	x	x	x	x	MZUEL17679
Curimatidae																		
Cyphocharax cf. *santacatarinae* (Fernández-Yépez, 1948)	2.67	1.3/22.7/M	AU/LC	x	x	x	x	x	x	x	x	x	x	x	x	x	x	MZUEL16272
Steindachnerina brevipinna (Eigenmann & Eigenmann, 1889)	2.87	2.0/22.0/M	AU/LC	x	x	x	x	x	x	x	x	x	x	x	x	x	x	MZUEL17613
Prochilodontidae																		
Prochilodus lineatus (Valenciennes, 1837)	0.03	19.6/36.0/M**	AL/LC	x			x	x	x	x			x	x	x	x	x	MZUEL13315
Anostomidae																		
Megaleporinus macrocephalus Garavello & Britski, 1988	0.03	15.3/39.6/M	AL/LC	x			x	x	x	x	x				x	x		MZUEL15870
*Megaleporinus piavussu*Britski, Birindelli & Garavello, 2012	0.02	16.4/41.2/L	AL/LC	x			x		x				x	x		x		MZUEL17944
Megaleporinus obtusidens (Valenciennes, 1837)	0.02	16.0/43.0/L	AL/LC	x			x	x		x	x			x	x	x	x	MZUEL15836
Schizodon borellii (Boulenger, 1900)	*	29.5/35.0/M	AL/LC				x									x		MZUEL17941
Crenuchidae																		
Characidium sp.	0.38	1.7/9.9/S	END	x	x	x	x	x	x	x	x	x	x	x	x	x	x	MZUEL17568
Serrasalmidae																		
Piaractus mesopotamicus (Holmberg, 1887)	0.04	10.5/68.0/L	AL/NT	x			x	x	x	x		x	x			x		MZUEL17986
Characidae																		
Astyanax dissimilis Garavello & Sampaio, 2011	3.14	2.0/14.4/S	END/LC	x	x	x	x	x	x	x	x	x	x	x	x	x	x	MZUEL16339
Astyanax lacustris Lütken, 1875	6.69	1.0/16.4/S	AL/LC	x	x	x	x	x	x	x	x	x	x	x	x	x	x	MZUEL16359
Astyanax minor Garavello & Sampaio, 2010	5.50	2.2/28.7/M	END/LC	x	x	x	x	x	x	x	x	x	x	x	x	x	x	MZUEL16346
Astyanax serratus Garavello & Sampaio, 2011	*	9.7/13.0/S	END/LC				x										x	MZUEL15827
Bryconamericus ikaa Casciotta, Almirón & Azpelicueta, 2004	10.83	0.7/8.3/S	END/LC	x	x	x	x	x	x	x	x	x	x	x	x	x	x	MZUEL17521
Bryconamericus pyahu Azpelicueta, Casciotta & Almirón, 2003	0.08	2.3/5.8/S	END/LC	x	x		x	x	x				x	x	x	x	x	MZUEL15830
Charax stenopterus Fowler, 1932	0.01	6.9/9.6/S	AL/LC													x	x	MZUEL13309

Taxonomic position/Species	% N	SL (cm) / Size	Origin/ Threat level	Sampling sites														Voucher specimens
				T1	T2	C1	T3	C2	T4	C3	C4	T5	T6	C5	T7	T8	T9	
Diapoma aff. *alburnus* (Hensel, 1870)	2.40	1.1/30.0/M	AU/LC	x	x	x	x	x	x	x	x	x	x	x	x	x	x	MZUEL13243
Hyphessobrycon boulengeri Ellis, 1911	0.01	2.7/4.3/S	AU	x	x			x				x						MZUEL17979
Oligosarcus longirostris Menezes & Géry, 1983	4.46	2.2/36.4/M	END/LC	x	x	x	x	x	x	x	x	x	x	x	x	x	x	MZUEL17522
Psalidodon bifasciatus (Garavello & Sampaio, 2010)	20.71	2.0/38.9/M	AU/LC	x	x	x	x	x	x	x	x	x	x	x	x	x	x	MZUEL16267
Psalidodon gymnodontus (Eignmann, 1911)	7.68	2.0/16.3/S	END/LC	x	x	x	x	x	x	x	x	x	x	x	x	x	x	MZUEL16353
Psalidodon gymnogenys Eignmann, 1911	0.10	6.0/14.5/S	END/EN	x		x	x	x	x			x	x		x	x	x	MZUEL20821
Bryconidae																		
Brycon hilarii (Valenciennes, 1850)	0.01	18.0/30.6/M	AL/LC	x			x		x	x		x				x	x	MZUEL15855
Salminus brasiliensis (Cuvier, 1816)	0.02	18.0/41.0/L	AL/LC	x			x		x	x		x	x					MZUEL13302
Erythrinidae																		
Hoplias sp. 1	0.30	5.5/48.2/L	AU	x	x	x	x	x	x	x	x	x	x	x	x	x	x	MZUEL13264
Hoplias sp. 2	0.30	5.5/52.0/L	AU	x	x	x	x	x	x	x	x	x	x	x	x	x	x	MZUEL17662
SILURIFORMES																		
Trichomycteridae																		
Cambeva davisi (Haseman, 1911)	0.01	3.8/13.4/S	AU/LC									x	x					MZUEL15841
Cambeva stawiarski (Miranda Ribeiro, 1968)	0.01	3.5/13.0/S	END/LC									x	x					MZUEL17950
Callichthyidae																		
Corydoras carlae Nijssen & Isbrücker, 1983	*	5.5/6.0/S	END/LC						x								x	MZUEL17500
Corydoras ehrhardti Steindachner, 1910	0.09	1.7/4.5/S	AU/LC	x	x	x	x	x	x						x		x	MZUEL17475
Corydoras longipinnis (Jenyns, 1842)	0.27	1.5/14.6/S	END/LC	x	x	x	x	x	x		x	x	x	x			x	MZUEL17681
Loricariidae																		
Ancistrus agostinhoi Bifi, Pavanelli & Zawadzki, 2009	*	4.8/12.0/S	END/LC						x			x					x	MZUEL15856
Ancistrus mullerae Bifi, Pavanelli & Zawadzki, 2009	1.22	1.5/16.1/S	END/LC	x	x	x	x		x	x							x	MZUEL15862
Hisonotus yasi (Almirón, Azpelicueta & Casciotta, 2004)	0.11	1.2/19.0/S	END	x	x		x	x	x	x	x	x	x	x	x	x		
Hypostomus albopunctatus (Regan, 1908)	0.03	11.0/35.5/M	AU/LC	x		x	x	x	x				x				x	MZUEL15849
Hypostomus commersoni Valenciennes, 1836	0.17	3.3/43.5/L	AU/LC	x		x	x	x	x	x	x	x	x			x	x	MZUEL15887
Hypostomus derbyi (Haseman, 1911)	0.53	13.8/40.5/L	AU/LC	x	x	x	x	x	x	x	x	x	x	x	x	x	x	MZUEL17495
Hypostomus myersi (Gosline, 1947)	3.29	13.4/37.5/M	AU/LC	x	x	x	x	x	x	x	x	x	x	x	x	x	x	MZUEL16348
Loricariichthys cf. *rostratus* Reis & Pereire, 2000	1.44	5.0/28.5/M	AU/LC	x		x	x	x	x	x	x	x	x	x	x	x	x	MZUEL17604
Pareiorhaphis cf. *parmula* Pereira, 2005	*	2.5/2.5/S	END/LC									x						
Heptapteridae																		
Heptapterus sp.	*	11.0/16.0/S	END				x											MZUEL15845
Imparfinis hollandi Haseman, 1911	0.02	3.7/25.8/M	END	x	x		x	x				x	x				x	MZUEL17985
Pariolus sp.	0.01	8.5/18.5/S	END				x					x						
Rhamdia branneri Haseman, 1911	0.19	6.3/39.0/M	END/LC	x	x	x	x	x	x	x	x		x	x	x	x	x	MZUEL13276
Rhamdia voulezi Haseman, 1911	0.41	5.0/36.8/M	END/LC	x	x	x	x	x	x	x	x	x	x	x	x	x	x	MZUEL15871
Ictaluridae																		
Ictalurus punctatus (Rafinesque, 1818)	0.03	11.0/73.8/L	EX	x			x	x	x			x				x	x	MZUEL13246

Taxonomic position/Species	% N	SL (cm) / Size	Origin/ Threat level	T1	T2	C1	T3	C2	T4	C3	C4	T5	T6	C5	T7	T8	T9	Voucher specimens
Auchenipteridae																		
Glanidium ribeiroi Haseman, 1911	3.75	5.1/29.0/M	END/LC	x	x	x	x	x	x	x	x	x	x	x	x	x	x	MZUEL16268
Tatia jaracatia Pavanelli & Bifi 2009	0.10	3.9/7.4/S	END/LC	x	x	x	x	x	x	x	x	x	x	x		x	x	MZUEL16278
Clariidae																		
Clarias gariepinus (Bourchell, 1822)	0.03	19.8/85.0/L	EX	x			x	x	x	x	x					x	x	MZUEL15858
Pimelodidae																		
Leiarius marmoratus (Gill, 1870)	*	35.5/35.5/M	AL/LC						x									MZUEL15874
Pimelodus britskii Garavello&Shibatta, 2007	10.12	1.0/40.2/L	END/LC	x	x	x	x	x	x	x	x	x	x	x	x	x	x	MZUEL17494
Pimelodus ortmanni Haseman, 1911	0.79	9.0/32.0/M	END/LC	x	x	x	x	x	x	x	x	x	x	x	x	x	x	MZUEL16275
Pseudoplatystoma corruscans (Spix& Agassiz, 1829)	*	42.5/58.0/L	AL/NT													x	x	MZUEL20820
Steindachneridion melanodermatum Garavello, 2005	0.01	17.4/72.5/L	END/EN			x			x				x				x	MZUEL17620
GYMNOTIFORMES																		
Gymnotidae																		
Gymnotus inaequilabiatus (Valenciennes, 1839)	0.04	8.0/21.4/M	AL/LC	x			x		x				x	x	x		x	MZUEL16279
Gymnotus sylvius Albert & Fernandes-Matioli, 1999	0.25	2.5/34.0/M	AL/LC	x	x	x	x	x	x	x	x	x	x	x	x	x	x	MZUEL13300
Apteronotidae																		
Apteronotus sp.	*	26.7/27.5/M	AU				x										x	MZUEL13271
ATHERINIFORMES																		
Atherinopsidae																		
Odontesthes bonariensis (Valenciennes, 1835)	0.31	4.8/34.5/M	AL/DD	x		x	x	x	x	x	x	x	x			x	x	MZUEL13290
CYPRINODONTIFORMES																		
Poeciliidae																		
Phalloceros harpagos Lucinda, 2008	0.21	1.0/4.1/S	AU/LC	x	x		x	x	x			x	x	x	x	x	x	MZUEL17981
Poecilia reticulata Peters, 1859	*	1.4/1.7/S	AL										x					MZUEL15839
SYNBRANCHIFORMES																		
Synbranchidae																		
Synbranchus marmoratus Bloch, 1795	0.15	6.8/41.0/L	AL/LC	x	x	x	x		x			x	x	x	x	x	x	MZUEL13245
CICHLIFORMES																		
Cichlidae																		
Australoheros kaaygua Casciotta, Almirón & Gómez, 2006	0.01	2.7/9.0/S	END/LC										x	x			x	MZUEL15854
Coptodon rendalli (Boulenger, 1897)	0.07	3.2/42.3/L	EX	x	x	x	x	x	x	x	x	x			x	x	x	MZUEL16254
Crenicichla iguassuensis Haseman, 1911	2.68	1.8/36.6/M	END/LC	x	x	x	x	x	x	x	x	x	x			x	x	MZUEL17614
Crenicichla lepidota Heckel, 1840	0.06	4.8/17.2/S	AU/LC	x			x	x	x				x				x	MZUEL15847
Crenicichla sp. Casciotta, Almirón & Gómez, 2006	0.97	2.0/29.1/M	AU/LC	x	x	x	x	x	x	x	x	x	x	x	x	x	x	MZUEL13301
Crenicichla tapii (Piálek, Dragová, Casciotta, Almirón y Rícan, 2015)	*	10.0/10.0/S	END										x					MZUEL20809
Crenicichla tesay Casciotta & Almirón, 2009	0.15	3.0/19.6/S	END/LC	x	x	x	x	x	x	x		x	x	x	x	x	x	MZUEL20811
Crenicichla tuca (Piálek, Dragová, Casciotta, Almirón y Rícan, 2015)	*	9.6/9.6/S	END												x			MZUEL20810
Geophagus iporangensis Haseman, 1911	2.28	1.1/41.5/L	AU/LC	x	x	x	x	x	x	x	x	x	x	x	x	x	x	MZUEL17616

Taxonomic position/Species	%N	SL (cm) / Size	Origin/Threat level	T1	T2	C1	T3	C2	T4	C3	C4	T5	T6	C5	T7	T8	T9	Voucher specimens
Gymnogeophagus taroba Casciotta, Almirón, Piálek & Rican, 2017	0.73	1.3/11.1/S	END/EN	x	x	x	x	x	x	x	x	x	x	x	x		x	MZUEL16354
Oreochromis niloticus (Linnaeus, 1758)	0.09	3.3/43.0/L	EX	x	x	x	x	x	x	x		x	x	x		x	x	MZUEL13318
Hybrid																		
Piaractus mesopotamicus X *Colossoma macropomum*	*	33.5/36.9/M	HY	x			x											MZUEL15832
Piaractus mesopotamicus X *Piaractus brachypomus*	*	31.6/31.6/M	HY							x								
Pseudoplatystoma corruscans X *Pseudoplatystoma fasciatum*	*	28.0/46.0/L	HY												x	x		MZUEL15877

* Relative numerical abundance (%) smaller than 0.01

** Species less than 40 cm in length, but considered large in the literature (Baumgartner et al. 2012).

most abundant families and comprising approximately 80% (Fig. 2b). Seven species were identified to only the genus level: *Apteronotus* sp., *Characidium* sp., *Crenicichla* sp., *Heptapterus* sp., *Hoplias* sp. 1, *Hoplias* sp. 2, and *Pariolius* sp.

Species richness was greater (76 species) at sites in the tributaries than in the main channel (58 species). The tributaries with the highest species richness were T9 (62 species) and T4 (58 species). Species richness was less in T7 (39 species). Eighteen species were caught only in tributaries. The following species had a restricted occurrence: *Heptapterus* sp. in T2, *Leiarius marmoratus* in T4, *Poecilia reticulata* in T5, *Pareiorhaphis* cf. *parmula* and *Crenicichla tapii* in T6, *Crenicichla tuca* in T7, and *Hypophthalmichthys nobilis* in T9. In the main channel, the greatest species richness was at C2 (46 species) and the lowest at C4 and C5 (40 species each). The hybrid *Piaractus mesopotamicus* × *P. brachypomus* had restricted capture in the main channel (C3). The most frequent species at all sampling sites (main channel and tributaries) were *Psalidodon bifasciatus* (21%), *Bryconamericus ikaa* (11%), and *Pimelodus britskii* (10%).

The fish fauna was characterized chiefly by small and medium-sized species (74% of total numerical abundance; Table 2), represented mainly by *Psalidodon bifasciatus* (24%), *P. gymnodontus* (13%), and *B. ikaa* (9%). Nineteen large species were shared between the main channel and tributaries, with *P. britskii* (71%) being the most frequent and *Steindachneridion melanodermatum* the rarest (Table 2). Some large species were recorded only in the tributaries: *Ctenopharyngodon idella*, *Megaleporinus piavussu*, and *Pseudoplatystoma corruscans*.

On the biogeographic origin of the species in terms of richness, 42% are endemics, 24% autochthonous, 21% allochthonous, 9% exotic, and 4% hybrids. In terms of abundance, endemic and autochthonous species represented 92% of the total abundance (54% and 38%, respectively). In general, the most frequent endemic species were *B. ikaa* (10.83%), *P. britskii* (10.12%), and *P. gymnodontus* (7.68%). *Psalidodon bifasciatus* (20.71%) was most frequent autochthonous species, *Astyanax lacustris* (6.69%) the most frequent allochthonous species, *Oreochromis niloticus* (0.09%) and *Coptodon rendalli* (0.07%) the most frequent exotic
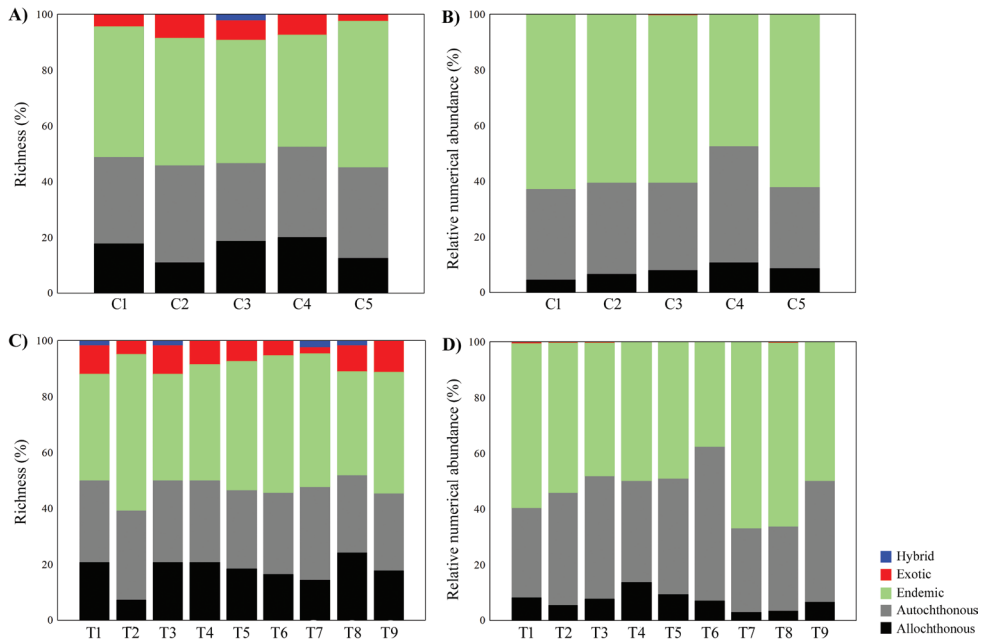
Figure 3. Richness (%, **A–C**) and relative numerical abundance (**B–D**) of fish species according to the origin (AL: allochthonous; AU: autochthonous; END: endemic; EX: exotic; HY: hybrid) recorded between 2010 and 2016 in the tributaries (**C, D**) and main channel (**A, B**) Lower Iguaçu river basin, Brazil.

species, and *Pseudoplatystoma corruscans* × *P. fasciatum* (<0.001%) was the most frequent hybrid (Table 2).

The results of the GLMMs indicated that the relative numerical abundance of allochthonous (F = 2.54; p = 0.007), autochthonous (F = 3.80; p = 0.0001), and endemic (F = 4.30; p < 0.0001) species differed among sites (Table 3; Fig. 3). For exotic species and hybrids, there were no significant relationships with sites (F = 1.32; p = 0.23; F = 0.97; p = 0.49, respectively). The main channel (C1 and C4) and tributaries (T2, T3, T4, T6, and T9) were the sites related with higher abundance of endemic species. In addition, C1, C4 and tributaries (T3, T6, and T9) also related to a great abundance of autochthonous species, and the main channel (C1 and C4) and tributaries outside of INP (T4 and T5) were most abundant in allochthonous species. Despite non-significant results, exotic and hybrid species were also richer and highly abundant in the tributaries, especially in those areas outside of INP, and in areas with intense urban and agricultural activities (Fig. 3; Table 2). The indicator species analysis (Table 4) showed that, among the 76 species considered, only a few species were significantly related with biogeographic origin: *O. bonariensis* (allochthonous) was an indicator species of the main channel, *P. harpagos* (autochthonous) and *I. punctatus* (exotic) were indicator species of tributaries located outside of INP, and *A. mullerae* (endemic) and *R. branneri* (endemic) were indicator species of tributaries inside INP.

Table 3. Effects of the sampling sites on the relative numerical abundance of autochthonous, allochthonous, and endemic species evaluated in the generalized linear mixed models (GLMMs).

Sites	Endemic					Autochthonous					Allochthonous					
	Estimate	Std. Error	df	t value	Pr(>|t|)	Estimate	Std. Error	df	t value	Pr(>|t|)	Estimate	Std.	Error	df	t value	Pr(>|t|)
C1	63.97	4.20	56.08	15.24	**< 0.0001**	30.64	3.77	63.08	8.12	**< 0.0001**	5.20	5.20	1.68	56.44	3.09	**0.003**
C2	-4.35	5.90	59.28	-0.74	0.464	2.62	5.51	59.35	0.48	0.636	1.97	1.97	2.36	59.50	0.83	0.409
C3	-1.52	5.90	59.28	-0.26	0.797	-1.66	5.51	59.35	-0.30	0.764	3.27	3.27	2.36	59.50	1.38	0.172
C4	-17.99	5.61	58.87	-3.21	**0.002**	12.01	5.24	58.69	2.29	**0.026**	6.12	6.12	2.25	59.12	2.72	**0.008**
C5	-6.30	5.61	58.87	-1.12	0.266	3.72	5.24	58.69	0.71	0.481	2.69	2.69	2.25	59.12	1.20	0.237
T1	1.97	5.61	58.87	0.35	0.727	-3.91	5.24	58.69	-0.75	0.459	1.71	1.71	2.25	59.12	0.76	0.450
T2	-11.77	5.61	58.87	-2.10	**0.040**	9.11	5.24	58.69	1.74	0.088	2.70	2.70	2.25	59.12	1.20	0.235
T3	-17.63	5.90	59.28	-2.99	**0.004**	15.07	5.51	59.35	2.74	**0.008**	2.67	2.67	2.36	59.50	1.13	0.262
T4	-13.14	5.61	58.87	-2.34	**0.023**	5.34	5.24	58.69	1.02	0.313	7.80	7.80	2.25	59.12	3.47	**0.001**
T5	-11.14	5.61	58.87	-1.99	0.052	6.66	5.24	58.69	1.27	0.209	4.57	4.57	2.25	59.12	2.03	**0.047**
T6	-22.91	5.90	59.28	-3.89	**< 0.0001**	20.74	5.51	59.35	3.77	**< 0.0001**	2.10	2.10	2.36	59.50	0.89	0.378
T7	0.57	5.90	59.28	0.10	0.923	0.62	5.51	59.35	0.11	0.911	-1.16	-1.16	2.36	59.50	-0.49	0.624
T8	3.30	5.90	59.28	0.56	0.578	-1.54	5.51	59.35	-0.28	0.780	-1.97	-1.97	2.36	59.50	-0.84	0.407
T9	-17.55	5.61	58.87	-3.13	**0.003**	16.71	5.24	58.69	3.19	**0.002**	0.89	0.89	2.25	59.12	0.40	0.693

Table 4. Species indicators defined by IndVal analysis, performed for main channel and tributaries outside and inside Iguaçu National Park – INP.

Species indicator	stat	*p*
	Main channel	
O. bonariensis	0.70	0.001
	Tributaries outside of INP	
P. harpagos	0.74	0.001
I. punctatus	0.49	0.024
	Tributaries inside of INP	
A. mullerae	0.95	0.001
R. branneri	0.74	0.004

Three Endangered (EN) species were sampled in low abundance (<1%) (Table 2): *Psalidodon gymnogenys*, captured at most sites in the tributaries and the main channel but especially at C1 (0.38%); *Steindachneridion melanodermatum*, captured at T4, T6, and T9 in the tributaries but principally in the main channel at C1 (0.07%), and *Gymnogeophagus taroba*, captured widely in the study but especially at T9.

Discussion

This study is the first ichthyofaunistic survey carried out on a dam-free stretch of the Iguaçu River and its tributaries between the Salto Caxias Dam and the Iguaçu Falls. The number of identified species accounted for 72% of the number of species observed in a previous study for the Lower Iguaçu basin (Baumgartner et al. 2012), of which seven species had not been recorded (*Schizodon borellii*, *Charax stenopterus*, *Leiarius marmoratus*,

Poecilia reticulata, *Crenicichla lepidota*, *C. tapii*, and *C. tuca*). Other species identified only to genus level still have unresolved taxonomy (*Apteronotus* sp., *Characidium* sp., *Heptapterus* sp., *Hoplias* sp. 1, *Hoplias* sp. 2, and *Pariolius* sp.). These results are important, as the stretch of river studied by Baumgartner et al. (2012) was over 250 km long and included five reservoirs upstream of our study area. The high species richness we found may be due, in part, to the unprecedent collections within a conservation area, the INP.

The richness and abundance of Siluriformes and Characiformes species were higher than those of other orders, both in the Iguaçu River and in its tributaries. Similarly, the same pattern was pointed out by previous studies along the Lower Iguaçu river basin: in reservoirs (Baumgartner et al. 2006), in rivers (Bifi et al. 2006), and in streams (Sereia et al. 2017; Delariva et al. 2018). This pattern in the Iguaçu river basin demonstrates a trend in many Neotropical watersheds, as observed by Lowe-McConnell (1999).

Small water bodies are as refuges for small species and provide a greater diversity of food resources from riparian vegetation and a larger diversity of microhabitats (Castro and Polaz 2020). Our study finds a more remarkable small-bodied species richness in tributaries than in the main channel. Additionally, the results of GLMM also showed the tributaries importance for conserving endemic species, both outside of (T2, T3, T4, T9) and inside INP (T6). The autochthonous *Pareiorhaphis* cf. *parmula* and *C. tapii* were recorded only in tributaries within INP (T6), which suggests the park's role in the conservation of the fish fauna. Other species also had restricted capture in tributaries, but outside INP: the autochthonous *Heptapterus* sp. (T2), the allochthonous *P. reticulata* (T5), and *L. marmoratus* (T4), and the exotic *Hypophthalmichthys nobilis* (T9), indicating that tributaries without the protection afforded by being outside of the INP are more susceptible to anthropic threats.

Other small species, mainly belonging to the genera *Astyanax*, *Psalidodon*, and *Crenicichla*, occurred at all sampling sites. These species are generalists with high trophic plasticity, favoring their wide distribution within the basin and in varied habitats (Pini et al. 2019; Delariva and Neves 2020; Kuhn et al. 2020). Some *Astyanax* species were described in the last decades (Alcaraz et al. 2009; Garavello and Sampaio 2010), but taxonomic relationships and the identity of some of these remains uncertain (Rossini et al. 2016), caused by phenotypic plasticity (Pavanelli and Oliveira 2009), which will require full taxonomic review.

The introduction of species is among the leading causes of species extinction in worldwide (Matthews 1998), and this problem has already been highlighted in the Lower Iguaçu river basin. The transfer of these species to the Iguaçu basin has multiple reasons but may be a result of commercial and sport fishing (using live bait), aquaculture, fish stocking, and aquarium fish release (Garavello et al. 1997; Daga et al. 2016; Larentis et al. 2019). The exotic *P. reticulata* was recorded only in the Monteiro River (T5), whose basin is highly impacted by the urbanization of the city Capitão Leonidas Marques near the sampling site. Allochthonous species were also recorded elsewhere in the Iguaçu river basin, such as in the Segredo reservoir (Garavello et al. 1997) and the Salto Osório reservoir (Baumgartner et al. 2006), where the migratory *P. lineatus* was introduced. The allochthonous *Astyanax lacustris* is commonly reported for the Upper Paraná river basin, and its introduction is uncertain.

Fish farms are potential sources of invasive species (Orsi and Agostinho 1999; Daga et al. 2016) and impact the basin (Agostinho et al. 1999). The capture of the allochthonous *Salminus brasiliensis* is due to escapes and releases, possibly originating from fish farms to increase sport fishing potential, as reported by residents in the region. *Salminus brasiliensis* is considered potentially invasive and can cause serious harmful effects to the ecosystem where it is introduced (Vitule et al. 2014). The exotic Tilapia species, *Oreochromis niloticus* and *Coptodon rendalli*, were probably escapes from fish farms. Tilapia culture already has an alarmingly poor record of high-risk invasions into natural environments (Frota et al. 2019). Records of introduced species were also found in Iguaçu reservoirs (Foz do Areia, Segredo, Salto Santiago, Salto Osório and Salto Caxias) where 20 species are known, with Tilapia being among the most common (Daga and Gubiani 2012). The presence of hybrids is associated with fish farming (*Piaractus mesopotamicus* × *Colossoma macropomum*, *Piaractus mesopotamicus* × *Piaractus brachypomus*, *Pseudoplatystoma corruscans* × *Pseudoplatystoma fasciatum*) (Valladão et al. 2018).

Due to their multiple uses of water, the implementation of hydroelectric projects has also been associated with facilitating the introduction and dissemination of exotic species (Agostinho et al. 1999). In addition, changes in the river's physical and chemical characteristics promote non-measurable pressure on fish fauna, especially for species with greater sensitivity and specific ecological requirements. *Psalidodon gymnogenys*, *Steindachneridion melanodermatum*, and *Gymnogeophagus taroba*, could be most severely affected as they are already Endangered (ICMBio 2018). *Steindachneridion melanodermatum* is the largest fish in the Iguaçu River. It is an endemic and possibly migratory (Agostinho and Gomes 1997; Ludwig et al. 2005; Brehm et al. 2016), living in fast-flowing, deep waters in stretches of the Iguaçu River and tributaries where the natural flow of water is still preserved (Garavello 2005). In addition to the losses of their habitat and connectivity caused by the successive hydroelectric dams, fishing also contributes to declines in this species population (Assumpção et al. 2017). Stocks of this species have been under pressure from prohibited fishing (Assumpção et al. 2021) and are a challenge to monitor because the species occurs in two countries (Brazil and Argentina), and the fishing is most intense on weekends and holidays (UNIOESTE 2017). The extinction of *S. melanodermatum* could harm other trophic levels as it is a top-of-the-chain species. *Gymnogeophagus taroba*, a species of fast waters (Paiz et al. 2017), is widely distributed in the studied area. However, with the construction of the new hydroelectric reservoir, the species can disappear in the flooded area, and its distribution can be fragmented, which will lead to loss of genetic diversity and a population decline (Souza-Shibatta et al. 2018).

Conclusions

The last dam-free stretch of the Lower Iguaçu River upstream of the Iguaçu Falls exhibits a rich endemic fish fauna, rare endangered species restricted to this region, and new

species for science. This diversity is threatened with extinction by biotic and abiotic factors. Exotic species have occurred in low abundance, but their presence in most sampling sites and the Iguaçu National Park is worrisome, requiring actions to mitigate its harmful effects and to avoid new introductions. The presence of hybrids of allochthonous species escaped from fish farms requires strict supervision of these commercial operations. Another source of threats is the construction of the Baixo Iguaçu HPP, which will promote hydrological changes in the main channel and severe damage to many fish species. Thus, tributaries will play an essential role in maintaining the diversity of fish in the Iguaçu river basin since many species of the Iguaçu River also frequent in the tributaries, besides the species that occur only in these environments. The protection of free-flowing tributaries has been an appeal worldwide (Grill et al. 2019; Makrakis et al. 2019), as they support endangered species populations, provide various environmental conditions, access to spawning habitat, and refugia for early life stages (Silva et al. 2019). The correct identification of species and taxonomic research are also essential, as they will help the development of strategies for the management and conservation of environments (Assumpção et al. 2021). Thus, preserving the free stretch below the Baixo Iguaçu HPP to the Iguaçu Falls is crucially necessary and the last resource to conserve endemic and endangered species. In addition, to enable the management of ichthyofauna, efforts should be concentrated on monitoring populations.

Acknowledgements

References

Abell R, Thieme ML, Revenga C, Bryer M, Kottelat M, Bogutskaya N, Coad B, Mandrak N, Contrerasbalderas S, Bussing W, Stiassny MLJ, Skelton P, Allen GR, Unmack P, Naseka ANGR, Sindorf N, Robertson J, Armijo E, Higgins JV, Heibel TJ, Wikramanayake E, Olson D, López HL, Reis RE, Lundberg JG, Sabaj-Pérez MH, Petry P (2008) Freshwater ecoregions of the world: a new map of biogeographic units for freshwater biodiversity conservation. BioScience 58(5): 403–414. https://doi.org/10.1641/B580507

Agostinho AA, Gomes LC (1997) Reservatório de Segredo: bases ecológicas para o manejo. Eduem, Maringá, 387 pp.

Agostinho AA, Gomes LC, Pelicice FM (2007) Ecologia e manejo de recursos pesqueiros em reservatórios do Brasil. Eduem, Maringá, 501 pp.

Agostinho AA, Gomes LC, Suzuki HI, Júlio Jr HF (2003) Migratory fishes of the upper Paraná River Basin, Brazil. In: Carolsfeld J, Harvey B, Ross C, Baer A (Eds) Migratory Fishes of South America: Biology, Fisheries and Conservation Status. World Fisheries Trust, Ottawa, 19–98.

Agostinho AA, Miranda LE, Bini LM, Gomes LC, Thomaz SM, Suzuki HI (1999) Patterns of colonization in Neotropical reservoirs, and prognoses on aging. In: Tundisi JG, Straskraba M (Eds) Theoretical Reservoir Ecology and its Applications. International Institute of Ecology, São Carlos, 227–265.

Alcaraz HSV, Pavanelli CS, Bertaco VA (2009) *Astyanax jordanensi*s (Ostariophysi: Characidae), a new species from the rio Iguaçu basin, Paraná, Brazil. Neotropical Ichthyology 7(2): 185–190. https://doi.org/10.1590/S1679-62252009000200008

Assumpção L, Makrakis S, Silva PS, Makrakis MC (2017) Espécies de peixes ameaçadas de extinção no Parque Nacional do Iguaçu. Biodiversidade Brasileira 7: 4–17.

Assumpção L, Fávaro LF, Makrakis S, Silva PS, Pini SFR, Kashiwaqui EAL, Makrakis MC (2021) Population structure and reproduction of *Steindachneridion melanodermatum* (Siluriformes: Pimelodidae), a large catfish endemic to Neotropical ecoregion. Marine and Freshwater Research 1: 1–15. https://doi.org/10.1071/MF19373

Barbosa FAR, Padisak J, Espindola ELG, Borics G, Rocha O (1999) The cascading Reservoir Continuum Concept (CRCC) and its application to the River Tietê basin, São Paulo State, Brazil. In: Tundisi JG, Straskaba M (Eds) Theoretical Reservoir Ecology and its Applications. Brazilian Academy of Sciences and Backhuys Publishers, São Carlos, 425–437.

Bartozek ECR, Bueno NC, Feiden A, Rodrigues LC (2016) Response of phytoplankton to an experimental fish culture in net cages in a subtropical reservoir. Brazilian Journal of Biology 76(4): 824–833. https://doi.org/10.1590/1519-6984.00115

Bates D, Maechler M, Bolker B, Walker S (2015) Fitting linear mixed-effects models using lme4. Journal of Statistical Software 67(1): 1–48. https://doi.org/10.18637/jss.v067.i01

Baumgartner G, Pavanelli CS, Baumgartner D, Bifi AG, Debona T, Frana VA (2012) Peixes do Baixo rio Iguaçu. Eduem, Maringá, 203 pp. https://doi.org/10.7476/9788576285861

Baumgartner D, Baumgartner G, Pavanelli CS, Silva PRL, Frana VA, Oliveira LC, Micheon MRO (2006) Fish, Salto Osório Reservoir, Iguaçu river basin, Paraná state, Brazil. Check List 2(1): 1–4. https://doi.org/10.15560/2.1.1

Bifi AG, Baumgartner D, Baumgartner G, Frana VA, Debona T (2006) Composição específica e abundância da ictofauna do rio dos Padres, bacia do rio Iguaçu, Brasil. Acta Scientiarum Biological Sciences 28(3): 203–211. https://doi.org/10.4025/actascibiolsci.v28i3.193

Brehm M, FIlippin RF, de Moura RR (2016) O impacto ambiental causado à ictiofauna do rio Iguaçu pela exploração do potencial hidrelétrico: o caso do surubim do Iguaçu (*Steindachneridion melanodermatum*). Revista Brasileira de Energia 1: 30–47. https://sbpe.org.br/index.php/rbe/article/view/350/331

Bueno-Krawczyk ACD, Guiloski IC, Piancini LDS, Azevedo JC, Ramsdorf WA, Ide AH, Guimarães ATB, Cestari MM, Silva de Assis HC (2015) Multibiomarker in fish to evaluate a river used to water public supply. Chemosphere 135: 247–264. https://doi.org/10.1016/j.chemosphere.2015.04.064

Cáceres MD, Legendre P (2009) Associations between species and groups of sites: indices and statistical inference. Ecology 90(12): 3566–3574. https://doi.org/10.1890/08-1823.1

Carvalho DR, Flecker AS, Alves CBM, Sparks JP, Pompeu PS (2019) Trophic responses to aquatic pollution of native and exotic livebearer fishes. Science of the Total Environment 681: 503–515. https://doi.org/10.1016/j.scitotenv.2019.05.092

Casciotta J, Almirón A, Ciotek L, Giorgis P, Říčan O, Piálek L, Dragová K, Croci Y, Montes M, Iwaszkiw J, Puentes A (2016) Visibilizando lo invisible. Un relevamiento de la diversidad de peces del Parque Nacional Iguazú, Misiones, Argentina. Historia Natural 6: 5–77. https://ri.conicet.gov.ar/handle/11336/65608

Castro R, Polaz CN (2020) Small-sized fish: the largest and most threatened portion of the megadiverse neotropical freshwater fish fauna. Biota Neotropica 20(1): e20180683. https://doi.org/10.1590/1676-0611-bn-2018-0683

Daga VS, Gubiani ÉA (2012) Variations in the endemic fish assemblage of a global freshwater ecoregion: associations with introduced species in cascading reservoirs. Acta Oecologica 41: 95–105. https://doi.org/10.1016/j.actao.2012.04.005

Daga VS, Debona T, Abilhoa V, Gubiani ÉA, Vitule JRS (2016) Non-native fish invasions of a Neotropical ecoregion with high endemism: a review of the Iguaçu River. Aquatic Invasions 11(2): 209–223. https://doi.org/10.3391/ai.2016.11.2.10

Delariva RL, Hahn NS, Kashiwaqui EAL (2013) Diet and trophic structure of the fish fauna in a subtropical ecosystem: impoundment effects. Neotropical Ichthyology 4: 891–904. https://doi.org/10.1590/S1679-62252013000400017

Delariva RL, Neves MP, Larentis C, Kliemann BCK, Baldasso MC, Wolff LL (2018) Fish fauna in forested and rural streams from an ecoregion of high endemism, lower Iguaçu river basin, Brazil. Biota Neotropica 18(3): e20170459. https://doi.org/10.1590/1676-0611-bn-2017-0459

Delariva RL, Neves MP (2020) Morphological traits correlated with resource partitioning among small characin fish species coexisting in a Neotropical river. Ecology of Freshwater Fish 29(4): 640–653. https://doi.org/10.1111/eff.12540

Dufrêne M, Legendre P (1997) Species assemblages and indicator species: the need for a flexible asymmetrical approach. Ecological Monographs 67(3): 345–366. https://doi.org/10.1890/0012-9615(1997)067[0345:SAAIST]2.0.CO;2

Fox J, Weisberg S (2019) An {R} Companion to Applied Regression, 3rd edn. Thousand Oaks CA: Sage. https://socialsciences.mcmaster.ca/jfox/Books/Companion/ [Accessed 23 June 2020]

Fricke R, Eschmeyer WN, Van der Laan R [Eds] (2020) Eschmeyer's Catalog of Fishes: Genera, Species, References. http://researcharquive.calacademy.org/research/ichthyology/catalog/fishcatmain.asp [Accessed 23 June 2020]

Frota A, Oliveira RCD, Benedito E, Graça WJD (2019) Ichthyofauna of headwater streams from the rio Ribeira de Iguape basin, at the boundaries of the Ponta Grossa Arch, Paraná, Brazil. Biota Neotropica 19(1): e20180666. https://doi.org/10.1590/1676-0611-bn-2018-0666

Garavello JC (2005) Revision of genus *Steindachneridion* (Siluriformes: Pimelodidae). Neotropical Ichthyology 3(4): 607–623. https://doi.org/10.1590/S1679-62252005000400018

Garavello JC, Britski HA, Zawadzki CH (2012) The cascudos of the genus *Hypostomus Lacépède* (Osteichthyes: Loricariidae) from the rio Iguaçu basin. Neotropical Ichthyology 10: 263–283. https://doi.org/10.1590/S1679-62252012000200005

Garavello JC, Pavanelli CS, Suzuki HI (1997) Caracterização da ictiofauna do rio Iguaçu. In: Agostinho AA, Gomes LC (Eds) Reservatório de Segredo: bases ecológicas para o manejo. Eduem, Maringá, 61–84.

Garavello JC, Sampaio FAA (2010) Five new species of genus *Astyanax* Bird & Girard, 1854 from Rio Iguaçu, Parana, Brazil (Ostariophysi, Characiformes, Characidae). Brazilian Journal of Biology 70(3): 847–865. https://doi.org/10.1590/S1519-69842010000400016

Graça WJ, Pavanelli CS (2007) Peixes da planície de inundação do alto rio Paraná e áreas adjacentes. Eduem, Maringá, 241 pp.

Grill G, Lehner B, Thieme M, Geenen B (2019) Mapping the world's free-flowing rivers. Nature 569: 215–221. https://doi.org/10.1038/s41586-019-1111-9

ICMBio [Instituto Chico Mendes de Conservação da Biodiversidade] (2018) Livro Vermelho da Fauna Brasileira Ameaçada de Extinção. ICMBio/MMA, Brasília, 492 pp.

IBGE [Instituto Brasileiro de Geografia e Estatística] (2015) Indicadores de desenvolvimento sustentável: Brasil. Coordenação de Recursos Naturais e Estudos Ambientais e Coordenação de Geografia, Rio de Janeiro, 352 pp.

Kliemann BCK, Delariva RL (2015) Pequenas Centrais Hidrelétricas: cenários e perspectivas no estado do Paraná. Ciência e Natura 37(3): 274–283. https://doi.org/10.5902/2179460X17111

Kuhn F, Neves MP, Bonato KO, Fialho CB (2020) Relationship between diet and pharyngeal jaw morphology of *Crenicichla* species (Cichliformes: Cichlidae) in streams from Uruguay and Jacuí basins, southern Brazil. Environmental Biology of Fishes 103: 377–388. https://doi.org/10.1007/s10641-020-00963-y

Kuznetsova A, Brockhoff PB, Christensen RHB (2017) lmerTest package: tests in linear mixed effects models. Journal of Statistical Software 82(13): 1–26. https://doi.org/10.18637/jss.v082.i13

Langeani F, Corrêa e Castro RM, Oyakawa OT, Shibatta OA, Pavanelli CS, Casatti L (2007) Diversidade da ictofauna do Alto Rio Paraná: composição atual e perspectvas futuras. Biota Neotropica 7(3): 181–197. https://doi.org/10.1590/S1676-06032007000300020

Larentis C, Delariva RL, Gomes LC, Baumgartner D, Ramos IP, Sereia DAO (2016) Ichthyofauna of streams from the lower Iguaçu river basin, Paraná state, Brazil. Biota Neotropica 16(3): e20150117. https://doi.org/10.1590/1676-0611-BN-2015-0117

Larentis C, Baldasso MC, Kliemann BCK, Neves MP, Zavaski AG, Sandri LM, Ribeiro AC, Xavier DPSS, Costa GON, Delariva RL (2019) First record of the non-native *Xiphophorus hellerii* (Cyprinodontiformes: Poeciliidae), in the Iguazu river basin, Paraná, Brazil. Journal of Applied Ichthyology 35(5): 1164–1168. https://doi.org/10.1111/jai.13965

Lowe-Mcconnell RH (1999) Estudos ecológicos de comunidades de peixes tropicais. Edusp, São Paulo, 534 pp.

Ludwig LAM, Gomes E, Artoni RF (2005) Um método de reprodução induzida para o surubim *Steindachneridion melanodermatum* (Siluriformes: Pimelodidae) do Rio Iguaçu. Publicatio UEPG Ciências Biológicas e da Saúde 11: 23–27. https://doi.org/10.5212/Publ.Biologicas.v.11i3.0003

Maack R (1981) Geografa física do Estado do Paraná. J. Olympio, Rio de Janeiro, 442 pp.

Makrakis S, Bertão APS, Silva JFM, Makrakis MC, Sanz-Ronda Fco J, Celestino LF (2019) Hydropower development and fishways: a need for connectivity in rivers of the Upper Paraná Basin. Sustainability 11(3749): 1–24. https://doi.org/10.3390/su11133749

Matthews WJ (1998) Patterns in Freshwater Fish Ecology. Chapman & Hall, New York, 784 pp. https://doi.org/10.1007/978-1-4615-4066-3

Mise FT, Fugi R, Pagotto JPA, Goulart E (2013) The coexistence of endemic species of Astyanax (Teleostei: Characidae) is propitiated by ecomorphological and trophic variations. Biota Neotropica 13(3): 21–28. https://doi.org/10.1590/S1676-06032013000300001

Neves MP, Silva JC, Baumgartner D, Baumgartner G, Delariva RL (2018) Is resource partitioning the key? The role of intra-interspecific variation in coexistence among five small endemic fish species (Characidae) in subtropical rivers. Journal of Fish Biology 93: 238–249. https://doi.org/10.1111/jfb.13662

Nimet J, Guimaráes ATB, Delariva RL (2017) Use of Muscular Cholinesterase of *Astyanax bifasciatus* (Teleostei, Characidae) as a Biomarker in Biomonitoring of Rural Streams. Bulletin of Environmental Contamination and Toxicology 99: 232–238. https://doi.org/10.1007/s00128-017-2111-9

Orsi ML, Agostinho AA (1999) Introdução de espécies de peixes por escapes acidentais de tanques de cultivo em rios da Bacia do Rio Paraná, Brasil. Revista Brasileira de Zoologia 16(2): 557–560. https://doi.org/10.1590/S0101-81751999000200020

Paiz LM, Baumgartner L, Graça WJ, Margarido VP, Pavanelli CS (2017) Cytogenetics of *Gymnogeophagus setequedas* (Cichlidae: Geophaginae), with comments on its geographical distribution. Neotropical Ichthyology 15(2): e160035. https://doi.org/10.1590/1982-0224-20160035

Pavanelli CS, Oliveira AM (2009) A redescription of *Astyanax gymnodontus* (Eigenmann, 1911), a new combination, a polymorphic characid fish from the rio Iguaçu basin, Brazil. Neotropical Ichthyology 7(4): 569–578. https://doi.org/10.1590/S1679-62252009000400003

Pelicice FM, Azevedo-Santos VM, Esguícero ALH, Agostinho AA, Arcifa MS (2018) Fish diversity in the cascade of reservoirs along the Paranapanema River, southeast Brazil. Neotropical Ichthyology 16(2): e170150. https://doi.org/10.1590/1982-0224-20170150

Pini SFR, Abelha MCF, Kashiwaqui EAL, Delariva RL, Makrakis S, Makrakis MC (2019) Food resource partitioning among species of Astyanax (Characiformes: Characidae) in the Lower Iguaçu River and tributaries, Brazil. Neotropical Ichthyology 17(4): e190028. https://doi.org/10.1590/1982-0224-20190028

Pinheiro J, Bates D, DebRoy S, Sarkar D, Team RC (2021) NLME: linear and nonlinear mixed effects models. R package version 3.1-137. https://CRAN.R-project.org/package=nlme [Accessed 23 April 2021]

R Core Team (2021) R: A language and environment for statistical computing. Vienna: R Foundation for Statistical Computing. http://www.R-project.org/ [Accessed 10 January 2021]

Reis RB, Frota A, Depra GDC, Ota RR, Graca WJ (2020) Freshwater fishes from Paraná State, Brazil: an annotated list, with comments on biogeographic patterns, threats, and future perspectives. Zootaxa 4868(4): 451–494. https://doi.org/10.11646/zootaxa.4868.4.1

Reis RE, Albert JS, Dario F di, Mincarone MM, Petry P, Rocha LA (2016) Fish biodiversity and conservation in South America. Journal of Fish Biology 89: 12–47. https://doi.org/10.1111/jfb.13016

Reis RE, Kullander SO, Ferraris Jr CJ (2003) Check list of the freshwater fishes of South and Central America. Edipucrs, Porto Alegre, 742 pp.

Rossini BC, Oliveira CAM, Melo FAG, Bertaco VA, Astarloa JMD, Rosso JJ, Foresti F, Oliveira C (2016) Highlighting *Astyanax* species diversity through DNA barcoding. PLoS ONE 11(12): e0167203. https://doi.org/10.1371/journal.pone.0167203

Santos NCL, García-Berthou E, Dias JD, Lopes TM, Affonso IP, Severi W, Gomes LC, Agostinho AA (2018) Cumulative ecological effects of a Neotropical reservoir cascade across multiple assemblages. Hydrobiologia 819: 77–91. https://doi.org/10.1007/s10750-018-3630-z

Sereia DAO, Duarte GSC, Debona T (2017) A importância das unidades de conservação para a preservação da diversidade de peixes em riachos. Estudo de caso: riacho Sanga 2 do Poço Preto, um afluente da bacia do rio Iguaçu, Parque Nacional do Iguaçu. Revista Latino-Americana de Estudos Avançados 1(2): 39–56. https://revistas.unila.edu.br/relea/article/view/630

Severi W, Cordeiro AAM (1994) Catálogo de Peixes da Bacia do Rio Iguaçu. IAP/GTZ, Curitiba, 118 pp.

Silva PS, Miranda LE, Makrakis S, Assumpcão L, Dias JHP, Makrakis MC (2019) Tributaries as biodiversity preserves: an ichthyoplankton perspective from the severely impounded Upper Paraná River. Aquatic Conservation 29: 258–269. https://doi.org/10.1002/aqc.3037

Souza-Shibatta L, Kotelok-Diniz T, Ferreira DG, Shibatta OA, Sofia SH, de Assumpção L, Pini SFR, Makrakis S, Makrakis MC (2018) Genetic Diversity of the Endangered Neotropical Cichlid Fish (*Gymnogeophagus setequedas*) in Brazil. Frontiers in Genetics 9: e13. https://doi.org/10.3389/fgene.2018.00013

Teresa FB, Casatti L (2017) Trait-based metrics as bioindicators: responses of stream fish assemblages to a gradient of environmental degradation. Ecological Indicators 75: 249–258. https://doi.org/10.1016/j.ecolind.2016.12.041

Valladão GMR, Gallani SU, Pilarski F (2018) South American fish for continental aquaculture. Reviews in Aquaculture 10(2): 351–369. https://doi.org/10.1111/raq.12164

Vitule JRS, Bornatowski H, Freire CA, Abilhoa V (2014) Extralimital introductions of *Salminus brasiliensis* (Cuvier, 1816) (Teleostei, Characidae) for sport fishing purposes: A growing challenge for the conservation of biodiversity in neotropical aquatic ecosystems. BioInvasions Records 3(4): 291–296. https://doi.org/10.3391/bir.2014.3.4.11

UNESCO [United Nations Educational, Scientific and Cultural Organization] (2012) World Heritage Committee. Report: 36th Session. WHC-12/36. COM/7B. Add. Convention Concerning the Protection of the World Cultural and Natural Heritage. Saint-Petersburg. http://whc.unesco.org/archive/2012/whc12-36com-7BAdd-en.pdf [Accessed 23 June 2020]

UNIOESTE (2017) Avaliação da ictiofauna e do ciclo reprodutivo na área de influência da UHE Baixo Iguaçu – Setembro de 2013 a Dezembro de 2016: Relatório. Getech/Instituto Água Viva, Toledo, 129 pp.